

STRUCTURAL STUDIES
OF
HYDROGEN-BONDED FERROELECTRICS

Thesis

presented by

/ / /
VESTEINN RUNI EIRIKSSON

for the degree of

DOCTOR OF PHILOSOPHY

UNIVERSITY OF EDINBURGH

MAY, 1974.

ACKNOWLEDGEMENTS

Throughout my candidature for this degree I have been fortunate in the generous measure of personal and financial assistance I have received.

I am very grateful for the award of a maintenance grant from the Atomic Energy Authority. I thank Professor W. Cochran and Dr. B.T.M. Willis for their essential contribution in making this award a reality - for maintenance grants from the Icelandic Science Foundation and the Icelandic Students Loan Foundation (a "Candidates grant") - and for grants from the Brodie Memorial Fund and the Wardlaw Memorial Fund; I thank Professors W. Cochran and N. Feather for their support for the last two awards.

I am very grateful to the Atomic Energy Authority and the Science Research Council for granting me access to the neutron beam facilities at the Atomic Energy Research Establishment, Harwell, and sincere thanks are also due to Professor N. Feather for extending to me the facilities of the Department of Natural Philosophy, Edinburgh University.

The work presented in this thesis forms a part of a collaborative effort between the Solid State Physics Group of this University, led by Professor W. Cochran, and the Neutron Scattering Group of A.E.R.E., led by Dr. B.T.M. Willis. In particular the data collection on DTGS was carried out in collaboration with Dr. A. Hewat and Mr. K.D. Rouse of A.E.R.E. Some of the analysis on DTGS were carried out with Mr. K.D. Rouse, who also collected data on KDP in continuation of the data collection on DKDP. I am truly grateful for the experience of participating in scientific life at A.E.R.E. Harwell, and in particular of working with the group of Dr. B.T.M. Willis.

I consider myself fortunate in having had the opportunity to work in the Solid State Group of Edinburgh University. I highly value the support I have received to participate frequently in international conferences and summer schools. It is a great pleasure to thank the members of this group for generous scientific and personal assistance, for many highly valuable discussions and interesting arguments and, in general for the pleasure of their company.

I express my sincere thanks to Dr. R.J. Nelmes for his enthusiastic interest, guidance, scientific and personal assistance and appreciation of the work.

I am grateful to Dr. G.S. Pawley for making available his very flexible basic least squares program; to Dr. F. Placido for collaboration on crystal growing and testing.

Without meaning to throw anyone into the shade, above all my most sincere thanks are offered to Professor W. Cochran who introduced me to the subject of Solid State Physics and whose guidance and support in all aspects of the work, throughout my candidature, has been my greatest source of confidence and encouragement.

Most of the analysis was carried out using the facilities of the Edinburgh Regional Computing Centre. I thank Mr. R.R. McLeod of the E.R.C.C. for assistance with non-standard procedures in data transfer.

I cannot leave without thanking my very good friends Drs. G. Zaccai and K. Hisano, who always saw bright spots within the horizon, for enlightenment.

I happily extend my thanks to Mrs. R. Chester for carrying out the task of typing my manuscript; also to Mrs. M. McDonald for cheerfully typing the tables.

It is hard to see how I could have as much as started this work without the backing of my parents, the family of my parents-in-law and my sisters and their families. My wife, my children and I, who have all shared the pleasures and other aspects of this work, must pay tribute to the unselfish and reassuring assistance of these people in the achievement of the completion of this thesis.

ABSTRACT

This thesis is concerned with structural studies of hydrogen-bonded ferroelectrics, in particular the structures of DKDP, KDP and of DTGS in their paraelectric phases.

The methods of least squares with constraints and of hypothesis testing are considered in detail.

These methods are then applied to assess the significance of structural features of interest in DKDP and in KDP at room temperature and at $T_c + 5^\circ\text{K}$ (213.8(3) and 127°K respectively).

The principal conclusions are that in the paraelectric phases of DKDP and of KDP the D, H atoms on the short O - O hydrogen-bonds are disordered in double minimum potential wells and that a line joining these sites is inclined to the O - O line. Marked isotope and temperature effects are found on many of the structural features considered.

Suggestions are made as to future work.

The problem of structural studies on paraelectric DTGS is included as an illustrative example of some of the problems met in structural studies on ferroelectrics. In particular we point out that the problem of DTGS cannot successfully be tackled in terms of conventional crystallography if the questions on structural features of interest, such as that on the extent of disorder, are to be meaningfully answered. Alternative approaches are discussed.

C O N T E N T S

Page

CHAPTER I INTRODUCTION

I.1	Objectives	1
I.2	Ferroelectricity	2
I.3	Ferroelectric Phase Transitions	2
I.4	Classification of Ferroelectrics	7
I.5	Ferroelectricity and Lattice Dynamics	8
I.6	Problems of Structural Studies of Ferroelectrics	17
I.7	Outline of the Thesis	20

CHAPTER II METHODS OF STUDY

II.1	Neutron Diffraction	22
II.1.a	Structure factors	22
II.1.b	Neutron instruments	25
II.1.c	Observations	29
II.2	Least Squares	33
II.2.a	The general theory of least squares	33
II.2.b	Constraints and hypothesis testing	38
II.2.c	Application to Crystallography.	44
II.3	Fourier Methods	49
II.4	Structural Studies of Ferroelectrics	51

CHAPTER III SAMPLE PREPARATION

III.1	Crystal Growing from Solution	53
III.1.a	In theory	53
III.1.b	In practice, DTGS.	55

C O N T E N T S (Contd.)

		Page
III.2	Crystal Testing and Grinding	58
III.2.a	DTGS	58
III.2.b	DKDP	59
III.2.c	KDP	60
III.2.d	Grinding	60
<u>CHAPTER IV</u>	<u>STRUCTURAL STUDIES OF THE SYSTEM KDP - DKDP</u>	
IV.1	Introduction	62
IV.2	Data Collection and Handling	74
IV.2.a	The room temperature data collection	74
IV.2.b	The low temperature data collection	77
IV.2.c	Data handling	79
IV.3	Structural Features to be Tested in KDP - DKDP	80
IV.4	The Models of KDP - DKDP and their Formalism	83
IV.5	The Room Temperature Experiment on DKDP	87
IV.5.a	The refinements	87
IV.5.b	The results	89
IV.5.c	The room temperature structure of DKDP	90
IV.6	The Low Temperature Experiment on DKDP	91
IV.6.a	The refinements	91
IV.6.b	The results	93
IV.6.c	The structure of DKDP at $T_c + 5^\circ K$	94

C O N T E N T S (Contd.)

		Page
IV.7	The Room Temperature Experiment on KDP	95
IV.7.a	The refinements	95
IV.7.b	The results	96
IV.7.c	The room temperature structure of KDP	97
IV.8	The Low Temperature Experiment on KDP .	98
IV.8.a	The refinements	98
IV.8.b	The results	98
IV.8.c	The structure of KDP at $T_c + 5^\circ\text{K}$	99
IV.9	Interpretation of the Results.	100
IV.10	Application of Results	104
<u>CHAPTER V</u>	<u>STRUCTURE STUDY OF DTGS</u>	
V.1	Introduction	108
V.2	The Experiment on DTGS at 80°C	115
V.2.a	Experimental setup	115
V.2.b	Data collection and handling	115
V.3	Refinements and Results	116
V.4	Discussion	120
<u>CHAPTER VI</u>	<u>CONCLUSIONS</u>	
VI.1	KDP - DKDP	124
VI.2	DTGS	126

C O N T E N T S (Contd.)

Appendix I

The F distribution and α .

Appendix II

The Cooper-Rouse extinction correction.

Appendix III

DKDP structure factors at R.T.

Appendix IV

DKDP structure factors at $T_c + 5^\circ\text{K}$.

Appendix V

KDP structure factors at R.T.

Appendix VI

KDP structure factors at $T_c + 5^\circ\text{K}$.

Appendix VII

DTGS structure factors at 80°C

Appendix VIII

Published Work.

REFERENCES

CHAPTER I

INTRODUCTION

I.1 Objectives

The object of this study is to contribute to the foundations of a deeper understanding of ferroelectric phase transitions that should lead to a better understanding of phase transitions in general and at the same time add to our understanding of interatomic forces.

By the essential foundations referred to above we mean the detailed crystal structure of the compounds concerned, that is a static, time averaged, picture of their interatomic arrangements.

This work is concerned with the crystal structures of potassium dideuterium (and dihydrogen) phosphate (KD_2PO_4 and KH_2PO_4) and of deuterated triglycine sulphate $(\text{ND}_2\text{CD}_2\text{COOD})_3 \cdot \text{D}_2\text{SO}_4$.

The compounds KD_2PO_4 , KH_2PO_4 and $(\text{ND}_2\text{CD}_2\text{COOD})_3 \cdot \text{D}_2\text{SO}_4$ will be referred to as DKDP, KDP and DTGS hereafter.

I.2 Ferroelectricity

A ferroelectric crystal possesses a spontaneous polarization that can be switched by the application of an external field (or pressure).

Out of the 32 crystal classes (point groups) 21 are non-centrosymmetric; 20 of these are piezoelectric. 10 of the piezoelectric classes are polar. The polar classes show the pyroelectric effect and possess spontaneous polarization.

Being pyroelectric is however only a necessary but not sufficient condition for a crystal to be ferroelectric. Only when the forces within the polar structure are so delicately balanced as to permit switching of the polarization by the application of an external field is the crystal ferroelectric.

A ferroelectric crystal is therefore a pyroelectric crystal with switchable polarization.

It is customary to use the term "ferroelectric" for a crystal which has a ferroelectric phase.

The present discussion will be limited to "proper" ferroelectrics in which the spontaneous polarization is the primary order parameter.

I.3 Ferroelectric Phase Transition

In general a ferroelectric has a non-ferroelectric phase of higher symmetry with a transition temperature T_c associated with the transition between the low temperature ferroelectric phase and the high temperature non-ferroelectric phase. A ferroelectric may have transitions between two or more ferroelectric phases.

There is a wide range of T_c , $\text{LiTlC}_4\text{H}_6 \cdot \text{H}_2\text{O}$ lithium thallium tartrate monohydrate has a T_c of 10°K while NaNbO_3 sodium niobate becomes ferroelectric on cooling at 913°K , (Zheludev, 1971, p. 52, p. 102).

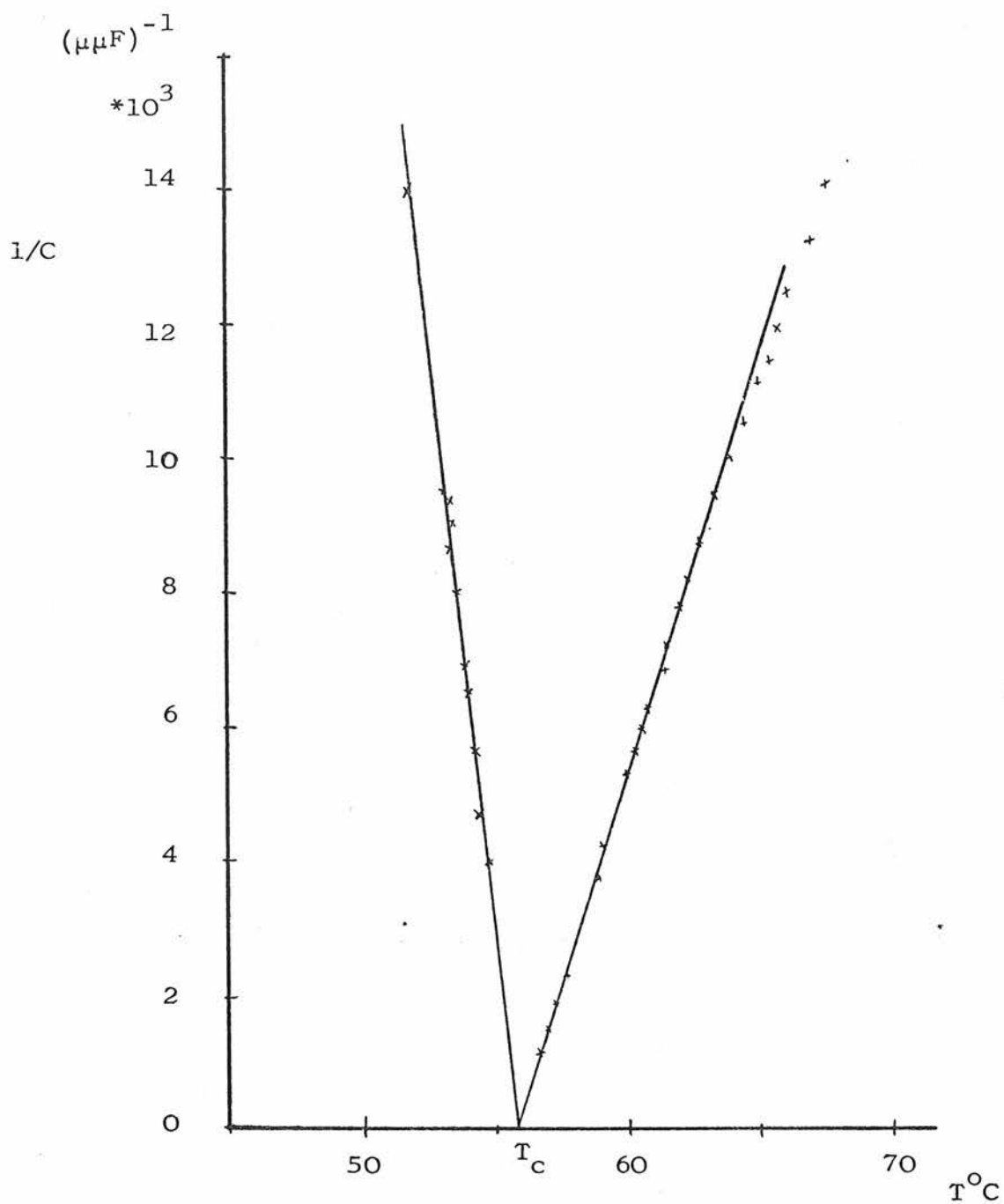
It is customary to refer to the non-ferroelectric phase as the 'paraelectric' phase.

Ferroelectrics may have none (at atmospheric pressure at least), one or more than one paraelectric phases. Rochelle salt, sodium potassium tartrate tetrahydrate, $\text{NaKC}_4\text{H}_6 \cdot 4\text{H}_2\text{O}$, is ferroelectric between 255 and 297°K ; and Ammonium hydrogen sulphate, $(\text{NH}_4)\text{HSO}_4$, is ferroelectric between 154 and 270°K (Jona and Shirane, 1962).

Associated with a ferroelectric transition is an anomaly in the static dielectric constant $\epsilon(0)$ in the direction(s) in which spontaneous polarization develops. $\epsilon(0)$ diverges as T_c is approached and can reach values as high as 10^5 . The falling off of $\epsilon(0)$ in the paraelectric phase follows a Curie-Weiss law, see Fig. I.1 (of DTGS after Eiriksson and Placido, 1971).

$$\epsilon(0) \propto (T - T_c)^{-1}.$$

For ferroelectrics therefore the divergence of the susceptibility $\epsilon(0) - 1$ at T_c can be demonstrated directly by relatively simple measurements. In the ferroelectric phase it is usually straight forward to observe hysteresis in the switching of polarization under the action of an externally applied a.c. field. The value of the saturated polarization extrapolated to zero applied field gives the spontaneous polarization. The spontaneous polarization corresponds to the order parameter. Thus in ferroelectric phase transitions



Reciprocal of capacitance, $1/C$ (of a plate of DTGS perpendicular to (010)), proportional to $1/\epsilon$, the reciprocal of the dielectric constant, vs. temperature; demonstrating, near T_c , the Curie-Weiss law for DTGS. (After Eiriksson and Placido, 1971)

Fig. I.1.

we have this favourable situation of being able to observe directly and measure the temperature dependence of the susceptibility and of the order parameter. This makes ferroelectric phase transitions a particularly important class of structural phase transitions.

The ferroelectric phase is derived from the paraelectric phase by relative atomic displacements small compared with the unit cell dimensions and/or by the ordering of certain structure elements that were disordered in the paraelectric phase. The delicate balance of the possible configurations in the ferroelectric phase, making possible the switching polarization and obtained from one another by these small changes, require the free energy of the two phases to be nearly equal (see, for example, Jona and Shirane, 1962). The distinction between the purely displacive and order-disorder phase transition becomes unclear in the limit of site separation of the relevant disordered atoms, being comparable with the mean thermal amplitude of these atoms or in the limit of the energy barrier separating the possible sites being comparable with or less than $k_B T$. In these limits the dynamics (see Section I.5) of a disordered atom approaches equivalence to that of an ordered atom but with anharmonic effects being somewhat more important.

Purely displacive ferroelectric phase transitions are almost a unique class of phase transitions in that they occur between two perfectly ordered phases.

Examples are provided by the structural phase transitions between ferroelectric phases which are common among ferroelectric perovskites. Devonshire, 1954, lists the order which will always be cubic, tetragonal polar, orthorhombic polar,

rhombohedral-polar, tetragonal non-polar and orthorhombic non-polar. But any particular perovskite might only exist in one or some of these phases. BaTiO_3 , barium titanate, exists in the four first listed forms, it is ferroelectric in its polar forms and therefore has two structural transitions between ferroelectric phases.

At a ferroelectric transition the relative atomic displacements are generally very small; a structure of higher symmetry in the paraelectric phase becomes, in the ferroelectric phase a pseudosymmetric variation of that structure. There is a large number of possible symmetry changes, displacements and ordering processes (which themselves may be linked with other displacements) involved in ferroelectric phase transitions. In most ferroelectrics the pseudosymmetry is confined to the ferroelectric phase but more complicated situations arise in, for example, NH_4HSO_4 where the paraelectric phase (upper) is pseudosymmetric (Nelmes, 1971). In hydrogen bonded ferroelectrics the transition commonly involves ordering of hydrogens that in the paraelectric phase are disordered between two possible sites on a hydrogen bond, as in KDP; but in NH_4HSO_4 the hydrogen bonds as a whole are involved in the ordering process (Nelmes, 1971). In addition some ferroelectrics lack a centre of symmetry in the paraelectric phase (and are generally piezoelectric; example: KDP) whereas others (like TGS) are centrosymmetric in the paraelectric phase.

There is a connection between the way in which lowering of symmetry at a transition takes place and the onset of spontaneous polarization through the fact that both the

change in symmetry and the change in polarization come about as a direct consequence of the small displacements.

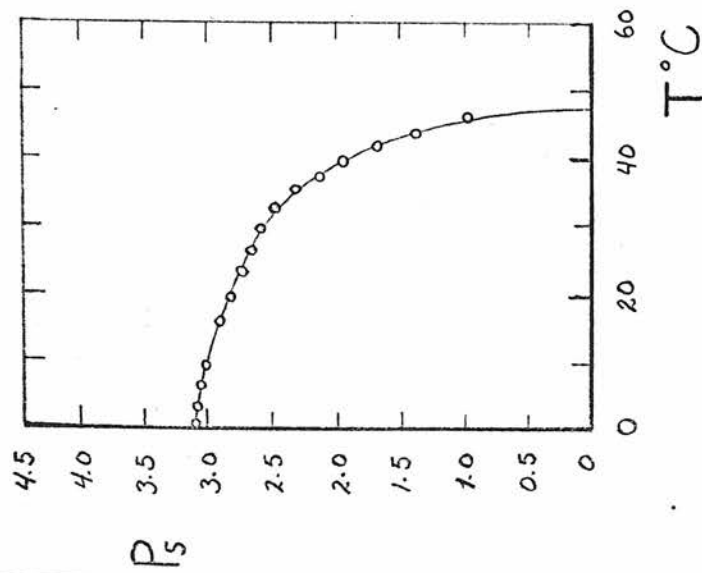
We only take this as far as relating (see below) abrupt discontinuity in one with abrupt discontinuity in the other.

A transition can be first or second order (see, for example, Pippard, 1964). As stated earlier the free energies of the para and ferroelectric phases must be nearly equal away from the transition. The free energy also must vary continuously through the transition.

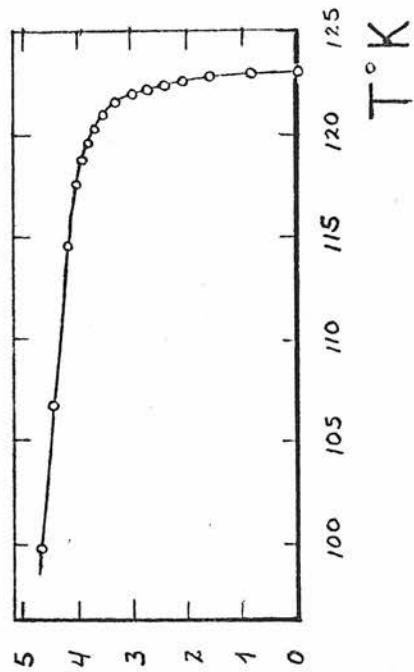
By expanding the free energy (see Section I.5) of the crystal as a power series in polarization with temperature dependent coefficients, assuming, depending on the choice of free energy, either zero stress or zero strain, it can be shown (Devonshire, 1954 or for brief accounts: Jona and Shirane, 1962, p. 15; or Zheludev, 1971, p. 262) that the spontaneous polarization should change discontinuously at T_c , see Fig. I.2.c, for a first order transition (BaTiO_3) but continuously, see Fig. I.2.a, for a second order transition (TGS).

Fig. I.2.b shows the temperature dependence of the spontaneous polarization for KDP which is very nearly second order.

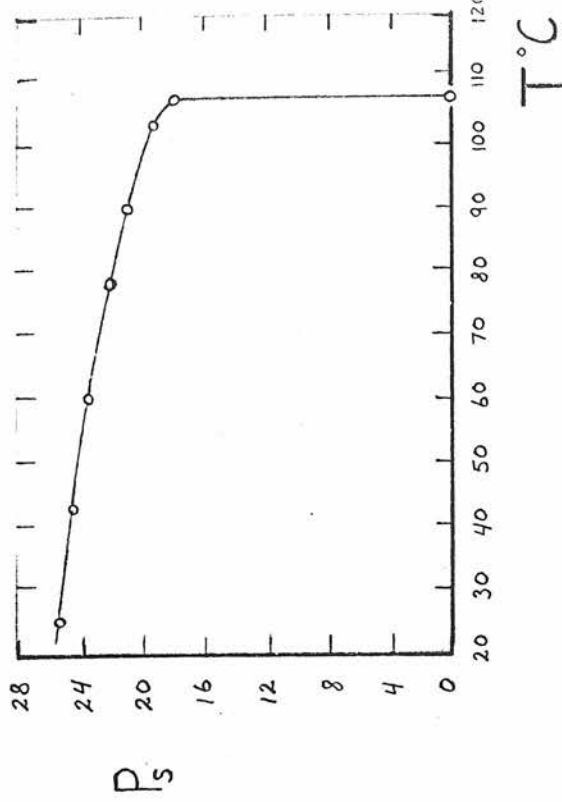
We expect therefore as a feature of second order ferroelectric structural phase transitions that the symmetry will be lowered without abrupt discontinuity in the interatomic arrangement. In TGS the change in symmetry across the second order transition is from $P2_1/m$ to $P2_1$ in the ferroelectric phase and comes about as a "statistical mirror plane" disappears (Chapter V).



a) TGS



b) KDP



c) BaTiO_3

P_s , the spontaneous polarization in $\mu\text{-coulombs/cm}^2$, vs. temperature for three ferroelectrics.
 (This figure is copied from figures II.4, III.4 and IV.7 of Jona and Shirane, 1962)

Fig. I.2.

The structural approach aims at identifying the time averaged distribution of the atoms in the phases on either side of the transition temperature and thereby answering the question what happens when a transition takes place.

Detailed knowledge of the paraelectric phase provides the essential basis for microscopic modelling involved in attempting to answer the questions how and why the transition occurs (see Section I.5). The phase transitions involve a change in thermodynamic equilibrium state; if how this happens is to be understood, the changes in equilibrium crystal structure have to be known.

The main difficulties of the structural approach to ferroelectric transitions stem from the smallness of the displacements, giving rise to the pseudosymmetry, and from the desire to distinguish static disorder from pronounced thermal motion wherever possible.

I.4 Classification of Ferroelectrics

There is no one classification of ferroelectrics. The most important criteria in relation to this thesis are:

i) One group is hydrogen bonded; these are usually mechanically soft, water soluble and have a low melting point. The other group includes oxygen octahedra materials, usually ionic mechanically hard of a high melting point, water-insoluble and have a spontaneous polarization an order of magnitude higher than that of the hydrogen bonded ferroelectrics. Both DTGS and KDP, DKDP are hydrogen bonded ferroelectrics.

ii) In one group the ferroelectric transition involves the ordering of structure elements that were disordered in the paraelectric phase, e.g. hydrogen atoms on asymmetric hydrogen bonds. In the other group the transition is purely displacive. As touched upon in Section I.3, this distinction is not always clear and indeed one aspect of this thesis is the clarification of whether the assumption of disorder in paraelectric KDP and DKDP holds good.

iii) It is possible clearly to put all ferroelectrics that have a paraelectric phase in one of two groups: those with centrosymmetric paraelectric phase and those with non-centrosymmetric (piezoelectric in general, see Section I.2) paraelectric phase. DTGS and KDP are examples of these two groups respectively (other examples appear in Section I.3).

The importance of the last two classifications lies in the difference in the dynamical models needed to explain their properties (see Section I.5).

I.5 Ferroelectricity and Lattice Dynamics

Theories of ferroelectricity can be divided into phenomenological theories and model theories.

Phenomenological theories treat the crystal as a thermodynamic system in terms of entropy, temperature, strain tensor, stress tensor, polarization vector and electric field vector. The transition is examined in terms of the free energy usually with temperature, stress and polarization as independent variables and useful relationships are derived between the various macroscopic properties of the crystal (Devonshire, 1954). Phenomenological theories are independent of any

particular microscopic model and do not establish relationship between dielectric properties, atomic displacements and lattice vibrations.

Model theories attempt to derive the macroscopic properties of crystals in terms of a microscopic model of their structure and interatomic forces. Model theories pre 1960 have generally been restricted in their application and have often applied only to one material.

Slater's theory of KDP (Slater, 1941), for example, based on the structural study of West (West, 1930), although quite successful as applied to KDP, does not explain why DKDP has a much higher transition temperature.

A more general approach and a major break-through in the investigation of at least ferroelectric phase transitions was presented by Cochran (1960, 1961). Cochran utilized the significance of the implication to ferroelectric phase transitions born in the Lyddane-Sachs-Teller relationship. The Lyddane-Sachs-Teller formula (Lyddane, Sachs and Teller, 1941) for a diatomic diagonally cubic crystal:

$$\epsilon_0/\epsilon_\infty = (\omega_{LO}/\omega_{TO})^2 \quad \text{I.1}$$

(where ϵ_0 is the static (clamped) dielectric constant and ϵ_∞ is the high frequency dielectric constant. ω_{LO} and ω_{TO} are the frequencies of the longitudinal and transverse optic modes (often, LO and TO modes) of wave vector $\underline{q} = \text{zero}$).... implies that since ϵ_0 , following Curie-Weiss law (Section I.3), goes as $(T - T_c)^{-1}$ as the transition is approached and diverges at T_c , ω_{TO} should tend to zero as T_c is approached, in fact ω_{TO}^2 should go as $(T - T_c)$. Denoting $\tilde{\omega}_f$ as the quasi harmonic frequency of the ferroelectric mode

the theory predicts $\tilde{\omega}_f^2 \propto (T - T_c)$.

The condition for crystal stability against all small deformations is that all frequencies of the normal modes should be real. At $\omega = 0$ the displacements of the atoms are no longer oscillatory but static, so the crystal structure becomes unstable as $\omega \rightarrow$ zero.

By extending the Lyddane-Sachs-Teller formula to crystals with any number of atoms in the primitive unit cell and the idea to more general symmetries, Cochran (1961) showed that ferroelectric structural phase transitions could be treated as a problem in lattice dynamics, in particular that the instability of the crystal structure is associated with a particular transverse optic mode, of wave vector zero, whose frequency approaches zero as the transition temperature is approached.

He identifies the structural changes that occur at a transition with "frozen in" displacements of the atoms due to the TO mode. That is the atomic displacements at the transition are identified with the eigenvectors of the transverse optic mode against which the structure has become unstable.

This theory found immediate support in experiments on strontium titanate SrTiO_3 (Cowley, 1962) where a mode of the characteristics of the ferroelectric mode was found (referred to generally as a soft mode). Subsequently the theory has led to a much better understanding of the phase transitions in perovskites where, in general, a ferroelectric phase transition is associated with a soft zone centre mode, while an antiferroelectric phase transition is associated with a soft zone boundary mode. There are other features of the phase

transitions in perovskites that await further investigation (Riste, Samuelsen and Otnes, 1971).

The extension of the original theory to include order-disorder type ferroelectrics (Sections I.4 and I.3) has found support, for example, in experiments on KDP (Kaminow and Damen, 1968) and in DKDP (Skalyo, Frazer and Shirane, 1970). The two last examples are of particular relevance to this thesis, see Chapter IV.

In order to show the present day connection between structural work, as is presented in this thesis, and lattice dynamics we, following Cochran 1969, present some results of lattice dynamics, in particular the differential coherent, inelastic neutron scattering cross-section.

The lattice dynamical treatment of the various materials under investigation can be divided into 3 main systems which can be described in terms of: 1) The ordinary phonon-coordinates Hamiltonian, BaTiO_3 , 2) a Tunnelling Hamiltonian or a mixed phonon-tunnelling Hamiltonian, KDP and 3) an Ising system as a limiting case of the tunnelling model, NaNO_2 .

In the quasi-harmonic approximation where each mode is behaving as an independent damped oscillator but with frequency and damping constant, $\tilde{\Gamma}$, depending on temperature, the one phonon neutron scattering cross section is proportional to

$$S_i(\underline{K}\omega) = 2NE(\omega) \sum_j \left| F_j(\underline{K}) \right|^2 \frac{2\tilde{\Gamma}_j(\underline{q})}{(\tilde{\omega}_j^2(\underline{q}) - \omega^2)^2 + 4\tilde{\Gamma}_j^2(\underline{q})\omega^2} \quad \text{I.2}$$

where $E(\omega) = \left(1 - \exp(-\beta \hbar \omega) \right)^{-1} \hbar \omega$ with $\beta = 1/k_B T$
this tends to $k_B T$ as

$\omega\hbar/k_B T \ll 1$. $\tilde{\omega}_j(\underline{q})$ is the quasi-harmonic frequency of a particular wave vector \underline{q} and of branch j .

$F_j(\underline{K})$ is the dynamic structure factor:

$$F_j(\underline{K}) = \sum_{\chi} b_{\chi} \exp(-W_{\chi}(\underline{K})) \underline{K} \cdot \underline{e}_{j\chi}(\underline{q}) \exp(i \underline{K}_h \cdot \underline{r}_{\chi}) \quad \text{I.3}$$

where b_{χ} is the scattering length, $\exp(-W_{\chi}(\underline{K}))$ is the Debye-Waller factor and $\underline{e}_{j\chi}(\underline{q})$ is the eigenvector of the χ th atom; \underline{K}_h is a reciprocal lattice vector ($\underline{K} + \underline{q} = \underline{K}_h$) and \underline{r}_{χ} is the atomic position. The sum is taken over all atoms in the primitive unit cell.

Excitations other than phonons are possible in disordered materials. In particular a H atom can be disordered between two sites separated by an energy barrier, (2Ω , the ground state separation of the two levels depends on wave function overlap), through which the H atoms could tunnel. If there were no H - H or H-other atoms interactions, the excitations would have frequency

$$\Omega(\underline{q}) = 2\Omega / \hbar \quad \text{I.4}$$

independent of \underline{q} . Allowing H-H interactions and treating the system in terms of fictitious spin $\frac{1}{2}$ we have:

$$\hbar^2 \Omega^2(\underline{q}) = 4\Omega^2 \frac{T - T_c(\underline{q})}{T} \quad \text{I.5}$$

Hoping by analogy with equation I.2 to take anharmonic coupling to phonons into account, the neutron scattering cross-section is proportional to:

$$S(\underline{K}\omega) = N |\widetilde{f}(\underline{K})|^2 \frac{8/\hbar^2 \Omega \tanh(\beta\Omega) E(\omega)}{(\Omega^2(\underline{q}) - \omega^2)^2 + 4\omega^2 \Gamma^2(\underline{q})} \quad \text{I.6}$$

where $\beta = 1/(K_B T)$ and $\Gamma(\underline{q})$ is an experimental parameter. The structure factor for the tunnelling mode $\widetilde{f}(\underline{K})$ is

$$\widetilde{f}(\underline{K}) = \sum_{\underline{x}} b_{\underline{x}} \exp(-W_{\underline{x}}(\underline{K})) \sin(\underline{K} \cdot \underline{U}_{\underline{x}}) \exp(i \underline{K}_h \cdot \underline{r}_{\underline{x}}) \quad \text{I.7}$$

where $2\underline{U}_{\underline{x}}$ is the site separation of the tunnelling atoms.

Equation I.7 is to be compared with equation I.3, the dynamic structure factor for the phonon model.

In a mixed tunnelling and phonon model interaction of H with other atoms is taken into account. It turns out that the mixed mode can be approximately regarded as a pure tunnelling mode with all the atoms tunnelling, the respective $\underline{U}_{\underline{x}}$ being the difference in equilibrium positions of the atoms in the para and ferroelectric phases.

The Ising model can be looked upon as a limiting case of the tunnelling model when the term involving the kinetic energy of the tunnelling protons has been eliminated from the conventional tunnelling Hamiltonian. This leads to the simple result that

$$S(\underline{K}) = N |\widetilde{f}(\underline{K})|^2 T/(T - T_c(\underline{q})) \quad \text{I.8}$$

This is to be compared with equation I.6.

Considering now the neutron scattering cross-section of the soft mode integrated over the range of frequencies of the soft mode

$$S(\underline{K}) = \int S(\underline{K}\omega) d\omega / (2\pi) = N K_B T |F_{j_1}(\underline{K})|^2 / (\tilde{\omega}^2(\underline{q}_1 j_1)) \quad \text{I.9}$$

where $S(\underline{K}\omega)$ and $F_j(\underline{K})$ are from equations I.2 and I.3. q_1 and j_1 denote q and j of the soft mode. Since $\tilde{\omega}^2$ of the soft mode is expected to vary as $(T - T_c)$ the form of equations I.9 and I.8 is the same and the intensity should diverge as T_c is approached. Equations I.8 and I.9 then differ, apart from a factor of k_B , only in the different forms of the inelastic structure factors $\mathcal{F}(\underline{K})$ and $F(\underline{K})$, see equations I.7 and I.3.

Equations I.7 and I.3 require, if the dynamic structure factors are to be evaluated, in the first instance knowledge of the detailed crystal structure; in particular, the positional and thermal parameters of all the atoms in the unit cell; thus making clear the connection between dynamical and structural studies.

Before further connecting structural studies with dynamical studies we mention some practical and theoretical aspects of the dynamical study, in particular the difficulty in extracting the soft mode intensity when the mode is heavily damped and also the role of anharmonicity near the phase transition.

The scattering from a soft mode is indistinguishable from other contributions to critical scattering so far as temperature dependence of the intensity is concerned. The identification of a soft mode becomes the more difficult the more damped the mode is. The scattered intensity of an overdamped mode will peak at $\omega = 0$ so that no definable phonon peaks are observed.

Cochran's theory involves the harmonic approximation and the quasi-harmonic approximation involves no further mode-mode interactions. When the paraelectric phase is non-

centrosymmetric (and piezoelectric) even in the harmonic approximation the ferroelectric mode interacts with the transverse acoustic modes (of low q).

Anharmonic coupling of the ferroelectric mode to other modes, lowering their frequencies, gives rise to further contributions to the critical scattering.

In the harmonic approximation we have the energy of a mode (Cochran, 1973)

$$\frac{1}{2} \omega_j^2(q) |B_j(q)|^2 = \tilde{E}(\omega_j(q)) \quad \text{I.10}$$

where $B_j(q)$ is the amplitude of the mode, $\tilde{E}(\omega)$ tends to $k_B T$ as $\hbar\omega/k_B T \ll 1$ (). For the soft mode therefore as $\omega \rightarrow 0$ the amplitude can be arbitrarily large. The anharmonic character of the crystal limits the amplitude.

Also the eigenvectors will no longer be amplitude independent and will depend on anharmonicity to some extent.

Assuming that anharmonic effects other than those taken into account in the quasi-harmonic approximation will not invalidate equations I.2, I.6, I.3 and I.7, we are in a position to connect the work presented in this thesis with the dynamical approach outlined earlier in this section.

A conventional crystal structure determination (Section I.6) of the para and ferroelectric phases of a material gives, if carried out using neutrons, the time averaged mean relative positions of the atomic nuclei and their mean square thermal amplitudes, in both phases.

From these two structures the net relative atomic displacements associated with the transition are obtained. We

wish to compare these with the eigenvectors of the ferroelectric or soft mode.

Given that a soft mode was found in the phonon spectrum of a material, it is possible (with neutron spectroscopy) to determine its eigenvectors at a given temperature; this is more difficult, the more damped the mode is. Equations I.2 and I.6 show how the moduli of the dynamic structure factors, equations I.3 and I.7 respectively, are related to the neutron scattering cross-sections. We can thus obtain for a particular $\omega_j(\underline{q})$ a set of dynamic structure factors varying \underline{K} ($\omega_j \underline{q}$ fixed) which, knowing the structure of the paraelectric phase, give different projections of the eigenvectors which then can be obtained by fitting the set of the dynamic structure factors, varying the eigenvectors in much the same way as fitting is carried out in conventional crystallography (see Chapter II).

The anisotropic Debye-Waller factors obtained as a result of a successful crystal structure determination represent the mean square amplitudes of the individual atoms (see Chapter II).

If, in a ferroelectric as the temperature approaches T_c , a large section of a particular energy surface, representing modes of vibrations, went soft there should be a change in the mean square amplitude of some of the atoms. In principle, therefore, an accurate determination of anisotropic Debye-Waller factors in the paraelectric phase should show the corresponding change between these temperatures. However, since the modes relatively unaffected by temperature, as T_c is approached, greatly outnumber the modes that soften, the

effect on the mean square amplitude is expected to be small. This aspect of structural work on ferroelectrics is not gone into in any detail in this thesis.

The question, mentioned earlier (see Section I.3), whether or not one or more atoms are disordered between two (or more) possible sites in the paraelectric phase is a question of how the dynamics of the material should be modelled. The importance of this question and any other question about finer details of the crystal structure of the paraelectric phase of a ferroelectric is, in the light of the dynamical approach, determined by the accuracy of the relevant dynamical experiment.

We see from equations I.3 and I.7, the expressions for the dynamic structure factors for the phonon and the tunneling models respectively, that these expressions are relatively insensitive to minor details of the crystal structure for low values of \underline{K} ($\approx \underline{K}_h$ for a soft ferroelectric mode) (see Chapter IV). For larger values of \underline{K} and for accurate determination of the displacements associated with the transition, however, the finer structural details become of central importance. This thesis is concerned with obtaining and assessing the significance of these structural details in hydrogen bonded ferroelectrics.

I.6 Problems of Structural Studies of Ferroelectrics

The requirement that a ferroelectric must have switchable polarization implies a delicate balance between the possible configurations of the structure in the ferroelectric phase. These configurations are derived from a structure of higher

symmetry in the paraelectric phase and are pseudosymmetric variations of that structure through small relative atomic displacements and/or ordering of some structure elements.

It is the pseudosymmetry, the smallness of the relative atomic displacements, and the difficulty in distinguishing disorder from pronounced thermal motion which gives rise to the problems of structural studies of ferroelectrics as compared with the general problems of conventional crystallography.

The two main methods of structural investigation are the methods of X-ray and neutron diffraction.

The X-ray method, in principle, yields the time averaged electron density in the unit cell. Maxima in the electron density are identified with the positions of the nuclei which is not a good approximation for light atoms, hydrogen atoms in particular. The X-ray method is capable of giving the absolute configuration of a polar structure (Jona and Shirane, 1962, p. 379).

The neutron method yields the time averaged neutron scattering density in the unit cell. Maxima (in some cases minima) of the scattering density are identified with the positions of the nuclei.

For X-rays the scattering off the various types of atoms is very different, being the higher the heavier the atom (roughly goes as the number of electrons), whereas for neutrons the scattering lengths vary in relative magnitude mostly within a factor of 4. This makes the neutron method superior in studying hydrogen bonded ferroelectrics since light atoms can be readily located in the neighbourhood of heavy ones. The small displacements and the need to distinguish between

disorder and pronounced thermal motion call for data capable of giving high resolution which in turn (by Bragg's law) calls for accurate determination of high angle data. For X-rays the atomic scattering factor (form factor) is scattering angle dependent, with decreasing scattering for increasing scattering angle, this decrease being more pronounced the lighter the atom.

For neutrons, on the other hand, the scattering lengths can be taken to be constant with scattering angle thus making the collection of high angle data, capable of good resolution, relatively easier with neutrons. Yet another fact is that during refinement (Chapter II) parameter correlation is likely to be different for X-ray and neutron data; this being less for neutrons in the particular case of BaTiO_3 (see below).

A classic example of a structural study of a ferroelectric is to be found in the long history of attempts to solve the crystal structure of tetragonal BaTiO_3 (Frazer, 1971). This example is particularly striking because of the apparent simplicity of the structure as compared with many of the complex structures considered as solved (BaTiO_3 has five atoms in the unit cell with 3 positional and 9 anisotropic temperature parameters to determine).

The structural problem of BaTiO_3 illustrates: 1) the difficulty in an X-ray determination to locate light atoms in the neighbourhood of much heavier ones (illustration in Jona and Shirane, 1962, p. 376), 2) the ambiguity in parameter determination due to strong parameter interactions in a pseudosymmetric structure, 3) that the problem of parameter interactions is not as serious in a neutron study

as it is with X-rays in this case and, at the same time, that the neutron method is not immune to these difficulties, 4) the value of giving some consideration to X-ray results in a neutron study, and 5) how the question of partially disordered model would introduce, at present, an indeterminate problem in a conventional refinement of tetragonal BaTiO_3 .

What particularly favours using neutrons when concerned with hydrogen bonded ferroelectrics is the difficulties in an X-ray study to assess the structural parameters of hydrogen atoms. The problem of radiation damage of X-rays as is, for example, observed by Keve et al. (Keve, 1973) in TGS may cause the structure to be indeterminable in details by the X-ray method. One drawback of the neutron method is that extinction (secondary, see Section II.1.a) is more likely to be a problem due to the much larger crystals needed in a neutron experiment as a consequence of the lower flux and the much lower scattering cross-section.

I.7 Outline of the Thesis

This thesis is concerned with structural studies of hydrogen bonded ferroelectrics, in particular the paraelectric structures of DKDP, KDP and that of DTGS. In Chapter II we describe the methods of study with a detailed description of the method of least squares, as used in application to problems (DKDP and KDP) where we desire to assess the validity of various proposed models of the structure. In describing the various hypotheses and the associated constrained least squares refinement, we try to bring to light

all assumptions made on the way so as to enable the reader to make some assessment of the methods himself.

We also try to show that the small differences in the usually delicately balanced structures of ferroelectrics make them a particularly suitable material for application of statistical testing of the various hypotheses then involving structural models with only small differences.

In Chapter III we describe sample preparation with some emphasis on crystal growing of DTGS.

Chapter IV describes the refinement of the room temperature crystal structures of DKDP and KDP with assessment of the validity of various structural models describing the finer structural details (application of ideas described in Chapter II). Chapter IV also describes assessment of various structural features of DKDP and KDP 5°K above their respective transition temperatures but due to experimental limitations resolution obtainable with the corresponding data sets does not result in quite the same detailed description as does the room temperature study.

Chapter V is an account of an attempt to solve the detailed crystal structure of paraelectric DTGS at 80°C , included as an illustrative example of some of the problems met in structural studies of ferroelectrics.

Chapter VI sums up the conclusions to be drawn from the work.

CHAPTER II

METHODS OF STUDY

II.1 Neutron Diffraction

II.1.a Structure factors

In its simplest form the structure factor, proportional to the scattered amplitude per unit cell, is expressed in terms of a reciprocal lattice vector, the relative atomic positions (within one unit cell) and scattering lengths.

$$\hat{f}(\underline{h}) = \sum_{i=1}^n b_i \exp(2\pi i \underline{H} \cdot \underline{x}_i) \quad \text{II.1}$$

where $\underline{h} = (h, k, \ell)$ the Miller indices, $\underline{H} = (\underline{a}^* h + \underline{b}^* k + \underline{c}^* \ell)$ = a reciprocal lattice vector*, $\underline{x}_i = (x_i, y_i, z_i)$ the coordinates of the i^{th} atom with respect to some origin and b_i the scattering length of the i^{th} atom. The sum is taken over all n atoms in one unit cell.

Account is taken of the thermal vibrations of the atoms about their mean position by expanding their potential in a Taylor series and terminating wherever the limit of information the data contains (given errors and resolution) is reached.

Terminating at second order terms is equivalent to assuming strictly harmonic potential wells, representing the atomic thermal distributions as ellipsoids such that:

$$\hat{f}(\underline{h}) = \sum_{i=1}^n b_i \exp(2\pi i \underline{H} \cdot \underline{x}_i) \exp(-\underline{H} B_i \underline{H}') \quad \text{II.2}$$

where B_i is a 3×3 matrix with elements $\beta_{rs} = \beta_{sr}$. B_i , the thermal matrix of the i^{th} atom, is related to the matrix of mean square displacements, U_i , by $B_i = 2\pi^2 U_i$.

*omitting the factor of 2π

Only harmonic thermal motion is considered in the analysis presented in this thesis.

In Section I.6 a brief comparison of the neutron and the X-ray diffraction methods was made. For a comprehensive comparison of these methods see Arndt and Willis, 1966. As mentioned in Section I.6 one drawback of the neutron method is the much lower flux as compared with X-rays (3 to 4 orders of magnitude; see Arndt and Willis, 1966, p. 312); this necessitates the use of larger crystals with typically 10 times the path lengths of samples used for X-ray diffraction. Also the cross-section of neutron scattering is much lower for neutrons than for X-rays. Although linear absorption is, in general, much less of a problem with neutrons than X-rays, the much increased path lengths introduce the more serious problem of extinction.

Extinction is the effect of attenuation of the incident beam as it passes through the crystal by non absorbing processes and can be divided into two types.

Primary extinction is the attenuation of the incident beam in a perfect crystal due to the large fraction of the beam being (Bragg) scattered by each set of planes. The intensity of the incident beam is further reduced because the twice reflected beam is π out of phase with the incident beam and interferes deconstructively.

In real crystals, due to dislocations, impurities and other imperfections, regions in the crystal are misaligned with respect to one another (without any well defined boundaries between them, necessarily) much reducing the effect of primary extinction.

So far as neutron diffraction is concerned, in general, due to the relatively (as compared with X-rays) low scattering cross-section, primary extinction is not usually as serious as secondary extinction, see below, no correction was made for primary extinction in any of the present work.

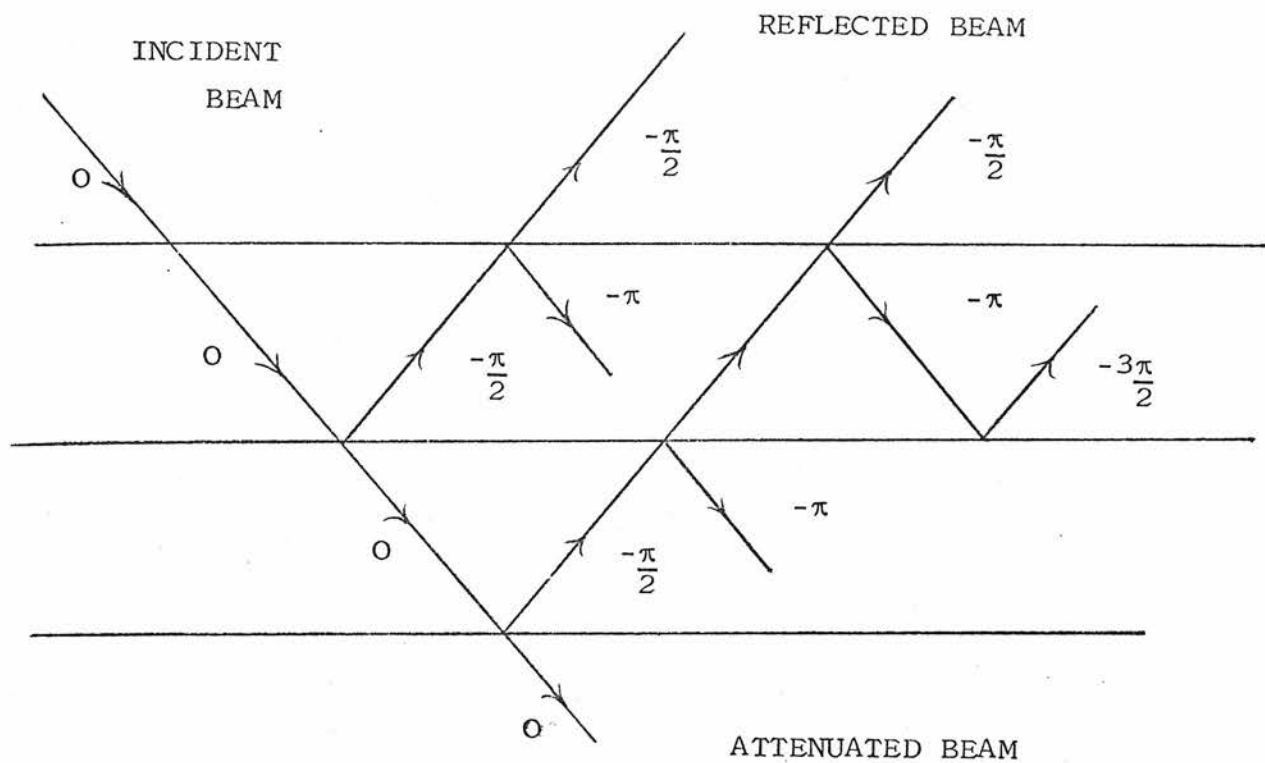
Secondary extinction is the effect of attenuation of the incident beam by regions in the crystal oriented to give a Bragg reflection reducing the incident beam before it is being Bragg scattered off some other similar regions (not adjacent) in the crystal which also happen to satisfy Bragg's condition. (The crystal can be looked upon as effectively being built up of slightly misaligned "mosaic blocks" of the order of 1-2 thousand unit cells across having a mean angular deviation of a few hundreds of a degree).

Fig. II.1(a) shows how the incident beam is reflected off a set of crystal planes with the phase of each reflected beam, relative to that of the incident beam, marked on the diagram. There is a phase lag of $\pi/2$ on each reflection so that the twice reflected beam aids attenuation of the incident beam (for the same reason the three times reflected beam will serve to decrease the reflected beam). Fig. II.1(b) illustrates how secondary extinction arises; attenuation by Bragg reflection out of the incident beam takes place by some sections of the crystal all simultaneously satisfying Bragg's Law.

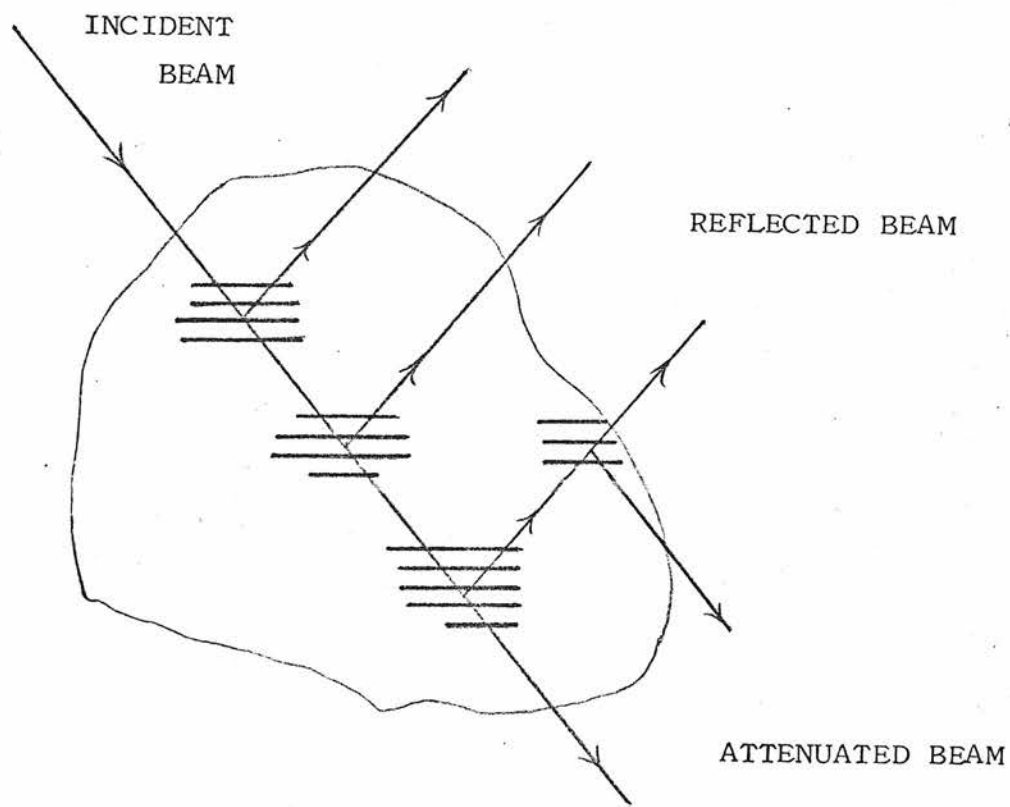
The greater the reflecting power of the scattering planes of the crystal, the greater will be the effect of extinction for that reflection.

The effect of secondary extinction is usually taken into

a)



b)



The effect of extinction a) Primary and b) Secondary

Fig. II.1.

account by a correction term in the structure factor expression (equation II.2) in least squares analysis, see Section II.2. The expression used in the analysis of DKDP and KDP was that of Cooper and Rouse, 1970, for a spherical crystal which takes into account angular dependence of the effect and claims, based on experiments on CaF_2 and on SrF_2 , validity of the correction up to extinction of 80% of the intensity. The expression for this correction appears in Appendix II.

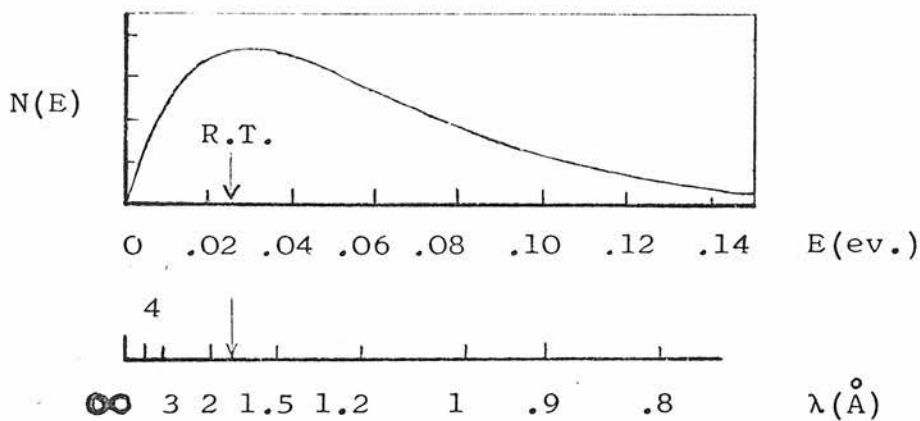
Extinction, its extent and degree of isotropy is clearly dependent on the condition of sample preparation; in particular, extinction must depend on the crystal growing procedure and the subsequent mechanical and thermal treatment of the sample. Implications of such effects particular to ferroelectrics grown in their ferroelectric phase, are discussed in Section II.4.

II.1.b Neutron instruments

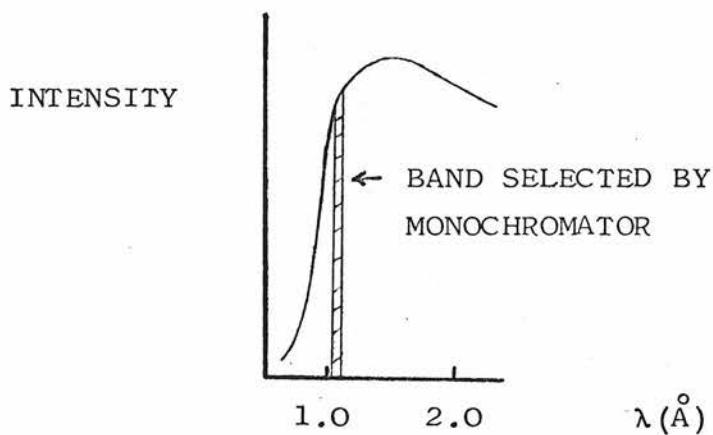
The neutrons from a reactor come to thermal equilibrium with the moderator when $\frac{1}{2}m\overline{v^2} = \frac{3}{2}k_B T$ and have a Maxwellian energy spectrum.

Fig. II.2.(a) shows a typical Maxwellian spectrum from a reactor, after Brockhouse, 1966, p. 111, where $N(E)$, the energy distribution of the neutrons, is shown with an auxiliary wavelength scale.

A narrow band of neutrons is selected from the spectrum by Bragg reflection of a monochromating crystal; this is illustrated in Fig. II.2.(b) (after Arndt and Willis, 1966, p. 4), showing an intensity distribution of neutrons with wavelength and how a narrow band is selected by the



- a) The form of a typical Maxwellian spectrum from a reactor; with auxiliary wavelength scale ($k_B T = 0.03 \text{ eV}$). (After Brockhouse, 1966, p.111)



- b) The form of a typical Intensity curve for slow neutrons from a reactor; showing a band of wavelengths selected by a monochromator (Copied from fig.1 of Arndt and Willis, 1966, p.4)

Fig. II.2.

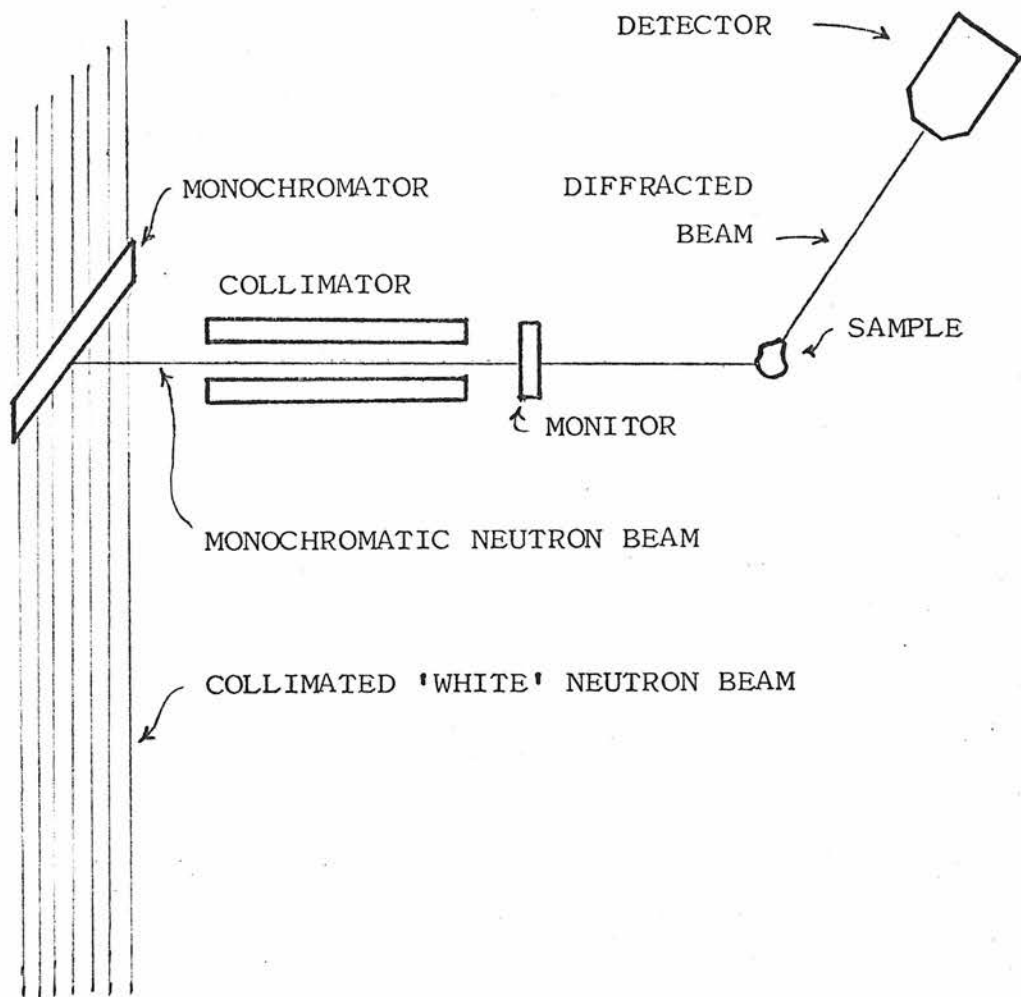
monochromating crystal.

Fig. II.3 shows a neutron diffraction assembly. The collimated "white" beam of neutrons from the moderator are monochromized by a single crystal (Bragg reflection). The resulting monochromatic beam is collimated to take care of spread due to insufficient collimation of the beam from the moderator. In order to take into account fluctuations in the reactor power a low efficiency fission chamber is used to monitor the beam before the sample.

After being Bragg reflected off the sample the neutron beam is detected by a BF_3 counter; counting for a predetermined number of monitor counts. The distance between sample and counter or monitor is about 0.5m; other distances in Fig. II.3 are arbitrary. Due to incoherent, inelastic and fast neutron scattering the Bragg peak is superimposed on background scattering that has to be estimated and subtracted; see Section II.1.c.

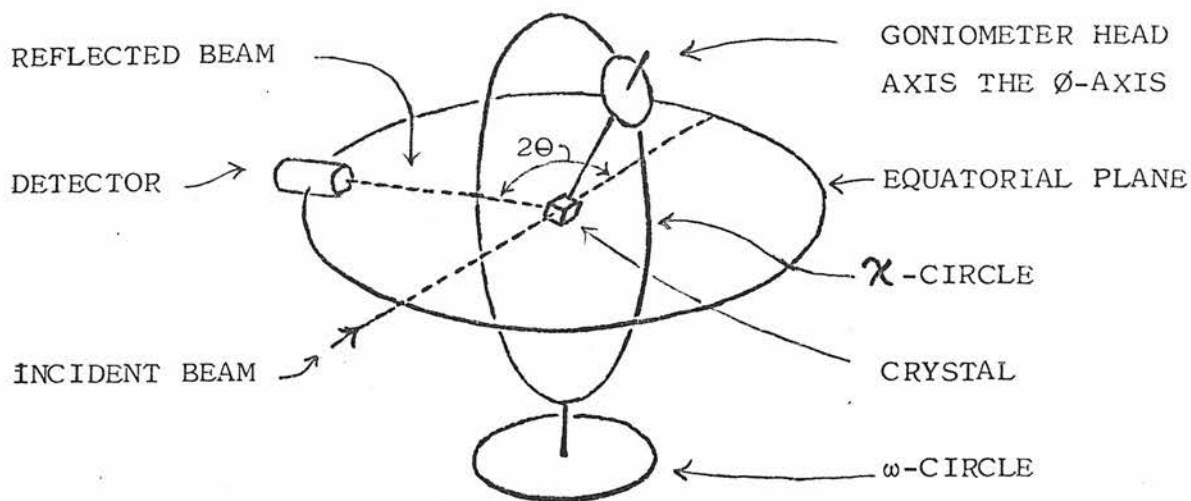
The sample is located at the centre of a diffractometer. The diffractometer is designed to allow the sample to be rotated (about the sample centre) to align any vector within the sample parallel to any direction specified (in the laboratory frame). The arm supporting the counter is a part of the diffractometer but its possible movements are in general more restricted due to its bulk, see below.

The centre of a diffractometer is defined as the point of intersection of all axes of rotation. Fig. II.4.(a) (after Arndt and Willis, 1966, p. 8) shows the diffractometer in its normal beam equatorial geometry. The counter is restricted to move in the equatorial plane, while the sample can be rotated to any orientation by the operation of the ϕ , χ and ω rotations.

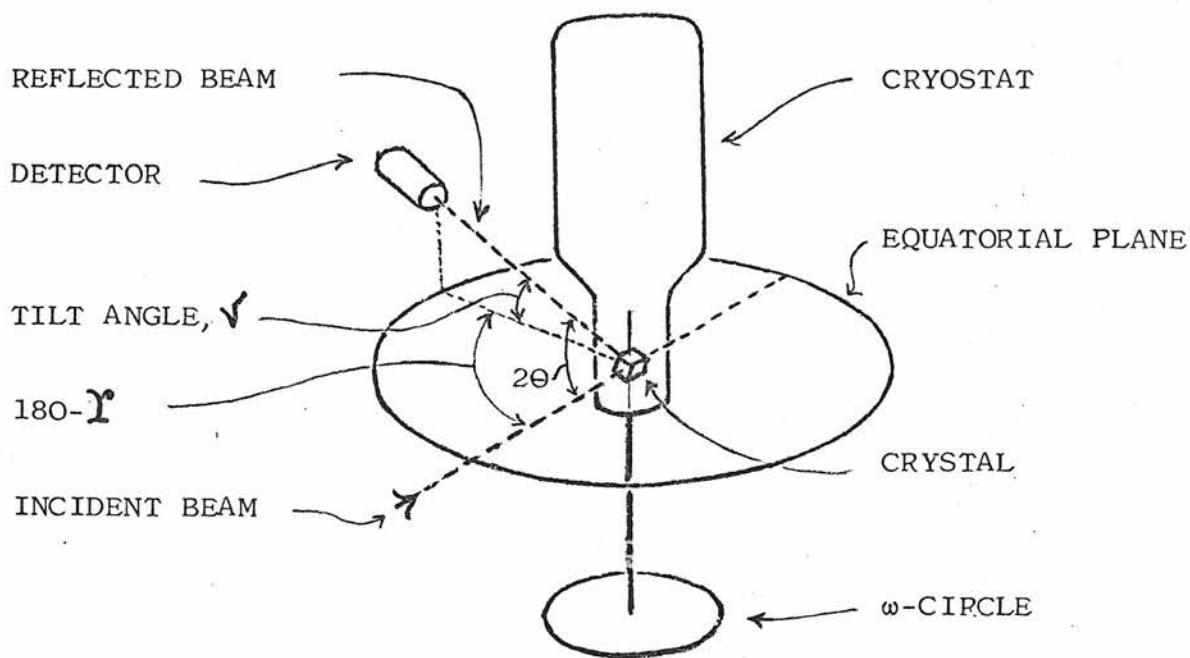


A schematic diagram of a neutron diffraction assembly.

Fig. II.3.



a) Normal beam equatorial geometry of a 4-circle diffractometer.
(Copied from fig.3 of Arndt and Willis, 1966, p.8)



b) Normal beam tilting counter geometry of a 2-circle diffractometer.

Fig. II.4.

The crystal is mounted on a goniometer head attached to the ϕ axis. The ϕ assembly as a whole is rotated around the vertical χ circle, which itself is rotated about the vertical axis ω .

Limitations to the possible Bragg reflections, at a given wavelength, are firstly the limited θ value, possible due to the bulk of the counter running into the reactor shielding, or blocking the incident beam (also for very small θ angles the incident beam runs directly into the counter) and secondly, a few reflections might be inaccessible due to the assembly getting into the incident or reflected beams.

The normal beam equatorial geometry was employed during the data collection at room temperature (DKDP, KDP and DTGS) and at 80°C (DTGS).

For the low temperature work (DKDP and KDP) a cryostat was needed which meant, due to the bulk of the cryostat, that a different setup had to be used; see below. Fig. II.4 (b) shows a diffractometer deprived of its χ assembly due to the use of a cryostat. For this setup, however, a tilting counter is employed which can also be rotated in the equatorial plane. The cryostat containing the sample can be rotated about the vertical ω axis.

Due to the finite collimation of the beam before the monochromator there is a focusing effect to be considered. Rewriting Bragg's law we have:

$$\underline{k}_0 \cdot \underline{d}_0 = \pi \quad \text{II.3}$$

differentiating with respect to \underline{k}_0 (\underline{d}_0 is a constant ignoring any imperfections of the monochromator), we have:

$$\underline{\partial k}_0 \cdot \underline{d}_0 = 0 \quad \text{II.4}$$

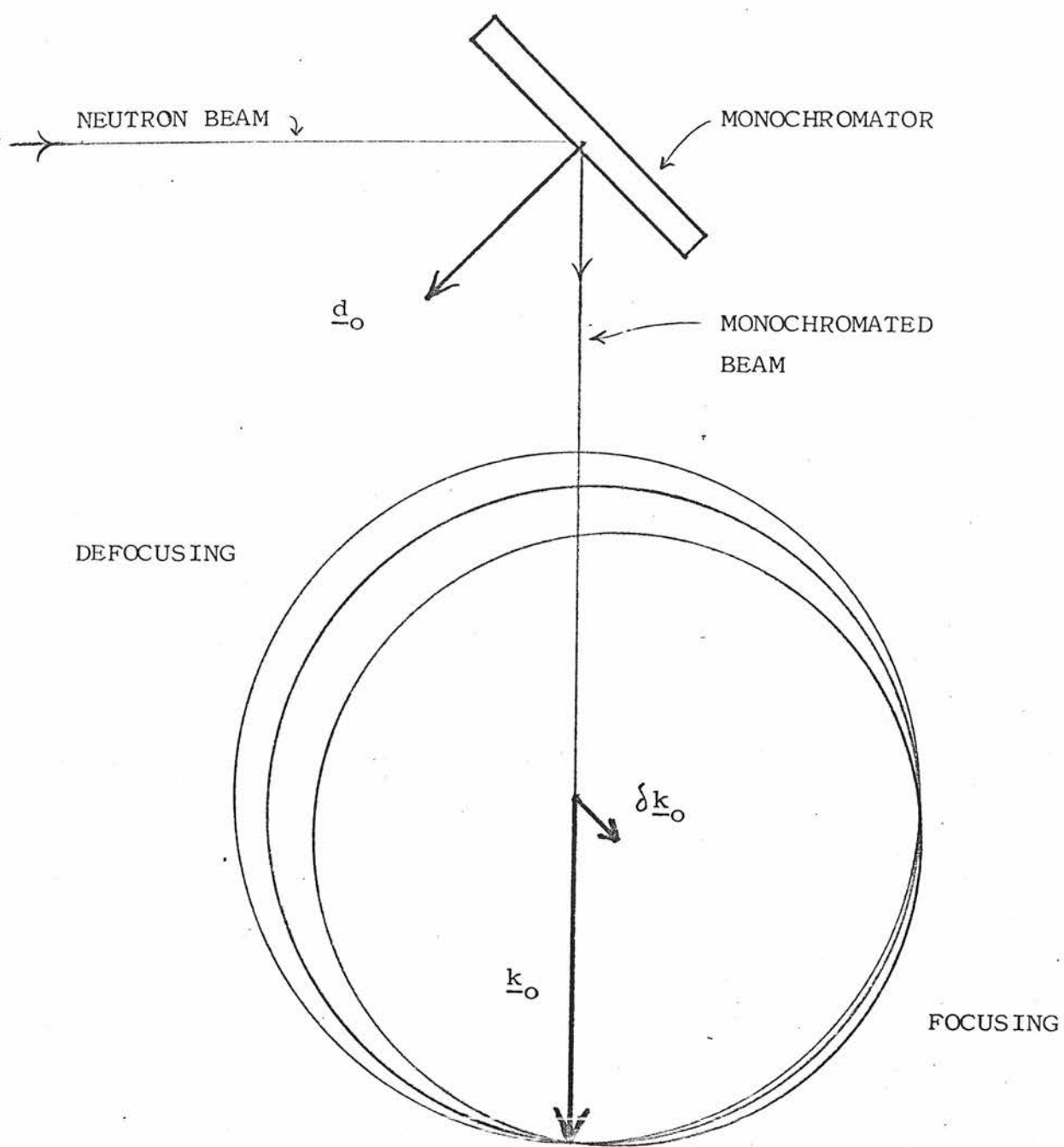
therefore $\underline{\partial k}_0$ must be perpendicular to \underline{d}_0 . This is illustrated in Fig. II.5 for a 90° take-off angle and by constructing the Ewald spheres for some possible \underline{k} values in reciprocal space, we see that the focusing occurs when the diffracted beam is parallel to the white beam before the monochromator. In practice the situation is more complicated due to the finite spread in \underline{d}_0 of the monochromator, giving rise to a focusing ellipsoid in reciprocal space (see, for example, Peckham, Saunderson and Sharp, 1967).

Due to the focusing effect the width of the Bragg peaks as observed will be relatively small near the focusing position of the relevant instrument and care must be taken to ensure that sufficient number of measurements are made in the angular range of these Bragg peaks, see Section II.1.c below.

The diffractometer is automatic and is controlled by a PDP8 computer (or by a paper tape). Each shaft can be stepped in 0.01° steps except the detector shaft, which can be stepped in 0.02° steps. Counting for any particular setting is carried out for a specified number of monitor counts. The ω and counter shafts (or 2θ shaft) are often coupled together to move in the ratio 1:2 ($\omega - 2\theta$ scans).

The data is collected onto a magnetic tape together with other information relevant to the experimental setup.

The instruments used were diffractometers of the reactors Pluto and Dido at the Atomic Energy Research Establishment, Harwell. In Pluto the diffractometers used



Focusing effect due to finite collimation of the neutron beam.

Fig. II.5.

were, at channels I and II, the Hilger and Watts automatic diffractometers, Mk. II, and a modified version thereof on Channel I to take a tilting counter. In Dido the instrument used was a Mk. VI diffractometer on channel II designed for low temperature work employing a tilting counter. The focusing positions on these instruments were for $2\theta_f \approx 90, 60$ and 45 respectively.

II.1.c Observations

In all cases the profile of each Bragg reflection was obtained employing the moving crystal-moving detector method (Section II.1.b); the $\omega/2\theta$ scan type. The reflections were scanned in steps through the Bragg angle, counting at each step. The integrated intensity was obtained by summing the total number of counts in the scan and subtracting from it an estimated background level.

The criteria for deciding a particular scan involve focusing, accuracy, efficiency and instrumental setup. The step width must be small enough to allow the profile of the Bragg peaks to be obtained over the whole range of Bragg angles at which measurements are made in the experiment; in particular at and near the focusing position of the relevant instrument. The accuracy depends on the number of counts in the scan since the estimated standard deviation of a statistical quantity, N , say, is the square root of that quantity. However the accuracy of a given structure factor can only beneficially be increased by increasing the number of monitor counts per step until the standard deviation, as

obtained from the counting statistics, is less than the difference obtained between symmetry equivalent structure factors. In the work presented in this thesis the criterion used here was that if symmetry equivalent structure factors agreed within 3 or 4 standard deviations (equations II.11 below) a sufficiently large number of monitor counts had been specified.

The accuracy also depends on the applicability of the background correction. In the room temperature work a background level (the average background over the angular range of the peak scan) was estimated for each reflection from the tails of the peak scan (the levelled off sections at either end of the peak scan, that is). When a heater or a cryostat is used the possibility of a powder peak from the cryostat, coinciding with some of the scans, has to be considered. In order to eliminate errors due to powder peaks, or uneven background, the scan type $\omega/2\theta$ was carried out and then the background was obtained by offsetting the crystal by one or two degrees on ω and repeating the same scan. It is important that the background scan should be carried out in an identical way to the peak scan (but with ω offset) since this is the only way to ensure that the powder peaks are detected in the same detail in both scans; thus permitting a closer approximation of their elimination. The reason for wanting to decrease the number of steps in a given scan of a given total number of monitor counts by increasing the step width is that the time spent setting the diffractometer can be an appreciable fraction of the total time spent on the scan.

Fig. II.6 shows how the integrated intensity for two

Bragg reflections compare with the area under a free hand smooth curve through the points. Fig. II.6 shows part of scans from a preliminary study on DKDP, on Pluto Channel I Mk. II take-off angle 90° , the step width is 0.04° in both cases. The Bragg angle is 66° for the higher peak and 47° for the lower one which is near θ -focus. It is clear from Fig. II.6 that the step width used is sufficiently small since even near the focusing position, by omitting every second point in the scan, a close representation of the profile is still obtainable.

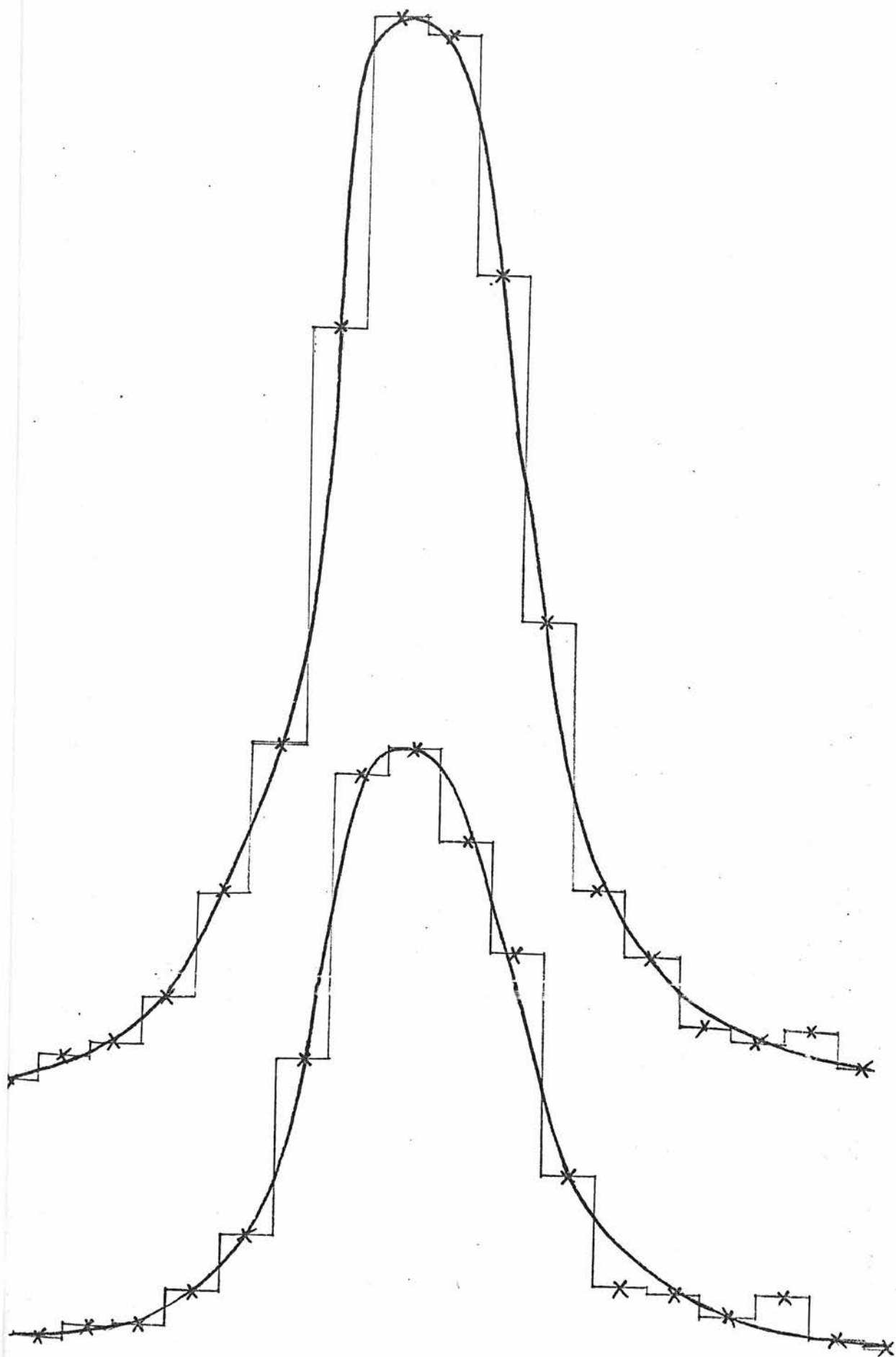
The profiles obtained are processed to give the integrated intensities, INTC:

$$\text{INTC} = \sum p - (\sum b_1 + \sum b_2)/(n_1+n_3) \times n_2 \quad m_2/m_1 \quad \text{II.5}$$

where p is a peak count b_1 and b_2 are background counts, n_1 , n_2 and n_3 are the number of steps in background one, the peak and in background two (if there are two background scans) respectively; m_2 and m_1 are the monitor counts for the peak and the background steps; m_2 was $= m_1$ and n_3 was $= n_1$ in all the experiments. $(b_1 + b_2)/(n_1+n_3)$ is the average background level per step $= \bar{B}$. When the scan type: peak - peak offset background is used this becomes $\sum b/n_1$; the average background level is subtracted from each peak count. The intensity is put on a fixed scale (comparing with unit step width and unit monitor count), INT:

$$\text{INT} = \text{INTC} \times w_2/m_2 \quad \text{II.6}$$

The intensities are also corrected to take account of the variation with setting angles, of the various reflections,



Integrated intensity v. area under free hand curve.

Fig. II.6.

of the rate of passing through the reflecting position for a given rate of rotation of the specimen, the Lorentz factor. For the normal beam of equatorial geometry this correction is $\sin(2\theta)$ and for the tilting counter normal beam geometry the general expression for the Lorentz factor (Arndt and Willis, 1966, p. 282) reduces to: $\cos \nu \sin \gamma$, see Fig. II.4. After these corrections the intensities are on a common (but arbitrary) scale when they can be equated to the square of the modulus of the structure factor ff .

$$ff = INT \times K \times \sin(2\theta) \quad \text{II.7}$$

$$\text{or: } ff = INT \times K \times \cos \nu \sin \gamma \quad \text{II.8}$$

with K an arbitrary scale factor ($= 10^5$ usually).

Finally the observed structure factors, f , are obtained as the square root of ff .

The standard deviation is estimated for each observed structure factor by considering: s_1 , s_2 and s_3 the sums of the counts in background one, the peak and in background two, see equation II.5, and \bar{B} the average background level:

$$\sigma(\bar{B}) = \sqrt{(s_1 + s_3)} / (n_1 + n_3) \quad \text{II.9}$$

$$\sigma(ff) = \sqrt{(s_2 + n_2^2 \sigma^2(\bar{B}))} \times \omega_2/m_2 \times K \times \sin(2\theta) \quad \text{II.10}$$

$$\sigma(f) = \sigma(ff)/2f \quad \text{II.11}$$

In equation II.10 $\sin(2\theta)$ is replaced by $\cos \nu \sin \gamma$ when data has been collected using the tilting counter setting. The observed structure factors are then compared with the calculated (or estimated) structure factors, \hat{f} , in evaluation of the validity of the estimates of the structural parameters for the crystal structure studied; the \hat{f} 's

involving as many terms in harmonic and anharmonic thermal factors as the interest of the experimenter and the accuracy of his measurements call for.

Thermal diffuse scattering was not corrected for in the work described in this thesis nor was there any correction made for absorption.

In order to avoid accidental errors more than one representative of each set of symmetry equivalent observed structure factors was collected to enable an estimate. Each set of equivalent observed structure factors was averaged to give one non-equivalent observed structure factor for the set.

II.2 Least Squares

In view of the importance of understanding clearly the least squares procedure when evaluating the methods of hypothesis testing, discussed below, a fairly comprehensive treatment of the least squares method will be presented.

II.2.a The general theory of least squares

The basic underlying idea is that one unbiased estimator of a population parameter is preferred to another if the first has a smaller variance.

The method of least squares is an application of this idea to a multivariate problem.

Consider n experimental observations f_1, f_2, \dots, f_n linearly dependent on m parameters x_1, x_2, \dots, x_m associated with each observation is a random error e_i then the equations of condition read:

$$\begin{aligned} f_1 &= a_{11} x_1 + a_{12} x_2 + \dots + a_{1m} x_m + e_1 \\ f_2 &= a_{21} x_1 + a_{22} x_2 + \dots + a_{2m} x_m + e_2 \\ &\vdots \\ f_n &= a_{n1} x_1 + a_{n2} x_2 + \dots + a_{nm} x_m + e_n \end{aligned} \quad \text{II.12}$$

or in a matrix form:

$$\tilde{F}_{n,1} = \tilde{A}_{n,m} \tilde{X}_{m,1} + \tilde{E}_{n,1} \quad \text{II.13}$$

\tilde{X} are the parameters of importance, $\hat{\tilde{X}}$ are the estimates we seek to obtain. \tilde{A} is the design matrix. We assume the errors e_i to have a joint distribution with zero mean, i.e.

$$\varepsilon \{ \tilde{F} \} = \tilde{F}^0 = \tilde{A} \tilde{X} \quad \text{II.14}$$

where $\varepsilon \{ \tilde{F} \}$ is the expectation value of \tilde{F} . We further assume the errors to have a variance covariance matrix \tilde{M}_F with elements $m_{ij} = m_{ji} = \varepsilon \{ e_i e_j \} = \text{cov}(f_i, f_j) \cdot \text{var}(f_i) =$ the variance of f_i . $\text{cov}(f_i, f_j) = \rho_{ij} \sigma_i \sigma_j$ where ρ_{ij} is the correlation coefficient and σ_i is the standard deviation of f_i . $\text{cov}(f_i, f_i) = \text{var}(f_i)$.

Note that no assumption has been made about the form of the distribution function of the e_i 's; only that it has finite second moment.

It can be shown that there exist estimators $\hat{\tilde{X}}$ such that for any linear function of X

$$\tilde{L} = \tilde{G}_{1,m} \tilde{X}_{m,1} ; \quad \text{II.15}$$

the estimator

$$\hat{\tilde{L}} = \tilde{G} \hat{\tilde{X}} \quad \text{II.16}$$

is a minimum variance unbiased estimator of \underline{L} . $\underline{\hat{X}}$ with this property is independent of \underline{G} .

The problem of minimizing the sum of the squares of residuals, the differences between estimated and observed quantities, see below, gives rise to the same best values of $\underline{\hat{X}}$ as does the problem of minimizing the variance of an arbitrary linear combination of $\underline{\hat{X}}$.

The least squares estimate of \underline{X} is the estimate which minimizes the variance of the estimate of any linear function of the parameters.

Consider now the case when $\underline{M}_F = \underline{I}$; this, in effect, means no correlation between observations and strictly unit weight to each observation. We seek to minimize the sum of squares of residuals

$$S = \sum_{i=1}^n (f_i - \hat{f}_i)^2 \quad \text{where } \hat{f}_i$$

are the elements of $\underline{\hat{F}} = \underline{A} \underline{\hat{X}}$. If we define a matrix of residuals

$$\underline{V}_{n,l} = \underline{F} - \underline{\hat{F}} = \underline{F} - \underline{A} \underline{\hat{X}} \quad \text{II.17}$$

the minimization of S is equivalent to the minimization of

$$\underline{V}' \underline{V} = S \quad \text{II.18}$$

In the general case of $\underline{M}_F \neq \underline{I}$

$$\underline{V}' \underline{M}_F^{-1} \underline{V} = S \quad \text{II.19}$$

we have

$$\begin{aligned} \underline{V}' \underline{M}_F^{-1} \underline{V} &= (\underline{F} - \underline{A} \underline{\hat{X}})' \underline{M}_F^{-1} (\underline{F} - \underline{A} \underline{\hat{X}}) \\ &= \underline{F}' \underline{M}_F^{-1} \underline{F} - \underline{F}' \underline{M}_F^{-1} \underline{A} \underline{\hat{X}} - \underline{\hat{X}}' \underline{A}' \underline{M}_F^{-1} \underline{F} + \underline{\hat{X}}' \underline{A}' \underline{M}_F^{-1} \underline{A} \underline{\hat{X}} \end{aligned} \quad \text{II.20}$$

introducing the differential operator ∂ :

$$\begin{aligned}
 \partial(V' \tilde{M}_f^{-1} V) &= - \tilde{F}' \tilde{M}_f^{-1} \tilde{A} \partial \tilde{X} - \partial \tilde{X}' \tilde{A}' \tilde{M}_f^{-1} \tilde{F} + \partial \tilde{X}' \tilde{A}' \tilde{M}_f^{-1} \tilde{A} \tilde{X} \\
 &\quad + \tilde{X}' \tilde{A}' \tilde{M}_f^{-1} \tilde{A} \partial \tilde{X} \\
 &= 2 \partial \tilde{X}' (\tilde{A}' \tilde{M}_f^{-1} \tilde{A} \tilde{X} - \tilde{A}' \tilde{M}_f^{-1} \tilde{F}) \\
 &= 0 \quad \text{for minimum,}
 \end{aligned}
 \tag{II.21}$$

which means that the condition for minimum is equivalent to:

$$(\tilde{A}' \tilde{M}_f^{-1} \tilde{A}) \tilde{X} = \tilde{A}' \tilde{M}_f^{-1} \tilde{F} ; \tag{II.22}$$

these are the normal equations:

$$\tilde{B} \tilde{X} = \tilde{A}' \tilde{M}_f^{-1} \tilde{F} \tag{II.23}$$

where $\tilde{B} = \tilde{A}' \tilde{M}_f^{-1} \tilde{A}$ is the matrix of the normal equations.

We usually only know \tilde{M}_f to within a scale factor, σ^2

$$\tilde{M}_f = \sigma^2 \tilde{N} ; \quad \tilde{M}_f^{-1} = 1/\sigma^2 \tilde{N}^{-1}$$

defining \tilde{N} ; substituting into the normal equations we have

$$1/\sigma^2 \tilde{A}' \tilde{N}^{-1} \tilde{A} \tilde{X} = 1/\sigma^2 \tilde{A}' \tilde{N}^{-1} \tilde{F} ,$$

which means that the solutions, \tilde{X} , are independent of the scale of \tilde{M}_f . We introduce the weight matrix $\tilde{P} = \tilde{N}^{-1}$, then:

$$\tilde{X} = (\tilde{A}' \tilde{P} \tilde{A})^{-1} \tilde{A}' \tilde{P} \tilde{F} .$$

If $p_{ij} = 0$ when $i \neq j$ and $p_{ii} = \omega_i$ (i.e. a diagonal weight matrix); this is equivalent to multiplying through every equation of condition by $\sqrt{\omega_i}$ and then treating the system as unweighted (i.e. $a_{ij} \rightarrow \sqrt{\omega_i} a_{ij}$ and $f_i \rightarrow \sqrt{\omega_i} f_i$).

Errors in the parameter estimates:

Consider the variance covariance matrix M_X of the parameter estimates

$$\tilde{M}_X = \epsilon \left\{ (\tilde{X} - \hat{\tilde{X}})(\tilde{X} - \hat{\tilde{X}})' \right\}$$

$$\tilde{M}_X = \epsilon \left\{ B^{-1} \tilde{A}' \tilde{M}_f^{-1} (\tilde{F} - \tilde{F}^0)(\tilde{F} - \tilde{F}^0)' \tilde{M}_f^{-1} \tilde{A} (B^{-1})' \right\}$$

$$\tilde{M}_X = \tilde{B}^{-1} \tilde{A}' \tilde{M}_f^{-1} \epsilon \left\{ (\tilde{F} - \tilde{F}^0)(\tilde{F} - \tilde{F}^0)' \right\} \tilde{M}_f^{-1} \tilde{A} \tilde{B}^{-1}$$

$$\tilde{M}_X = \tilde{B}^{-1} \tilde{A}' \tilde{M}_f^{-1} \tilde{M}_f \tilde{M}_f^{-1} \tilde{A} \tilde{B}^{-1}$$

$$\tilde{M}_X = \tilde{B}^{-1} \tilde{A}' \tilde{M}_f^{-1} \tilde{A} \tilde{B}^{-1} = \tilde{B}^{-1} \tilde{B} \tilde{B}^{-1} = \tilde{B}^{-1}$$

$$\therefore \tilde{M}_X = \tilde{B}^{-1}$$

$$\tilde{B} = \tilde{A}' \tilde{M}_f^{-1} \tilde{A} = 1/\sigma^2 \tilde{A}' \tilde{P} \tilde{A}$$

$$\therefore \tilde{M}_X = \sigma^2 (\tilde{A}' \tilde{P} \tilde{A})^{-1} \quad \text{II.27}$$

We have thus shown that \tilde{M}_X , the variance covariance matrix of the parameter estimates, is equal to the inverse of the matrix of the normal equations.

We must know σ^2 , in which case \tilde{M}_X is completely determined, or have an unbiased estimate of σ^2 . It can be shown that σ^2 , an unbiased estimator of σ^2 , is available from the least squares treatment.

By considering $\epsilon \left\{ \tilde{V}' \tilde{P} \tilde{V} \right\} = \sigma^2 \epsilon \left\{ \tilde{V}' \tilde{M}_f^{-1} \tilde{V} \right\}$ after some manipulation we find:

$$\epsilon \left\{ \tilde{V}' \tilde{M}_f^{-1} \tilde{V} \right\} = \epsilon \left\{ (\tilde{F} - \tilde{F}^0)' \tilde{M}_f^{-1} (\tilde{F} - \tilde{F}^0) \right\} - \epsilon \left\{ (\tilde{X} - \hat{\tilde{X}})' \tilde{B} (\tilde{X} - \hat{\tilde{X}}) \right\}. \quad \text{(II.28)}$$

We now state the result of the theory of statistics that

since $\underline{F} - \underline{F}^0$ and $\underline{X} - \underline{\hat{X}}$ are random variables with zero means $\epsilon \{ \underline{V}' \underline{M}_F^{-1} \underline{V} \} = n - m$, where n and m are the ranks of \underline{M}_F^{-1} and \underline{B} respectively (Hamilton, 1964, p. 129-130). Then we have

$$\epsilon \{ \underline{V}' \underline{P} \underline{V} \} = \sigma^2 (n - m) , \quad \text{II.29}$$

which gives $\hat{\sigma}^2 = \underline{V}' \underline{P} \underline{V} / (n - m)$ as an unbiased estimator of σ^2 , which in turn gives:

$$\underline{M}_X = \frac{\underline{V}' \underline{P} \underline{V}}{n - m} (\underline{A}' \underline{P} \underline{A})^{-1} \quad \text{II.30}$$

as an unbiased estimator of \underline{M}_X the variance covariance matrix of the parameter estimates.

II.2.b. Constraints and hypothesis testing.

The least squares process can readily be adapted to include constraints on the parameters; see section on application to crystallography II.2.c.

When we have imposed restrictions on some parameters or when we have carried out the least squares procedure with some relationship between the parameters, we want to compare the fits obtained for each case and we want to be able to make statements about the relative validity of the different models tried. First we consider linear restrictions only, i.e. linear hypothesis:

$$\omega_i = \sum_j \theta_{ij} x_j , \quad \text{II.31}$$

where we constrain the parameters, x_j , by fixing the values of ω_i which are some linear combinations determined by some constants θ_{ij} .

The F distribution represents the probability

distribution of a ratio of two estimates, y_1 and y_2 , of the same variance such that if y_1 with ν_1 degrees of freedom is distributed as χ^2 , defined below, and y_2 with ν_2 degrees of freedom, and independent of y_1 , is distributed as χ^2 , then the ratio

$$\frac{y_1 / \nu_1}{y_2 / \nu_2} = F_{\nu_1, \nu_2} \quad \text{II.32}$$

where F_{ν_1, ν_2} has a known distribution function, $\phi(F)$, see Appendix I, for $F > 0$ but zero otherwise. We work out, see Appendix I :

$$\alpha = P(F > F_{\nu_1, \nu_2}) \quad \text{II.33}$$

the probability of being wrong in rejecting the hypothesis; the hypothesis being that the constraint of the parameters is correct, (see below).

If we are to utilize the F distribution we must therefore be able to assign the χ^2 distribution to our various estimates of the variance of our fit. The definition of the χ^2 distribution follows:

"If k observations are made from a normal population with zero mean and unit variance, the sum of the squares of the observations is distributed as χ^2 with k degrees of freedom. The sum of two random independent variables, each distributed as χ^2 , is again a χ^2 distributed random variable (with $k_1 + k_2$ degrees of freedom" (Hamilton, 1964, p. 81).

It is here where we must make the additional assumption, not necessary for the least squares procedure to work, that the errors follow a normal distribution.

If we know that the contributions to the errors come from many additive independent random variables, each with different distribution, we can quote in support of this assumption the central limit theorem, CLT, (Hamilton, 1964, p. 67):

"Given x_i , $i = 1, n$ set of independent random variables, each with an arbitrary probability distribution function with finite mean μ_i and second moment, (variance) σ_i^2 , the CLT states that as n increases the distribution of y , a linear function of x_i such that

$$y = \sum_{i=1}^n a_i x_i, \quad \text{II.34}$$

approaches the normal distribution with mean

$$\mu_y = \sum_{i=1}^n a_i \mu_i \quad \text{II.35}$$

and variance

$$\sigma^2(y) = \sum_{i=1}^n a_i^2 \sigma_i^2. \quad \text{II.36}$$

If the errors of observations, e_i , are normally distributed then the errors of the parameter estimates obtained from such observations also are normally distributed.

We have that $\tilde{V}' \tilde{P} \tilde{V}$, the weighted sum of the squares of the residuals is distributed as $\sigma^2 \chi_{n-m}^2$ ($\tilde{V}' \tilde{M}_f^{-1} \tilde{V}$ as χ_{n-m}^2).

$\tilde{V}'_c \tilde{P} \tilde{V}_c - \tilde{V}' \tilde{P} \tilde{V}$ where $\tilde{V}'_c \tilde{P} \tilde{V}_c$ represents the constraint case is distributed as χ_b^2 where b is the difference in the number of degrees of freedom between the free and the constraint models. The ratio:

$$\frac{\tilde{V}'_c \tilde{P} \tilde{V}_c - \tilde{V}' \tilde{P} \tilde{V}}{\tilde{V}' \tilde{P} \tilde{V}} \quad \text{II.37}$$

is therefore distributed as:

$$\frac{b}{n-m} F_{b, n-m} \quad \text{II.38}$$

or:

$$F_{b, n-m} = \frac{n-m}{b} \frac{\sum_{c=1}^m \frac{V_c' P V_c}{V_c' P V_c} - \frac{V' P V}{V' P V}}{\sum_{c=1}^m \frac{V_c' P V_c}{V_c' P V_c}}, \quad \text{II.39}$$

which means that the corresponding point of the F distribution is immediately obtainable from the sum of the squares of the residuals of the different least squares procedures.

So far we have considered only linear hypothesis and linear least squares problems. The least squares method can be applied to non-linear problems provided we can make the assumption of linear increments of the functions describing the observations with parameter increments over the range of parameters considered, i.e. that we can expand \tilde{f}_i in a Taylor series:

$$\tilde{f}_i(x_1, \dots, x_m) \approx \tilde{f}_i(x_1^0, \dots, x_m^0) + \sum_{j=1}^m \frac{\partial \tilde{f}_i}{\partial x_j}(x_j - x_j^0) + \dots \quad \text{II.40}$$

and that we can terminate the series at first order

$$\Delta f_i \approx \sum_{j=1}^m \frac{\partial \tilde{f}_i}{\partial x_j} \Delta x_j \quad \text{II.41}$$

where $\Delta f_i = f_i(x_1, \dots, x_m) - \tilde{f}_i(x_1^0, \dots, x_m^0)$ and $\Delta x_j = x_j - x_j^0$.

If these approximations hold good, the problem has been reduced to the linear one where:

$$\left. \begin{aligned} A &= \{a_{ij}\} = \left\{ \frac{\partial f_i}{\partial x_j} \right\} \\ F &= \{f_i\} \\ X &= \{x_j\} \end{aligned} \right\} \begin{aligned} i &= 1, n; \\ j &= 1, m. \end{aligned} \quad \text{II.42}$$

The design matrix \underline{A} is now a function of the parameters calling for some initial values of the parameters to enable the setting up of \underline{A} .

When we have carried out the least squares procedure, the estimates we obtain must in general be used as initial values for a repeat of the process, since the design matrix is parameter dependent.

It is therefore, in general, necessary to iterate until the parameter shifts are so small as to leave \underline{A} practically unchanged, or less than the estimated error.

A usual condition for convergence, that the initial parameter estimates are to be close to the correct parameters, follows from the limits of the range of approximate validity of the Taylor expansion. The procedure of successive iterations in a converging least squares is often referred to as a "refinement" of the parameters.

When we want to apply some linear constraints to the parameters of the non-linear least squares problem and then test the hypothesis postulated, we find we rely on:

- 1) the validity of $\underline{V}' \underline{P} \underline{V} / (n - m)$ as an unbiased estimator of σ^2 and
- 2) the invariance of \underline{B} or $\underline{A}' \underline{P} \underline{A}$ over the range of parameters considered in the hypothesis.

The testing of non-linear hypothesis

We can test non-linear hypothesis of the form

$$\omega_i = f_i(x_1, \dots, x_m) \quad \text{II.43}$$

say, so far as we can make the approximation:

$$\partial \omega_i \approx \sum_j^m \frac{\partial f_i}{\partial x_j} \partial x_j \quad \text{II.44}$$

It should also be mentioned that the concept of degrees of freedom depends on linear relations with implication of an effective number of degrees of freedom.

When we want to test a non-linear hypothesis in a non-linear least squares problem, all the above mentioned approximations have to hold simultaneously. Fig. II.7 shows schematically the assumptions that have to be made for the least squares procedure and hypothesis testing to work. One important point to note is that we assume validity of $\tilde{V}' \tilde{P} \tilde{V} / (n - m)$ as an estimator of σ^2 when assessing the significance of the various constraints; but that the resulting $F_{b, n-m}$, equation II.39, is independent of any constant factor common to $\tilde{V}_c' \tilde{P} \tilde{V}_c$ and $\tilde{V}' \tilde{P} \tilde{V}$. We thus do not rely on knowing the absolute magnitude of $\tilde{V}' \tilde{P} \tilde{V}$ and $\tilde{V}_c' \tilde{P} \tilde{V}_c$ but only the relative magnitudes. This, however, is not the case when with the results of an unconstrained least squares procedure we want to estimate the errors in the parameter estimates from $\tilde{M}_{\tilde{x}} = \sigma^2 (\tilde{A}' \tilde{P} \tilde{A})^{-1}$, see equation II.27; because here we must rely on the absolute magnitude of $\tilde{V}' \tilde{P} \tilde{V}$ as an estimator of σ^2 . For this reason we claim that assessment of significant features of the parameter estimates is more likely

HYPOTHESIS			
	NONE	LINEAR	NON-LINEAR
LINEAR	Assume errors to be <u>randomly distributed</u> with <u>zero mean</u> and <u>finite variances</u>	Assume errors to be <u>normally distributed</u>	Assume; if hypothesis is: $\omega_i = f_i(x_1, \dots, x_m)^*$; then: $\Delta \omega_i \approx \sum_j \frac{\delta f_i}{\delta x_j} \Delta x_j$
LEAST SQUARES	Assume*: $\Delta f_i \approx \sum_j \frac{\delta f_i}{\delta x_j} \Delta x_j$	Assume validity* of $\frac{V'PV}{n-m}$ as an estimator of σ^2 and the invariance* of B or A'PA	Assume that all assumptions mentioned are simultaneously valid
NON LINEAR			

The assumptions necessary for the methods of least squares and hypothesis testing to work. *over the range of parameters considered in the analysis

Fig. II.7.

to be meaningful in a study employing the method of constraint least squares procedure (refinement) and hypothesis testing than it would be in a study based on the errors in the parameter estimates as obtained from the unconstrained least squares procedure only.

We have tried in this section to make it clear what assumptions have to hold for the methods of least squares and hypothesis testing to work. The validity of these assumptions in any particular case of application is a measure of the extent to which we can equate statistical significance to physical significance.

II.2.c. Application to Crystallography

The problem of fitting structure factors is clearly, see equations II.1 and II.2, a very non-linear one due to the trigonometric and exponential dependence of the structure factors on positional and thermal parameters, respectively. The trigonometric terms give rise to the possibility of oscillations in the least squares procedure of some parameter estimates when some of the initial parameter values are some way from the correct values. It is sometimes possible to overcome this problem and still have convergence of the least squares procedure by introducing damping of the calculated parameter shifts and update the parameters by:

$$x_j = x_j^0 + \underline{q} \ x_j \quad \text{rather than by} \quad x_j = x_j^0 + x_j$$

where $0 \leq \underline{q} \leq 1$. When the initial parameters are quite some way from the correct values, the conventional least squares procedure is, due to the oscillary^{to} terms in the structure factor expressions, unlikely to converge, at least

to the correct minimum, in parameter space. There is, however, a very powerful method of increasing the range of convergence of the least squares procedure and this is by applying some constraints (e.g. let some molecules be rigid units) to the parameters in the initial stages of the least squares procedure (Pawley, 1972). The problem of correlations between some parameters is properly assessed only by using constraints (Pawley, 1972) and testing the significance of the extra parameters.

A great number of the features examined in crystal structures involve linear hypothesis such as: atomic coordinates have specific values, e.g. are located on symmetry sites or: atoms are isotropic in their thermal vibrations;

$$u_{33} = u_{22} = u_{11} ; \quad u_{12} = u_{13} = u_{23} = 0. \quad \text{II.45}$$

Others involving fixed bondlengths and angles are more than often non-linear, involving the squares of linear combinations of atomic coordinates or trigonometric functions of these.

A very flexible method of including constraints in the least squares procedure was proposed and put to use by Dr. G.S. Pawley of this department (Pawley, 1969). The essence of this approach is to divide the variables into dependent variables (constrained variables) and independent variables and when setting up the design matrix \underline{A} , taking account of the parameter relations by updating the usual derivatives through:

$$\frac{\partial f_i}{\partial p_j} = \sum_k \frac{\partial f_i}{\partial P_k} \frac{\partial P_k}{\partial p_j} \quad \text{II.46}$$

where the P_k 's are the dependent variables and the p_j 's

are the independent variables. The P_k 's are the usual positional and thermal parameters of the atoms, so the:

$$\frac{\partial f_i}{\partial P_k} \quad \text{II.47}$$

are provided by any conventional least squares program. The p_j 's can be any of the P_k 's or indeed any function of the P_k 's.

An example of linear hypothesis formulated in this way: $u_{33} = u_{22} = u_{11}$ for an atom; treating u_{11} as dependent and $u'_{11} = u_{11}$ as an independent variable, we form the derivative such that

$$\frac{\partial f_i}{\partial u'_{11}} = \frac{\partial f_i}{\partial u_{11}} + \frac{\partial f_i}{\partial u_{22}} + \frac{\partial f_i}{\partial u_{33}} \quad \text{II.48}$$

which now represents the true derivative of f_i with respect to u'_{11} taking the constraints into account.

For a non-linear hypothesis we must, as stated before, rely on the approximation that the increments of the dependent variables are linear in the increments of the independent ones over the range of parameters considered.

For example, in tetragonal KDP (see Chapter IV) a $\bar{4}$ axis (down z) through the origin at which a P atom is located, operates on an oxygen atom at (x, y, z) to form a PO_4 tetrahedron which is a regular tetrahedron if, for the oxygen atom:

$$x^2 + y^2 = 2z^2 \quad \text{II.49}$$

We treat $y' = y$ and $z' = z$ as independent variables and we have:

$$\frac{\partial f_i}{\partial y'} = \frac{\partial f_i}{\partial y} + \frac{\partial f_i}{\partial x} \frac{\partial x}{\partial y} = \frac{\partial f_i}{\partial y} + \frac{\partial f_i}{\partial x} \left(\frac{-y}{x} \right)$$

and

$$\frac{\partial f_i}{\partial z'} = \frac{\partial f_i}{\partial z} + \frac{\partial f_i}{\partial x} \frac{\partial x}{\partial z} = \frac{\partial f_i}{\partial z} + \frac{\partial f_i}{\partial x} \left(\frac{2z}{x} \right)$$

Referring to Figure II.7 we try to evaluate the applicability of the assumptions made to crystallographic problems.

The two assumptions made that need most consideration are:

1) in the least squares procedure: the assumption of random errors with zero means i.e. we assume our data sets and models to be nearly free of systematic errors.

2) When testing hypothesis: the assumption that \underline{B} or $\underline{A}' \underline{P} \underline{A}$ is approximately invariant over the range of parameters considered in the hypothesis, i.e. that the weights must be the same and that the non-linearities are not so great over the range of parameters considered so as to alter the design matrix \underline{A} too much for the approximation of the invariance of $\underline{A}' \underline{P} \underline{A}$ to hold good over that parameter range. The systematic errors depend on how well we represent the experimental setup in handling of data and in our model. There are various known systematic effects like extinction, see Section II.1a, that we can to a large extent include in our model.

The effects of non-linearity simply depend on the validity of the linear approximations over the range of parameters considered. It is important, once we have decided to apply hypothesis testing, to realize what conclusions are possible from the results.

We apply constraints; our hypothesis is that some

parameter relations hold good.

$\alpha = P(F > F_{\nu_1, \nu_2})$ is the statistical probability of being wrong in rejecting the hypothesis.

Taking the theory of the statistics involved for granted and trusting that our data has normally distributed errors with zero means, with our models closely representing the physical situation of our sample, we still have one important limitation to realize, namely:

A failure to reject a hypothesis does not mean the hypothesis is true.

E.g. an α of .5 means that the statistical probability of being wrong in rejecting the corresponding hypothesis, say that an atom i had isotropic thermal motion, is 50% but we cannot, on that basis alone, make the statement: atom i has isotropic thermal motion. If, however, in the above example α came to .001, we can make the statement that there is strong experimental evidence that atom i is anisotropic. The validity of that statement, as is explained in Section II.2.b and summarized in Fig. II.7, depends on the degree to which the assumptions made (necessary to enable the application of the statistical approach) really hold good,

An attempt has been made by Pawley, 1972, to establish a general relationship between statistical and physical significance, based on a comparison (for particular types of constraints) of the results of hypothesis testing with some other physical evidence. But for a meaningful comparison to be made we not only require the assumptions in each individual case to be approximately valid, but also we must now assume, in addition, that the assumptions are valid to

the same extent in all cases considered. This approach is not considered further in this thesis.

A program was written, see Appendix I, to work out, to any desired accuracy, α , the level of statistical significance for a given $\tilde{V}' \tilde{P} \tilde{V}$, $\tilde{V}_c' \tilde{P} \tilde{V}_c$, $n - m$ and b (specifying a point of the F distribution, see equation II.39).

This program thus obviates: 1) the use of an approximation for the F distribution (Pawley, 1970), 2) the use of statistical tables where extrapolations are necessary (Hamilton, 1964, 1965) and 3) the use for an S value (Pawley, 1972) as a means of expressing low values of α .

II.3 Fourier Methods

We will include a brief mention of the Fourier methods since these methods were qualitatively used in the early stages of the DTGS problem (Chapter V).

Considering the scattering from each element of volume $v \, dx \, dy \, dz$ in the unit cell separately with $\rho(x,y,z)$, the density of scattering matter, the structure factor expression more fundamentally^{*} reads:

$$\hat{f}(\underline{h}) = \int_{\text{unit cell}} V \rho(\underline{r}) \exp(2\pi i \underline{h} \cdot \underline{r}) dx \, dy \, dz \quad \text{II.51}$$

since the crystal is periodic in 3-D ρ can be expressed as a Fourier series in 3-D

$$\rho(\underline{r}) = \sum_{\underline{h}'} \sum \sum C(\underline{h}') \exp(2\pi i \underline{h}' \cdot \underline{r}) \quad \text{II.52}$$

the summations are over all values of each component of \underline{h}'

^{*}compare with equation II.1

from $-\infty$ to ∞ for each point \underline{r} in the unit cell. Substituting into equation II.51, we soon find

$$\rho(\underline{r}) = 1/V \sum \sum_{\underline{h}} \sum \hat{f}(\underline{h}) \exp(-2\pi i \underline{H} \cdot \underline{r}) \quad \text{II.53}$$

We can thus construct a map of ρ , a Fourier map, throughout the unit cell. By using $f(\underline{h})$ as coefficients in equation II.53, rather than $\hat{f}(\underline{h})$, but with calculated phases we hope to gain some information as to the correctness of the calculated phases. This is the f synthesis.

The termination of \underline{h} at some value, limited by the highest value of $\sin \theta/\lambda$ obtained, causes ripples to appear in the Fourier maps. Such difficulties can be overcome (for example, Bacon and Pease, 1953), but in the present work only qualitative use was made of Fourier maps.

The difference synthesis

$$\delta\rho(\underline{r}) = 1/V \sum \sum_{\underline{h}} \sum (f(\underline{h}) - \hat{f}(\underline{h})) \exp(-2\pi i \underline{H} \cdot \underline{r}) \quad \text{II.54}$$

does not suffer from termination ripples as does the f -synthesis. We can eliminate any terms from the difference synthesis, for example those we are not able to phase with any certainty (e.g. \hat{f} near zero and f large). The resulting synthesis should then serve to show up inadequacies of our proposed model that then can be corrected to give more accurate phasing.

One point should be brought up here in connection with using this method parallel to the least squares method when the parameters are still some way off their correct values.

The criterion for minimizing σ_p is equivalent to the statement of the normal equations of least squares (Cochran, 1951). The weights given to each observation are different (for neutron data fairly uniform weights are applied) from those usually employed in the least squares process. It is, of course, possible to introduce weights into the difference synthesis.

An account of this approach is given by Lipson and Cochran, 1966.

II.4 Structural Studies of Ferroelectrics

In Section I.6 we pointed out some of the structural problems, particularly relevant to ferroelectrics using Ba Ti O_3 as an illustrative example. In particular we pointed out that in order to resolve the finer details of the often delicately balanced structures we need data capable of giving good resolution, and even then there could be serious problems due to correlation.

We want here to consider further the problems particular to structural studies of ferroelectrics in assessing the applicability of the methods of least squares and hypothesis testing to ferroelectrics.

1) Extinction (see Section II.1.a): There are some indications (Bunn and Emmett, 1949) that the growth of a ferroelectric crystal in its ferroelectric phase is influenced by the dipole moments of the crystal formed. This effect is believed to ease crystal growth (see Chapter III). In ferroelectrics this effect is directional and hence could give rise to anisotropic extinction. Anisotropic extinction,

if not corrected for, would give rise to systematic errors and the application of the method is based on random errors in the data.

As the transition temperature of a ferroelectric is passed, in the crystal, strains build up and relax. Not only does this give rise to variable extinction of the crystal with T near T_c but also it means that extinction is history dependent in some cases, i.e. in those crystals where the building up and relaxation of strains is not a reversible process. An extinction parameter should therefore always be refined individually for each dataset on a ferroelectric when changes in temperature are involved.

2) Often in ferroelectric crystal structural studies our main interest lies in the finer details of delicately balanced structure. The correlations which often result from such situations are best tackled by the method of constraint refinements and hypothesis testing but the main point we wish to make is that, since the differences involved are small, the assumptions needed for valid test of relevant hypothesis are likely to hold good, see Figure II.7.

In particular we point out that since the range of parameters considered is often quite small, the assumption of the invariance of \tilde{B} or $\tilde{A}^1 \tilde{P} \tilde{A}$ over that range is likely to be a fair assumption. In principle, therefore, at least, the methods of constraints and hypothesis testing are particularly applicable to structural studies of ferroelectrics.

CHAPTER III

SAMPLE PREPARATION

III.1 Crystal Growing from Solution

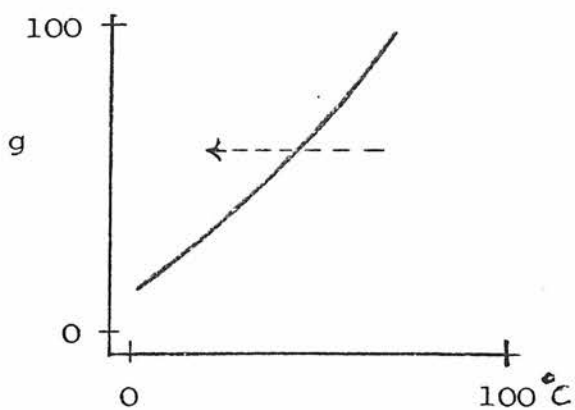
III.1.a In theory

Here we briefly deal with the main factors involved in crystal growing from solution.

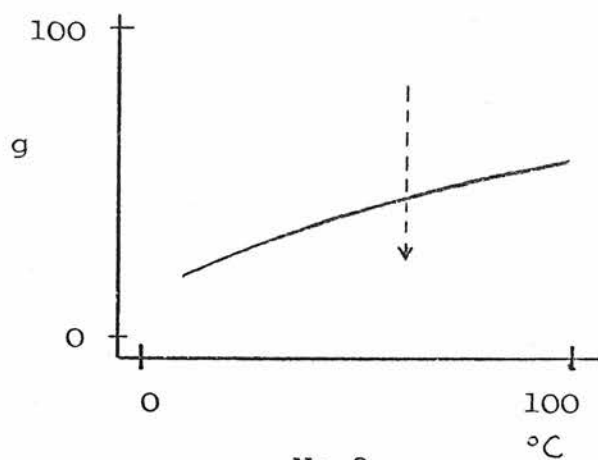
1) Solubility. At the temperature of growth or in the temperature range of growth the material should be at least 10⁰/o soluble in the solvent to be used (grams of the material dissolved in 100 grams of solvent). Figure III.1 shows 4 possible solubility curves: No. 1 shows a steep solubility curve where the method of slow cooling at constant supersaturation would be applied, indicated by an arrow, since this method would give a reasonable growth rate; No. 2 shows a flat solubility curve that would call for the method of slow evaporation at constant temperature; No. 3 shows a solubility curve suitable for the method of transport of material across a thermal gradient to work; No. 4 shows a solubility curve where some other means of growing the crystal has to be used.

It should be emphasized that the solubility curves are obtained by joining together a set of equilibrium points. The crystal growing process is a steady state process and the solubility curves can therefore only be used as a guide.

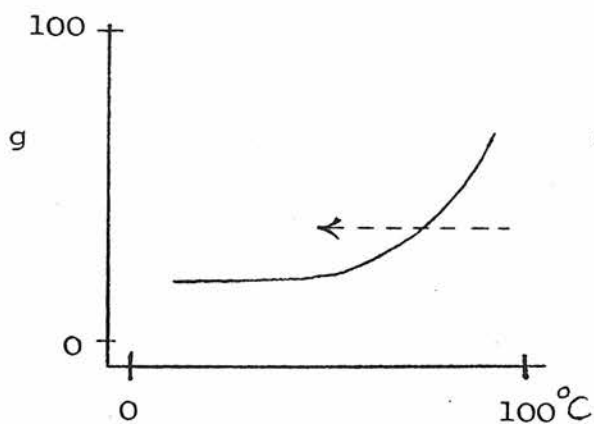
2) Forces of growth. We consider here two forces of growth: the change in temperature, T , and the change in concentration, n . By a force of growth we mean a variable parameter of



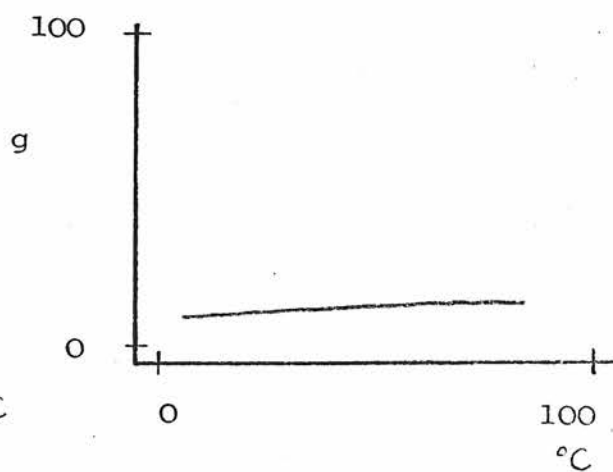
No 1



No 2



No 3



No 4

Four possible types of solubility curves;
 g = grams of material / 100 grams of solvent

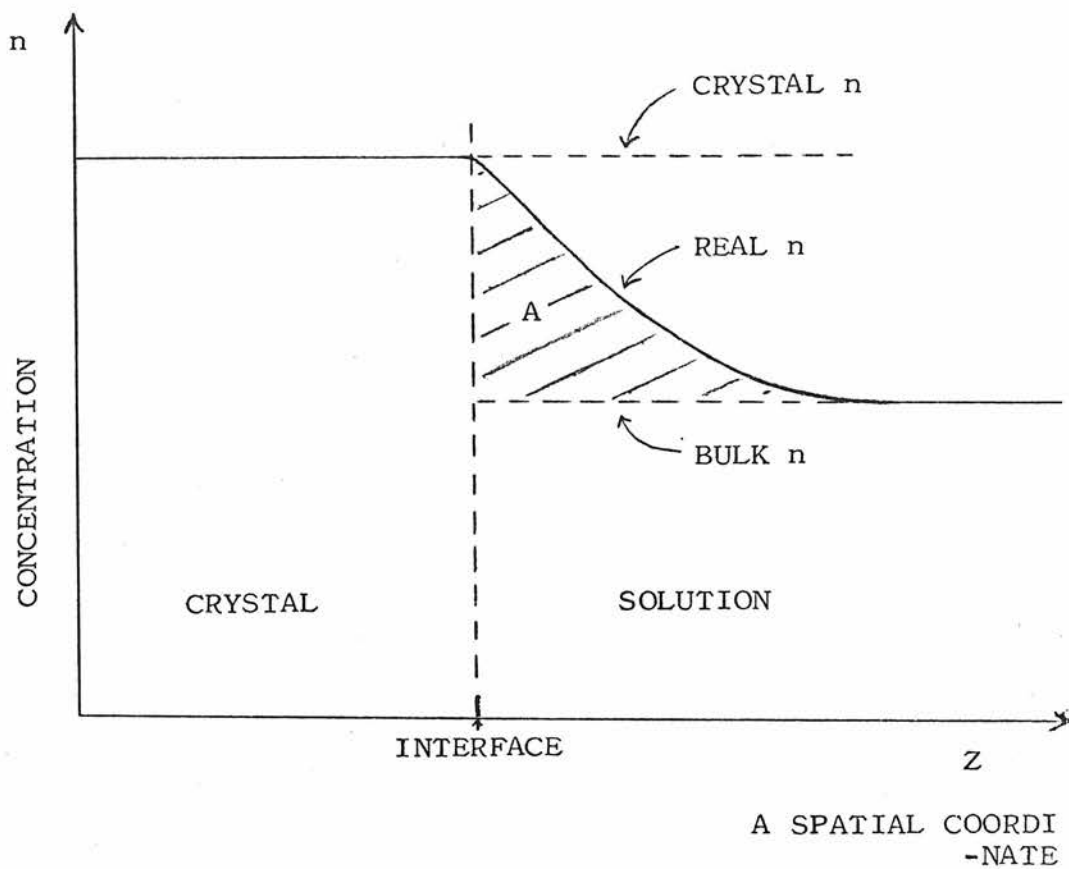
Fig. III.1.

the controlled phase change (crystal growth). The selection of a particular force of growth is, as is explained in 1) above, dependent on the solubility curve.

3) Supersaturation, mobility and the mechanism of growth.

An important point to make is that supersaturation of some degree is an absolutely essential property of a solution if a single crystal is to be grown by the usual methods. Both the quality of temperature control needed and the mechanism of growth are directly related to the degree of supersaturation. Figure III.2 shows what could be the situation near an interface of a crystal and the solution it is growing from. The principle is that the less the area A penetrates into the solution the better the result is likely to be. This can be achieved by stirring and by increasing the mobility of the solution (where possible). Stirring must not cause turbulence (this leads to uneven growth). The mobility of a solution can often be increased by raising the temperature of growth. Effects of concentration gradients, causing uneven growth, are much lessened by periodically reversing the stirring action (see 5) below).

At a very low degree of supersaturation ($1^{\circ}/o$, say) the layer growth mechanism becomes virtually impossible, due to the difficulty in forming a new layer. The growth at low supersaturation necessarily involves the dislocation mechanism such as the screw dislocation mechanism, where it is impossible to complete a layer. A very high degree of supersaturation means a greater probability of nucleation in the solution.



A possible concentration gradient
 near a CRYSTAL-SOLUTION interface.

Fig. III.2.

4) Control of temperature. If a crystal grows, dissolves a little and then grows again, shaded regions appear inside the crystal due to strains associated with irregular growth. It is therefore essential to control the temperature such that no dissolving of the growing crystal is possible at any time; also, sharp drops in temperature cause uneven growth and possible nucleation.

5) Environment. The effects of impurities can be any of the following:

- a) alteration of the physical properties of the crystal;
- b) alteration of the crystal growth habit and/or growth rate;
- c) change in the degree of supersaturation that the system will support (usually lessens the possible degree of supersaturation).

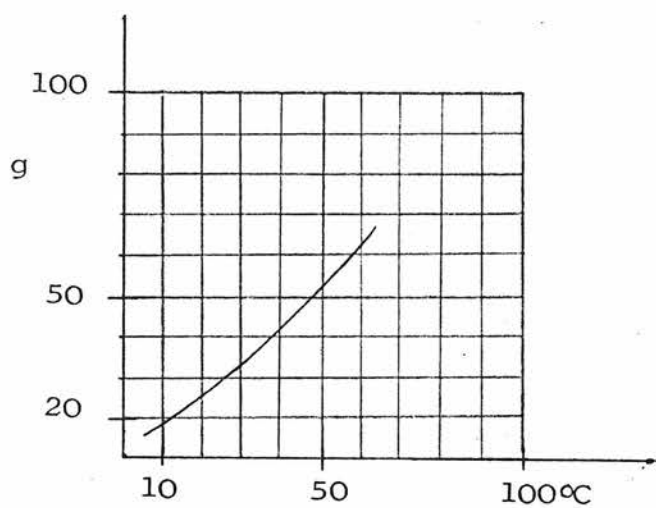
One important general rule of crystal growing is that the less the fractional change that the growing of the crystal in the solution causes, the better is the chance of success, i.e. at best the solution should be an infinite sea.

The nearest environment of the crystal should be as free from concentration gradients as can possibly be achieved with non-turbulent and periodically reversed stirring.

III.1.b In practice, DTGS

Figure III.3 shows the solubility curve for TGS in water (Nitsche, 1958).

In view of Section III.1.a above we can readily appreciate that TGS should have a reasonable growth-rate, whether we choose



The solubility curve for TGS in H₂O;

g = grams TGS / 100 grams H₂O

(after Nitsche, 1958)

Fig. III.3.

to select T or Ω as a force of crystal growing. (TGS has also been grown by Nitsche, 1958, using the method of transport across a gradient).

Crystals of TGS could readily be obtained by simply dissolving TGS in water, reacting the solution with the proper amount of H_2SO_4 , $(NH_2CH_2COOH \times 3 + H_2O \times \Omega + H_2SO_4 \times 1)$, and then leaving this, in a beaker say, to evaporate slowly. The resulting crystals necessarily suffered from inadequate T control and/or the effects of concentration gradients (see Section III.1.a).

Further problems were introduced when a deuterated crystal was needed. In glycine the CH_2 groups are less likely to exchange H for D than are the NH_2 and $COOH$ groups. Rather than to try the simple method of dissolving and regrowing the protonated crystals repeatedly in D_2O , only deuterated materials were used. Because of the limited availability of glycine - d_5 and therefore the excessive cost of this material, the amount of the solution available was limited to 40 grams of glycine d_5 .

In order to avoid exchange the solution had to be produced in and only kept in contact with a hydrogen free atmosphere. This meant that the whole experimental setup had to be enclosed in a "drybox" under a slight +ve pressure of a gas such as N_2 .

Figure III.4 shows the experimental setup used for growing the DTGS crystals. The solution is kept in a glass vessel which is enclosed by a water jacket through which temperature controlled water is pumped. The vessel containing

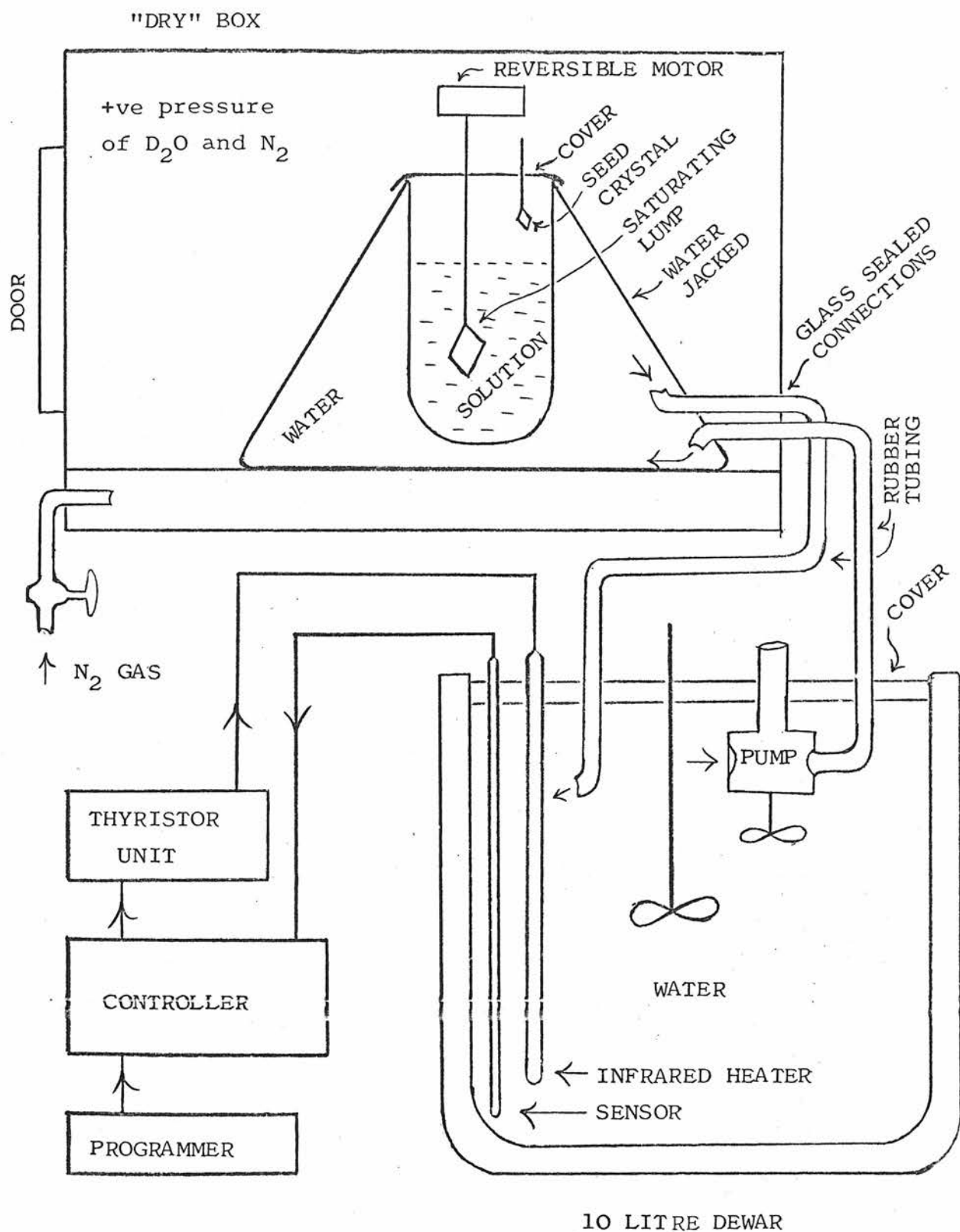


Fig. III.4.

The crystal growing setup for DTGS

the solution is covered in order to keep the temperature above the solution near to the temperature of the solution. This has a double purpose: 1) to avoid thermal shock to the grown crystal when it is lifted out of the solution and 2) to ensure that the seed crystal has a temperature very close to that of the solution when it is lowered into the solution. The temperature controlling water is completely sealed from the inside of the "drybox" in which the crystal growing vessel is situated. The inside of the "drybox" is kept under a slight +ve pressure of N_2 gas (and some D_2O vapour) to avoid exchange. The water used for temperature control is pumped through rubber tubing from a 10 litre water heat bath in a covered double wall Dewar flask. Temperature control is achieved via infrared heater and platinum resistor (as sensor) connected to a West Instrument controller/programmer with proportional integral and differential controlling actions. The programmer makes it possible gradually to decrease or increase the setpoint at an adjustable rate.

The procedure followed was first to obtain some crystals by the simple method described earlier (but inside the "drybox"). Some of the smaller crystals were then selected as potential seeds and one of the larger ones as a saturating lump. The saturated solution was time consuming to obtain but equilibrium condition was assumed when no growing or dissolving could be detected on or off the saturating lump for four days. The seed was cut so as to expose maximum relative surface of the faces of easiest (fastest) growth since the first growth on a seed is the most critical.

The seed crystal was suspended with a platinum wire and kept above the solution under a cover, see Fig. III.4, before being lowered into it. When the seed had been lowered into the solution and growth had already started, the saturating lump was lifted out. The seed (and the saturating lump) was kept moving in the solution by the action of the reversible motor. The setup was meant to enable growth of large crystals of DTGS and the final result was a crystal of ~ 6 grams.

III.2 Crystal Testing and Grinding

III.2.a DTGS

A suitable crystal grown of DTGS (Section III.1) was selected for a test of its dielectric constant as a function of temperature. A slab was cleaved perpendicular to the b axis - the ferroelectric axis. After painting silver electrodes onto the b faces, the crystal was put into an oven and connected to an a.c. bridge operating at 1592Hz. This experiment was carried out with Mr. F. Placido of this Department.

The resulting capacitance C and $1/C$ are shown plotted in Figures III.5 and III.6, respectively, as a function of temperature. The sample can be seen to be well behaving, giving a transition temperature of about 57°C . The measurements were made to give a rough idea of the state of the sample (to detect depression of the dielectric anomaly due to strains caused by irregular growth) and no attempt was made to correct for capacitance of the leads. A systematic error in temperature, of the order of 2° , is also possible.

The deuterium content of a DTGS crystal grown (see Section III.1), was inspected in the Chemistry Department

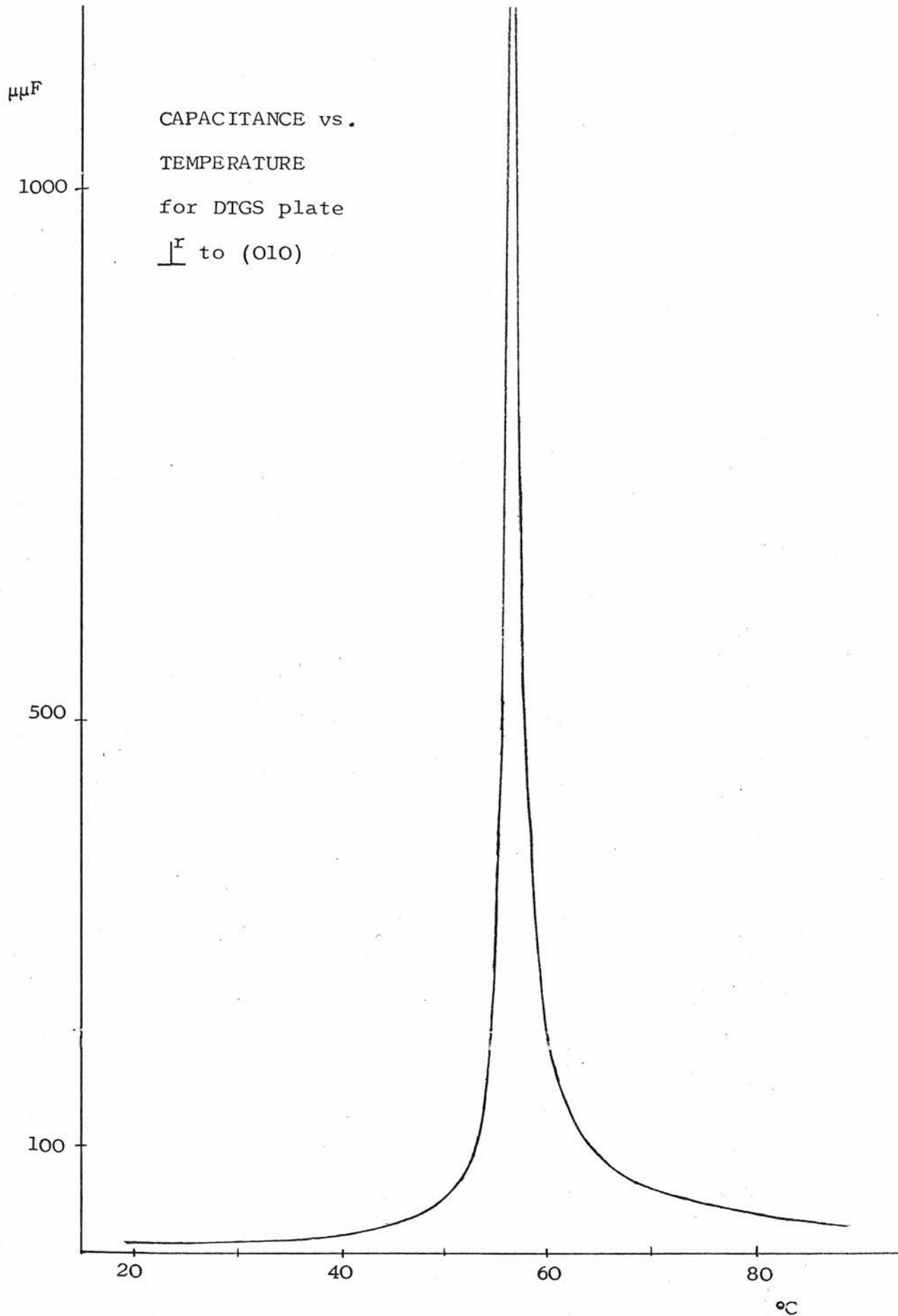


Fig. III.5.

RECIPROCAL of CAPACITANCE vs.

TEMPERATURE for DTGS plate

\perp to (010)

$(\mu\mu F)^{-1}$
 $\times 10^3$

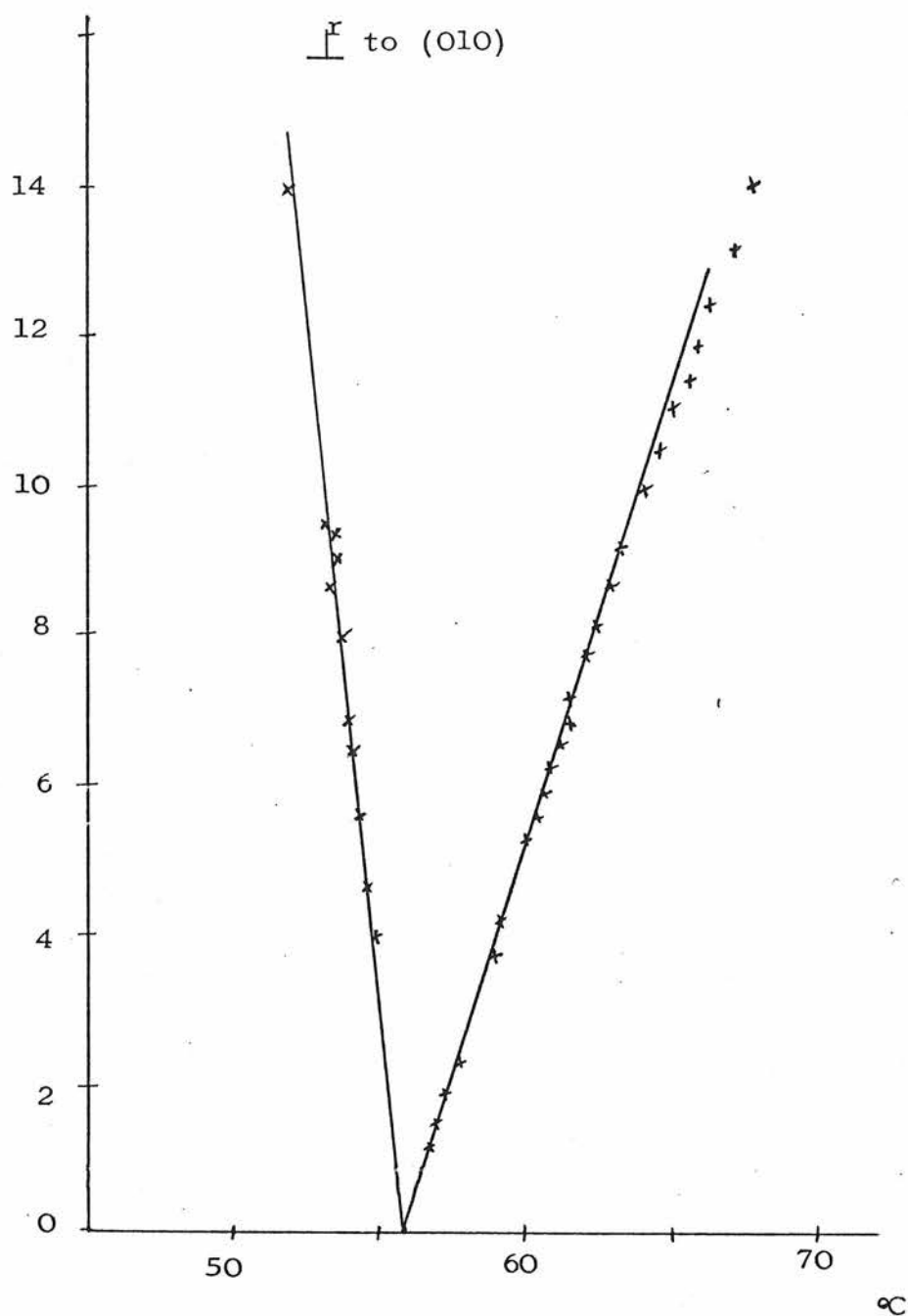


Fig. III.6.

of this University, by running the NMR spectrum (100 MHz) of the crystal dissolved in very pure D_2O ; this run was arranged by Dr. R.O. Gould. The conclusion from the NMR run was that the sample was better than 99% fully deuterated.

III.2.6 DKDP

Deuteration of KDP is not as much of a problem as it is with TGS, and DKDP crystals are available from commercial sources (but see effects at high deuteration levels, Section IV.1).

A commercially grown rectangular block of DKDP (tetragonal, see Section IV.1) of approximate dimensions 1 cm. \times 1 cm. \times 1.5 cm. was provided by Professor W. Cochran of this Department. This block is referred to hereafter as DKDPI.

DKDPI was sent to Dr. B.J. Isherwood (of the General Electric Company, Wembley, Middlesex) for estimation of its deuteration. His results (Isherwood, 1972), using a multiple diffraction method and a relationship between cell dimensions (a in fact) and the deuteration percentage, were:

$a, \text{\AA}$	$c, \text{\AA}$	% D
at a face centre:		
7.46785 ± 0.00010	6.97890 ± 0.00020	88 ± 1
at an edge:		
7.46810 ± 0.00010	6.97905 ± 0.00030	89.5 ± 1

The deuteration percentage, % D, was obtained by applying the formula

$$a = (7.45239 + 1.759/100 \times X) \text{ \AA} \quad \text{III.1}$$

where: $X = D/(D + H)$.

III.2.c. KDP

A crystal of KDP was obtained by Mr. K.D. Rouse from the Royal Radar Establishment, Malvern.

The crystal as grown was in the form of a rectangular prism 4 cm. long and 4 mm. \times 4 mm. average cross-section.

III.2.d Grinding

In order to make the correction for extinction effects simpler and to lessen the possible effect of beam non-uniformity during the diffraction experiments to come, the crystals used, both of DTGS and of KDP-DKDP, were ground to spheres ranging from 2-4 mm. in diameter.

The grinding was done by blowing the crystals round inside a tube of cylindrical cross-section lined with an abrasive material. The gas used was N_2 .

The crystals cut and ground from DKDPI (Section II.2.b) were designated: $DKDPI_1$, $DKDPI_2$ and $DKDPI_3$: they were 4 mm., 2 mm. and 3 mm. diameter spheres, respectively. A crystal of KDP (Section III.2.c) was ground to a 2 mm. diameter sphere. The variation in diameter over these spheres was within $\pm \frac{1}{4}$ mm.

The crystal used of DTGS was ground to a sphere of 4 mm. diameter ($\pm \frac{1}{2}$ mm.).

The spherical crystals were mounted on 1 mm. thick glass rods 3.5 cm. long, with the aid of glue such as "Durofix". The rods, holding the crystals, were then attached

to goniometer heads for the room temperature experiment (KDP, DKDP) or to a furnace which itself was attached to a goniometer head for the higher temperature experiment (DTGS at 80°C). For the low temperature experiments (KDP and DKDP) the crystals were glued with 'quickfill', a glue with good low temperature properties, to an aluminium wire of about 1 mm. diameter, which then was attached to a cryostat (see Section IV.2.b).

CHAPTER IV

STRUCTURAL STUDIES OF THE SYSTEM KDP-DKDP

IV.1 Introduction

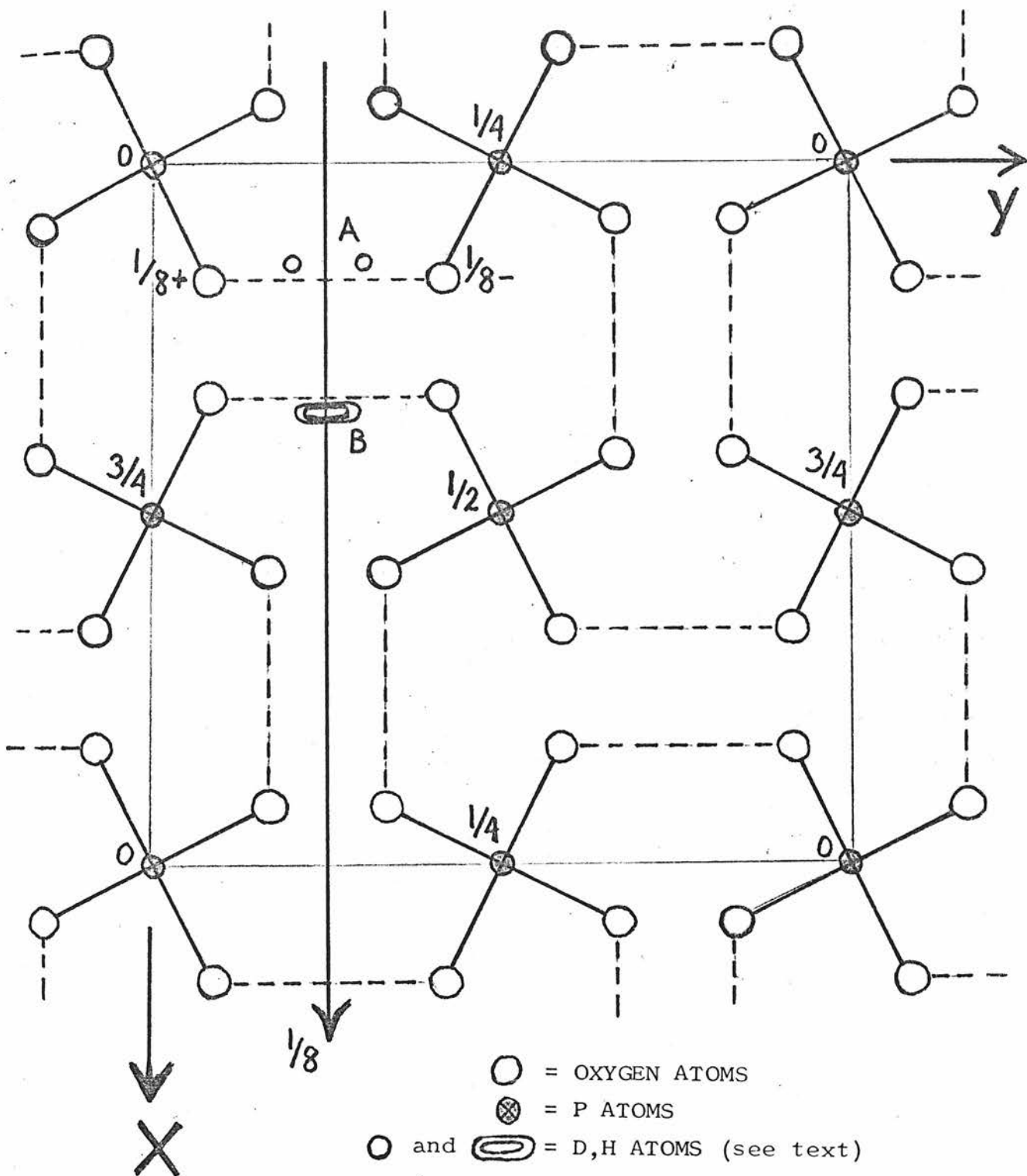
A ferroelectric phase transition at 122°K in KDP was first discovered by Busch and Scherrer (1935).

KDP is piezoelectric above this transition and many of the numerous studies on KDP and isomorphous compounds are concerned with this property, and with the dielectric and the electrooptic properties (Jona and Shirane, 1962).

Because of the relative simplicity of its structure (see below) as compared with other hydrogen bonded ferroelectrics, KDP has received much theoretical attention; see, for example, reviews by: Tokunaga and Matsubara, 1966; Tokunaga, 1966; Cochran, 1969; Moore and Williams, 1972.

A crystal structure determination of KDP was first carried out by West (1930) at room temperature, using X-rays. West found the space group to be $I\bar{4}2d$ (see International Tables, 1962) and the tetragonal unit cell ($a = 7.43$, $c = 6.97$) to contain $4 \times \text{KH}_2\text{PO}_4$. West found the positional parameters of the K, P and O atoms, see Fig. IV.1, and associated the H atoms (correctly in fact) with the $X, \frac{1}{4}, \frac{1}{8}$ eightfold positions rather than the alternative $0, 0, Z$ in light of the O-O distances and, assuming hydrogen bonds, identified the X_{H} parameter with X_{O} (Fig. IV.1).

In West's Fourier analysis, however, no actual evidence appeared supporting the above location of the H atoms.



One unit cell of KDP. The structure is built up by PO₄ groups linked by hydrogen-bonds (dotted lines) nearly \perp^r to Z. The K atoms are half way between the P atoms along Z. A and B show the two possible D,H distributions considered (see text). One symmetry element is shown.

Fig. IV.1.

On the basis of West's structure Slater (1941) put forward the first microscopic theory of the ferroelectric phase transition in KDP, postulating as a mechanism of the transition an ordering process for the H atoms that were to be disordered in the paraelectric phase. Slater assumes that each proton can take one of two possible sites along a hydrogen bond connecting two PO_4 groups but only two protons (of four possible) can at any one time be nearer to any PO_4 group. Any configurations with other than two protons nearer to a PO_4 group are considered energetically unfavourable and are discarded. This model obtained experimental support from the structural study of Bacon and Pease (1953 and 1955), see below. The Slater theory and later versions thereof (see above mentioned reviews 1966, 1972) were able to explain well some properties of KDP, but the theory had the serious limitation of being unable to explain the large increase in the transition temperature on deuteration. In Slater's theory T_c depends solely on the energy difference between the two possible configurations and this quantity is not thought to be much dependent on the mass of the particle.

In attempting to explain this isotope effect Pirre (1949, 1955) proposed a model where the kinetic energy of the protons played an important role. This idea was further developed by Blinc (1960) in a tunnelling model (see Section I.5).

The most serious limitation of this approach is that the motion of the protons is mostly confined to the a-b plane, while the ferroelectric axis is the c-axis. It was emphasized by Cochran (1961) that the motion of the protons was not something independent of the other atoms (see below).

On the structural side Ubbelohde and Woodward (1947) and de Quervain (1944) established the space group of the ferroelectric phase to be the orthorhombic $Fdd2$. Frazer and Pepinsky (1953), carrying out further Fourier analysis on West's data using the difference synthesis (Section II.3), showed that there were indications from the difference maps of elongated electron density centred about the proposed proton sites. Frazer and Pepinsky concentrated their attention on the structural changes that take place and confined their attention to KDP at $T_c + 4^\circ K$ and at $T_c - 4^\circ K$. Their analysis did not give concrete evidence for the location of the protons in either phase. The difference observed between the R.T. structure of West and that of Frazer and Pepinsky at $T_c + 4^\circ K$ is thought to be mostly explainable in terms of the inaccuracy of West's data (Bacon and Pease, 1953). Structural studies of KDP, using neutrons, were carried out by Bacon and Pease (1953 and 1955), by Peterson, Levy and Simonsen (1953) and by Levy, Peterson and Simonsen (1954).

Only the work of Bacon and Pease will be considered here since their study is the most detailed and extensive to date. In their neutron study Bacon and Pease were able to locate the protons conclusively and obtain more accurate parameters for the O atoms.

In their study of the room temperature structure of KDP Bacon and Pease (1953) concluded, on the basis of Fourier projections (hko and hol data) that the diffraction method was unable to distinguish between the two possible descriptions of the proton distribution: 1) a pronounced thermal motion along the bond, possibility B in Fig. IV.1; or 2) protons

disordered between two sites separated by $.35 \text{ \AA}$, possibility A in Fig. IV.1; i.e. the protons are disordered in a double minimum well.

The nuclear density distribution obtained from the Fourier maps was elliptical elongated along the bond but was circular as viewed along the bond. Bacon and Pease argued that since their reliability index was low already for the ordered model, it seemed unlikely that the disordered model would give a significantly better fit. With $\lambda = .81 \text{ \AA}$ Bacon and Pease measured reflections out to interplanar spacing of $.46 \text{ \AA}$ but they felt that the accuracy of their data would not permit a conclusive distinction between the two models. Bacon and Pease also showed that the two models would introduce only small differences to the Fourier peak and considered that these differences would be within experimental error. Bacon and Pease hoped that by determining the crystal structure of KDP at much lower temperature, just above the transition temperature, the thermal motion of the protons would have decreased sufficiently to allow the two models to be distinguished. In a later study Bacon and Pease (1955) concluded from Fourier maps, this time based on hko and hhl projections, that, in spite of the improvement in resolution, the two models could still not be resolved on the basis of their data.

Figure IV.1 shows schematically the structure of KDP in its paraelectric phase. The PO_4 groups are linked with hydrogen bonds indicated by dotted lines. One symmetry element is shown, a diad at the height $z = 1/8$, the K atoms along z . The two possible proton distributions discussed here are illustrated in Fig. IV.1 and labelled A

for the disordered case and B for the ordered case.

Bacon and Pease (1955) determined the crystal structure of KDP in its ferroelectric phase conclusively (at $T_c - 45^\circ\text{K} = 77^\circ\text{K}$). It is convenient to use for the purpose of comparison the alternative space group $F\bar{4}2d$ for the paraelectric structure. The unit cell volume doubles, if \underline{a}_1 , \underline{a}_2 and \underline{c}_1 are the unit cell vectors for $I\bar{4}d2$ then $\underline{a} = \underline{a}_1 + \underline{a}_2$, $\underline{b} = \underline{a}_1 - \underline{a}_2$ and $\underline{c} = \underline{c}_1$ will be those for $F\bar{4}2d$ (see The International Tables, 1962) and will be very close to those of the $Fdd2$ unit cell below T_c .

In this study, as mentioned before, Bacon and Pease demonstrated the ordering of the H atoms onto one of two possible sites previously proposed by Slater (1941). They were also able to demonstrate that reversal of \underline{E} , the applied electric field, shifted the protons from one set of ordered positions to the other.

The relative parameter shifts found by Bacon and Pease for KDP, as it goes ferroelectric, were: in Å

<u>atom</u>	<u>X-shift</u>	<u>Z-shift</u>
P	0	0.073
K	0	- 0.047
O	0	- 0.007
H	0.20	0

which means that the protons move solely in the x-y plane whereas, as pointed out above, the ferroelectric axis is the c-axis.

In 1961 Cochran extended his theory of ferroelectricity (Cochran, 1960) (see Chapter I) to crystals of more general symmetries to include materials such as KDP. (It should be

noted here that for crystals of low symmetry such as Rochelle salt (see, for example, Jona and Shirane, 1962) modes cannot be described as purely longitudinal or purely transverse.)

From the structural studies of Bacon and Pease (1953, 1955) Cochran (1961) proposed a set of eigenvectors of the ferroelectric mode that should, according to the theory, exist in KDP and be coupled to the mode involving the redistribution of the hydrogen atoms. (This is not the current picture, see Cochran, 1969.)

The first observation supporting the ferroelectric or soft mode approach to KDP was made by Kaminow and Damen (1968). Using Raman scattering Kaminow and Damen detected a heavily damped mode in KDP and deduced a $((T - T_c)/T)^{\frac{1}{2}}$ variation for its undamped frequency. Plessner and Stiller (1969) used diffraction effects in incoherent neutron scattering to determine the proton distribution in KDP at room temperature and to demonstrate that the protons tunneled between two sites.

Plessner and Stiller claimed that 1) the protons were concentrated at two sites separated by 0.400 ± 0.025 Å, 2) the hydrogen bonds were inclined $6 \pm 3^\circ$ to the a-b plane and 3) the protons tunneled between these sites and there was considerable correlation in the proton fluctuations. In 2) above, what is meant is that a line joining the two sites of proton concentration is inclined to the c-axis.

Paul, Cochran, Buyers and Cowley (1970) carried out an experiment on the dynamics of D-KDP, using inelastic coherent neutron scattering. The choice of D-KDP rather than KDP is due to the large incoherent scattering cross-

section of the H atoms.

The object of this experiment was to detect the dispersion relation for phonon modes and to study any modes associated with the ferroelectric transition. They found that none of the undamped modes is directly associated with the ferroelectric transition, their frequencies being essentially independent of temperature. Their result resembles the result of Kaminow and Damen on KDP in that they found no well defined peak in the phonon spectrum whose frequency tended to zero as T tended to T_c^+ .

They measured the quasi-elastic scattering intensity and found that it could be reasonably well fitted with an Ising model (see equation I.8), using in the expression for the \underline{u}_χ in equation I.7 the displacements deduceable from Bacon and Pease's work on KDP, see table on p. 66.

From their data they were able to deduce $|F(\underline{K})|$, the moduli of some dynamic structure factors but did not report on attempts to fit these with new displacements \underline{u}_χ since Skalyo, Frazer and Shirane, see below, had carried out more extensive measurements.

Paul, Cochran, Buyers and Cowley considered that even though a reasonable fit was obtained by using the Ising model, this did not disprove the tunnelling model since in D-KDP the tunnelling integral Ω (see Section I.5) is small (the dynamics of the tunnelling model approaches the Ising model as $\Omega \rightarrow 0$, see Section I.5 and Cochran, 1969).

One point we want to emphasize here is that the assumption has been made that the structural parameters of DKDP were well approximated by those of KDP.

Skalyo, Frazer and Shirane (1970) deduced for DKDP, by careful study of the temperature dependence of the over-damped optic branch, the soft mode intensity at the zone centre of 60 Brillouin zones (at 225°K).

Least squares calculations fitting the intensities rather well, calculating the inelastic structure factors permitted a deduction of the relative atomic movements (eigenvectors) of the soft mode. (The soft mode intensity is equated with the temperature dependent contribution as extrapolated to $q = 0$.)

In addition to the eigenvectors proposed by Cochran (1961) from the structural study on KDP of Bacon and Pease, large z motion of the D atoms and a large distortional motion in the x - y plane of the oxygen tetrahedra were found. Skalyo, Frazer and Shirane used in expression I.3 anisotropic temperature factors then

$$W = \underline{K} \underline{B} K' / (16\pi^2)$$

where \underline{B} is the matrix of anisotropic Debye-Waller factors (see Chapter II).

Skalyo, Frazer and Shirane refined the diagonal terms in B_D assuming cross terms to be zero and that the thermal motion was the same for the two directions perpendicular to the bond, leaving two thermal parameters to be determined. The validity of these assumptions and indeed the assumption that the paraelectric phase was ordered, are later discussed in the light of the results presented in this chapter.

Further work on the eigenvectors of DKDP was carried out by Wallace, Cochran and Stringfellow (1972). They used the

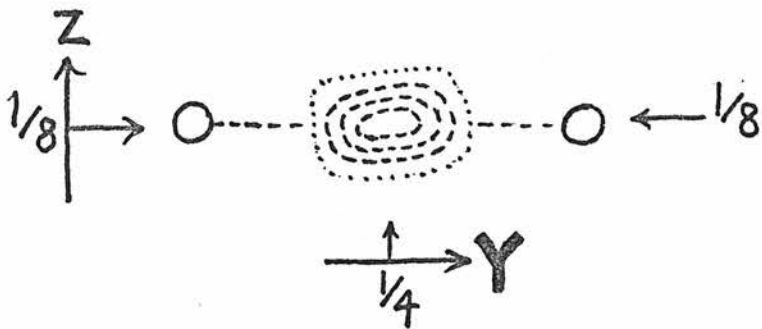
inelastic structure factors of Skalyo, Frazer and Shirane (see below) to determine the pattern of displacement of the atoms in the ferroelectric mode in DKDP by Fourier method, in which they constructed "eigenvector density maps".

Their results are in good general agreement with those of Skalyo, Frazer and Shirane and they find that not only is \underline{u}_D not directed along the hydrogen band but makes an angle of 22° to it. This large value of 22° for DKDP suggested an isotope effect of surprisingly large magnitude when compared with KDP ($6 \pm 3^\circ$), see above. It should be pointed out that we are, in DKDP, talking about an eigenvector making an angle with the O-O line, while in KDP we refer to a line joining maxima in the proton distribution making an angle with the O-O line. We do not, however, expect much difference between these angles.

This result pressed for re-examination of the validity of the assumption that KDP structural parameters were a close approximation to those of DKDP and also pressed for an accurate structural study of both KDP and DKDP with particular attention paid to the protons/deuterons on the short O-O bands.

The structure of DKDP had not been determined. Cochran (1972), after re-examining Bacon and Pease's structural work, pointed out that there was a suggestion of inclination of the elongated contours for the H atoms (from the Fourier map) to the O-O line, see Fig. IV.2.

This point was taken up by Nelmes, Eiriksson and Rouse (1972) who applied the methods described in Chapter II both to the 132°K data of Bacon and Pease and to preliminary room temperature DKDP data. Their results showed that the H, D atoms were disordered between two sites and that a line



A view down the X-axis of Fourier projection contours of the H atom distribution in KDP (after Bacon and Pease, 1955).

The distribution of the H atoms is elongated and there is a suggestion of a slight tilt of the direction of elongation to the O - O line.

Fig. IV.2.

joining these sites did make an angle with the 0-0 line. The results of Nelmes, Eiriksson and Rouse indicated an isotope effect and further data collection and analysis were planned (see later sections of this chapter).

When planning structural work on KDP and DKDP it was soon discovered that there were further complications arising from surprising temperature and isotope effects, some of which had been known for some time.

It was thought earlier that KDP decomposed from the tetragonal phase at 450°K (Kiehl and Wallace, 1927). Also Ubbelohde and Woodward (1939) found that at high deuteration levels the stable form of $\text{K}(\text{H}_{1-x}\text{D}_x)_2\text{PO}_4$ at room temperature was monoclinic. The point we wish to bring up immediately in this connection is that the samples of DKDP used in the dynamical neutron scattering experiments mentioned were claimed to be of high deuteration concentration and could, therefore, have been near a point when the tetragonal form no longer was stable; underlining the potential dangers of assuming the KDP structure for DKDP. Using dielectric and I.R. measurements, Grunberg, Levin, Pelah and Wiener (1967) found a high temperature transition near 450°K in KDP (the previously assumed decomposition temperature) that they concluded was not decomposition. They also examined DKDP and found two transitions on heating at 386°K and at 450°K . They concluded that since there was no isotope effect after the 450°K transition, tunnelling no longer took place at this temperature.

The high temperature phase transition in KDP was found by O'Keeffe and Perrino (1967) from conductivity measurements.

They also concluded this was not just decomposition.

Blinic et al. (1968) examined the high temperature transition in KDP by a variety of methods. They confirm the transition but conclude that it does not involve breakdown of H bonds and associate the transition with disordered hindered rotation of H_2PO_4 . From their X-ray powder studies they conclude that the crystal structure of KDP does not change in the temperature interval 293-450°K.

Blinic et al. (1969A) carried out a study of the high temperature transition in $\text{Rb H}_2\text{PO}_4$ and $\text{Rb D}_2\text{PO}_4$. They find that $\text{Rb D}_2\text{PO}_4$ (not known to be ferroelectric) is monoclinic at high T and propose it is isomorphous with room temperature monoclinic DKDP.

Blinic et al. (1969B) find a high pressure phase of $\text{Rb D}_2\text{PO}_4$ but do not find such drastic effects in KDP and do not conclude that there is a high pressure phase in KDP.

Rapaport (1970) claims six solid phases and a liquid phase from his PT phase diagram for KDP, using differential thermal analysis, and some data collected by other investigators (to whom he gives references). He claims that from room temperature up there are two solid-solid transitions, at 456°K and at 506°K and a solid-liquid transition at 531°K at atmospheric pressure.

Grünberg, Levin, Pelah and Gerlich (1972) examine KDP and DKDP in the temperature range 300-500°K, using dielectric and I.R. measurements. They find the transition, designated T_1 , at 448°K for both KDP and DKDP to be metastable below T_1 and to be dependent on PO_4 rotation. In DKDP they find the transition, designated T_ρ , at 383°K to be metastable below

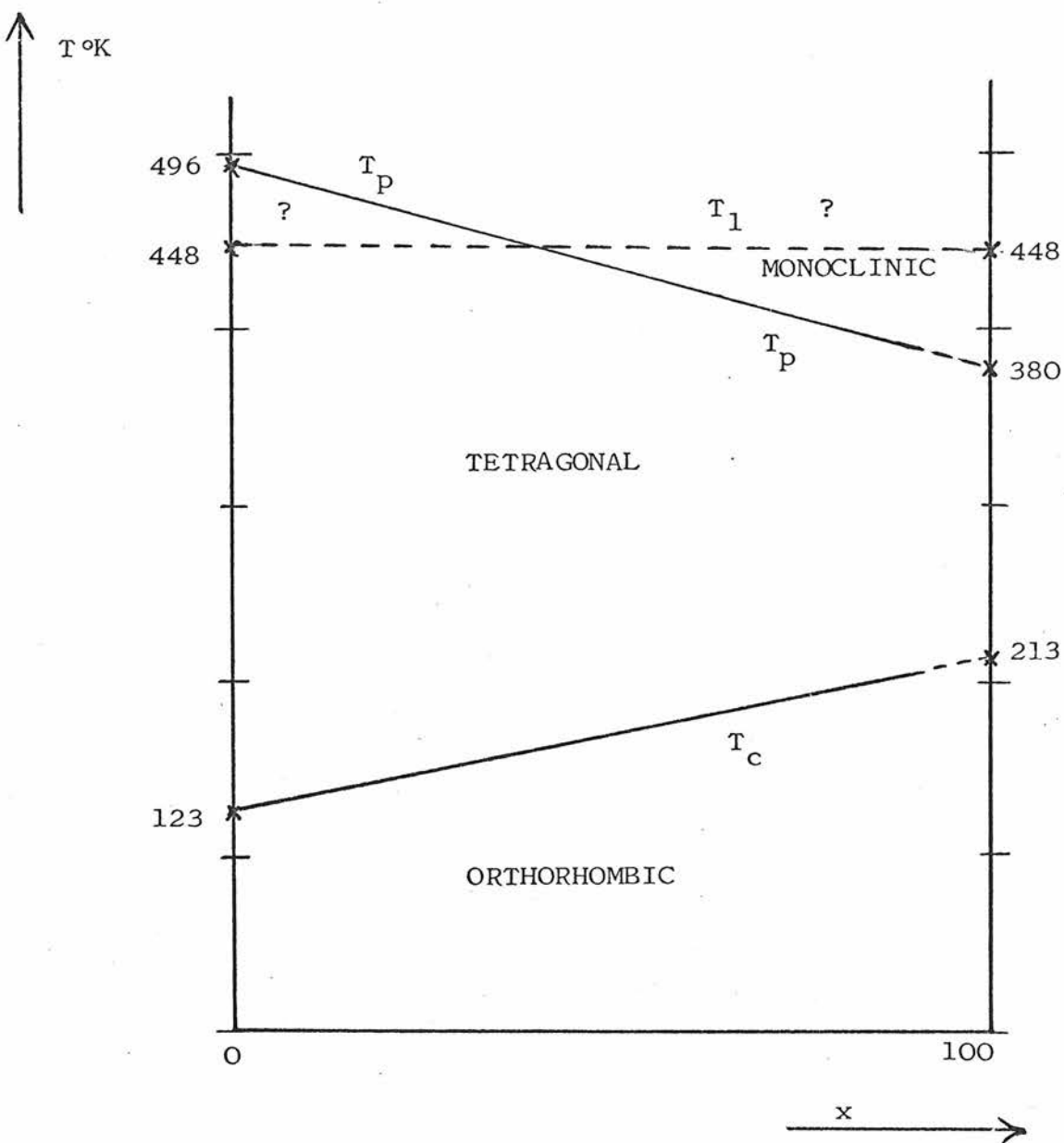
T_p they associate with change in H bond and a transition from tetragonal to monoclinic form.

Nelmes, (1972), determined the room temperature X-ray crystal structure of monoclinic DKDP. He finds, in view of the apparent ease by which the tetragonal to monoclinic phase change takes place, that surprisingly large relative atomic displacements are needed to bring one structure into the other.

Fig. IV.3 shows what is thought to be the most probable T-x phase diagram of the system $K(H_{1-x}D_x)_2PO_4$ on the basis of the experimental results published to date. But there is much uncertainty and the lines drawn are suggestions mostly. This uncertainty is illustrated by comparing Fig. IV.3 with Fig. IV.4, in which we present a possible phase diagram based on the work of Pereverzeva et al. (1972), who find two types of transitions in KDP and DKDP from their microwave dielectric measurements. T_1 , associated with PO_4 rotations, and T_2 "that can hardly be due to re-arrangement in crystal structure".

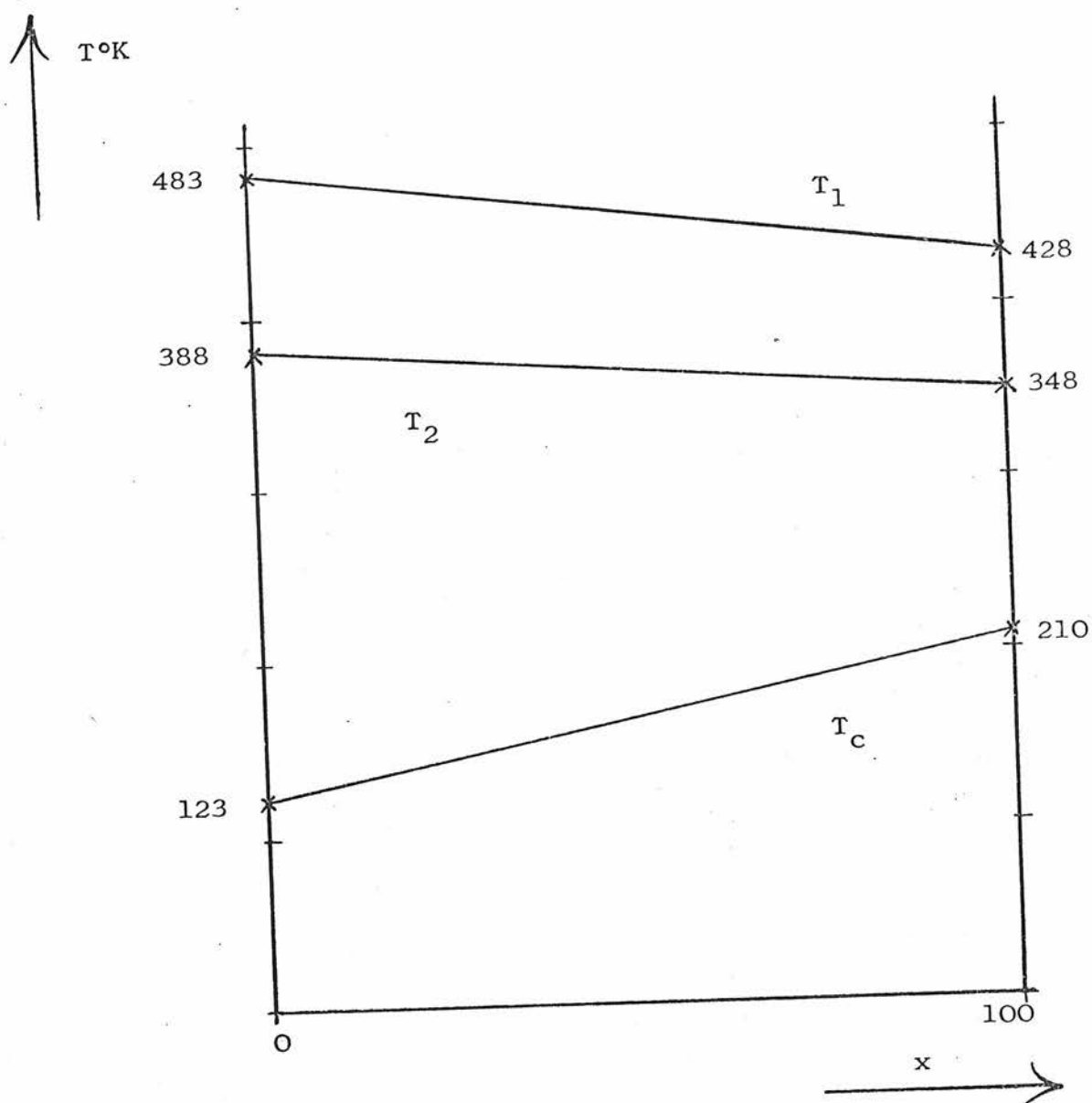
Before the work presented in this thesis was started, the only structural work in this whole phase diagram (x - T - P) were the studies at room temperature, $127^\circ K$ and $77^\circ K$ on KDP.

For any meaningful dynamical study on a crystal, involving the determination of eigenvectors, the crystal structure has to be known. One striking example of this need is provided by the work of Skalyo, Frazer and Shirane on DKDP, where uncertainty in an oxygen positional parameter, at that time, threw doubts upon their eigenvector determination.



The T-x phase diagram of the system $K(D_xH_{1-x})PO_4$ at atmospheric pressure; thought, on the basis of experimental work published to date, to be the most probable.

Fig. IV.3.



A possible T-x phase diagram of the system $K(D_xH_{1-x})_2PO_4$ based on the work of Pereverzeva et al (1972), at atmospheric pressure; compare with fig. IV.3.

Fig. IV.4.

The isotope effects on deuteration, resulting in a monoclinic phase on very high levels of deuteration, casts further doubts on the validity of assuming the structural parameters of KDP for DKDP, since dynamical experiments are usually carried out on samples of high deuteration near regions on the phase diagram where the monoclinic phase is the more stable phase.

There is thus a strong case for a comprehensive study of the whole system KDP - DKDP.

The present work on KDP and on DKDP is a part of a program undertaken to study crystal structure as it varies with deuteration and temperature over the $x - T - P$ diagram at atmospheric pressure.

IV.2 Data Collection and Handling

IV.2.a The room temperature data collection

For the data collection at room temperature the diffractometer was used in its normal beam equatorial setting shown in Fig. II.4.a and described in Section II.1.b. The cell dimensions, by fitting peak positions at low and high θ , were found to be in \AA :

	a	c
DKDPI	$7.468 \pm .003$	$6.979 \pm .003$
KDP	$7.453 \pm .001$	$6.959 \pm .001$

The scan type employed was the $\omega/2\theta$, or moving crystal-moving detector, type of scan (Section II.1.6) counting at 60 steps with step width of 0.04° (on ω). 5 steps at each end of the scans were used to estimate the average

background level. The step width was chosen as large as was reasonable within the limits of obtaining accurate representation of the reflections profile; in particular, care was taken to ensure that this condition was fulfilled near the focusing position of each instrument (Section II.1.b). Fig. II.6 shows two Bragg scans from a preliminary study of DKDP on Pluto channel I (Mk. II), takeoff angle 90° (see Section II.1.b); peak a in Fig. II.6 is at a Bragg angle of near 47° and peak b at 66° . Figure II.6 serves to illustrate that the step width is not unreasonably large. The counting time for each step, or the number of monitor counts specified for each step, was set to give a standard deviation of an average observed structure factor of about 1% (see Section II.1.c; in particular equations II.9-11). The equivalent structure factors then mostly agreed within 3-4 standard deviations. The point of this being that the accuracy in the observed structure factors is limited by the agreement of equivalent reflections rather than the counting statistics.

At regular intervals a reference reflection was measured as a means of checking the stability of the instrument and the alignment of the crystal; also at regular intervals all shafts of the diffractometer were stepped to their datum positions to check that their positioning was correct. Only data collected between checks that gave correct positioning and alignment (within 0.02°) was used in the analysis.

In all cases the c-axis, the tetrad, was oriented parallel to the ϕ axis of the instrument, see Fig. II.4.a.

The data sets collected were:

On sample DKDPI₁ (see Section III.2.c) on Pluto channel I (Mk II):

at $\lambda = 1.15\text{\AA}$:

A: in theta range 40° - 70° 6 equivalents in general

B: in theta range 1° - 40° 2 " " "

at $\lambda = 0.869\text{\AA}$:

C: in theta range 40° - 71.76° 6 " " "

D: in theta range 1° - 40° 2 " " "

On the same sample on Pluto channel II (Mk II)

at $\lambda = 1.14\text{\AA}$:

E: in theta range 1° - 70° some systematically

absent reflections examined and some low angle data collected for comparison of the reproducibility of the various data sets.

On sample DKDPI₂ (see Section II.2.c) on Pluto channel II (Mk II):

at $\lambda = 1.14\text{\AA}$:

F: in theta range 1° - 40° some data collected to enable the effect of extinction to be observed and estimated.

So far only data sets A, B, C and D, above, have been used quantitatively in the analysis of the room temperature structure of DKDP. Data set E was used to check some systematic absences and to check if there was an appreciable $\lambda/2$ component in the incident beam. Data set F was used to show that an extinction correction was needed throughout the data.

On sample KDP (see Section III.2.c) on Pluto channel I (Mk II)

at $\lambda = 1.147 \text{ \AA}$

G: in theta range 1° - 70° 6 equivalents in general.

This data set, G, was collected by Mr. K.D. Rouse of A.E.R.E., Harwell.

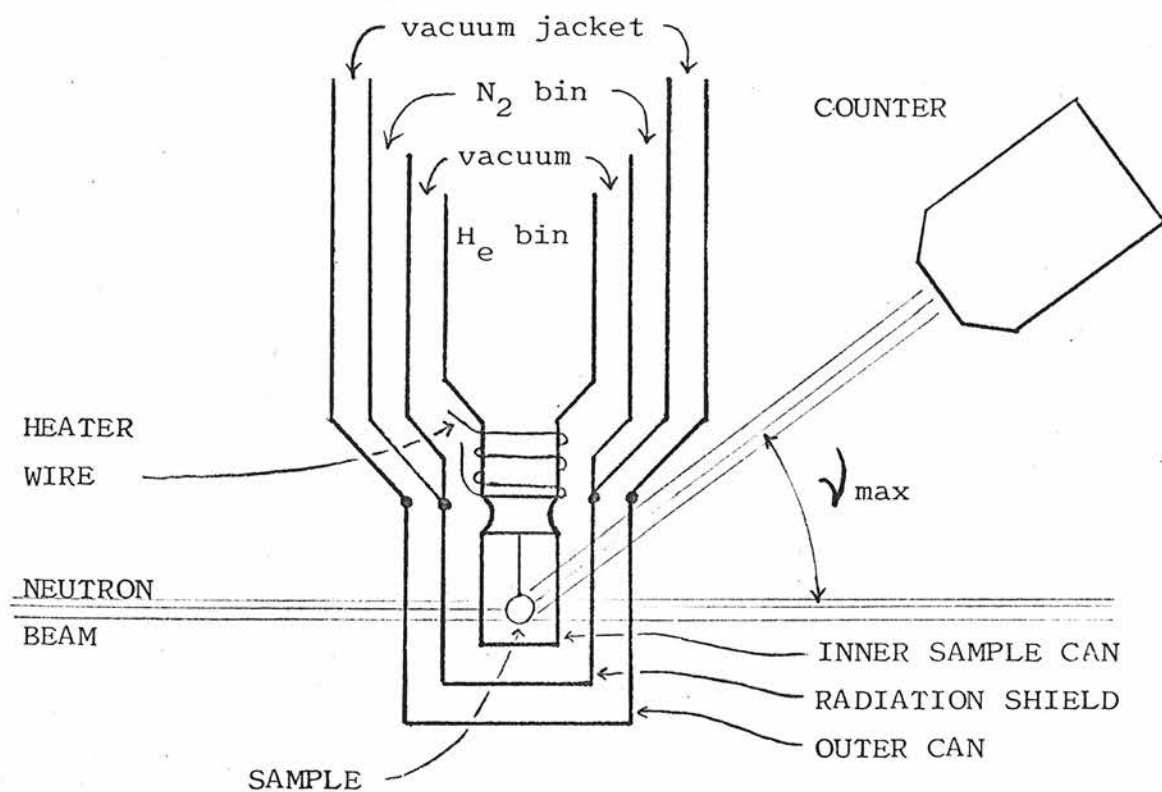
Iv.2.b The low temperature data collection

For the data collection at low temperatures a cryostat was used on a two circle diffractometer with a tilting counter as described in Section II.1.b. The cryostat used was an 'American Association' cryostat designed to give any temperature at the sample from liquid Helium to room temperature when used in conjunction with a 'Thor' 3 term temperature controller. With this set-up it was possible to maintain the temperature of the sample to within $\pm 1/8$ of a degree.

Fig. IV.5 shows the relevant section of the cryostat schematically. The important point to note is that, in tilting counter setting of the diffractometer with a cryostat, care has to be taken to limit ν (see Fig. II.4.b) of the experiment so as to avoid a situation where the scattered beam goes through the thicker sections of the cryostat, see ν_{\max} in Fig. IV.5.

The crystals were mounted with the c axis, the tetrad, vertical; parallel to the axis of ω rotation (and the symmetry axis of the cryostat).

The cell dimensions were found by fitting peak positions as in the room temperature study but due to the limited ν range of the tilting counter the uncertainty in c is rather large.



A schematic drawing of the cryostat illustrating the practical limitation on ν .

Fig. IV.5.

The cell dimensions found were, in \AA :

	a	c	$T_c + 5^\circ\text{K}$
DKDPI	7.433 ± 0.006	6.978 ± 0.010	213.8 ± 0.3
KDP	7.413 ± 0.002	6.918 ± 0.012	127

The transition temperature of DKDP was measured by observing the splitting of the 440 reflection on slow cooling and the reverse effect on slow heating. No thermal hysteresis was observed within the experimental error of $\pm 0.3^\circ\text{K}$.

The transition temperature of KDP was taken from the literature (see Jona and Shirane, 1962).

In order to eliminate possible errors in the observed intensities, as obtained from $\omega/2\theta$ scans through the Bragg peaks, due to powder diffraction from the aluminium windows of the cryostat, the background was estimated, using the peak offset scan (see Section II.1.c). In this case the background is effectively subtracted point for point from the peak scan so that whatever the detail of the unwanted scattering is in the peak scan it is, in the background scan, explored in the very same detail.

Other considerations and procedures were identical with those of the room temperature data collection, Section IV.2.a.

The data sets collected were:

on sample DKDPI_3 (Section III.2.c) on Dido channel II (Mk VI):
at $\lambda = 1.084 \text{\AA}$

H: in theta range $1^\circ-60^\circ$; with $0 \leq l \leq 3$;

2 equivalents in general;

at $\lambda = 0.882 \text{\AA}$

I: in theta range $1^\circ-60^\circ$; with $0 \leq l \leq 4$,

2 equivalents in general.

Data sets H and I, above, were collected both at $T_c + 5$ and at $T_c + 10$ but only the data set I, and of that only data collected at $T_c + 5$, has been used, so far, in the analysis of the structure of DKDP close to its transition temperature. The reason for limiting the range of theta values in the collection of data sets H and I was the low focusing angle ($2\theta_{\text{focus}} \approx 45^\circ$) of the instrument as installed.

On sample KDP (Section III.2.c) on Pluto channel I (Mk II, but modified to take a tilting counter) at $\lambda = 0.871 \overset{\circ}{\text{A}}$

J: in theta range $1^\circ - 70^\circ$; with $0 \leq \ell \leq 3$,
equivalents in general.

The data collected on KDP was collected by Mr. K.D. Rouse of A.E.R.E., Harwell.

IV.2.c Data handling

Data as collected was recorded on the magnetic tapes of the PDP-8 computers controlling the experiments.

All of the data collected on DKDP (Section IV.2.b) was transferred onto a large magnetic tape, using a program of Mr. I. Ferguson of A.E.R.E., Harwell.

From this tape all further data handling was carried out on the multi-access system (EMAS) of the Edinburgh Regional Computing Centre (E.R.C.C.). The transfer of the data onto EMAS was carried out by Mr. R.R. McLeod of the E.R.C.C.

It was found during data collection that occasionally pulses of electronic nature, in particular from teleprinters, caused excessively large numbers of counts to be recorded at one or more steps in a scan.

In order to eliminate errors arising from such effects a program was written to flag spurious counts in all scans.

The spurious counts were discarded and replaced by the mean value of the counts at either side.

The corrections made were assessed in each individual case and scans were discarded wherever the interpolation was thought not to give a reasonable representation of the peak profile.

The moduli and standard deviations of the observed structure factors were extracted from the data using the procedure described in Section II.1.c.

With the observed structure factors and their standard deviations, as estimated using the counting statistics, a program was written to assess the agreement within all sets of symmetry equivalent structure factors. The mean value of each set was used to represent the corresponding non-equivalent observed structure factor.

The data collected by Mr. K.D. Rouse of A.E.R.E. Harwell on KDP, was reduced to structure factors using the formulae of Section II.1.c. The program used was that of Dr. B.H. Bracher of A.E.R.E., Harwell.

The averaging of equivalent reflections was carried out using a program written by Mr. K.D. Rouse.

IV.3 Structural features to be tested in KDP - DKDP

What follows is a verbal description of the structural features that were tested and assessed in KDP and DKDP; the mathematical modelling of these features is described in detail

in Section IV.4 (in order of constraint number as indicated below).

In Chapter I and in Section IV.1 we have summarized the relationship of structural work to the more general study of phase transitions and dynamical work in particular. In this context the structural details of KDP and DKDP have been examined in the light of the previous studies of their dynamics.

We first of all concentrate attention on the distribution of the D, H atom in the short hydrogen bond.

The first question we ask is whether the D, H atom is disordered between two sites or is ordered, being in a special position on a twofold axis (constraints 10, 11, 12 and 13 in Section IV.4). The second question about the distribution of the D, H atoms, which stems from the dynamical work described in Section IV.1, is whether the D, H atoms actually do lie, if disordered, on the O-O line or - if not disordered - whether their principal thermal motion is directed along that line (constraints 14 and 8 in Section IV.4).

The angle made by either a line joining the D, H sites or by the direction of principal thermal motion with the O-O line is to be compared with the values from the dynamical experiments (noting however that when we compare this angle with that obtained for eigenvectors, we are comparing static distribution with dynamical results and there is not a direct comparison, see Section I.5).

In the work of Skalyo, Frazer and Shirane (1970) it became important to know whether the z coordinate of the O atom happened to have the value $c/8$ (see Section IV.1), because

if this were the case some of their resulting eigenvectors would be undetermined, due to overlap of the O atoms in the particular projection concerned $[0\ 1\ 0]$ (Wallace, Cochran and Stringfellow, 1972). We therefore ask the question whether z of O is $c/8$ (constraint 5 in Section IV.4).

Another question asked was whether the D, H atoms have the same x coordinate as the O atom, or better, whether the distribution of the D, H atom is centred about the centre of the O-O line (constraint 7 in Section IV.4). In order to assess the possibilities of disorder further we test the thermal motion of all atoms, asking whether that of the K, P, O and D, H atom is isotropic. In particular we looked to see if there is any pronounced thermal motion of the K and the P atoms along the c - the ferroelectric - axis; and if the principal thermal motion of the D, H atom - if disordered - is directed along the D, H - D, H line.

From the point of view of more general structural interest we tested whether the PO_4 group forms a regular tetrahedron (constraint 6 in Section IV.4) and whether for the D, H atom - if disordered - there is any significant thermal motion along directions forbidden by symmetry for the ordered model, e.g. a x - y component (constraints 9, 10 and 11 in Section IV.4).

The modelling of these features is described in the following section (IV.4) in numerical order of constraint number.

IV.4 The Models of KDP - DKDP and their Formulation

The models or constraints described in Section IV.3 are formulated below.

constraints 1 and 2: By symmetry the P and the K atoms, when treated as anisotropic in their thermal motion, have:

$U_{22} = U_{11}$ and $U_{ij} = 0$ for $i \neq j$. This constraint is a special case of constraints 3 and 4 below.

constraints 3 and 4: The P and K atoms have isotropic thermal motion; this particular constraint was formulated in Section II.2.c.

We require $U_{33} = U_{22} = U_{11} = U'_{11}$, where we only refine U'_{11} , and $U_{ij} = 0$ for $i \neq j$.

We treat U'_{11} as the independent variable, and find the derivative of f_j with respect to U'_{11}

$$\frac{\partial f_j}{\partial U'_{11}} = \frac{\partial f_j}{\partial U_{11}} + \frac{\partial f_j}{\partial U_{22}} + \frac{\partial f_j}{\partial U_{33}}.$$

This is equivalent to constraints 1 and 2 above when we treat U_{33} as an additional independent variable and therefore omit the last term in the above equation.

constraint 5: The z coordinate of the O atom is $= c/8$ in which case a line joining the hydrogen bonded O atoms is confined to the x-y plane, see Fig. IV.2.

constraint 6: The PO_4 group forms a regular tetrahedron.

The O atoms, in a general position, are operated on by the $\bar{4}$ operation. An atom O at x y z relative to P is brought into positions $\bar{y} \bar{x} \bar{z}$, $\bar{x} \bar{y} \bar{z}$ and into $y \bar{x} \bar{z}$. For the resulting tetrahedron to be regular we require all angles between any pairs of P-O bonds to be identical. We

form the scalar product of each pair of vectors directed along the 4 bonds and equate the cosines of the two possible angles:

$$\cos(-z^2/d) = \cos((-x^2 - y^2 + z^2)/d)$$

where $d = PO$ distance. Apart from the trivial solution when $y^2 = x^2 = 0$ we have that:

$$x^2 + y^2 = 2z^2$$

We choose to treat $y' = y$ and $z' = z$ as independent variables with

$$\frac{\partial f_j}{\partial y'} = \frac{\partial f_j}{\partial y} + \frac{\partial f_j}{\partial x} \left(\frac{-y}{x}\right)$$

$$\frac{\partial f_j}{\partial z'} = \frac{\partial f_j}{\partial z} + \frac{\partial f_j}{\partial x} \left(\frac{2z}{x}\right)$$

representing the true derivative of f_j with respect to y' and z' .

constraint 7: The x coordinate of the D, H atom has the same value as the x coordinate of the O atom, see Fig.

IV.1. Treating $x' = x_O = x_{D,H}$ as an independent variable, we have:

$$\frac{\partial f_j}{\partial x'} = \frac{\partial f_j}{\partial x_O} + \frac{\partial f_j}{\partial x_{D,H}}$$

This constraint cannot be applied (in this form) simultaneously with constraint 6.

constraint 8: The D, H atoms vibrate along the O-O line, that is: a principal axis of their thermal ellipsoid is directed along a line joining the two nearest O atoms.

This constraint is not strictly relevant to the results since it was primarily intended to be applied in the case when the D, H atoms were ordered, which turned out not to be the case; its formulation is analogous to that of constraint 9.

constraint 9: The D, H atoms vibrate along the D,H - D,H line, see Fig. IV.2; or, a principal axis of their thermal ellipsoid is directed along a line joining the two possible D, H sites.

This constraint is only relevant when the D, H atoms are considered to be disordered.

The constraint is that for the D, H atoms:

$$U_{23} = (U_{22} - U_{33}) \tan \theta / (1 - \tan^2 \theta)$$

where $\tan \theta = (c/4 - 2z)/(b/2 - 2y)$. Treating

$$U'_{22} = U_{22} \text{ and } U'_{33} = U_{33}, z' = z \text{ and } y' = y$$

as independent variables but U_{23} as a dependent variable, we proceed as in previous examples with

$$\frac{\partial U_{23}}{\partial U'_{22}} = \tan \theta / (1 - \tan^2 \theta)$$

$$\frac{\partial U_{23}}{\partial U'_{33}} = - \frac{\partial U_{23}}{\partial U'_{22}}$$

$$\frac{\partial U_{23}}{\partial y'} = \frac{1 + \tan^2 \theta}{(1 - \tan^2 \theta)} \times \frac{2(c/4 - 2z)}{(b/2 - 2y)^2}$$

$$\frac{\partial U_{23}}{\partial z'} = \frac{1 + \tan^2 \theta}{(1 - \tan^2 \theta)^2} \times \frac{-2}{(b/2 - 2y)}$$

which then are substituted into equation II.46.

constraints 10, 11, 12 and 13: By symmetry we have for the D, H atoms: 10) $U_{12} = 0$, 11) $U_{13} = 0$, 12) $y = b/4$ and 13) $z = c/8$.

constraint 14: The D, H sites lie on the 0-0 line, see Fig. IV.2. This constraint applies only when the D,H atoms are considered to be disordered. The constraint is that

$$z_{D,H} = \tan \theta (y_{D,H} - b/4) + c/8$$

where

$$\tan \theta = (c/4 - 2z_0)/(b/2 - 2y_0) \quad ;$$

with $z' = z_0$ and $y' = y_0$ as independent variables, this constraint can be applied together with constraint 6 since in both cases $y' = y_0$ and $z' = z_0$ are independent variables.

constraints 15, 16: The D, H atoms, (15), and the O atoms, (16), are isotropic in their thermal motion.

constraint 17: The U_{33} thermal parameters of the P and K atoms are related by

$$U_{33}(P) = 0.5 \times U_{33}(K) \quad .$$

This constraint was applied during the refinement of low temperature DKDP data for reasons given later, see Section IV.6a.

IV.5 The Room Temperature Experiment on DKDP

IV.5.a The refinements

The refinements were carried out on data sets A, B, C and D simultaneously (see Section IV.2.a). One set of extinction parameter and scale factor was used for data sets A and B and another set for data sets C and D, since the wavelength was different for these two pairs of data sets, see Section IV.2.a. The extinction correction used was that of Cooper and Rouse (1970); see Appendix II. This correction was used in all subsequent refinements on KDP and DKDP data.

The starting parameters for the room temperature refinements were the parameters found by Bacon and Pease (1955).

In the initial stages of refinement the distribution of residuals (Section II.2) was examined both with f_i and with $\sin \theta/\lambda$. A weighting scheme was employed that smoothed the distribution of residuals with f_i and with $\sin \theta/\lambda$. The finally adapted weighting scheme made use of the counting statistics $\sigma(f_i)$ (see Section II.1.c)

$$\omega_i \propto 1/\sigma^2(f_i)$$

multiplied by an exponential function found to smooth the distribution

$$\omega_i \propto 1/\sigma^2(f_i) \times \exp(-\alpha f_i + \beta \sin \theta/\lambda)$$

where α and β were chosen from logarithmic plots of the residuals as a function of f_i and of $\sin \theta/\lambda$, these plots giving roughly straight lines.

The increased weight with $\sin \theta/\lambda$ is understood to be a consequence of the larger number of equivalent reflections

being collected at higher angles giving more accurate estimates at higher angles. The decreasing weight with f_i is taken simply to represent how the $\sigma(f_i)$ systematically fail to give the true random error. The exponential term otherwise remains unexplained.

The method of least squares with constraints (Section II.2) was applied, using the constraints described in Sections IV.3 and 5, refining separately the various models of interest.

All atomic positional coordinates and thermal parameters, not restricted by symmetry, were refined together with the 2 scale factors, 2 extinction parameters and the scattering length of the D, H atoms.

The extinction correction was up to 50% on \hat{f}_i .

The first model refined was the free disordered model, free meaning: without constraints other than those imposed by symmetry.

The point of central interest was to establish whether or not the free disordered model gave a significant improvement in fit as compared with the free ordered model.

It was established that the disordered model gave a very much better fit, see Table IV.1, to the data, making it pointless to carry out refinements on the ordered model with constraints on the principal direction of the D, H atoms.

All the refinements carried out converged properly.

IV.5.b The results

The significance of the parameters of the various refinements was assessed, using the method of hypothesis testing. The results are summarized in Table IV.1.

The first column briefly describes the model and also numbers the constraints involved for reference to Sections IV.3 and 4. Following the constraints in the table are: the number of parameters, $V' M_f^{-1} V$, the sum of residuals (Section II, 2); the conventional R-factor defined by

$$R = \frac{\sum (f_i - |\hat{f}_i|)}{\sum f_i}$$

where f_i and \hat{f}_i are the observed and estimated structure amplitudes respectively; b the difference in the number of parameters from the reference model, the free disordered model; α the level of statistical significance obtained on testing the constraint model against the reference model, α , as is explained in Section II.2, is the probability of being wrong in rejecting the hypothesis.

$n-m$, the number of observations - the number of parameters of the reference model, was $= 771 - 27 = 744$.

Correlations between parameters were nowhere large, less than 0.6, except between the scale factors and the extinction parameters (greatest values are quoted)

scale 1	-	scale 2	=	0.62
scale 1	-	extinction 1	=	0.91
scale 2	-	extinction 2	=	0.80

where 1 refers to data sets A and B and 2 refers to

data sets C and D; collected at $\lambda = 1.15 \text{ \AA}$ and at $\lambda = 0.882 \text{ \AA}$ respectively, see Section IV.2.a.

IV.5.c. The room temperature structure of DKDP

The D, H atoms are disordered and a line joining the two possible sites is inclined to the O-O line. The z coordinate of the O atoms does differ from $c/8$. The K and P atoms are anisotropic in their thermal motion. The thermal motion of the K atoms is more pronounced in the x-y plane than is their thermal motion along z.

The D, H atoms are anisotropic in their thermal motion but a principal axis of their thermal ellipsoid is not directed along the D,H - D,H line. $U_{13}(D,H)$ is different from zero but $U_{12}(D,H)$ is zero (since the data is not capable of detecting a difference of $U_{12}(D,H)$ from zero if there is any).

The PO_4 groups do not form a regular tetrahedron.

The question whether $x(D,H) = x(O)$ cannot be answered as clearly as most of the other questions asked. The level of statistical significance here is $\alpha = 0.0035$ which is the probability of being wrong in rejecting the hypothesis that $x(D,H) = x(O)$. We take this to mean that there is a strong experimental evidence that the x coordinate of the D,H atoms differs from that of the O atoms.

$U_{12}(D,H)$ aside, the experimental evidence is very strong for all the extra parameters to give a significant improvement to the fit - i.e. all of the constraints rejected.

The final parameters adapted for the room temperature structure of DKDP were those of the free disordered model but with $U_{12}(D,H) = 0$. The coordinates of the P and K atoms are fixed by symmetry to be (0,0,0) and (0,0, $\frac{c}{2}$) respectively. Also by symmetry, for the thermal parameters of the P and K atoms, we have that all cross terms $U_{ij} = 0$ and that $U_{22} = U_{11}$.

The final coordinates are given in Table IV.2; positional parameters (x,y,z) are given in $\frac{O}{A}$ units and thermal parameters U_{ij} are given in units of $\frac{O}{A^2/2\pi^2}$ (the U_{ij} 's, given in Table IV.2, are thus the elements of the matrix of the mean square displacements of thermal motion multiplied by $2\pi^2$).

Bondlengths (in $\frac{O}{A}$ units) and angles (in degrees) of particular interest are given in Table IV.3, Theta (θ) and phi (ϕ) are the angles made with the X-Y plane by, respectively, the line joining the D,H sites and the line joining the hydrogen bonded $\frac{O}{O}$ atoms, see Fig. IV.6.a. The X-P-O angle in Table IV.3 is the angle made with the X-Z plane by the P-O line, see Fig. IV.6.b.

IV.6 The Low Temperature Experiment on DKDP

IV.6.a The refinements

The refinements were carried out on one set collected off sample DKDPI₃ at $T_c + 5^\circ K$ (213.8 $^\circ K$) with $\lambda = 0.882 \frac{O}{A}$, see Section IV.2.b.

It is to be noted that the basic limitations to the refinement of the structure of DKDP at low temperature are due to the limited resolution of the data along the z-axis. The important questions of the disordering of the D, H atoms

Table IV.2

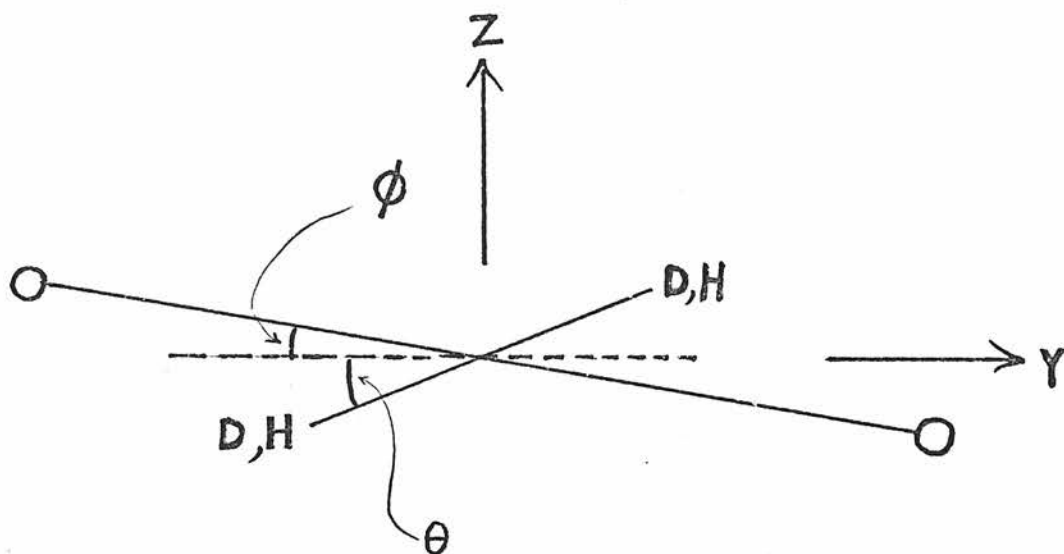
Atom	Param.	DKDP		KDP	
		<u>R.T.</u>	<u>L.T.</u>	<u>R.T.</u>	<u>L.T.</u>
K	U_{11}	0.4363(66)	0.2465(176)	0.3806(131)	0.1948(109)
	U_{33}	0.2780(11)	0.6942(144)	0.2483(247)	0.7686(2337)
P	U_{11}	0.2498(111)	0.1139(127)	0.2215(81)	0.1069(67)
	U_{33}	0.3225(74)	0.3471*(72)	0.2595(192)	0.4722(1581)
O	x	1.1117(5)	1.1117(13)	1.1089(8)	1.1075(9)
	y	0.6055(5)	0.6015(15)	0.6160(8)	0.6136(11)
	z	0.8818(6)	0.8865(70)	0.8715(15)	0.8851(35)
	U_{11}	0.3082(35)	0.1639(119)	0.3043(70)	0.1390(57)
	U_{22}	0.3235(35)	0.1752(113)	0.2867(95)	0.1428(53)
	U_{33}	0.3955(45)	0.3316(864)	0.3610(77)	0.4841(693)
	U_{23}	-0.0729(24)	-0.0942(224)	-0.0859(48)	-0.0174(124)
	U_{13}	-0.1046(27)	-0.1004(257)	-0.1192(84)	-0.0375(161)
	U_{12}	0.0395(19)	0.0170(62)	0.0425(51)	0.0199(50)
D,H	b(D,H)	0.642(10)**			
	x	1.1081(10)	1.1102(33)	1.0974(26)	1.1037(42)
	y	1.6453(9)	1.6380(37)	1.6736(29)	1.6802(40)
	z	0.8392(15)	0.8330(179)	0.8454(61)	0.8844(154)
	U_{11}	0.3981(74)	0.2318(165)	0.4606(147)	0.3794(162)
	U_{22}	0.4342(81)	0.2636(271)	0.4606*(147)	0.3794*(162)
	U_{33}	0.4637(103)	0.8446(1819)	0.4606*(147)	0.3794*(162)
	U_{23}	-0.0469(79)	-0.1807(701)		
	U_{13}	-0.0455(72)	0.0757(493)		
	U_{12}	0.0*	-0.0155(99)		

** corresponding to 98±1% deuteration (Bacon, 1972)

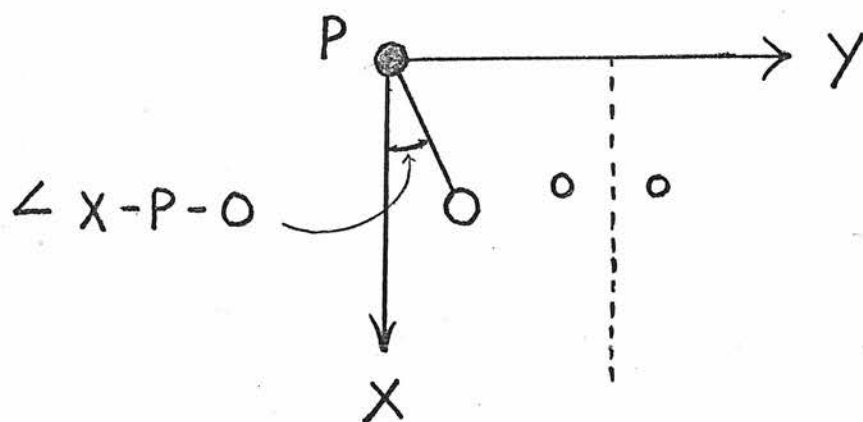
*these parameters were constrained.

Table IV.3

Structural features	DKDP		KDP	
	R.T.	L.T.	R.T.	L.T.
D,H - D,H bond	0.4483 (27)	0.4478 (105)	0.3806 (101)	0.3468 (79)
O - O bond	2.5230 (18)	2.5140 (44)	2.4944 (19)	2.4802 (24)
D,H - O bond	1.0407 (13)	1.0379 (44)	1.0596 (50)	1.0667 (41)
RATIO D,H - D,H/O - O	0.1777 (11)	0.1781 (42)	0.1526 (4)	0.1398 (32)
THETA angle	8.5 (4)	10.2 (4.5)	8.8 (2.9)	1.2 (7.2)
PHI angle	0.43 (4)	0.66 (33)	0.099 (78)	1.0 (2)
O - D,H - O angle	176.62 (13)	176.07 (90)	177.44 (43)	178.38 (84)
P - O - D,H angle	111.49 (13)	110.98 (90)	112.06 (43)	112.67 (84)
PO ₄ distortion:	1.51%	0.8%	2.85%	0.98%
tetrahedral angle minus:				
O(xyz) - P - O($\bar{x}\bar{y}z$)	0.40 (4)	0.22 (34)	0.75 (8)	0.26 (19)
O(xyz) - P - O($y\bar{x}\bar{z}$)	-0.81 (6)	-0.43 (36)	-1.51 (10)	-0.53 (20)
P - O bond	1.5427 (7)	1.5440 (43)	1.5392 (12)	1.5457 (24)
X - P - O angle	28.57 (2)	28.41 (7)	29.06 (4)	28.97 (5)



- a) A view of the hydrogen-bond down the X-axis, see figs. IV.1. and IV.2., illustrating the meaning of PHI, ϕ , and THETA, θ .



- b) An illustration of the meaning of the X-P-O angle, see fig. IV.1.

Some structural features in KDP-DKDP illustrated.

Fig. IV.6.

and of the D, H - D, H and O-O separations can, however, be answered since they primarily depend on the resolution in the x-y plane.

The starting parameters were the positional and thermal parameters of the room temperature structure (see Table IV.2), a scale factor and an extinction parameter (the extinction correction was up to 44% on \hat{f}_1).

The scattering length of the D, H atoms was fixed to the value found in the room temperature experiment.

The refinement of the free disordered model proved to be unstable when the P and K atoms were made anisotropic in their thermal motion; $U_{33} \neq U_{11}$ that is, for these atoms. $U_{33}(P)$ and $U_{33}(K)$ tended to a negative value and to a very high value respectively. It was decided to use the ratio of the thermal parameters of these two atoms, as refined when both atoms were made isotropic in their thermal motion, to predetermine the ratio of $U_{33}(P)$ to $U_{33}(K)$ such that the constraint

$$U_{33}(P) = 0.5 \times U_{33}(K)$$

was imposed. Imposing this constraint did not have an appreciable effect on the other parameters as compared with the refinement where the thermal motion of the P and the K atoms was made isotropic.

As a means of checking the data separate refinements were carried out, in the first instance, on the layers $\ell = 0, \dots, 4$ to see if there were systematic deviations with ℓ . This turned out not to be the case; the overall agreement from layer to layer was nearly the same and did not systematically change with ℓ .

Apart from the difference in number of parameters and the constraint imposed on the thermal motion of the P and K atoms, the refinements were carried out in an identical way to those of the room temperature DKDP experiment (Section IV.5.a).

There was a strong correlation between the scale factor and the extinction parameter together with three thermal parameters:

scale factor:	extinction parameter	0.8263
	- $U_{11}(P)$	0.7593
	- $U_{11}(0)$	0.8085
	- $U_{22}(0)$	0.7330

Other correlations were all less than 0.6.

IV.6.b The results

The method of hypothesis testing was applied in order to assess the significance of the various constraints. The results are summarized in Table IV.4, as described in Section IV.6.b.

$n-m$, the number of observations - the number of parameters of the reference model, = $211 - 23 = 188$.

The results are not conclusive wherever a z -dependent parameter is involved. With data of such low resolution along z the refinements are not expected to be sensitive to models involving z dependent parameters.

Table IV.4
DKDP L.T.

Constraint	No. of parameters	$V^1 M_f^{-1} V$	R- factor	b	a
'free' disordered	23	.58174	.091	0	-
5, Z(O) = $\frac{c}{8}$	22	.58777	.092	1	.1633
6, PO ₄ regular	22	.58609	.091	1	.2360
7, X(D,H) = X(O)	22	.58226	.091	1	.6844
12, 13, 'free' ordered	19	1.7243	.154	4	< .0000
14, D,H on O-O line	22	.58890	.093	1	.1289
15, D,H isotropic	18	.64590	.096	5	.0011

$$n - m = 211 - 23 = 188$$

IV.6.c The structure of DKDP at $T_c + 5^\circ\text{K}$

The D, H atoms are disordered but the questions whether the D, H atoms do lie on the O-O line and whether $z(0) = c/8$ cannot conclusively be answered. The relative thermal vibration of the K atoms along z , as compared with that in the x - y plane, cannot be assessed since the relevant refinement did not converge properly.

No significant improvement was obtained by letting $x(\text{D,H})$ be different from $x(0)$. The thermal motion of the D, H atoms is very probably anisotropic. The final parameters adapted for the low temperature structure of DKDP were those of the disordered model but with $U_{33}(\text{P})$ constraint, see Table IV.2.

The structural features of particular interest are given in Table IV.3.

IV.7 The Room Temperature Experiment on KDP

IV.7.a The refinements

The refinements were carried out on data set G, (see Section IV.2.a). The starting positional and thermal parameters were those of the room temperature structure of DKDP, see Table IV.2. In addition a scale factor and an extinction parameter were refined but the scattering length of the H atoms was fixed (all scattering lengths used in this thesis are those given by Bacon, 1972).

The extinction correction was up to 50% on \hat{f}_1 . It was found necessary, as it was with DKDP, to introduce a weighting scheme (described in Section IV.5.a) in order to smooth the distribution of residuals with f_1 and $\sin\theta/\lambda$.

It was expected that the H atoms, if disordered, were not disordered between sites as well separated as were those of DKDP. It was therefore expected that it would be more difficult in KDP, as opposed to DKDP, to distinguish between the ordered and the disordered models for the D,H atoms. The refinement procedure described in Section IV.5.a was carried out and the disordered model was established to give a significantly better fit (see Table IV.5) than did the ordered model. (The improvement in fit is, however, not quite as striking as it was in DKDP. It would therefore possibly be worth considering yet another model where higher order terms are used in the description of the thermal motion of the H atoms; this was not done here.)

All models refined converged properly or did so after introduction of damping factors to the parameter shifts, see Section II.2.c.

There was some correlation between parameters. We

give correlation coefficients greater than 0.6:

scale factor - extinction parameter		0.9706
	- $U_{11}(P)$	0.6175
	- $U_{11}(O)$	0.6936
	- $U_{22}(O)$	0.7156
extinction parameter	- $U_{11}(O)$	0.6039
	$U_{22}(O)$	0.6391
	y(H) - $U_{22}(H)$	0.8046
	z(H) - $U_{23}(H)$	0.6659

It is interesting to note that in spite of correlation coefficient of 0.8 between $y(H) - U_{22}(H)$ the disordered model does give a significant improvement in fit, see Table IV.5, over the ordered model. (When refining the disordered model with H isotropic there was a correlation of 0.6187 between the scale factor and $U_{11}(P)$.)

IV.7.b The results

The method of hypothesis testing was used to assess the significance of the improvement in fit between the various models as before. The results are summarized in Table IV.5; for explanation of Table IV.5, see Section IV.5.b. Where $\alpha = 1.0$ in Table IV the data is completely insensitive to the value of the relevant parameter, $U_{12}(H)$; this, however, is not surprising in view of the fact that the data is very insensitive to any possible anisotropy in the thermal vibration of the H atoms.

$n-m$, the number of observations - the number of parameters

Table IV.5
KDP R.T.

	Constraint	No. of parameters	$V^1 M_F^{-1} V$	R- factor	b	a
	free disordered	24	.10860	.045	0	-
3,	K isotropic	23	.11980	.048	1	< .0000
4,	P isotropic	23	.11012	.046	1	.0704
5,	Z(O) = $c/8$	23	.10962	.046	1	.1379
6,	PO ₄ regular	23	.18816	.059	1	< .0000
7,	X(H) = X(O)	23	.11881	.048	1	< .0000
9,	H vibrates along H-H line	23	.10882	.045	1	.4900
10,	U ₁₂ (H) = 0	23	.10860	.045	1	1.0000
11,	U ₁₃ (H) = 0	23	.10940	.045	1	.1886
12, 13,	free ordered	20	.12120	.047	4	< .0000
14,	H on O-O line	23	.11317	.047	1	.0018
15	H isotropic	19	.10958	.046	5	.8252

$$n - m = 259 - 24 = 235$$

for the reference model = $259 - 24 = 235$.

IV.7.c The room temperature structure of KDP

The H atoms are disordered and the H - H line is very probably inclined to the O-O line (although the level of statistical significance for the H atoms to lie on the O-O line is not quite as high as is that for R.T. DKDP).

As to the question whether $z(0)$ is different from $c/8$ we note that the significance of the better fit, obtained by relaxing that constraint, is not very great, $\alpha = 0.14$ in Table IV.5. This should be interpreted as indicative (that $z(0) \neq c/8$) rather than entirely conclusive.

The anisotropy of the thermal motion of the K and P atoms is less pronounced in KDP than it is in DKDP but the thermal motion of the K atoms is still more pronounced in the x-y plane than it is along z.

The $x(H)$ does differ from the $x(0)$.

The H atoms are very probably isotropic in their thermal motion, $\alpha = 0.83$ in Table IV.5.

The PO_4 group does not form a regular tetrahedron.

The final parameters adapted for the room temperature structure of KDP were those of the disordered model with the thermal motion of the H atoms constrained to be isotropic; these are listed in Table IV.2, with, as is explained in Section IV.5.c, (x, y, z) in $\overset{O}{A}$ units and U_{ij} in units of $\overset{O}{A}^2/2\pi^2$.

Structural features, bondlengths and angles, of particular interest are given in Table IV.3.

IV.8 The Low Temperature Experiment on KDP

IV.8.a The refinements

The refinements were carried out on data set J (see Section IV.2.b.) The starting parameters were those of the corresponding R.T. study, see Section IV.7.

The extinction correction was up to 43°/o on \hat{f}_1 .

The data is limited to give much less resolution up z than in the x - y plane, see Section IV.2.b.

The procedure followed was that of the R.T. refinements, Section IV.7.a. All refinements of the various models proved stable and converged properly.

The correlations found, quoting values greater than 0.6, were:

scale factor	-	extinction	0.9432
	-	$U_{11}(0)$	0.6566
$z(H)$	-	$U_{23}(H)$	0.7227

IV.8.b The results

The method of hypothesis testing was applied to the various models refined and the results are summarized in Table IV.6, as described in Section IV.5.b.

$n-m$, the number of observations - the number of parameters = $171 - 24 = 147$ for the reference model.

It should be stressed here that, as in Section IV.6, all conclusions based on values of z dependent parameters are necessarily limited in validity due to the limited resolution up z .

Table IV.6
KDP L.T.

	Constraint	No. of parameters	$V_M^{-1}V_F$	R- factor	b	α
	free disordered	24	.54806	.039	0	-
5,	$Z(O) = \frac{c}{8}$	23	.68245	.043	1	< .0000
6,	PO_4 regular	23	.56984	.041	1	.0095
7,	$X(H) = X(O)$	23	.54971	.040	1	.4715
12, 13,	free ordered	20	.65719	.049	4	< .0000
14,	H on O-O line	23	.54806	.039	1	1.0000
15,	H isotropic	19	.56005	.041	5	.5693

$$n - m = 171 - 24 = 147$$

The results show (Table IV.6) that although the data is completely insensitive to the $z(H)$ parameter ($\alpha = 1.0$), the constraint that $z(0) = c/8$ is rejected at a very high level of statistical significance ($\alpha < 0.0000$).

IV.8.c. The structure of KDP at $T_c + 5^\circ K$

The H atoms are disordered and the H atoms very probably do lie on the O-O line (or, to be precise, a line parallel to the O-O line).

The $z(0)$ is not $= c/8$. (This striking contrast in the sensitivity of the data to $z(0)$ as compared with that to $z(H)$ is truly remarkable).

The thermal motion of both the K and P atoms is more pronounced along z than it is in the x - y plane but in view of the low resolution up z no attempt is made to interpret this.

The $x(H)$ very probably does not differ from $x(0)$.

The H atoms are very probably isotropic in their thermal motion.

The PO_4 group does not form a regular tetrahedron.

The final parameters adapted for the structure of KDP at $T_c + 5^\circ K$ ($127^\circ K$) were those of the disordered model with the thermal motion of the H atoms constrained to be isotropic; these were listed in Table IV.2, with, as is explained in Section IV.5.c, (x, y, z) in $\overset{O}{A}$ units and U_{ij} in units of $\overset{O}{A}^2/2\pi^2$.

Structural features, bondlengths and angles, of particular interest are given in Table IV.3.

IV.9 Interpretation of the Results

Table IV.7 shows a summary of the results of the tests applied to the various data sets.

In Table IV.7 we list the questions asked and the answers deduced from our results; see Tables IV.1, 4, 5 and 6.

In the extreme cases, where the results are conclusive at a high level of statistical significance (α at least smaller than 0.01) and where the data is very insensitive to the tested parameters (α as large as 0.5 or greater), we give the answers as 'NO' and 'VERY PROBABLY', respectively in Table IV.7.

Where the value of α lies somewhere between the two extremes we give, in Table IV.7, the actual value of α obtained for the constraint involved. The smaller the value of α the smaller is the probability of being wrong in giving the answer 'NO' to the question concerned.

Where $\alpha = 0.16, 0.24$ and 0.13 for the L.T. DKDP data and where $\alpha = 0.07, 0.14$ and 0.19 for the R.T. KDP data, we can only say that the experimental evidence, for the additional parameters involved to give a significant improvement in fit, is weak and inconclusive (the stronger the smaller the α value).

It should be restated here that the limited sensitivity of the data to some of the parameter values could be a consequence of the limited resolution, to some extent, but no concrete assessment as to what extent is possible.

Where $\alpha = 0.49$ in R.T. KDP we understand this to be a

Table IV.7
Summary of tests on KDP - DKDP

QUESTION	ANSWERS			
	DKDP		KDP	
	R.T.	L.T.	R.T.	L.T.
is K isotropic	No	-	No	-
is P isotropic	No	-	$\alpha = .07$	-
is $Z(O) = \frac{c}{g}$	No	$\alpha = .16$	$\alpha = .14$	No
is PO_4 regular	No	$\alpha = .24$	No	No
is $X(D,H) = X(O)$	No	Very probably	No	Very probably
does D,H vibrate along D,H - D,H line	No	-	$\alpha = .49$	-
is $U_{12}(D,H) = 0$	Very probably	-	Very probably	-
is $U_{13}(D,H) = 0$		-	$\alpha = .19$	-
is D,H ordered	No	No	No	No
is D,H on O-O line	No	$\alpha = .13$	No	Very probably
is D,H isotropic	No	No	Very probably	Very probably

consistent consequence of the fact that the H atoms are VERY PROBABLY isotropic in their thermal motion.

Comparison of the tested features between:

1) DKDP and KDP at R.T.

shows that there is very little difference apart from

a) for DKDP $z(0)$ does differ from $c/8$ at a high level of significance (α less than 0.0000), while in KDP this difference is not very significant ($\alpha = 0.14$), and

b) the thermal motion of the D, H atoms in DKDP is anisotropic, while the thermal motion of the H atoms in KDP is VERY PROBABLY isotropic.

2) DKDP at R.T. and DKDP at L.T.

shows that $x(D,H)$ is significantly different from $x(0)$ at R.T., while at L.T. no significant improvement can be obtained by relaxing the constraint on $x(D,H)$.

3) KDP R.T. and KDP L.T.

shows, as for DKDP, that at R.T. $x(H) \neq x(0)$ but that $x(H) = x(0)$, VERY PROBABLY, at L.T.; but more important is that unlike the situation in DKDP, the H-H line, VERY PROBABLY, ($\alpha = 1.0$), is not inclined to the O-O line at L.T. This shows a marked isotope and temperature effect on the inclination of the D,H - D,H line to the O-O line. It is remarkable that $z(0)$ does, for KDP L.T., differ from $c/8$ at a high level of statistical significance (α less than 0.0000), while in KDP R.T. the difference is only significant at $\alpha = 0.14$. This is opposite to the temperature dependence of the difference of $x(0)$ from $c/8$ found in DKDP.

Table IV.3 gives structural features, bondlengths in A

units and angles in degrees. As expected, the D,H - D,H bond is shorter in KDP than it is in DKDP and the ratio, D,H - D,H bond to the O-O bond, also is shorter in KDP. This ratio does not change with temperature in DKDP (within error) while in KDP this ratio decreases with decreasing temperature by $9 \pm 3\%$.

The angles Theta, Phi and x-P-O are explained in Fig..IV.6. The PO_4 is elongated along z so that the angle $O(xyz)-P-O(\bar{x} \bar{y} z)$ is smaller than the tetrahedral angle, while $O(xyz)-P-O(y \bar{x} \bar{z})$ is larger than the tetrahedral angle.

The change in the various angles calculated and tabulated in Fig. IV.3, is generally small over the range of deuteration level and temperature considered; the P-O-D,H, O-D,H-O and the x-P-O angles show no marked variation (though significant). However, as discussed earlier, there is a marked effect on the angles Theta and Phi.

The most important conclusions to be drawn from the work are:

- a) Disordering of the D,H atoms is finally clearly established in DKDP and in KDP in their paraelectric tetragonal phases.
- b) The D,H - D,H line is inclined to the O-O line in R.T. DKDP and KDP by $8.9(4)$ and $8.9(3.0)$ degrees respectively and there is a marked isotope effect on the temperature dependence of this angle. The H-H to O-O angle found for R.T. KDP is, within error, consistent with the angle claimed by Plessner and Stiller (1969).

There is a surprisingly large and unexpected difference between the value of Theta (see Table IV.3) for DKDP and the angle (22°) made by the soft mode eigenvector of the D,H atoms with the x-y plane; as found by Wallace, Cochran and Stringfellow (1972), using the dynamical data of Skalyo, Frazer and Shirane (1970).

- c) No indication of soft motion in the thermal vibration of the K or the P atoms is observed.
- d) There is a marked isotope effect on the D,H - D,H bondlength and the ratio between the D,H - D,H and the O-O bondlengths. There is also a marked isotope effect on the temperature dependence of these.
- e) The z parameter of the O atoms does differ from $c/8$ (which means that Phi differs from zero, see Table IV.b.a) for R.T. DKDP and for L.T. KDP. This difference of $z(0)$ from the value of $c/8$ is not very significant in L.T. DKDP and in R.T. KDP, which indicates both temperature and isotope effects on the angle Phi.

IV.10 Application of Results

It is of interest to examine the effect of the structural assumptions made in the dynamical investigations on DKDP.

In investigations of KDP and of DKDP the structural parameters of KDP, as found by Bacon and Pease (1953 and 1955), are commonly assumed. In particular the D, H atoms are assumed to be ordered in single minimum wells.

We want to examine the difference this assumption makes to the contribution of the D, H atoms to the dynamic structure factor expression used by Skalyo, Frazer and Shirane (1970).

Skalyo, Frazer and Shirane (1970) used, in the dynamic structure factor expression (equation I.3), anisotropic temperature factors for the D, H atoms in which case:

$$W(\underline{K}) = \underline{K} B_{D,H} \underline{K}' / (4\pi^2) ,$$

where B is the matrix of anisotropic temperature factors related to the matrix of mean squares displacements U through: $B = 2\pi^2 U$. They then refined the thermal parameters of the D, H atoms with $B_{33} = B_{11}$ and $B_{13} = B_{23} = B_{12} = 0$ (B_{11} and B_{22} are thus the two independent variables). We compare the structural parameters of Table IV.2 for the R.T. DKDP data, disordered model, with the following which were obtained from the same dataset but with the ordered model:

x	U_{11}	U_{22}	U_{33}	U_{23}
1.1052	0.3402	2.0837	0.4545	0.2035

x is in $\overset{\circ}{\text{\AA}}$ units and U_{ij} are in units of $\overset{\circ}{\text{\AA}}^2/(2\pi^2)$ (by symmetry $y = 1.8669$ and $z = 0.8724$ for the ordered model).

The point we wish to make is that the use of structural parameters which are as different from the correct ones as are the structural parameters of the ordered model, when applied to DKDP, introduces systematic errors over the whole range of \underline{K} considered in the analysis of Skalyo, Frazer and Shirane (1970). The most straight forward way of finding out exactly how serious the structural assumptions made in dynamical analysis really are, is to re-analyse the dynamical data.

We therefore feel that the structural results presented in this chapter should be applied to the dynamical data of Skalyo, Frazer and Shirane (1970) with particular emphasis on the z component of the eigenvectors of the D, H atoms.

The suggestion of application naturally extends to the analysis of Wallace, Cochran and Stringfellow (1972) who used the results of Skalyo, Frazer and Shirane (1970) and data, relying on KDP structural parameters to work out the signs (phases = 0 or π) and relative magnitudes of the dynamic structure factors which they then used to construct "eigenvector density" maps.

In order to obtain some idea of the possible effects of introducing the new structural parameters into the dynamic structure factor expression, we work out the contribution of the D, H atoms to the dynamic structure factors considered in the analysis of Skalyo, Frazer and Shirane. We

work out on an arbitrary scale the contribution of the D, H atoms for four different models:

- a) ordered phonon model
- b) disordered phonon model
- c) ordered tunnelling model
- d) disordered tunnelling model

There is a contradiction of terms here but we include the "ordered tunnelling" model since this is what was considered in the analysis of Skalyo, Frazer and Shirane (1970).

Table IV.8 lists, for each $h k l$, the contribution of the D, H atoms in the following order: for model a), for model b), the phase angle between a) and b), for model c), for model d) and the phase angle between c) and d). The phase angle difference is labelled $\delta\psi$ in Table IV.8.

In order to assess the relative differences between the different possibilities we least square fit, by varying a scale factor, one set (of relative contribution of the D, H atoms to the dynamic structure factor) to another. We work out

$$D^2 = \sum_i^n (f_i' - K f_i'')^2$$

for the n structure factors considered, with K a scale factor chosen to minimize D^2 ; the f' and f'' are any of the sets from Table IV.8.

Table IV.9 shows the result of the comparison. When we least square fit the f' 's for the ordered phonon model with the f' 's for the "ordered tunnelling" model

TABLE IV.8.

H	K	L	PHONON MODEL		$\delta\psi$	TUNNELING MODEL		
			F-ORD	F-DRD		F-ORD	F-DRD	$\delta\psi$
2.	0.	0.	0.000	0.000	0.	0.000	0.000	0.
4.	0.	0.	0.000	0.000	0.	0.000	0.000	0.
6.	0.	0.	0.000	0.000	0.	0.000	0.000	0.
8.	0.	0.	0.000	0.000	0.	0.000	0.000	0.
10.	0.	0.	0.000	0.000	0.	0.000	0.000	0.
12.	0.	0.	0.000	0.000	0.	0.000	0.000	0.
1.	0.	1.	0.870	0.887	0.	0.862	0.880	0.
3.	0.	1.	2.173	2.460	0.	2.071	2.346	0.
5.	0.	1.	2.469	3.065	0.	2.222	2.757	0.
7.	0.	1.	1.790	1.923	0.	1.524	1.629	0.
9.	0.	1.	0.707	0.495	-180.	0.544	0.293	-180.
11.	0.	1.	0.033	2.633	-0.	0.096	1.563	-0.
0.	0.	2.	0.000	0.000	0.	0.000	0.000	0.
2.	0.	2.	0.556	0.625	0.	0.511	0.577	0.
4.	0.	2.	1.230	1.350	0.	1.126	1.224	0.
6.	0.	2.	0.753	0.741	-0.	0.662	0.630	-0.
8.	0.	2.	0.303	0.547	0.	0.343	0.497	0.
10.	0.	2.	0.594	1.036	-0.	0.601	0.753	-0.
12.	0.	2.	0.079	0.635	0.	0.079	0.179	-0.
1.	0.	3.	1.985	2.001	-0.	1.951	1.966	-0.
3.	0.	3.	3.761	4.011	-0.	3.618	3.851	-0.
5.	0.	3.	2.133	2.672	0.	1.882	2.359	0.
7.	0.	3.	0.171	0.305	-0.	0.071	0.061	180.
9.	0.	3.	0.041	1.124	180.	0.105	0.862	-0.
11.	0.	3.	0.644	1.934	-180.	0.583	0.848	-180.
2.	0.	4.	2.057	2.166	0.	1.956	2.059	0.
4.	0.	4.	0.690	0.413	0.	0.854	0.617	0.
6.	0.	4.	0.980	0.939	0.	1.121	1.108	0.
8.	0.	4.	0.499	0.050	-180.	0.422	0.050	-0.
10.	0.	4.	0.993	0.008	-180.	0.964	0.499	-0.
1.	0.	5.	0.424	0.363	0.	0.456	0.397	0.
3.	0.	5.	0.019	0.302	-0.	0.121	0.138	180.
5.	0.	5.	1.942	2.319	0.	1.687	2.004	0.
7.	0.	5.	2.644	2.478	0.	2.391	2.272	0.
9.	0.	5.	1.081	0.137	180.	0.942	0.198	0.
11.	0.	5.	0.606	2.783	0.	0.640	1.669	0.
0.	0.	6.	0.000	0.000	103.	0.000	0.000	5.
2.	0.	6.	1.246	1.367	-0.	1.124	1.234	-0.
8.	0.	6.	0.667	1.242	0.	0.733	1.060	0.
10.	0.	6.	1.319	2.292	-0.	1.302	1.584	0.
1.	0.	7.	2.094	2.098	-0.	1.954	1.958	-0.

TABLE IV.8. CONTD.

H	K	L	PHONON MODEL		$\delta\psi$	TUNNELING MODEL		$\delta\psi$
			F-ORD	F-DRD		F-ORD	F-DRD	
3.	0.	7.	3.617	3.733	0.	3.320	3.410	0.
5.	0.	7.	1.223	1.474	0.	0.984	1.184	0.
7.	0.	7.	0.966	1.030	0.	1.082	1.056	0.
9.	0.	7.	0.407	1.430	-0.	0.476	0.978	-0.
2.	0.	8.	2.641	2.668	0.	2.427	2.445	0.
4.	0.	8.	0.853	0.544	-0.	1.001	0.744	-0.
6.	0.	8.	1.225	1.184	0.	1.339	1.294	0.
8.	0.	8.	0.652	0.076	-180.	0.535	0.113	-0.
1.	0.	9.	0.977	0.852	0.	0.986	0.867	0.
3.	0.	9.	1.138	0.850	0.	1.229	0.977	0.
5.	0.	9.	1.029	1.155	0.	0.801	0.895	0.
7.	0.	9.	2.241	1.805	0.	1.990	1.700	0.
2.	0.	10.	1.157	1.210	0.	1.004	1.044	0.
4.	0.	10.	2.562	2.582	0.	2.211	2.204	0.
6.	0.	10.	1.585	1.336	0.	1.321	1.119	0.
1.	0.	11.	1.399	1.373	-0.	1.197	1.178	-0.
3.	0.	11.	2.281	2.257	0.	1.916	1.884	0.
1.	1.	0.	0.000	0.000	0.	0.000	0.000	0.
3.	3.	0.	0.000	0.000	0.	0.000	0.000	0.
5.	5.	0.	0.000	0.000	0.	0.000	0.000	0.

Table IV.9

$$D^2 = \sum (f' - kf'')^2 \text{ where } k \text{ minimises } D^2.$$

D^2 is therefore the sum of residuals in a least squares fit involving a scale-factor only

	Phonon model		Tunnelling model	
	f-ordered	f-disordered	f-ordered	f-disordered
Phonon model f-ordered		$D^2 = 22.584$ $K = 0.792$	$D^2 = 0.690$ $K = 1.079$	
Phonon model f-disordered				$D^2 = 9.193$ $K = 1.115$
Tunnelling model f-ordered				$D^2 = 8.254$ $K = 0.901$

$D^2 = 0.690$. This is the value of D^2 we want to compare with other values of D^2 , since Skalyo, Frazer and Shirane (1970) came to the conclusion that they could not distinguish between these two models, i.e. the ordered phonon model and the "ordered tunnelling" model. We argue that since D^2 is much larger for all other comparisons made, see Table IV.9, it should be relatively easier to distinguish between: order and disorder - phonon models and tunnelling models than it was in the analysis of Skalyo, Frazer and Shirane to distinguish the ordered phonon and ordered tunnelling models.

CHAPTER V

STRUCTURAL STUDY OF DTGS

V.1 Introduction

This chapter is included because of the interest in TGS, triglycine sulphate $(\text{NH}_2\text{CH}_2\text{COOH})_3 \cdot \text{H}_2\text{SO}_4$, and how the present state of the analysis illustrates some of the points mentioned earlier in connection with the problems met on the way to a detailed solution of the crystal structure of some ferroelectrics.

It should be emphasized that the analysis briefly described in this chapter constitute initial attempts to solve the crystal structure of paraelectric DTGS and are by no means final.

TGS was discovered to be ferroelectric by Matthias, Miller and Remeika (1956). Its Curie temperature is 49°C .

TGS has a complicated crystal structure with 37 atoms in the asymmetric unit (see below) but is relatively simple phenomenologically. The essential features of the ferroelectric transition can be described on the basis of the expansion of the free energy in terms of polarization only (Jona and Shirane, 1962).

The transition in TGS is regarded as nearly perfect second order from the continuity of the polarization v. temperature curve (see Fig. I.2.a).

The dynamical models of DTGS have been limited to the Ising model (see Chapter I) fitting of critical X-ray scattering data (see below).

For a general outline of TGS, as studied pre 1962, see Jona and Shirane (1962).

One major concern as regards the true crystal structure of TGS is the effect of radiation damage (see below).

Structural data of TGS were first given by Wood and Holden (1957), who confirmed the space group of the ferroelectric phase to be $P2_1$. The cell dimensions reported were $a = 9.15$, $b = 12.69$, $c = 5.73$ and $\beta = 105.67^\circ$. The space group of the paraelectric phase was given by Pepinsky, Okaya and Jona (1957) to be $P2_1/m$.

The symmetry changes at the transition involve, the creation of mirror planes at $y = b/4$ and at $y = 3/4b$; these together with the existing screw axis generate a centre of symmetry, for the paraelectric phase, at $(a/2, b/2, 0)$.

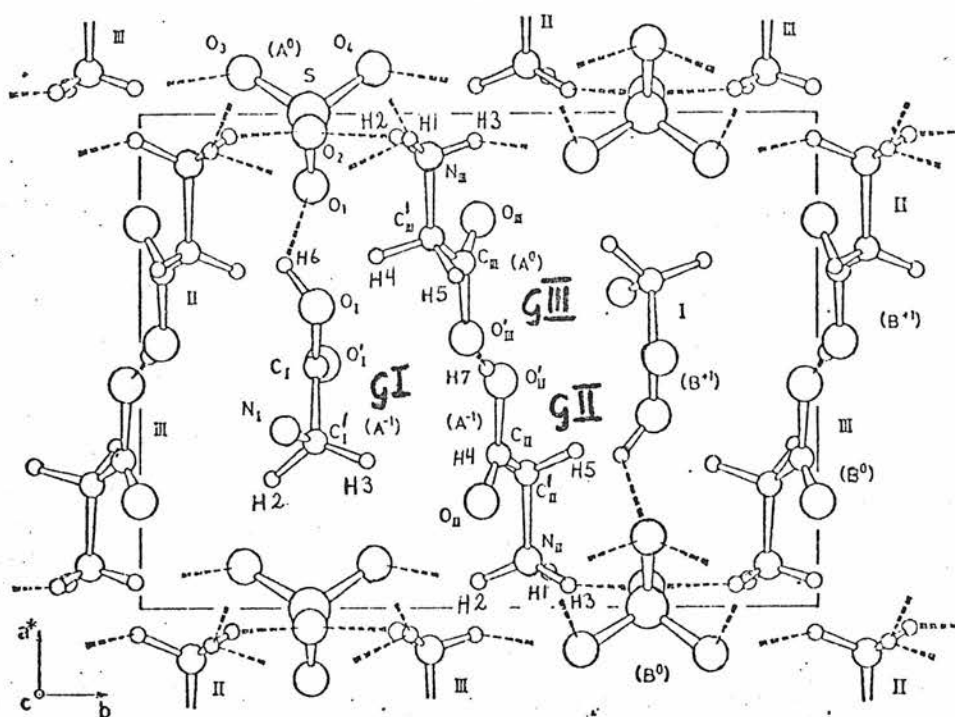
The first detailed structural study of TGS was the room temperature X-ray study of Hosino, Okaya and Pepinsky (1959); (cell dimensions $a = 9.41$, $b = 12.64$, $c = 5.73$ and $\beta = 110.38^\circ$).

They located all but the H atoms and proposed a system of hydrogen bonds (also illustrated in Jona and Shirane, 1962, p. 57).

TGS has 37 atoms in the asymmetric unit (one formula unit) thus 74 atoms in the unit cell.

The room temperature structure as viewed down the c axis is illustrated in Figure V.1 (after Itoh and Mitsui, 1973).

The labelling of atoms in Fig. V.1 follows the labelling of Hosino, Okaya and Pepinsky. Atoms S, O_1 and O_2 of the SO_4 group and atoms O, O', C and C' of glycine I are all located on (S) or near the plane $y = b/4$ which becomes a mirror plane in the paraelectric phase. The location of N_I is about $0.5\overset{o}{A}$ away from $y = b/4$ which implies that in the paraelectric phase N_I could be statistically distributed between sites separated by as much as $1\overset{o}{A}$, if



The crystal structure of TGS at 19°C viewed down the c -axis; after Itoh and Mitsui, 1973. The symbols A^0 , B^0 , A^{-1} and B^{+1} stand for atoms whose coordinates are (x, y, z) , $(1-x, y+\frac{1}{2}, 1-z)$, $(x, y, z-1)$ and $(1-x, y+\frac{1}{2}, 2-z)$ respectively. Dashed lines show the hydrogen-bond system reported by Itoh and Mitsui. G I, G II and G III stand for glycines 1, 2 and 3 respectively. Atom H7 links G II and G III. Atom H6 links G I with the SO_4 group.

Fig. V.1.

the transition was purely order disorder type. The atom H7 in Figure V.1 connects glycines II and III, by symmetry the mean value of the time averaged distribution of this atom coincides with the centre of symmetry in the paraelectric phase.

The dotted lines in Figure V.1 indicate the hydrogen bond system supported by Itoh and Mitsui (see below).

A problem of central importance is that of radiation damage. Chynoweth (1959) found that dosages of X-rays, small compared with those received during an X-ray structural investigation, changed the properties of TGS as observed by hysteresis loops. Chynoweth found these changes to be gradual with X-radiation with no threshold radiation.

These observations led Chynoweth to suspect all structural results from X-ray investigations on TGS and he asked the question whether the structure of TGS, as received from a crystal growing setup, could be determined at all by X-rays. Chynoweth went further and warned that there seemed to be the possibility of similar effects in a large number of compounds.

In continuation of the X-ray study of Hosino, Okaya and Pepinsky (1959), Hosino, Mitsui, Okaya and Pepinsky carried out some neutron diffraction studies on TGS in order to locate the H atoms, but the least squares calculation did not converge (see Itoh and Mitsui, 1973).

Interest in the improved pyroelectric properties of TGS with radiation damage (causing structural inhibition of ferroelectric switching) led Fletcher, Skapaski and Keve (1971) to undertake R.T. structural studies of TGS: a) with the minimum

of X-ray dosage consistent with the necessary diffraction data and b) heavily radiated; with a field applied.

They found that there was very little difference between the two resulting structures. They disagree with the structural study of Hosino, Okaya and Peipisky (1959) as to which glycine molecules are planar and which are non-planar. They find glycine I to be non-planar but glucines II and III to be planar, whereas Hosino, Okaya and Pepinsky found glycines I and III to be planar and glycine II non-planar, see Fig. V.1.

The results of Fletcher et al. (1971) agree with the R.T. results of Itoh and Mitsui (1973) (see below) on which glycines are planar, but disagree on the extent of "remnant molecular disorder" of which Fletcher et al. find none.

Another attempt to solve the R.T. structure of TGS, using neutrons, was carried out by Padmanabhan, V.M. (1971, private communication) from projection data (325 reflections in all. Padmanabhan felt that three dimensional structural analysis was needed and stopped his refinements.

The most detailed structural study of TGS at present is the X-ray study of Itoh and Mitsui (1973). Itoh and Mitsui solved the crystal structure of TGS at R.T. for all atoms but the three H atoms of the NH_3 group of glycine I (they state that this could be due to disorder or hindered rotation for the R.T. structure), see Fig. V.1, and for all but the H atoms for the structures at 37 and 57°C by constraining glycines II and III to be symmetry related.

We have already pointed out the serious implications of

of X-ray dosage consistent with the necessary diffraction data and b) heavily radiated; with a field applied.

They found that there was very little difference between the two resulting structures. They disagree with the structural study of Hosino, Okaya and Pepinsky (1959) as to which glycine molecules are planar and which are non-planar. They find glycine I to be non-planar but glycines II and III to be planar, whereas Hosino, Okaya and Pepinsky found glycines I and III to be planar and glycine II non-planar, see Fig. V.1.

The results of Fletcher et al. (1971) agree with the R.T. results of Itoh and Mitsui (1973) (see below) on which glycines are planar but disagree on the extent of "remnant molecular disorder" of which Fletcher et al. find none.

Another attempt to solve the R.T. structure of TGS, using neutrons, was carried out by Padmanabhan, V.M. (1971, private communication) from projection data (325 reflections in all). Padmanabhan felt that three dimensional structural analysis was needed and stopped his refinements.

The most detailed structural study of TGS at present is the X-ray study of Itoh and Mitsui (1973). Itoh and Mitsui solved the crystal structure of TGS at R.T., 37°C for all atoms but the three H atoms of the NH_3 group of glycine I (they state that this could be due to disorder or hindered rotation) for the R.T. structure, see Fig. V.1, and for all but the H atoms for the structures at 37 and 57°C by constraining glycines II and III to be symmetry related.

We have already pointed out the serious implications of Chynoweth's (1959) study of radiation damage in TGS. It seems from the similarities of the structural results of Fletcher,

Skapasky and Keve (1971) for the modestly and the heavily radiated samples of TGS on the one hand, and of these structural studies with Itoh and Mitsui's results on the other, that all these structural studies with X-rays are subject to very similar effects.

Of particular relevance to this thesis is Itoh and Mitsui's assessment of the structure of paraelectric TGS (at 57°C). They attempted to answer the question whether glycine I was disordered about the mirror plane at $y = b/4$, see Fig. V.1, or located on that mirror plane. They did this by: 1) refining all the glycine I atoms with starting positions off the mirror plane to some stable positions off the mirror plane and 2) by refining glycine I atoms from starting positions on the mirror plane.

The fact that the two refinements gave eventually the same structure led Itoh and Mitsui to conclude that this structure was the true one, which meant that TGS was disordered in the paraelectric phase.

The first point to make is that the derivative of any structure factor w.r.s.t a y coordinate is identical to zero when $y = b/4$ (or $y = 3/4b$). In this case the shift worked out by the least squares calculation is, in principle, infinite (depending on the accuracy of the computer, arithmetic rounding off might cause the shifts to be finite, but still quite arbitrary).

An atom will therefore tend to move away from whatever mirror plane it is placed on in a refinement.

The only meaningful way in which to ask the question concerned is by applying the methods of constrained refinements

and hypothesis testing (as is described in Chapter II). The application of these methods is quite trivial in this particular case since they consist simply of carrying out refinements with one or more atoms in turn constrained to lie on the mirror plane and comparing the results with those of the free refinement.

The final point on this is that although Itoh and Mitsui's conclusions seem very likely to hold good, they are not based on sound foundations (in the view of the writer, based on the approach to assessment described in Chapter II).

Itoh and Mitsui (1973) list a number of experiments, some of which indicate the displacive character and some of the order-disorder character of the transition. In particular they found the work of Shibuya and Mitsui (1961) on the temperature dependence of X-ray diffuse intensity in TGS consistent with the order-disorder model on the basis of comparison with dielectric data. This work was later extended by Fujii and Yamada (1971) who also examined the distribution of the diffuse intensity in reciprocal space.

Fujii and Yamada used an Ising model in their analysis and found its application to TGS not to be very good, in contrast with their results on Na NO_3 .

There is thus, as yet, no conclusive answer to the question whether the ferroelectric phase transition in TGS is of the order-disorder type or is, to some extent, displacive.

V.2 The Experiment on DTGS at 80°C

V.2.a Experimental setup

A crystal of DTGS, ground into a 4 mm diameter sphere (see Chapter III), was glued onto a hollow rod with thermocouple leads inside and placed inside a heater built by Dr. A. Hewat of A.E.R.E. Harwell.

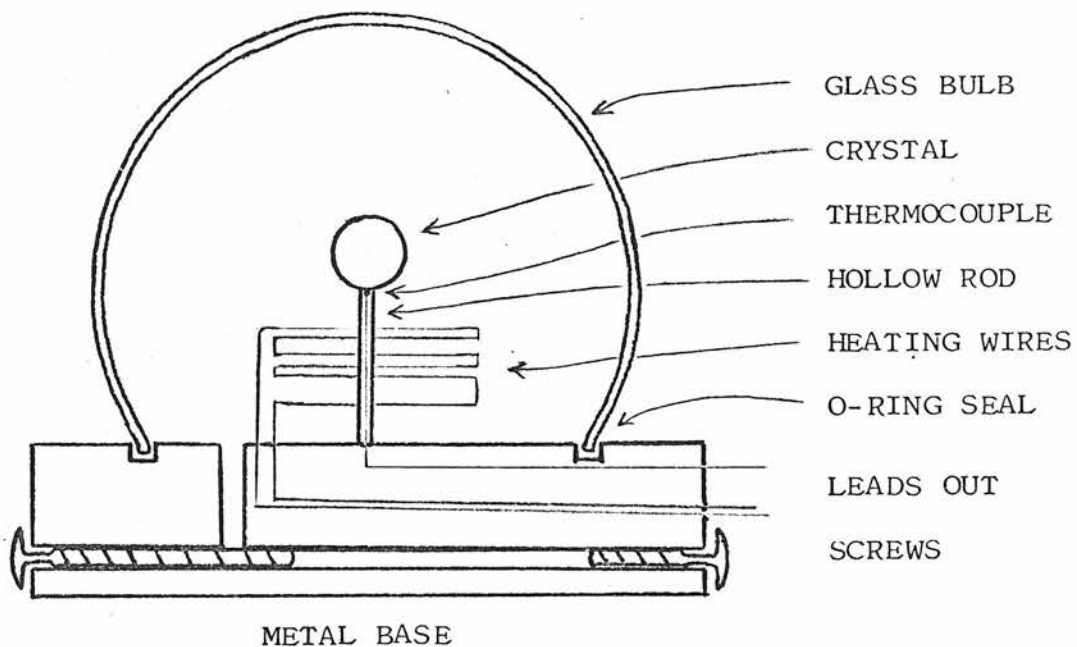
The heater (see Fig. V.2), placed on top of a goniometer head, consists of a silvered glass bulb vacuum sealed onto a metal base. The rod on which the crystal sits is attached to the metal base which also supports a resistance wire which heats the crystal by radiation (the glass bulb is evacuated during operation). The heater was controlled by Eurotherm instruments with proportional facilities for temperature control.

The heater was placed on a conventional goniometer head and with two small windows scratched on the silver coating the setup was ready for alignment and data collection. The crystal was oriented to have the C axis vertical. The data was collected at 80°C.

V.2.b Data collection and handling

Three-dimensional data was collected with $\lambda = 1.08\text{\AA}$ out to $\sin \theta/\lambda$ of 0.87\AA^{-1} but with $0 \leq l \leq 5$ on the Ferranti Mk. II diffractometer channel I in the reactor Pluto. This data was collected in collaboration with Dr. A. Hewat of A.E.R.E., Harwell.

Another three-dimensional dataset was collected with $\lambda = 1.141\text{\AA}$ out to $\sin \theta/\lambda$ of 0.62 on channel II of the Ferranti Mk II setup in the reactor Pluto. This data-set was collected in collaboration with Mr. K.D. Rouse of A.E.R.E., Harwell.



The heater used for the DTGS experiment
(built by Dr. A. Hewat).

Fig. V.2.

These data sets overlap to a considerable extent. In both cases the orientation of the crystal was with the c-axis vertical and the sample was kept at 80°C during data collection.

At first peak-peak offset background scans were employed but it was decided that the additional background due to the glass bulb of the heater (V.2.a) was sufficiently uniform over any one background-peak-background scan to allow the use of this type of scan without appreciable loss in accuracy. The reason for changing the type of scan was that for some unexplained reason, it was found that unreasonable differences occurred between the background of the peak offset scan and the background as determined from the levelling off of the counting rate in the peak scan itself.

The final background-peak-background scans had 60 steps of width 0.04°, 5 of which at either end were used to estimate the background.

The overlap of the data sets collected with the various collaborators made it possible to put all the data on a common scale, the data sets consisted of roughly equal number of intensities.

The data handling was carried out in the same way as that of the room temperature KDP data (IV.3) utilizing the data reduction program of Dr. B.H. Bracher of A.E.R.E., Harwell.

The final data set consisted of 1830 independent structure factors that were used in the analysis.

V.3 Refinement and Results

It should be restated that the analysis briefly described here constitutes initial attempts to solve the crystal

structure of paraelectric D-TGS and are by no means final.

No correction was made for extinction and no attempts were made to apply constraints in a systematic way.

The analysis was carried out in collaboration with Mr. K.D. Rouse.

At first, using the coordinates from the room temperature work of Hosino, Okaya and Pepinsky (1959) and calculating positions for the D atoms in accordance with their proposed network of hydrogen bonds, two-dimensional Fourier and difference Fourier maps were constructed (see Chapter II.3), using hko data. The program used was that of Dr. M. Harding of the Chemistry Department of this University,

This projection down the relatively short (5.73Å) ^oc-axis gives a good separation of quite a number of the atoms (see Fig. V.1) of the ferroelectric X-ray structure, ignoring the H atoms, but it soon was obvious that the overlap, in particular of D atoms, made this an exercise of little value.

With the three-dimensional data, using the more accurate room temperature parameters of Itoh and Mitsui (1971), Fourier and difference Fourier maps were constructed in 3 dimensions. The program used was the Fourier and difference Fourier programs of the system X-RAY 70 stored on the ICL computer in the Atlas computer laboratories.

Some attempts were made to approach a solution of the structure from the Fourier and difference Fourier maps.

A program was written that was capable of rotating any group of atoms about any axis (defined by two points) by a given number of degrees of rotation. The program could also be fed with a peak position associated with one or more

of the atoms (to be rotated) in which case the group of atoms was rotated so as to minimize the sum of the squares of the distances between the atoms and their associated peak positions. The idea was to feed the program with peak positions from either two or three dimensional Fourier maps (or difference Fourier maps) and approach solution of the structure with constraints applied to particular groups of atoms.

This approach was used to constrain, in the first instance, the ND_3 group of glycine I to be tetrahedrally arranged but free to rotate about an axis defined by the positions of the N_I and the C_I' atoms.

This gave little but rough indications as to the locations of the atoms considered and in general very little progress was made from the Fourier and difference Fourier maps.

The main difficulty was the near coincidence of glycines II and III as operated on by the centre of symmetry, and how close some of the atoms of glycine I and the SO_4 group were to the mirror plane (at $y = b/4$) if not on the mirror plane.

It was decided to try, with some care, least squares runs of the three-dimensional structure. Because of feared correlation between glycines II and III parameters, these two were never refined together but were refined in turn with glycine I and the SO_4 group.

The sulphur atom was fixed at $y = b/4$, on the mirror plane; N of glycine I was refined to a position nearly 0.5Å^o

away from the mirror plane. It was possible, in the circumstances, after obtaining some values for the anisotropic temperature factors from previous runs of refining parts of the structure at a time, to refine all positional parameters together (except $y(S)$ which was fixed) but as can be seen from the correlation coefficients listed in Table V.1, no certainty can be claimed in the atomic positions of glycines II and III. To attempt at this stage any free refinement of thermal parameters of glycines II and III would of course be quite pointless. The same applies to the atoms near the mirror plane, $y = b/4$, no certainty can, at this stage, be attached to their accurate positions. The R factor was 0.145 which is high even remembering that no extinction correction has been applied.

The point to make here is that it is of central importance whether (and to what extent) DTGS is disordered. It is the disorder which gives rise to the difficulties in solving the detailed structure of DTGS.

The case presented here is an obvious one for application of the methods of constraint refinement and hypothesis testing.

As to the question of how well the least squares parameters at present (listed in Table V.2) represent the structure of paraelectric DTGS, it is to be pointed out that the thermal parameters and the positional parameters of disordered atoms cannot be independently valued in this situation and the approach of constraint refinement has to be adapted.

Table V.1

Correlation coefficients from a least squares
refinement of atomic positions only

Correlation coefficient	parameters	
	glycine II	glycine III
.93	z(O)	z(O)
.81	y(C)	y(C)
.69	z(C)	z(C)
.72	x(C')	x(C')
.78	y(C')	y(C')
.76	z(N)	z(N)
.82	x(D1)	x(D1)
.87	y(D1)	y(D1)
.74	x(D2)	x(D3)
.87	z(D2)	z(D3)
.88	x(D3)	x(D2)
.91	y(D3)	y(D2)
.89	z(D3)	z(D1)

Table V.2

The following 5 pages list the parameters of DTGS at 80°C.

The atoms O_1 , O_2 , O_3 and O_4 are those of the SO_4 group.

The atoms O, O', C, C', N and D are pre-labelled G1, G2 or G3 according to which glycine they belong to G I, G II or G III in fig. V.1.

The atoms D6 and D7 which link G I to SO_4 and G II to G III respectively correspond to atoms H6 and H7 in fig. V.1.

The form factors in this table refer to the scattering lengths (Bacon, 1972). The atomic positions x, y and z are given as fractional coordinates. The $\beta(i,j)$ are the elements of the matrix of the mean square displacements and are given in units of \AA^2 .

PARAMETERS

PARAMETER			
SCALE FACTOR	1.5973721	O4	
OVERALL B	0.0	FORM FACTOR	0.5770000
		MULTIPLIER	1.0000000
S		X	1.0881996
FORM FACTOR	0.2850000	Y	0.3397000
MULTIPLIER	1.0000000	Z	0.2172000
X	1.0010757	BETA(1,1)	0.0055870
Y	0.2500000	BETA(2,2)	0.0032390
Z	0.2231364	BETA(3,3)	0.0309760
BETA(1,1)	0.0047290	BETA(1,2)	-0.0012850
BETA(2,2)	0.0023240	BETA(1,3)	0.0063010
BETA(3,3)	0.0079740	BETA(2,3)	-0.0008390
BETA(1,2)	0.0		
BETA(1,3)	0.0037080	G10	
BETA(2,3)	0.0	FORM FACTOR	0.5770000
		MULTIPLIER	1.0000000
O1		X	0.6051677
FORM FACTOR	0.5770000	Y	0.2633600
MULTIPLIER	1.0000000	Z	1.0696802
X	0.8595825	BETA(1,1)	0.0030180
Y	0.2531068	BETA(2,2)	0.0043280
Z	0.0060947	BETA(3,3)	0.0216180
BETA(1,1)	0.0035570	BETA(1,2)	-0.0006350
BETA(2,2)	0.0060760	BETA(1,3)	0.0028100
BETA(3,3)	0.0151450	BETA(2,3)	-0.0021520
BETA(1,2)	0.0018330		
BETA(1,3)	0.0013490	G10'	
BETA(2,3)	0.0000840	FORM FACTOR	0.5770000
		MULTIPLIER	1.0000000
O2		X	0.4936479
FORM FACTOR	0.5770000	Y	0.2658417
MULTIPLIER	1.0000000	Z	0.6609182
X	0.9652900	BETA(1,1)	0.0079900
Y	0.2533917	BETA(2,2)	0.0069550
Z	0.4529721	BETA(3,3)	0.0262940
BETA(1,1)	0.0101660	BETA(1,2)	-0.0020460
BETA(2,2)	0.0044190	BETA(1,3)	0.0050150
BETA(3,3)	0.0128960	BETA(2,3)	-0.0000570
BETA(1,2)	0.0001330		
BETA(1,3)	0.0070280	G1C	
BETA(2,3)	-0.0038030	FORM FACTOR	0.6610000
		MULTIPLIER	1.0000000
O3		X	0.4889796
FORM FACTOR	0.5770000	Y	0.2585622
MULTIPLIER	1.0000000	Z	0.8662099
X	1.0826616	BETA(1,1)	0.0053040
Y	0.1505539	BETA(2,2)	0.0023530
Z	0.2039541	BETA(3,3)	0.0223290
BETA(1,1)	0.0085180	BETA(1,2)	-0.0003090
BETA(2,2)	0.0016820	BETA(1,3)	-0.0040360
BETA(3,3)	0.0277830	BETA(2,3)	-0.0007740
BETA(1,2)	0.0011450		
BETA(1,3)	0.0053030		
BETA(2,3)	-0.0009910		

TABLE V.2 contd.

G1C1		G1D3	
FORM FACTOR	0.6610000	FORM FACTOR	0.6670000
MULTIPLIER	1.0000000	MULTIPLIER	1.0000000
X	0.3415431	X	0.4048004
Y	0.2557210	Y	0.2714259
Z	0.9124615	Z	1.2745142
BETA(1,1)	0.0030080	BETA(1,1)	0.0196220
BETA(2,2)	0.0035420	BETA(2,2)	0.0228460
BETA(3,3)	0.0251020	BETA(3,3)	0.0793300
BETA(1,2)	0.0006950	BETA(1,2)	0.0001370
BETA(1,3)	0.0011920	BETA(1,3)	0.0113070
BETA(2,3)	0.0021410	BETA(2,3)	-0.0242320
G1N		G1D4	
FORM FACTOR	0.9400000	FORM FACTOR	0.6670000
MULTIPLIER	1.0000000	MULTIPLIER	1.0000000
X	0.3547400	X	0.2626547
Y	0.2134110	Y	0.2030828
Z	1.1541147	Z	0.7756284
BETA(1,1)	0.0046100	BETA(1,1)	0.0093090
BETA(2,2)	0.0089810	BETA(2,2)	0.0113500
BETA(3,3)	0.0274580	BETA(3,3)	0.0369110
BETA(1,2)	0.0021910	BETA(1,2)	-0.0029610
BETA(1,3)	0.0053180	BETA(1,3)	0.0048190
BETA(2,3)	0.0006060	BETA(2,3)	-0.0012670
G1D1		G1D5	
FORM FACTOR	0.6670000	FORM FACTOR	0.6670000
MULTIPLIER	1.0000000	MULTIPLIER	1.0000000
X	0.2538950	X	0.2929249
Y	0.1936437	Y	0.3299279
Z	1.1750622	Z	0.8816685
BETA(1,1)	0.0149000	BETA(1,1)	0.0162150
BETA(2,2)	0.0184640	BETA(2,2)	0.0065360
BETA(3,3)	0.0585520	BETA(3,3)	0.0818990
BETA(1,2)	0.0054530	BETA(1,2)	0.0045710
BETA(1,3)	0.0184020	BETA(1,3)	0.0203550
BETA(2,3)	0.0112820	BETA(2,3)	0.0086500
G1D2		D6	
FORM FACTOR	0.6670000	FORM FACTOR	0.6670000
MULTIPLIER	1.0000000	MULTIPLIER	1.0000000
X	0.4155439	X	0.7041349
Y	0.1468375	Y	0.2381169
Z	1.1923552	Z	1.0353842
BETA(1,1)	0.0153300	BETA(1,1)	0.0097460
BETA(2,2)	0.0181550	BETA(2,2)	0.0080070
BETA(3,3)	0.0665520	BETA(3,3)	0.0497360
BETA(1,2)	0.0051780	BETA(1,2)	0.0008050
BETA(1,3)	0.0162880	BETA(1,3)	0.0061690
BETA(2,3)	0.0161650	BETA(2,3)	0.0025390

TABLE V.2 contd.

G20	
FORM FACTOR	0.5770000
MULTIPLIER	1.0000000
X	0.2217489
Y	0.4994522
Z	0.7749998
BETA(1,1)	0.0078170
BETA(2,2)	0.0057800
BETA(3,3)	0.0229040
BETA(1,2)	0.0000450
BETA(1,3)	0.0049240
BETA(2,3)	0.0054910

G20'	
FORM FACTOR	0.5770000
MULTIPLIER	1.0000000
X	0.4584325
Y	0.5300689
Z	0.7937699
BETA(1,1)	0.0050880
BETA(2,2)	0.0069530
BETA(3,3)	0.0108090
BETA(1,2)	0.0002540
BETA(1,3)	-0.0015060
BETA(2,3)	0.0037130

G2C	
FORM FACTOR	0.6610000
MULTIPLIER	1.0000000
X	0.3191598
Y	0.5288556
Z	0.6903702
BETA(1,1)	0.0049730
BETA(2,2)	0.0033260
BETA(3,3)	0.0106110
BETA(1,2)	0.0011320
BETA(1,3)	-0.0000920
BETA(2,3)	0.0011730

G2C'	
FORM FACTOR	0.6610000
MULTIPLIER	1.0000000
X	0.2684942
Y	0.5654467
Z	0.4206015
BETA(1,1)	0.0068870
BETA(2,2)	0.0043680
BETA(3,3)	0.0125860
BETA(1,2)	0.0000500
BETA(1,3)	0.0017390
BETA(2,3)	0.0029990

G2N	
FORM FACTOR	0.9400000
MULTIPLIER	1.0000000
X	0.1068338
Y	0.5665644
Z	0.3015986
BETA(1,1)	0.0061550
BETA(2,2)	0.0021550
BETA(3,3)	0.0174340
BETA(1,2)	0.0007720
BETA(1,3)	0.0017990
BETA(2,3)	0.0031200

G2D1	
FORM FACTOR	0.6670000
MULTIPLIER	1.0000000
X	0.0603490
Y	0.6030471
Z	0.1222102
BETA(1,1)	0.0126380
BETA(2,2)	0.0077410
BETA(3,3)	0.0363450
BETA(1,2)	0.0031050
BETA(1,3)	0.0044220
BETA(2,3)	0.0069760

G2D2	
FORM FACTOR	0.6670000
MULTIPLIER	1.0000000
X	0.0644855
Y	0.4982547
Z	0.2922460
BETA(1,1)	0.0244880
BETA(2,2)	0.0076870
BETA(3,3)	0.0369510
BETA(1,2)	-0.0045380
BETA(1,3)	-0.0000330
BETA(2,3)	-0.0002200

G2D3	
FORM FACTOR	0.6670000
MULTIPLIER	1.0000000
X	0.0567969
Y	0.6165497
Z	0.3874236
BETA(1,1)	0.0111150
BETA(2,2)	0.0124840
BETA(3,3)	0.0413920
BETA(1,2)	0.0020370
BETA(1,3)	0.0059780
BETA(2,3)	0.0007060

TABLE V.2 contd.

G2D4		G3N	
FORM FACTOR	0.6670000	FORM FACTOR	0.9400000
MULTIPLIER	1.0000000	MULTIPLIER	1.0000000
X	0.3219799	X	0.9164315
Y	0.5262434	Y	0.4231771
Z	0.3251621	Z	0.7047713
BETA(1,1)	0.0116450	BETA(1,1)	0.0077140
BETA(2,2)	0.0189540	BETA(2,2)	0.0031270
BETA(3,3)	0.0286280	BETA(3,3)	0.0085080
BETA(1,2)	0.0062430	BETA(1,2)	0.0000090
BETA(1,3)	0.0062030	BETA(1,3)	0.0031410
BETA(2,3)	0.0029360	BETA(2,3)	-0.0007520
G2D5		G3D1	
FORM FACTOR	0.6670000	FORM FACTOR	0.6670000
MULTIPLIER	1.0000000	MULTIPLIER	1.0000000
X	0.3194846	X	0.9370570
Y	0.6448804	Y	0.3957765
Z	0.4164817	Z	0.8690767
BETA(1,1)	0.0097780	BETA(1,1)	0.0332650
BETA(2,2)	0.0084790	BETA(2,2)	0.0095500
BETA(3,3)	0.0389510	BETA(3,3)	0.0350250
BETA(1,2)	-0.0074430	BETA(1,2)	-0.0035660
BETA(1,3)	-0.0029300	BETA(1,3)	0.0148570
BETA(2,3)	0.0062550	BETA(2,3)	-0.0025290
D7		G3D2	
FORM FACTOR	0.6670000	FORM FACTOR	0.6670000
MULTIPLIER	1.0000000	MULTIPLIER	1.0000000
X	0.4914359	X	0.9516442
Y	0.5018429	Y	0.3776005
Z	0.9421698	Z	0.5922301
BETA(1,1)	0.0259990	BETA(1,1)	0.0140910
BETA(2,2)	0.0112380	BETA(2,2)	0.0151540
BETA(3,3)	0.2766210	BETA(3,3)	0.0325660
BETA(1,2)	-0.0005150	BETA(1,2)	0.0012790
BETA(1,3)	0.0562370	BETA(1,3)	0.0066990
BETA(2,3)	-0.0213530	BETA(2,3)	0.0006230
G3C1		G3D3	
FORM FACTOR	0.6610000	FORM FACTOR	0.6670000
MULTIPLIER	1.0000000	MULTIPLIER	1.0000000
X	0.7483461	X	0.9590781
Y	0.4264939	Y	0.5017868
Z	0.5968240	Z	0.7147756
BETA(1,1)	0.0078180	BETA(1,1)	0.0309500
BETA(2,2)	0.0036040	BETA(2,2)	0.0102770
BETA(3,3)	0.0263430	BETA(3,3)	0.0481620
BETA(1,2)	0.0016700	BETA(1,2)	-0.0089320
BETA(1,3)	0.0076600	BETA(1,3)	-0.0000150
BETA(2,3)	0.0048240	BETA(2,3)	0.0064060

TABLE V.2 contd.

G3D4
 FORM FACTOR
 MULTIPLIER
 X
 Y
 Z
 BETA(1,1)
 BETA(2,2)
 BETA(3,3)
 BETA(1,2)
 BETA(1,3)
 BETA(2,3)

G3D
 FORM FACTOR 0.5770000
 MULTIPLIER 1.0000000
 X 0.5561011
 Y 0.4790137
 Z 0.2558166
 BETA(1,1) 0.0098760
 BETA(2,2) 0.0115410
 BETA(3,3) 0.0221330
 BETA(1,2) 0.0035350
 BETA(1,3) 0.0027710
 BETA(2,3) 0.0005450

G3D5
 FORM FACTOR
 MULTIPLIER
 X
 Y
 Z
 BETA(1,1)
 BETA(2,2)
 BETA(3,3)
 BETA(1,2)
 BETA(1,3)
 BETA(2,3)

G3C
 FORM FACTOR 0.6610000
 MULTIPLIER 1.0000000
 X 0.6983804
 Y 0.4726216
 Z 0.3407825
 BETA(1,1) 0.0047090
 BETA(2,2) 0.0032890
 BETA(3,3) 0.0130760
 BETA(1,2) 0.0001580
 BETA(1,3) 0.0007140
 BETA(2,3) 0.0003100

G30
 FORM FACTOR
 MULTIPLIER
 X
 Y
 Z
 BETA(1,1)
 BETA(2,2)
 BETA(3,3)
 BETA(1,2)
 BETA(1,3)
 BETA(2,3)

V.4 Discussion

The state of structural studies of TGS, at present, is:

- a) The X-ray results are suspect due to radiation damage.
- b) The X-ray structure of ferroelectric TGS has been solved.
- c) The X-ray structure of a constrained version of paraelectric TGS has been solved (for all but the H atoms) but the question whether TGS is disordered in its paraelectric phase has neither been asked to its full extent, nor has it been assessed properly (in the view of the writer, based on Chapter II). The constraint, that glycines II and III are symmetry related, applied to TGS in its paraelectric phase by Itoh and Mitsui (1973) is equivalent to assuming that the transition is partly displacive. This is because, in the ferroelectric phase, Itoh and Mitsui (1973), glycines II and III would not coincide under the operation assumed in the paraelectric phase to bring them into coincidence.

No free refinement has been carried out on paraelectric TGS.

- d) The two previous attempts to solve the structure of ferroelectric TGS, using neutrons, have failed (see Section V.1).
- e) The structures of DTGS have not been solved, but, in the light of the X-ray results and the present work, some of the problems involved in solving the structure of paraelectric TGS are clear.

In particular we have pointed out that in order to overcome the problems of correlations the method of constrained refinements has to be applied. One approach possible is to constrain glycines II and III to have particular shape(s)

and to refine them independently.

We finally consider a more empirical approach to the problem of solving the crystal structure of paraelectric DTGS. We require data on both phases to be collected on the same sample under identical conditions except for temperature, and the structure of the ferroelectric phase to be known.

We consider the possibility that DTGS was a perfect order-disorder ferroelectric and that the only change occurring at T_c was that imposed by symmetry on the y positional parameters (as a consequence of the creation or destruction of two mirror planes. In this case it can be straightforwardly shown that the structure factors $f(hol)$ should be equal (see equation V.1) for the two phases (apart from slight difference, increasingly important with angle, rising from the difference in thermal parameters, and possibly extinction, with temperature). Therefore, by collecting data under identical condition, except for temperature, in the two phases with particular reference to the $h o l$ projection, we should, without any refinement (but perhaps with a graph of structure factor ratios for identical $h o l$ v. scattering angle to estimate changes in temperature factors and v. structure factor for extinction effects), be able to tell straight away if there is any appreciable shift in x and z coordinates on going through the transition.

If we found this way that DTGS was a perfect order-disorder ferroelectric, this would ease enormously the

the analysis of the structure of the paraelectric phase since it would only be necessary to consider the y positional parameters.

In general, if the structural change was of the purely order-disorder type with only the change in statistical distribution of atoms between alternative sites taking place at the transition, the expression for the difference between the ferroelectric structure factor, \hat{f}_F , and the paraelectric structure factor, \hat{f}_P , would for any $h k \ell$, be:

$$\hat{f}_F - \hat{f}_P = \frac{i}{2} \sum_{\chi=1}^{N/2} b_{\chi} \sin 2\pi(hx_{\chi} + ky_{\chi} + \ell z_{\chi}) + \sin 2\pi(-hx_{\chi} + k(y_{\chi} + \frac{1}{2}) - \ell z_{\chi}) \quad V.1$$

where x , y and z are the fractional positional parameters of the ferroelectric structure, b_{χ} is the scattering length, the sum is taken over all atoms in one symmetric unit (half the number of atoms in the unit cell) and thermal parameters are left out as well as extinction correction.

It is to be noted that $\hat{f}_F - \hat{f}_P$ only has two possible phase angles, namely $\pm \pi/2$; it was pointed out above that for $k = 0$ in equation V.1, $\hat{f}_F - \hat{f}_P \equiv 0$ in this context.

It seems therefore feasible that the construction of a Fourier map, see Section II.3, where the coefficients were the observed values of $\hat{f}_F - \hat{f}_P$, phased $\pm \pi/2$ according to the most accurate structural study of the ferroelectric phase to date and equation V.1, would give some insight into the difference between the two structures. (In terms of Section II.3 this would be a Fourier synthesis of the difference structure).

In particular a Fourier map constructed, using the $h o \ell$

structure factors only would show up the difference between the real situation and the model based on the pure order-disorder picture. Unfortunately a projection along the b -axis (12.6 \AA) is likely to present excessive overlap.

The more involved task of a three-dimensional Fourier study - either using the observed values of $f_F - f_P$ as Fourier coefficients, phased according to equation V.1, or using $(f_F - f_P)$ minus the modulus of the right-hand side of equation V.1) as difference Fourier coefficients phased according to equation V.1 - should show if there is a set of parameters that satisfies equation V.1 or if there is no such set then point to the differences.

The application of equation V.1 to the structural changes at the ferroelectric phase transition in DTGS could, of course, also be tried on any of the more flexible least squares programs. Computer simulations to find the accuracy and resolution needed for such a project to give meaningful results, though time consuming, are, in the opinion of the writer, somewhat underestimated in value and should have a useful application in this problem.

CHAPTER VI

CONCLUSIONS

VI.1 KDP-DKDP

It is finally clearly established that the D, H atoms in paraelectric KDP and DKDP are disordered in double minimum potential wells. There are, that is, two maxima in the time averaged nuclear density distribution of the D, H atoms.

At room temperature in both KDP and DKDP a line joining the D, H sites, one the short O - O hydrogen bond, is inclined to the O - O line by $8.9(3.0)$ and $8.9(4)$ degrees respectively. There are marked isotope and temperature effects on the inclination of the D, H - D, H line to the O - O line but not as large as suggested by the inclination of the eigenvectors of the D, H atoms to the O - O line found in the dynamical investigation of Skalyo, Frazer and Shirane (1970) and Wallace, Cochran and Stringfellow (1972).

There are marked isotope and temperature effects on the D, H - D, H bondlengths and on the ratio of the D, H - D, H to the O - O bondlengths.

No indication of soft motion is observed in the thermal vibrations of the K and the P atoms.

There are marked isotope and temperature effects on the z parameter of the O atoms. The difference of this parameter from $c/8$ is important in relation to dynamical work in projection (0 1 0 or the equivalent 1 0 0), (Wallace, Cochran and Stringfellow, 1972).

The extent of anisotropy in the thermal vibration of the D, H atoms is isotope dependent and a principal axis of their thermal ellipsoids is not directed along the D, H - D, H line.

This work presents the first detailed structural investigation into DKDP.

As to KDP, this work presents the first detailed structural investigation to follow the studies on KDP by Bacon and Pease (1953 and 1955).

Coinciding, in time, with a report on this work (Eiriksson, Nelmes and Rouse, 1973) Nakano, Shiozaki and Nakamura (1973A) reported X-ray structural investigation on DKDP and KDP at various temperatures. The X-ray investigation, however, did not involve the D, H atoms and the principal interest lies in the O - D,H - O bonds.

In comparing the room temperature results presented in this thesis, as regards the structural parameters of the K, P and O atoms, with the X-ray work of Nakano, Shiozaki and Nakamura (1973B) it is remarkable to note that all positional and thermal parameters (including off diagonal terms in the thermal matrix of the O atoms) agree within the least squares estimated errors.

The results presented are of immediate relevance to dynamical studies on DKDP and on KDP and, in more general terms, are fundamental to the problem of understanding the

phase transitions in KDP and in DKDP.

Future work: In the short term the structural investigation on KDP and DKDP at their respective $T_c + 5^\circ\text{K}$ should be completed and full scale structural investigations into the ferroelectric phases at $T_c - 5^\circ\text{K}$, and at temperatures well below T_c , undertaken. In the long term structural studies should be undertaken over the whole of the $x - T$ phase diagram of $\text{K}(\text{D}_x\text{H}_{1-x})_2\text{PO}_4$ to investigate further the very interesting temperature and isotope effects. One major drawback of a program of structural investigations on this scale is the time, effort and expense involved. It is therefore of interest to look into the possibilities of applying the much faster method of powder diffraction with profile analysis (Hewat, 1973) to investigate slight structural changes in KDP and DKDP with temperature.

IV.2 DTGS

The state of the structural problem of paraelectric DTGS is, so far as distinction between ordered structure and disordered structure is concerned, somewhat analogous to that of KDP 21 years ago (Bacon and Pease, 1953). DTGS, however, presents a much more involved problem, not only for the much larger number of atoms in the asymmetric unit but also due to the uncertainty as regards the extent of disorder. In DTGS D, H atoms on O - O and on N - O bonds, molecules (glycines) or parts of molecules (e.g. ND_3) could be disordered in a large number of combinations which have to be assessed and compared.

No free refinement has been possible so far of the structural parameters of paraelectric DTGS (or TGS). We point out that the problem has to be approached employing the methods of constraints and hypothesis testing. We also point out that once the ferroelectric structure is known, it is possible to assess the difference between the para- and ferroelectric structures without inviting the problems of near overlap of molecules (as brought into the neighbourhood of one another by symmetry operation, glycines II and III) and thereby bypassing the formidable problems of parameter correlations.

The structural studies of paraelectric DTGS have underlined how, in general, considerations, uncommon in conventional crystal structure determinations, are necessary when dealing with the structural problems of ferroelectrics.

APPENDIX I

The F distribution and α : α is the level of statistical significance, i.e. the probability of being wrong in rejecting a hypothesis.

A point on the F distribution is specified through:

$$F_{b, n-m} = \frac{n-m}{b} \frac{V_c' P V_c - V' P V}{V' P V}$$

see section II.2.b. F has a known distribution $\phi(F)$ for F greater than zero.

$$\phi(F) = \frac{\Gamma((v_1 + v_2)/2)}{\Gamma(\frac{1}{2}v_1) \Gamma(\frac{1}{2}v_2)} \left(\frac{v_1}{v_2}\right)^{\frac{1}{2}v_1} F^{(v_1-2)/2} (1 + \frac{v_1}{v_2} F)^{-(v_1+v_2)/2}$$

v_2 corresponds to $n - m$ and v_1 to b (see section II.2.b).

The accumulative probability of F is

$$P(F|v_1, v_2) = \frac{v_1^{\frac{1}{2}v_1} v_2^{\frac{1}{2}v_2}}{B(\frac{1}{2}v_1, \frac{1}{2}v_2)} \int_0^F F^{(v_1-2)/2} (v_2 + v_1 F)^{-(v_1+v_2)/2} dF$$

We are interested in the probability $Q(F|v_1, v_2) = 1 - P(F|v_1, v_2)$ the probability of $F > F_{v_1, v_2}$ which is equal to α . Therefore

$$\alpha = - \int_{\infty}^F \phi(F) dF$$

We make the substitution

$$X = \frac{v_2}{v_2 + v_1 F}$$

in which case

$$\alpha = \frac{1}{B(\frac{1}{2}v_1, \frac{1}{2}v_2)} \int_0^X x^{\frac{1}{2}v_2-1} (1-x)^{\frac{1}{2}v_1-1} dx$$

This is equal to the Incomplete Beta function

$I_X(\frac{1}{2}v_2, \frac{1}{2}v_1)$: see Handbook of Mathematical Functions, p. 263, edited by M. Abramowitz and I.A. Stegun, 1965 New York, Dover.

The working out of $I_X(\frac{1}{2}v_2, \frac{1}{2}v_1)$ is carried out by a standard Fortran subroutine, BDTR (see the IBM System/360 Scientific Subroutine Package Version III, which itself uses the subroutine CDTR, NDTR and DLGAM of the same Subroutine Package).

Thus, by providing v_1, v_2 (= b and $n - m$ respectively), F (see equation II.3.9) and X (defined above) we obtain a value of α , the probability of being wrong in rejecting the hypothesis under test.

APPENDIX II

The extinction correction used in the analysis of the KDP-DKDP data was that of Cooper and Rouse (1970) for spherical crystals.

\hat{f}^2 is replaced, in the analysis, by $\hat{f}^2 y$ where y is an extinction correction:

$$y = \left[1 - \frac{1}{\hat{f}(\theta)} \right] + \frac{1}{5\hat{f}(\theta)} \left[\frac{4 \sinh^{-1} \sqrt{3/2 \hat{f}(\theta) x}}{\sqrt{3/2 \hat{f}(\theta) (1 + 3/2 \hat{f}(\theta) x) x}} + \frac{\tanh \sqrt{3 \hat{f}(\theta) x}}{\sqrt{3 \hat{f}(\theta) x}} \right]$$

where $\hat{f}(\theta) = 1 + 1/3 \sin^{2.5} \theta$ and $x = C \hat{f}^2 / L$ where L is the Lorentz correction, see section II.1.c., and C is the extinction parameter.

APPENDIX III

The room temperature DKDP experiment.

h , k , ℓ , f , \hat{f} , $\mathcal{O}(f)$ and e.c., the extinction correction factor that has been included in \hat{f} , are listed in the following 13 pages; in that order; one set per line.

The first 4 pages labelled λ_1 refer to data sets with $\lambda = 1.15 \text{ \AA}$. The final extinction parameter and scale factor were 0.01046 and 5.027 respectively.

The remaining 9 pages labelled λ_2 refer to data sets with $\lambda = 0.869 \text{ \AA}$. The final extinction parameter and scale factor were 0.00626 and 3.540 respectively.

H	K	L	f	\hat{f}	$\sigma(f)$	e.c.
0.	2.	0.	5.277	5.316	0.049	0.738
2.	2.	0.	9.146	10.345	0.065	0.618
1.	3.	0.	2.162	2.011	0.051	0.953
0.	4.	0.	8.710	8.458	0.055	0.688
2.	4.	0.	9.958	10.506	0.064	0.662
4.	4.	0.	10.140	11.236	0.055	0.691
1.	5.	0.	15.866	18.561	0.103	0.540
3.	5.	0.	10.435	11.395	0.056	0.686
0.	6.	0.	9.861	9.831	0.048	0.707
2.	6.	0.	12.697	13.565	0.064	0.639
4.	6.	0.	15.397	17.457	0.075	0.602
6.	6.	0.	12.546	12.059	0.042	0.680
1.	7.	0.	9.200	9.155	0.041	0.747
3.	7.	0.	4.997	4.702	0.031	0.893
5.	7.	0.	5.081	4.953	0.023	0.894
0.	8.	0.	9.279	9.346	0.033	0.757
2.	8.	0.	10.420	10.728	0.038	0.728
4.	8.	0.	12.811	12.492	0.039	0.679
6.	8.	0.	1.370	1.160	0.034	0.990
8.	8.	0.	2.560	2.292	0.015	0.964
1.	9.	0.	15.082	15.473	0.047	0.637
3.	9.	0.	8.900	9.122	0.025	0.778
5.	9.	0.	3.433	3.495	0.017	0.944
7.	9.	0.	1.568	1.386	0.018	0.985
0.	10.	0.	2.889	3.014	0.020	0.960
2.	10.	0.	5.686	5.567	0.017	0.875
4.	10.	0.	5.134	5.301	0.015	0.889
6.	10.	0.	15.716	16.424	0.031	0.637
1.	11.	0.	4.197	4.178	0.013	0.917
3.	11.	0.	3.253	3.346	0.012	0.943
5.	11.	0.	7.991	7.979	0.012	0.773
0.	12.	0.	11.682	12.734	0.018	0.691
2.	12.	0.	4.746	4.864	0.009	0.876
0.	1.	1.	10.146	11.095	0.073	0.481
1.	2.	1.	10.996	11.899	0.080	0.538
0.	3.	1.	13.960	15.292	0.105	0.504
2.	3.	1.	7.880	8.137	0.057	0.710
1.	4.	1.	8.502	8.360	0.056	0.704
3.	4.	1.	6.107	5.814	0.042	0.820
0.	5.	1.	1.141	1.044	0.076	0.991
2.	5.	1.	10.365	11.229	0.058	0.680
4.	5.	1.	6.885	7.348	0.039	0.815
1.	6.	1.	10.433	11.222	0.052	0.694
3.	6.	1.	13.602	14.687	0.065	0.629
5.	6.	1.	7.500	7.926	0.032	0.810
0.	7.	1.	15.704	16.667	0.077	0.594
2.	7.	1.	7.890	7.708	0.035	0.792
4.	7.	1.	4.607	4.669	0.026	0.908
6.	7.	1.	11.683	10.733	0.036	0.706
1.	8.	1.	10.976	10.976	0.041	0.712
3.	8.	1.	10.320	9.626	0.036	0.734
5.	8.	1.	9.086	8.533	0.028	0.772
7.	8.	1.	6.480	6.210	0.017	0.847
0.	9.	1.	7.308	7.208	0.026	0.824
2.	9.	1.	10.710	10.140	0.032	0.729
4.	9.	1.	7.540	7.245	0.022	0.818
6.	9.	1.	10.140	9.516	0.022	0.743
8.	9.	1.	8.705	8.258	0.013	0.753
1.	10.	1.	5.349	5.333	0.019	0.886
3.	10.	1.	3.651	3.435	0.016	0.937
5.	10.	1.	3.152	2.982	0.014	0.948
0.	11.	1.	7.294	7.539	0.016	0.818

λ_1

2.	11.	1.	4.190	4.162	0.013	0.916
4.	11.	1.	2.955	3.221	0.012	0.948
1.	12.	1.	8.555	8.799	0.013	0.757
1.	1.	2.	15.451	17.831	0.126	0.442
0.	2.	2.	7.292	7.225	0.059	0.696
1.	3.	2.	12.325	13.128	0.086	0.570
3.	3.	2.	11.086	11.578	0.068	0.638
0.	4.	2.	13.576	14.226	0.088	0.568
2.	4.	2.	1.165	1.182	0.083	0.990
1.	5.	2.	10.926	11.290	0.061	0.665
3.	5.	2.	10.236	10.306	0.052	0.701
5.	5.	2.	16.597	18.466	0.083	0.585
0.	6.	2.	20.356	22.454	0.137	0.507
2.	6.	2.	5.350	5.166	0.036	0.873
4.	6.	2.	11.962	12.449	0.050	0.679
1.	7.	2.	9.675	9.591	0.042	0.738
3.	7.	2.	9.175	9.067	0.036	0.759
5.	7.	2.	11.510	10.815	0.039	0.707
7.	7.	2.	9.441	8.826	0.024	0.763
0.	8.	2.	11.868	12.101	0.043	0.692
2.	8.	2.	2.381	1.918	0.031	0.972
4.	8.	2.	5.984	5.878	0.024	0.866
6.	8.	2.	0.862	0.408	0.068	0.996
1.	9.	2.	8.665	8.405	0.027	0.784
3.	9.	2.	8.109	7.809	0.024	0.801
5.	9.	2.	15.893	15.357	0.043	0.637
7.	9.	2.	9.622	9.093	0.018	0.745
0.	10.	2.	15.581	16.288	0.043	0.640
2.	10.	2.	2.158	1.959	0.020	0.976
4.	10.	2.	5.322	5.265	0.015	0.881
6.	10.	2.	6.817	6.548	0.013	0.816
1.	11.	2.	10.823	10.939	0.021	0.724
3.	11.	2.	8.601	8.512	0.016	0.771
0.	12.	2.	3.474	3.678	0.009	0.922
0.	1.	3.	10.440	11.078	0.074	0.603
1.	2.	3.	11.896	12.113	0.080	0.585
0.	3.	3.	15.263	16.298	0.106	0.527
2.	3.	3.	7.887	7.647	0.050	0.744
1.	4.	3.	9.032	8.973	0.052	0.715
3.	4.	3.	6.069	5.888	0.038	0.837
0.	5.	3.	3.422	3.433	0.038	0.934
2.	5.	3.	10.667	10.615	0.053	0.690
4.	5.	3.	6.506	6.034	0.034	0.837
1.	6.	3.	12.413	12.365	0.058	0.657
3.	6.	3.	12.274	12.589	0.053	0.671
5.	6.	3.	7.481	6.894	0.029	0.815
0.	7.	3.	13.731	14.064	0.057	0.643
2.	7.	3.	6.178	6.089	0.029	0.855
4.	7.	3.	5.708	5.476	0.025	0.874
6.	7.	3.	12.810	12.122	0.037	0.685
1.	8.	3.	10.565	10.273	0.036	0.728
3.	8.	3.	8.258	7.873	0.027	0.795
5.	8.	3.	9.199	8.521	0.025	0.770
7.	8.	3.	9.422	8.984	0.020	0.758
0.	9.	3.	10.834	10.624	0.031	0.728
2.	9.	3.	10.717	10.364	0.030	0.731
4.	9.	3.	5.813	5.450	0.018	0.870
6.	9.	3.	6.769	6.658	0.015	0.831
1.	10.	3.	2.122	2.155	0.021	0.977
3.	10.	3.	6.961	6.820	0.017	0.830
5.	10.	3.	1.601	1.351	0.017	0.984
0.	11.	3.	9.311	9.510	0.018	0.756
2.	11.	3.	5.114	5.185	0.012	0.878
4.	11.	3.	2.507	2.458	0.010	0.956

λ_1

0.	0.	4.	18.708	21.855	0.130	0.465
0.	2.	4.	13.240	14.034	0.084	0.582
2.	2.	4.	10.468	10.439	0.063	0.667
1.	3.	4.	2.287	2.253	0.046	0.966
0.	4.	4.	18.501	20.520	0.124	0.519
2.	4.	4.	10.183	10.142	0.052	0.702
4.	4.	4.	8.961	8.663	0.041	0.755
1.	5.	4.	16.221	17.159	0.087	0.575
3.	5.	4.	10.561	10.493	0.045	0.711
0.	6.	4.	9.982	9.749	0.042	0.729
2.	6.	4.	5.707	5.340	0.031	0.868
4.	6.	4.	3.056	2.376	0.027	0.955
6.	6.	4.	20.346	20.815	0.085	0.572
1.	7.	4.	8.471	8.384	0.032	0.783
3.	7.	4.	4.673	4.439	0.024	0.908
5.	7.	4.	4.821	4.659	0.021	0.904
0.	8.	4.	8.798	8.587	0.029	0.779
2.	8.	4.	7.151	6.872	0.025	0.829
4.	8.	4.	3.638	3.617	0.020	0.939
6.	8.	4.	13.372	12.785	0.031	0.677
8.	8.	4.	9.876	9.480	0.015	0.725
1.	9.	4.	14.102	14.224	0.039	0.663
3.	9.	4.	8.607	8.433	0.021	0.785
5.	9.	4.	3.341	3.309	0.014	0.943
7.	9.	4.	1.332	1.234	0.015	0.986
0.	10.	4.	13.371	13.827	0.030	0.677
2.	10.	4.	9.222	9.141	0.019	0.764
4.	10.	4.	8.747	8.467	0.017	0.768
1.	11.	4.	3.861	3.878	0.011	0.917
3.	11.	4.	3.139	3.190	0.009	0.934
0.	1.	5.	10.496	10.094	0.058	0.675
1.	2.	5.	11.159	11.752	0.060	0.665
0.	3.	5.	15.739	16.558	0.090	0.571
2.	3.	5.	8.393	8.095	0.042	0.763
1.	4.	5.	7.406	6.811	0.038	0.801
3.	4.	5.	4.114	3.974	0.030	0.920
0.	5.	5.	2.575	1.966	0.041	0.965
2.	5.	5.	10.230	9.641	0.042	0.725
4.	5.	5.	7.278	7.393	0.028	0.821
1.	6.	5.	11.022	10.840	0.042	0.711
3.	6.	5.	10.513	10.881	0.036	0.729
5.	6.	5.	7.089	6.630	0.024	0.831
0.	7.	5.	12.431	13.347	0.042	0.686
2.	7.	5.	7.443	7.304	0.026	0.819
4.	7.	5.	4.341	4.699	0.025	0.919
6.	7.	5.	12.018	11.696	0.028	0.703
1.	8.	5.	11.360	11.080	0.032	0.716
3.	8.	5.	7.119	7.000	0.020	0.830
5.	8.	5.	6.594	6.479	0.016	0.842
7.	8.	5.	5.873	5.830	0.012	0.846
0.	9.	5.	7.285	7.389	0.019	0.823
2.	9.	5.	8.853	8.607	0.021	0.777
4.	9.	5.	7.091	7.064	0.016	0.822
6.	9.	5.	7.530	7.155	0.012	0.787
1.	10.	5.	1.392	1.609	0.024	0.990
3.	10.	5.	5.474	5.388	0.012	0.864
1.	1.	6.	16.731	17.835	0.092	0.565
0.	2.	6.	7.029	6.777	0.036	0.813
1.	3.	6.	12.665	12.486	0.057	0.657
3.	3.	6.	9.204	8.757	0.038	0.755
0.	4.	6.	12.740	12.257	0.052	0.662
2.	4.	6.	1.451	1.541	0.045	0.989
1.	5.	6.	8.676	8.411	0.033	0.776
3.	5.	6.	9.403	9.778	0.032	0.759
5.	5.	6.	15.287	16.243	0.050	0.639
0.	6.	6.	17.860	19.952	0.073	0.591

λ_1

2.	6.	6.	4.469	4.155	0.022	0.915
4.	6.	6.	10.522	10.631	0.030	0.736
1.	7.	6.	8.882	8.899	0.026	0.778
3.	7.	6.	8.705	8.608	0.024	0.784
5.	7.	6.	9.972	9.542	0.023	0.748
7.	7.	6.	6.266	6.320	0.013	0.836
0.	8.	6.	10.241	10.016	0.026	0.743
2.	8.	6.	2.619	2.303	0.020	0.965
4.	8.	6.	5.242	5.068	0.015	0.884
6.	8.	6.	1.005	0.248	0.019	0.993
1.	9.	6.	7.361	7.225	0.017	0.815
3.	9.	6.	8.359	8.121	0.016	0.781
5.	9.	6.	12.546	12.345	0.020	0.672
0.	10.	6.	12.772	13.334	0.022	0.676
2.	10.	6.	3.557	3.766	0.011	0.923
0.	1.	7.	10.770	11.316	0.045	0.710
1.	2.	7.	10.524	10.567	0.042	0.720
0.	3.	7.	11.964	12.563	0.045	0.687
2.	3.	7.	6.001	6.032	0.027	0.863
1.	4.	7.	7.360	7.587	0.028	0.820
0.	5.	7.	0.200	0.183	0.233	1.000
2.	5.	7.	8.578	8.443	0.026	0.786
4.	5.	7.	4.379	4.213	0.020	0.917
1.	6.	7.	9.344	8.897	0.027	0.766
3.	6.	7.	11.868	11.957	0.031	0.706
5.	6.	7.	5.479	5.201	0.016	0.878
0.	7.	7.	12.486	12.723	0.032	0.694
2.	7.	7.	3.917	4.032	0.016	0.930
4.	7.	7.	4.505	4.344	0.014	0.908
6.	7.	7.	7.769	7.474	0.013	0.787
1.	8.	7.	6.710	6.946	0.016	0.836
3.	8.	7.	7.904	7.868	0.016	0.795
5.	8.	7.	7.060	6.794	0.012	0.802
0.	9.	7.	7.138	7.329	0.014	0.810
2.	9.	7.	8.620	8.507	0.015	0.763
0.	0.	8.	24.333	27.531	0.146	0.517
0.	2.	8.	5.699	5.749	0.025	0.875
2.	2.	8.	8.351	8.419	0.027	0.792
1.	3.	8.	2.273	2.314	0.025	0.975
0.	4.	8.	5.427	5.478	0.021	0.884
2.	4.	8.	8.417	8.574	0.025	0.792
4.	4.	8.	9.025	9.185	0.023	0.774
1.	5.	8.	13.213	13.209	0.036	0.679
3.	5.	8.	8.399	8.201	0.021	0.791
0.	6.	8.	7.244	7.674	0.019	0.825
2.	6.	8.	10.500	10.542	0.024	0.736
4.	6.	8.	11.903	12.453	0.025	0.702
6.	6.	8.	7.410	7.705	0.012	0.791
3.	7.	8.	3.257	3.574	0.014	0.943
5.	7.	8.	3.435	3.705	0.009	0.925
0.	8.	8.	6.560	6.604	0.014	0.828
2.	8.	8.	7.748	7.703	0.013	0.787
0.	1.	9.	8.590	8.421	0.025	0.787
1.	2.	9.	8.319	8.411	0.024	0.795
0.	3.	9.	11.501	11.754	0.030	0.714
2.	3.	9.	6.293	6.499	0.018	0.855
1.	4.	9.	4.307	4.348	0.016	0.918
3.	6.	9.	8.398	8.607	0.016	0.773
0.	7.	9.	10.242	10.575	0.017	0.723
2.	7.	9.	5.755	5.954	0.011	0.843
3.	5.	10.	6.362	6.550	0.011	0.818

λ_1

0.	2.	0.	4.058	4.263	0.074	0.841
2.	2.	0.	7.273	8.591	0.090	0.729
1.	3.	0.	1.227	1.467	0.154	0.987
0.	4.	0.	6.630	6.954	0.079	0.803
2.	4.	0.	7.406	8.797	0.085	0.788
4.	4.	0.	8.047	9.102	0.078	0.795
1.	5.	0.	12.928	15.451	0.135	0.638
3.	5.	0.	8.267	9.251	0.077	0.792
0.	6.	0.	7.692	7.962	0.080	0.814
2.	6.	0.	9.677	11.333	0.083	0.758
4.	6.	0.	12.238	14.422	0.097	0.706
6.	6.	0.	9.245	10.048	0.067	0.804
1.	7.	0.	6.964	7.364	0.062	0.854
3.	7.	0.	3.614	3.536	0.062	0.953
5.	7.	0.	3.624	3.730	0.050	0.957
0.	8.	0.	6.759	7.564	0.056	0.870
2.	8.	0.	8.091	8.653	0.056	0.834
4.	8.	0.	9.563	10.373	0.058	0.801
6.	8.	0.	0.870	0.823	0.112	0.998
8.	8.	0.	1.979	1.655	0.048	0.988
3.	9.	0.	6.870	7.255	0.048	0.878
5.	9.	0.	2.693	2.547	0.048	0.977
7.	9.	0.	1.446	0.984	0.057	0.993
0.	10.	0.	2.507	2.167	0.045	0.980
2.	10.	0.	4.282	4.240	0.036	0.947
4.	10.	0.	3.792	4.020	0.034	0.958
6.	10.	0.	13.332	13.355	0.055	0.736
8.	10.	0.	7.877	7.848	0.026	0.863
10.	10.	0.	1.005	1.206	0.040	0.997
3.	11.	0.	2.540	2.449	0.036	0.981
5.	11.	0.	6.612	6.502	0.028	0.894
7.	11.	0.	2.779	3.074	0.028	0.977
9.	11.	0.	5.842	5.941	0.017	0.909
0.	12.	0.	10.495	10.358	0.036	0.799
2.	12.	0.	3.980	3.736	0.025	0.955
4.	12.	0.	1.339	0.422	0.043	0.994
6.	12.	0.	5.981	5.801	0.020	0.909
8.	12.	0.	4.521	4.702	0.017	0.940
10.	12.	0.	1.349	1.065	0.019	0.993
1.	13.	0.	2.283	2.489	0.030	0.984
3.	13.	0.	1.612	1.247	0.030	0.992
5.	13.	0.	1.957	1.916	0.026	0.988
7.	13.	0.	1.404	0.169	0.022	0.993
9.	13.	0.	0.876	1.684	0.030	0.997
0.	14.	0.	12.205	12.273	0.029	0.762
2.	14.	0.	3.454	3.339	0.017	0.963
4.	14.	0.	1.301	0.781	0.026	0.994
6.	14.	0.	1.532	1.876	0.022	0.991
8.	14.	0.	2.573	2.442	0.010	0.970
1.	15.	0.	1.124	0.625	0.034	0.995
3.	15.	0.	0.180	1.268	0.155	1.000
5.	15.	0.	7.010	7.042	0.012	0.859
0.	16.	0.	3.180	3.142	0.010	0.958
2.	16.	0.	2.887	3.150	0.010	0.964
0.	3.	1.	11.142	13.059	0.132	0.611
1.	4.	1.	6.614	6.781	0.081	0.811
2.	5.	1.	8.322	9.093	0.082	0.782
4.	5.	1.	5.422	5.679	0.060	0.895
1.	6.	1.	8.392	9.040	0.075	0.794
3.	6.	1.	10.943	12.033	0.085	0.732
5.	6.	1.	6.312	6.074	0.049	0.882
0.	7.	1.	12.421	13.821	0.100	0.699
2.	7.	1.	6.207	6.028	0.051	0.880
4.	7.	1.	3.652	3.455	0.049	0.954

6.	7.	1.	8.335	8.955	0.051	0.837
1.	8.	1.	8.286	8.973	0.059	0.827
3.	8.	1.	7.606	7.860	0.054	0.851
5.	8.	1.	6.723	6.863	0.042	0.882
7.	8.	1.	4.842	4.827	0.033	0.935
0.	9.	1.	5.555	5.615	0.043	0.911
2.	9.	1.	8.008	8.282	0.046	0.846
4.	9.	1.	5.738	5.681	0.036	0.911
8.	9.	1.	6.864	6.856	0.028	0.888
1.	10.	1.	4.278	4.011	0.034	0.946
3.	10.	1.	2.639	2.524	0.038	0.978
5.	10.	1.	2.093	2.186	0.047	0.987
7.	10.	1.	4.591	4.378	0.025	0.942
9.	10.	1.	0.789	1.097	0.059	0.998
0.	11.	1.	5.703	5.938	0.032	0.915
2.	11.	1.	3.102	3.109	0.033	0.971
4.	11.	1.	2.564	2.344	0.055	0.980
6.	11.	1.	6.318	6.340	0.025	0.902
8.	11.	1.	4.273	4.275	0.019	0.948
10.	11.	1.	0.372	0.734	0.083	0.999
1.	12.	1.	7.230	7.192	0.028	0.879
3.	12.	1.	4.808	5.117	0.024	0.938
5.	12.	1.	4.782	4.837	0.022	0.938
7.	12.	1.	5.317	5.201	0.018	0.923
9.	12.	1.	4.180	4.372	0.013	0.944
11.	12.	1.	1.700	1.891	0.012	0.985
0.	13.	1.	8.221	8.270	0.026	0.854
2.	13.	1.	1.881	2.082	0.031	0.989
4.	13.	1.	1.186	0.837	0.041	0.995
6.	13.	1.	4.354	4.044	0.015	0.944
8.	13.	1.	1.159	1.240	0.027	0.995
1.	14.	1.	4.501	4.540	0.017	0.942
3.	14.	1.	3.626	3.605	0.016	0.959
5.	14.	1.	1.647	1.856	0.024	0.990
7.	14.	1.	4.829	4.941	0.011	0.921
0.	15.	1.	1.727	1.733	0.020	0.989
2.	15.	1.	5.282	5.105	0.012	0.916
4.	15.	1.	3.368	3.263	0.011	0.959
6.	15.	1.	2.777	2.810	0.009	0.965
1.	16.	1.	2.039	2.315	0.012	0.981
3.	16.	1.	3.332	3.507	0.008	0.949
1.	1.	2.	12.359	15.430	0.154	0.543
0.	2.	2.	5.767	5.847	0.087	0.800
1.	3.	2.	10.008	10.935	0.114	0.675
3.	3.	2.	8.844	9.525	0.096	0.745
0.	4.	2.	10.921	11.884	0.113	0.674
1.	5.	2.	8.768	9.187	0.082	0.769
3.	5.	2.	8.228	8.287	0.073	0.800
5.	5.	2.	13.417	15.154	0.106	0.682
0.	6.	2.	16.210	18.744	0.170	0.601
2.	6.	2.	4.227	3.884	0.058	0.932
4.	6.	2.	9.475	10.128	0.071	0.785
1.	7.	2.	7.494	7.702	0.060	0.841
3.	7.	2.	7.125	7.222	0.051	0.858
5.	7.	2.	8.190	9.018	0.051	0.837
7.	7.	2.	6.850	7.183	0.042	0.883
0.	8.	2.	9.360	9.827	0.061	0.799
2.	8.	2.	1.639	1.376	0.083	0.990
4.	8.	2.	4.646	4.467	0.041	0.935
6.	8.	2.	0.196	0.288	0.404	1.000
1.	9.	2.	6.643	6.671	0.043	0.883
3.	9.	2.	6.188	6.166	0.038	0.898
5.	9.	2.	11.909	12.866	0.057	0.758

λ_2

7.	9.	2.	7.525	7.477	0.032	0.871
9.	9.	2.	10.034	9.698	0.030	0.811
0.	10.	2.	12.232	13.405	0.062	0.748
2.	10.	2.	1.768	1.399	0.052	0.990
4.	10.	2.	3.870	4.024	0.034	0.957
6.	10.	2.	5.272	5.235	0.027	0.927
8.	10.	2.	2.789	2.935	0.025	0.977
1.	11.	2.	8.972	8.863	0.036	0.833
3.	11.	2.	6.988	6.870	0.028	0.884
5.	11.	2.	5.135	4.790	0.024	0.930
7.	11.	2.	4.665	4.540	0.020	0.940
9.	11.	2.	3.831	3.836	0.016	0.955
11.	11.	2.	3.713	3.954	0.011	0.949
0.	12.	2.	2.530	2.755	0.032	0.981
2.	12.	2.	1.690	1.615	0.040	0.991
4.	12.	2.	3.113	3.069	0.025	0.971
6.	12.	2.	4.696	4.679	0.019	0.939
8.	12.	2.	1.485	1.348	0.025	0.992
10.	12.	2.	3.959	3.931	0.010	0.942
1.	13.	2.	4.720	4.805	0.021	0.939
3.	13.	2.	4.248	4.397	0.020	0.949
5.	13.	2.	4.556	4.560	0.017	0.940
7.	13.	2.	3.484	3.338	0.014	0.960
9.	13.	2.	3.069	3.251	0.010	0.961
0.	14.	2.	1.842	1.548	0.024	0.989
2.	14.	2.	1.696	2.043	0.030	0.990
4.	14.	2.	3.337	3.337	0.016	0.964
6.	14.	2.	6.442	6.494	0.012	0.883
8.	14.	2.	3.219	3.618	0.009	0.953
1.	15.	2.	7.668	7.574	0.014	0.854
3.	15.	2.	5.488	5.451	0.011	0.907
5.	15.	2.	3.512	3.675	0.010	0.951
0.	16.	2.	1.737	1.597	0.013	0.986
2.	16.	2.	1.026	1.267	0.020	0.995
0.	1.	3.	8.802	9.001	0.101	0.696
1.	2.	3.	9.714	10.023	0.107	0.688
0.	3.	3.	12.558	13.571	0.150	0.624
2.	3.	3.	6.157	6.097	0.072	0.843
1.	4.	3.	7.273	7.173	0.075	0.812
3.	4.	3.	4.525	4.542	0.064	0.917
0.	5.	3.	2.582	2.508	0.075	0.970
2.	5.	3.	8.560	8.571	0.075	0.791
4.	5.	3.	4.808	4.668	0.061	0.919
1.	6.	3.	9.920	10.090	0.079	0.762
3.	6.	3.	9.827	10.227	0.073	0.774
5.	6.	3.	5.602	5.397	0.047	0.906
0.	7.	3.	10.775	11.581	0.078	0.752
2.	7.	3.	4.434	4.688	0.056	0.935
4.	7.	3.	4.294	4.154	0.049	0.942
6.	7.	3.	9.885	9.965	0.052	0.800
1.	8.	3.	8.098	8.323	0.052	0.838
3.	8.	3.	5.773	6.316	0.048	0.906
5.	8.	3.	7.200	6.797	0.041	0.872
7.	8.	3.	7.313	7.295	0.035	0.874
0.	9.	3.	8.216	8.660	0.056	0.842
2.	9.	3.	8.037	8.470	0.046	0.849
4.	9.	3.	4.399	4.164	0.035	0.944
6.	9.	3.	5.226	5.231	0.032	0.927
8.	9.	3.	6.022	5.924	0.026	0.909
1.	10.	3.	2.074	1.533	0.043	0.986
3.	10.	3.	5.419	5.335	0.032	0.922
5.	10.	3.	1.075	0.963	0.077	0.996
7.	10.	3.	1.810	1.627	0.036	0.990
9.	10.	3.	2.300	2.653	0.024	0.983

λ_2

0.	11.	3.	7.691	7.671	0.032	0.866
2.	11.	3.	4.046	3.963	0.029	0.954
4.	11.	3.	1.520	1.797	0.046	0.993
6.	11.	3.	4.097	3.766	0.024	0.953
8.	11.	3.	2.302	1.998	0.021	0.983
10.	11.	3.	1.751	2.212	0.021	0.989
1.	12.	3.	5.324	5.423	0.025	0.926
3.	12.	3.	6.115	6.275	0.024	0.907
5.	12.	3.	4.702	4.880	0.020	0.939
7.	12.	3.	4.155	3.824	0.016	0.949
9.	12.	3.	4.959	5.177	0.012	0.922
0.	13.	3.	5.973	6.005	0.020	0.909
2.	13.	3.	0.806	1.057	0.057	0.998
4.	13.	3.	2.715	2.417	0.018	0.977
6.	13.	3.	6.294	5.950	0.015	0.895
8.	13.	3.	2.521	2.737	0.014	0.975
1.	14.	3.	3.166	3.341	0.018	0.968
3.	14.	3.	5.293	5.199	0.014	0.920
5.	14.	3.	2.546	2.204	0.014	0.977
7.	14.	3.	2.023	2.358	0.013	0.982
0.	15.	3.	1.149	0.260	0.023	0.995
2.	15.	3.	4.871	4.847	0.011	0.923
4.	15.	3.	2.958	3.153	0.011	0.965
0.	0.	4.	14.862	18.708	0.184	0.566
0.	2.	4.	10.284	11.867	0.106	0.699
2.	2.	4.	8.488	8.459	0.086	0.768
1.	3.	4.	2.104	1.605	0.079	0.977
0.	4.	4.	14.326	17.468	0.152	0.627
2.	4.	4.	8.108	8.177	0.072	0.804
4.	4.	4.	7.003	6.890	0.060	0.853
1.	5.	4.	12.739	14.339	0.108	0.683
3.	5.	4.	8.427	8.435	0.063	0.811
0.	6.	4.	7.592	7.896	0.061	0.838
6.	8.	4.	10.788	10.461	0.049	0.787
8.	8.	4.	7.910	7.938	0.029	0.862
1.	9.	4.	11.159	11.652	0.055	0.771
3.	9.	4.	6.585	6.735	0.036	0.891
5.	9.	4.	2.720	2.416	0.035	0.978
7.	9.	4.	1.428	0.876	0.043	0.994
0.	10.	4.	10.936	11.263	0.047	0.783
2.	10.	4.	7.421	7.343	0.033	0.872
4.	10.	4.	7.042	6.855	0.029	0.883
6.	10.	4.	5.419	5.438	0.024	0.923
8.	10.	4.	1.864	1.416	0.026	0.989
10.	10.	4.	7.334	7.306	0.015	0.868
1.	11.	4.	3.132	2.891	0.027	0.971
3.	11.	4.	2.641	2.354	0.028	0.979
5.	11.	4.	6.066	5.918	0.023	0.908
7.	11.	4.	3.204	2.801	0.018	0.969
9.	11.	4.	5.481	5.319	0.014	0.914
0.	12.	4.	1.511	1.706	0.043	0.993
2.	12.	4.	5.381	5.644	0.022	0.924
4.	12.	4.	7.978	7.458	0.022	0.860
6.	12.	4.	2.324	2.353	0.021	0.983
8.	12.	4.	2.368	2.536	0.017	0.980
10.	12.	4.	4.496	4.484	0.009	0.920
1.	13.	4.	2.453	2.276	0.022	0.981
3.	13.	4.	1.555	1.187	0.028	0.992
5.	13.	4.	1.461	1.662	0.026	0.993
7.	13.	4.	1.125	0.120	0.024	0.995
0.	14.	4.	5.916	6.180	0.015	0.905
2.	14.	4.	4.137	4.097	0.015	0.947
4.	14.	4.	6.702	6.593	0.013	0.879
6.	14.	4.	4.194	4.152	0.010	0.936

λ_2

1.	15.	4.	1.180	0.680	0.021	0.994
3.	15.	4.	1.427	1.441	0.017	0.991
0.	1.	5.	8.223	8.258	0.082	0.784
1.	2.	5.	9.162	9.480	0.082	0.762
0.	3.	5.	12.336	13.897	0.109	0.681
2.	3.	5.	6.332	6.467	0.065	0.865
1.	4.	5.	5.987	5.272	0.052	0.880
3.	4.	5.	3.021	2.935	0.062	0.965
0.	5.	5.	1.825	1.415	0.105	0.987
2.	5.	5.	8.016	7.757	0.059	0.828
4.	5.	5.	5.733	5.719	0.044	0.902
1.	6.	5.	8.534	8.802	0.060	0.820
3.	6.	5.	8.725	8.616	0.056	0.820
7.	8.	5.	4.802	4.551	0.026	0.938
4.	9.	5.	5.554	5.561	0.031	0.919
6.	9.	5.	5.923	5.836	0.026	0.911
8.	9.	5.	5.704	5.522	0.021	0.916
1.	10.	5.	1.460	1.137	0.054	0.993
3.	10.	5.	4.714	4.125	0.026	0.939
5.	10.	5.	2.049	2.178	0.036	0.987
7.	10.	5.	1.612	1.525	0.038	0.992
9.	10.	5.	3.960	3.668	0.014	0.952
0.	11.	5.	7.076	6.992	0.026	0.883
2.	11.	5.	2.823	2.641	0.027	0.976
4.	11.	5.	2.090	1.719	0.032	0.987
6.	11.	5.	3.892	3.607	0.018	0.956
8.	11.	5.	3.092	2.737	0.015	0.969
10.	11.	5.	1.879	1.919	0.014	0.985
1.	12.	5.	5.840	5.793	0.020	0.913
3.	12.	5.	6.006	6.045	0.020	0.908
5.	12.	5.	4.198	4.026	0.017	0.948
7.	12.	5.	2.508	2.509	0.018	0.978
9.	12.	5.	3.944	4.157	0.010	0.941
0.	13.	5.	5.206	5.188	0.017	0.925
2.	13.	5.	1.233	1.052	0.035	0.995
4.	13.	5.	2.467	2.256	0.017	0.980
6.	13.	5.	5.437	5.122	0.011	0.911
8.	13.	5.	3.266	3.410	0.009	0.954
1.	14.	5.	1.925	1.558	0.018	0.987
3.	14.	5.	4.714	4.870	0.012	0.929
5.	14.	5.	2.028	2.065	0.013	0.983
0.	15.	5.	1.103	1.393	0.025	0.995
2.	15.	5.	4.078	4.188	0.009	0.935
0.	2.	6.	5.402	5.269	0.059	0.898
1.	3.	6.	9.945	10.253	0.073	0.766
3.	3.	6.	5.183	7.450	0.095	0.913
0.	4.	6.	9.797	10.122	0.070	0.777
2.	4.	6.	1.323	1.090	0.101	0.993
1.	5.	6.	6.611	6.682	0.054	0.876
3.	5.	6.	7.427	7.769	0.050	0.857
0.	6.	6.	14.035	16.435	0.105	0.692
2.	6.	6.	3.311	3.084	0.049	0.964
7.	7.	6.	5.013	4.966	0.028	0.933
6.	8.	6.	0.938	0.176	0.069	0.997
1.	9.	6.	5.702	5.710	0.032	0.915
3.	9.	6.	6.630	6.537	0.029	0.893
5.	9.	6.	10.501	10.333	0.036	0.799
7.	9.	6.	4.787	4.542	0.020	0.938
9.	9.	6.	8.994	8.458	0.021	0.831
0.	10.	6.	11.027	10.925	0.039	0.786
2.	10.	6.	3.026	2.796	0.028	0.973
4.	10.	6.	3.312	3.543	0.026	0.968
6.	10.	6.	4.353	4.248	0.020	0.947
8.	10.	6.	2.550	2.303	0.019	0.979

λ_2

1.	11.	6.	6.518	6.676	0.024	0.897
3.	11.	6.	5.391	5.671	0.024	0.924
5.	11.	6.	4.722	4.664	0.017	0.938
7.	11.	6.	5.047	4.972	0.015	0.927
9.	11.	6.	4.263	4.074	0.011	0.937
0.	12.	6.	2.515	2.205	0.023	0.980
2.	12.	6.	1.474	1.461	0.037	0.993
4.	12.	6.	2.530	2.624	0.022	0.980
6.	12.	6.	3.393	3.897	0.016	0.962
8.	12.	6.	1.028	1.252	0.027	0.995
1.	13.	6.	3.819	3.722	0.015	0.955
3.	13.	6.	3.630	3.869	0.017	0.958
5.	13.	6.	3.531	3.415	0.012	0.957
7.	13.	6.	3.369	3.510	0.009	0.952
0.	14.	6.	1.739	1.299	0.017	0.988
2.	14.	6.	1.906	1.734	0.014	0.986
4.	14.	6.	2.247	2.713	0.013	0.979
0.	1.	7.	9.061	8.949	0.066	0.797
0.	3.	7.	9.770	10.096	0.067	0.785
2.	3.	7.	4.405	4.614	0.070	0.937
1.	4.	7.	5.524	5.925	0.049	0.909
3.	4.	7.	4.114	4.305	0.059	0.947
0.	5.	7.	1.349	0.128	0.082	0.994
2.	5.	7.	6.818	6.642	0.042	0.878
4.	5.	7.	3.553	3.108	0.040	0.961
1.	6.	7.	7.229	7.114	0.045	0.870
3.	6.	7.	9.504	9.688	0.048	0.812
0.	7.	7.	9.744	10.432	0.050	0.808
6.	7.	7.	6.132	6.060	0.027	0.906
3.	8.	7.	6.324	6.271	0.029	0.900
5.	8.	7.	5.786	5.457	0.026	0.915
7.	8.	7.	4.801	5.184	0.024	0.937
0.	9.	7.	6.111	5.770	0.026	0.906
2.	9.	7.	7.166	6.907	0.028	0.880
6.	9.	7.	4.668	4.609	0.021	0.940
8.	9.	7.	4.967	4.826	0.016	0.931
1.	10.	7.	3.245	3.040	0.025	0.969
3.	10.	7.	2.650	2.483	0.026	0.979
5.	10.	7.	1.473	1.570	0.035	0.993
7.	10.	7.	3.177	3.259	0.018	0.968
9.	10.	7.	1.476	1.042	0.019	0.992
0.	11.	7.	4.117	4.079	0.021	0.952
2.	11.	7.	3.540	3.175	0.020	0.963
4.	11.	7.	1.653	1.421	0.031	0.991
6.	11.	7.	4.579	4.296	0.014	0.938
8.	11.	7.	3.224	3.050	0.012	0.962
1.	12.	7.	4.335	4.017	0.015	0.945
3.	12.	7.	3.356	3.542	0.017	0.965
5.	12.	7.	4.125	4.217	0.014	0.946
7.	12.	7.	5.163	4.853	0.010	0.911
0.	13.	7.	6.378	6.194	0.013	0.890
2.	13.	7.	2.574	2.444	0.014	0.977
4.	13.	7.	0.948	0.961	0.026	0.996
6.	13.	7.	3.154	3.134	0.009	0.957
1.	14.	7.	4.171	4.205	0.010	0.935
3.	14.	7.	2.459	2.462	0.010	0.973
0.	0.	8.	20.300	21.727	0.204	0.580
0.	2.	8.	4.453	4.342	0.045	0.938
2.	2.	8.	6.754	6.577	0.044	0.878
1.	3.	8.	1.381	1.661	0.083	0.993
0.	4.	8.	4.350	4.112	0.041	0.943
2.	4.	8.	6.872	6.706	0.041	0.879

λ_2

4.	4.	8.	7.553	7.222	0.038	0.865
1.	5.	8.	10.318	10.842	0.054	0.791
3.	5.	8.	6.783	6.461	0.038	0.885
0.	6.	8.	5.996	5.936	0.034	0.906
2.	6.	8.	8.570	8.475	0.036	0.840
4.	6.	8.	10.409	9.959	0.043	0.797
6.	6.	8.	6.320	6.185	0.025	0.901
1.	7.	8.	5.069	4.764	0.028	0.930
3.	7.	8.	2.479	2.620	0.038	0.981
5.	7.	8.	2.673	2.761	0.031	0.979
0.	8.	8.	5.632	5.153	0.029	0.918
2.	8.	8.	6.386	6.200	0.028	0.900
4.	8.	8.	7.435	7.136	0.027	0.874
6.	8.	8.	0.818	0.464	0.058	0.998
8.	8.	8.	2.495	2.604	0.020	0.980
1.	9.	8.	9.148	8.681	0.028	0.832
3.	9.	8.	5.322	5.264	0.023	0.926
5.	9.	8.	2.430	1.998	0.022	0.982
7.	9.	8.	0.903	0.629	0.041	0.997
0.	10.	8.	1.369	0.680	0.038	0.994
2.	10.	8.	2.784	2.728	0.022	0.977
4.	10.	8.	3.698	3.418	0.017	0.960
6.	10.	8.	9.545	9.360	0.020	0.817
8.	10.	8.	5.726	5.738	0.012	0.902
1.	11.	8.	2.257	2.291	0.022	0.984
3.	11.	8.	1.600	2.038	0.026	0.992
5.	11.	8.	4.658	4.394	0.013	0.935
7.	11.	8.	2.075	2.191	0.014	0.983
0.	12.	8.	7.209	7.317	0.016	0.871
2.	12.	8.	2.649	3.024	0.017	0.976
4.	12.	8.	1.655	0.710	0.017	0.990
1.	13.	8.	1.440	1.751	0.019	0.992
0.	1.	9.	6.844	6.634	0.041	0.880
1.	2.	9.	6.193	6.698	0.044	0.899
0.	3.	9.	9.330	9.471	0.046	0.817
4.	5.	9.	4.072	4.000	0.029	0.953
1.	6.	9.	5.001	4.842	0.029	0.932
3.	6.	9.	7.338	6.860	0.030	0.876
5.	6.	9.	3.902	3.469	0.024	0.957
0.	7.	9.	8.894	8.615	0.034	0.837
2.	7.	9.	4.921	4.647	0.024	0.935
4.	7.	9.	2.057	1.208	0.027	0.987
6.	7.	9.	5.834	5.504	0.020	0.913
1.	8.	9.	6.320	6.000	0.023	0.902
3.	8.	9.	4.711	4.779	0.024	0.939
5.	8.	9.	3.722	3.524	0.021	0.960
7.	8.	9.	1.473	1.156	0.025	0.993
0.	9.	9.	1.612	1.530	0.038	0.992
2.	9.	9.	4.336	4.204	0.020	0.947
4.	9.	9.	3.974	4.230	0.019	0.954
6.	9.	9.	5.482	5.434	0.015	0.917
8.	9.	9.	4.461	4.424	0.012	0.934
1.	10.	9.	2.399	2.563	0.022	0.982
3.	10.	9.	0.579	1.227	0.063	0.999
5.	10.	9.	1.825	1.638	0.022	0.988
7.	10.	9.	2.265	2.539	0.015	0.980
0.	11.	9.	3.267	3.272	0.016	0.966
2.	11.	9.	1.759	0.830	0.019	0.989
4.	11.	9.	1.878	1.861	0.018	0.987
6.	11.	9.	3.777	3.780	0.011	0.946
1.	12.	9.	5.049	5.132	0.012	0.919

λ_2

3.	12.	9.	3.256	3.486	0.011	0.960
5.	12.	9.	1.788	2.064	0.012	0.985
0.	13.	9.	4.475	4.698	0.009	0.921
2.	13.	9.	1.901	1.734	0.010	0.982
1.	1.	10.	9.628	9.954	0.041	0.814
0.	2.	10.	3.559	3.606	0.037	0.963
1.	3.	10.	7.417	7.142	0.034	0.872
3.	3.	10.	7.122	7.178	0.031	0.881
0.	4.	10.	6.913	6.308	0.030	0.886
2.	4.	10.	1.646	1.039	0.044	0.992
1.	5.	10.	6.889	6.694	0.028	0.887
3.	5.	10.	5.250	5.231	0.026	0.927
5.	5.	10.	8.100	8.163	0.028	0.857
0.	6.	10.	11.172	10.850	0.039	0.784
2.	6.	10.	2.144	1.983	0.035	0.986
4.	6.	10.	6.042	5.721	0.020	0.908
1.	7.	10.	4.431	4.426	0.024	0.946
3.	7.	10.	3.942	3.900	0.021	0.956
5.	7.	10.	5.079	4.887	0.017	0.930
7.	7.	10.	4.660	4.700	0.015	0.936
0.	8.	10.	5.729	5.155	0.020	0.915
2.	8.	10.	2.087	1.399	0.025	0.986
4.	8.	10.	2.577	2.693	0.020	0.979
6.	8.	10.	1.281	0.197	0.026	0.994
1.	9.	10.	3.944	3.891	0.017	0.954
5.	9.	10.	7.258	7.258	0.015	0.869
7.	9.	10.	5.481	5.459	0.011	0.905
0.	10.	10.	7.228	7.298	0.016	0.872
2.	10.	10.	3.170	2.728	0.014	0.967
4.	10.	10.	2.923	2.579	0.013	0.970
6.	10.	10.	2.812	2.753	0.011	0.968
1.	11.	10.	5.536	5.402	0.011	0.907
3.	11.	10.	3.779	4.116	0.011	0.948
5.	11.	10.	2.406	2.298	0.010	0.974
0.	12.	10.	1.292	1.413	0.017	0.992
2.	12.	10.	1.036	1.118	0.020	0.995
0.	1.	11.	4.947	4.909	0.027	0.934
1.	2.	11.	5.031	5.009	0.026	0.932
0.	3.	11.	7.255	6.621	0.026	0.878
2.	3.	11.	2.925	3.070	0.029	0.975
1.	4.	11.	4.244	3.943	0.023	0.950
3.	4.	11.	2.661	2.958	0.028	0.979
0.	5.	11.	2.024	1.223	0.030	0.987
2.	5.	11.	4.344	3.808	0.021	0.947
4.	5.	11.	1.234	1.161	0.040	0.995
1.	6.	11.	5.045	5.113	0.023	0.931
3.	6.	11.	5.420	5.302	0.018	0.922
0.	7.	11.	5.219	5.325	0.019	0.926
6.	7.	11.	4.785	4.464	0.013	0.930
5.	8.	11.	3.509	3.698	0.014	0.959
7.	8.	11.	4.192	4.293	0.010	0.935
2.	9.	11.	4.753	4.477	0.013	0.931
4.	9.	11.	1.172	1.540	0.027	0.995
6.	9.	11.	1.782	1.806	0.013	0.986

λ_2

1.	10.	11.	1.099	1.200	0.034	0.995
3.	10.	11.	2.678	2.766	0.011	0.972
5.	10.	11.	1.226	0.900	0.021	0.993
0.	11.	11.	2.538	3.518	0.016	0.971
2.	11.	11.	2.372	2.216	0.010	0.974
0.	0.	12.	8.025	8.066	0.028	0.859
2.	2.	12.	5.054	5.007	0.020	0.931
0.	4.	12.	9.340	9.018	0.026	0.826
2.	4.	12.	4.891	4.687	0.019	0.934
4.	4.	12.	3.114	2.915	0.017	0.970
1.	5.	12.	6.451	6.065	0.017	0.896
3.	5.	12.	4.040	3.814	0.016	0.952
0.	6.	12.	4.272	3.999	0.017	0.946
4.	8.	12.	1.614	1.828	0.017	0.989
6.	8.	12.	4.600	5.056	0.010	0.915
1.	9.	12.	5.102	5.137	0.011	0.913
3.	9.	12.	3.087	3.258	0.011	0.961
0.	10.	12.	5.000	5.041	0.009	0.903
0.	1.	13.	2.377	2.744	0.024	0.982
1.	2.	13.	3.277	3.257	0.019	0.967
4.	7.	13.	1.341	1.575	0.017	0.992
1.	8.	13.	3.516	3.725	0.009	0.949

λ_2

APPENDIX IV

The experiment on DKDP at $T_c + 5^\circ\text{K}$ ($213.8(3)^\circ\text{K}$).

h , k , l , f , \hat{f} , $\hat{O}(f)$ and e.c., the extinction correction factor that has been included in \hat{f} , are listed in the following 4 pages; in that order; one set per line.

$\lambda = 0.882 \overset{\circ}{\text{A}}$. The final extinction parameter and scale factor were 0.00975 and 1.853 respectively.

H	K	L	f	\hat{f}	$\sigma(f)$	e.c.
0.	2.	0.	2.783	2.249	0.047	0.876
2.	2.	0.	4.918	4.911	0.075	0.781
1.	3.	0.	1.088	0.888	0.116	0.985
0.	4.	0.	4.591	3.808	0.061	0.841
2.	4.	0.	5.589	4.964	0.065	0.806
4.	4.	0.	5.600	5.428	0.061	0.833
1.	5.	0.	8.977	9.390	0.118	0.686
3.	5.	0.	5.786	5.393	0.057	0.828
0.	6.	0.	5.538	4.944	0.051	0.841
2.	6.	0.	7.365	6.806	0.066	0.775
4.	6.	0.	8.623	9.254	0.075	0.747
6.	6.	0.	6.673	6.704	0.046	0.831
1.	7.	0.	5.288	4.632	0.040	0.866
3.	7.	0.	2.728	2.321	0.029	0.959
5.	7.	0.	2.423	2.064	0.032	0.969
0.	8.	0.	6.146	4.243	0.040	0.845
2.	8.	0.	6.139	5.599	0.039	0.848
4.	8.	0.	7.194	6.722	0.046	0.818
6.	8.	0.	1.551	0.559	0.030	0.988
8.	8.	0.	2.294	2.077	0.020	0.976
1.	9.	0.	8.854	8.445	0.062	0.766
3.	9.	0.	5.272	4.599	0.030	0.887
5.	9.	0.	2.306	1.870	0.024	0.975
7.	9.	0.	0.223	0.604	0.114	1.000
0.	10.	0.	1.514	1.542	0.029	0.989
2.	10.	0.	3.563	3.098	0.022	0.943
4.	10.	0.	3.009	2.772	0.021	0.959
6.	10.	0.	9.884	10.273	0.046	0.758
8.	10.	0.	6.230	6.485	0.017	0.865
10.	10.	0.	0.448	0.899	0.027	0.999
1.	11.	0.	2.207	2.466	0.020	0.977
3.	11.	0.	2.296	1.866	0.018	0.976
5.	11.	0.	5.182	5.285	0.017	0.898
7.	11.	0.	2.661	2.507	0.012	0.967
9.	11.	0.	5.121	5.153	0.010	0.894
0.	12.	0.	8.398	8.289	0.031	0.800
2.	12.	0.	2.902	3.053	0.015	0.962
4.	12.	0.	1.347	0.635	0.016	0.991
6.	12.	0.	4.594	4.649	0.012	0.914
8.	12.	0.	3.563	3.797	0.008	0.940
1.	13.	0.	1.066	1.680	0.019	0.994
3.	13.	0.	0.556	0.947	0.027	0.998
5.	13.	0.	1.460	1.510	0.012	0.989
0.	14.	0.	10.003	10.676	0.028	0.755
2.	14.	0.	2.447	2.677	0.009	0.970
0.	1.	1.	5.099	5.640	0.044	0.671
1.	2.	1.	5.662	5.954	0.063	0.720
0.	3.	1.	7.268	7.816	0.124	0.681
2.	3.	1.	4.292	3.711	0.057	0.850
1.	4.	1.	4.516	4.004	0.052	0.852
3.	4.	1.	2.988	2.582	0.040	0.934
0.	5.	1.	0.904	0.647	0.066	0.993
2.	5.	1.	5.900	5.332	0.056	0.817
4.	5.	1.	3.925	3.553	0.036	0.912
1.	6.	1.	5.960	5.350	0.051	0.827
3.	6.	1.	7.399	7.586	0.061	0.782
5.	6.	1.	4.133	3.706	0.029	0.916

0.	7.	1.	8.737	8.641	0.077	0.741
2.	7.	1.	4.172	3.645	0.031	0.911
4.	7.	1.	2.273	2.005	0.027	0.972
6.	7.	1.	5.894	6.087	0.059	0.865
1.	8.	1.	6.213	5.792	0.039	0.844
3.	8.	1.	5.512	5.087	0.053	0.873
5.	8.	1.	4.693	4.719	0.056	0.906
7.	8.	1.	1.502	3.640	0.076	0.989
0.	9.	1.	4.442	4.015	0.047	0.913
2.	9.	1.	6.030	5.479	0.050	0.860
4.	9.	1.	4.250	3.925	0.062	0.922
6.	9.	1.	5.913	5.555	0.050	0.873
8.	9.	1.	5.218	5.438	0.025	0.897
1.	10.	1.	1.820	2.755	0.093	0.984
3.	10.	1.	1.985	1.862	0.070	0.981
5.	10.	1.	2.005	1.268	0.037	0.981
7.	10.	1.	3.313	3.197	0.020	0.952
9.	10.	1.	1.479	0.939	0.019	0.989
0.	11.	1.	4.925	4.105	0.040	0.905
2.	11.	1.	3.063	2.276	0.031	0.958
4.	11.	1.	2.177	1.819	0.025	0.978
6.	11.	1.	4.800	4.671	0.021	0.910
8.	11.	1.	3.196	3.162	0.014	0.953
1.	12.	1.	5.492	5.421	0.026	0.888
3.	12.	1.	4.208	3.811	0.020	0.927
5.	12.	1.	3.749	3.906	0.017	0.940
7.	12.	1.	4.118	4.393	0.014	0.926
0.	13.	1.	6.671	6.846	0.025	0.851
2.	13.	1.	1.444	1.471	0.021	0.990
6.	13.	1.	3.713	3.792	0.012	0.936
1.	14.	1.	3.732	3.912	0.013	0.937
3.	14.	1.	3.433	3.543	0.011	0.944
1.	1.	2.	6.036	10.391	0.050	0.705
0.	2.	2.	3.713	3.526	0.040	0.855
1.	3.	2.	6.467	6.487	0.067	0.744
3.	3.	2.	5.868	5.483	0.054	0.801
0.	4.	2.	7.030	6.954	0.069	0.744
2.	4.	2.	1.088	0.568	0.049	0.990
1.	5.	2.	5.858	5.360	0.052	0.819
3.	5.	2.	5.379	5.213	0.045	0.851
5.	5.	2.	8.959	9.752	0.075	0.739
0.	6.	2.	10.733	12.019	0.165	0.664
2.	6.	2.	2.845	2.298	0.035	0.951
4.	6.	2.	6.429	6.310	0.044	0.829
1.	7.	2.	5.199	4.661	0.036	0.873
3.	7.	2.	5.022	4.381	0.031	0.885
5.	7.	2.	5.996	6.105	0.054	0.858
7.	7.	2.	4.832	4.951	0.042	0.905
0.	8.	2.	6.650	6.049	0.040	0.830
2.	8.	2.	1.951	0.980	0.047	0.980
4.	8.	2.	3.162	2.966	0.039	0.952
6.	8.	2.	1.205	0.369	0.056	0.993
1.	9.	2.	4.951	4.599	0.043	0.897
3.	9.	2.	4.312	3.961	0.041	0.920
5.	9.	2.	8.974	9.018	0.072	0.776
7.	9.	2.	5.558	5.741	0.030	0.886
9.	9.	2.	7.519	7.704	0.029	0.826
0.	10.	2.	8.563	9.588	0.072	0.786
2.	10.	2.	0.909	1.036	0.067	0.996

4.	10.	2.	3.242	2.823	0.030	0.953
6.	10.	2.	4.003	4.055	0.023	0.933
8.	10.	2.	2.672	2.283	0.016	0.967
1.	11.	2.	6.746	6.615	0.039	0.848
3.	11.	2.	5.253	5.228	0.028	0.895
5.	11.	2.	3.711	3.771	0.020	0.941
7.	11.	2.	3.707	3.513	0.016	0.941
9.	11.	2.	3.315	3.330	0.011	0.947
0.	12.	2.	2.108	1.606	0.021	0.979
2.	12.	2.	0.900	1.295	0.035	0.996
4.	12.	2.	2.774	2.570	0.017	0.965
6.	12.	2.	4.181	4.023	0.015	0.926
1.	13.	2.	3.758	3.890	0.016	0.939
3.	13.	2.	3.515	3.501	0.014	0.945
5.	13.	2.	3.702	3.644	0.012	0.938
0.	14.	2.	1.269	0.970	0.017	0.992
2.	14.	2.	2.088	1.863	0.012	0.978
1.	2.	3.	4.846	6.045	0.056	0.826
0.	3.	3.	7.586	8.383	0.103	0.716
2.	3.	3.	3.906	3.833	0.058	0.892
1.	4.	3.	4.730	4.237	0.065	0.862
3.	4.	3.	3.038	2.849	0.056	0.940
0.	5.	3.	1.297	1.081	0.079	0.988
2.	5.	3.	5.526	5.250	0.069	0.846
4.	5.	3.	3.368	2.882	0.051	0.937
1.	6.	3.	6.602	6.073	0.078	0.813
3.	6.	3.	6.742	6.265	0.070	0.816
5.	6.	3.	3.826	2.959	0.042	0.929
0.	7.	3.	7.574	6.893	0.079	0.790
2.	7.	3.	3.201	2.917	0.043	0.946
4.	7.	3.	2.917	2.704	0.040	0.957
6.	7.	3.	6.671	6.961	0.048	0.842
1.	8.	3.	5.834	5.310	0.052	0.863
3.	8.	3.	4.539	4.244	0.040	0.910
5.	8.	3.	4.896	4.849	0.035	0.902
7.	8.	3.	5.136	4.921	0.029	0.893
0.	9.	3.	6.163	6.179	0.046	0.858
2.	9.	3.	5.935	5.766	0.043	0.867
4.	9.	3.	3.416	2.863	0.028	0.948
6.	9.	3.	4.032	3.749	0.025	0.932
8.	9.	3.	4.749	4.805	0.020	0.911
1.	10.	3.	0.958	0.943	0.048	0.995
3.	10.	3.	3.830	3.703	0.026	0.937
5.	10.	3.	0.999	0.922	0.037	0.995
7.	10.	3.	1.802	1.567	0.019	0.985
9.	10.	3.	2.254	1.924	0.013	0.975
0.	11.	3.	5.650	5.051	0.029	0.883
2.	11.	3.	2.729	2.747	0.022	0.966
4.	11.	3.	1.768	1.348	0.022	0.985
6.	11.	3.	2.968	3.007	0.016	0.960
8.	11.	3.	1.969	1.872	0.013	0.981
1.	12.	3.	4.213	4.136	0.018	0.927
3.	12.	3.	4.929	5.006	0.019	0.905
5.	12.	3.	3.891	3.772	0.015	0.935
7.	12.	3.	3.172	3.229	0.011	0.952
0.	13.	3.	4.772	4.959	0.016	0.909
2.	13.	3.	0.676	0.663	0.030	0.993
4.	13.	3.	1.770	1.814	0.013	0.984
0.	2.	4.	4.852	6.895	0.025	0.846

2.	2.	4.	3.584	5.357	0.024	0.910
1.	3.	4.	0.950	1.576	0.034	0.993
0.	4.	4.	8.859	10.577	0.097	0.711
2.	4.	4.	4.779	4.917	0.032	0.875
4.	4.	4.	4.330	3.309	0.028	0.903
1.	5.	4.	8.370	8.454	0.065	0.745
0.	6.	4.	5.076	4.470	0.030	0.878
2.	6.	4.	2.576	1.788	0.022	0.963
6.	6.	4.	10.729	11.602	0.110	0.717
1.	7.	4.	4.505	4.181	0.025	0.906
3.	7.	4.	2.743	2.166	0.036	0.962
5.	7.	4.	2.405	1.801	0.032	0.972
0.	8.	4.	4.951	4.711	0.039	0.896
2.	8.	4.	3.827	2.991	0.033	0.933
4.	8.	4.	1.539	1.732	0.038	0.988
6.	8.	4.	7.432	7.374	0.043	0.824
8.	8.	4.	5.687	5.306	0.024	0.882
1.	9.	4.	7.938	7.737	0.055	0.803
3.	9.	4.	4.684	4.729	0.029	0.910
5.	9.	4.	1.986	2.218	0.025	0.981
7.	9.	4.	0.965	0.946	0.030	0.995
0.	10.	4.	7.705	7.712	0.045	0.816
2.	10.	4.	5.353	5.221	0.028	0.891
4.	10.	4.	5.148	4.811	0.025	0.899
6.	10.	4.	4.156	4.154	0.018	0.929
8.	10.	4.	0.981	0.935	0.021	0.995
1.	11.	4.	2.353	2.123	0.020	0.975
3.	11.	4.	2.051	2.029	0.019	0.980
5.	11.	4.	4.755	4.900	0.017	0.911
7.	11.	4.	2.634	2.336	0.012	0.967
0.	12.	4.	1.775	1.969	0.017	0.985
2.	12.	4.	4.421	4.178	0.016	0.921
4.	12.	4.	6.055	5.824	0.019	0.869
6.	12.	4.	2.035	2.072	0.012	0.979
1.	13.	4.	1.193	1.487	0.017	0.993
3.	13.	4.	1.539	1.037	0.013	0.988

APPENDIX V

The experiment on KDP at room temperature.

h , k , l , f , \hat{f} , $\check{O}(f)$ and e.c., the extinction correction factor that has been included in \hat{f} , are listed in the following 5 pages; in that order; one set per line.

$\lambda = 1.147 \overset{\circ}{\text{A}}$. The final extinction parameter and scale factor were 0.01138 and 3.445 respectively.

H	K	L	f	f^{\sim}	$\sigma(f)$	e.c.
9.	3.	0.	10.000	10.059	0.010	0.737
-6.	0.	-10.	7.260	7.433	0.020	0.775
-5.	3.	-10.	7.020	7.793	0.060	0.787
-7.	0.	-9.	6.000	5.979	0.010	0.833
-1.	0.	-9.	3.990	3.979	0.040	0.924
3.	0.	-9.	5.110	4.936	0.190	0.887
2.	1.	-9.	4.470	4.135	0.080	0.908
4.	1.	-9.	1.250	1.886	0.180	0.991
-7.	2.	-9.	5.390	6.046	0.040	0.848
3.	2.	-9.	8.960	8.804	0.160	0.766
-6.	3.	-9.	6.570	6.582	0.040	0.819
-8.	0.	-8.	3.470	3.582	0.070	0.928
0.	0.	-8.	14.580	14.451	0.040	0.629
2.	0.	-8.	10.120	10.079	0.460	0.730
4.	0.	-8.	3.900	3.680	0.070	0.927
6.	0.	-8.	4.400	4.576	0.080	0.909
3.	1.	-8.	7.280	7.154	0.260	0.815
5.	1.	-8.	4.560	4.380	0.110	0.905
-8.	2.	-8.	7.090	7.435	0.050	0.798
2.	2.	-8.	4.010	3.830	0.100	0.924
4.	2.	-8.	3.790	3.926	0.070	0.931
-7.	3.	-8.	2.630	2.967	0.060	0.958
5.	3.	-8.	9.050	8.599	0.040	0.763
-6.	4.	-8.	6.750	6.852	0.060	0.824
4.	4.	-8.	12.000	11.803	0.050	0.693
-7.	5.	-8.	1.940	2.178	0.060	0.970
-6.	6.	-8.	3.340	3.744	0.060	0.925
-9.	0.	-7.	2.710	3.183	0.060	0.953
1.	0.	-7.	5.740	5.128	0.260	0.858
3.	0.	-7.	5.160	5.002	0.210	0.882
5.	0.	-7.	1.430	1.734	0.240	0.989
7.	0.	-7.	5.820	5.522	0.050	0.862
-8.	1.	-7.	1.790	1.575	0.090	0.981
2.	1.	-7.	6.140	5.902	0.130	0.846
4.	1.	-7.	4.310	3.943	0.090	0.913
6.	1.	-7.	4.340	4.579	0.070	0.913
-9.	2.	-7.	6.450	6.703	0.090	0.818
3.	2.	-7.	10.160	9.645	0.170	0.724
5.	2.	-7.	3.470	2.858	0.130	0.940
7.	2.	-7.	6.500	6.087	0.050	0.839
-8.	3.	-7.	8.070	8.284	0.080	0.781
4.	3.	-7.	8.490	8.123	0.100	0.777
6.	3.	-7.	8.920	8.719	0.040	0.767
-7.	4.	-7.	3.650	3.996	0.050	0.930
5.	4.	-7.	2.240	1.915	0.250	0.973
-8.	5.	-7.	2.300	2.724	0.080	0.961
-6.	5.	-7.	2.570	2.580	0.070	0.963
-7.	6.	-7.	4.480	4.490	0.040	0.888
-10.	0.	-6.	7.180	7.286	0.020	0.795
-8.	0.	-6.	6.490	6.383	0.040	0.840
2.	0.	-6.	8.810	8.882	0.340	0.742
4.	0.	-6.	0.880	1.414	0.270	0.995
6.	0.	-6.	10.490	10.532	0.250	0.720
-9.	1.	-6.	6.850	7.230	0.060	0.822
1.	1.	-6.	9.140	8.367	0.040	0.729
3.	1.	-6.	11.040	10.842	0.200	0.684
5.	1.	-6.	6.580	6.457	0.100	0.834
7.	1.	-6.	6.680	6.568	0.100	0.835
-10.	2.	-6.	4.030	4.081	0.050	0.898
-8.	2.	-6.	1.400	1.419	0.120	0.989
4.	2.	-6.	8.000	7.431	0.090	0.783

6.	2.	-6.	3.700	3.785	0.070	0.933
-9.	3.	-6.	7.050	7.260	0.080	0.810
-7.	3.	-6.	6.780	7.195	0.150	0.832
3.	3.	-6.	9.740	9.095	0.050	0.728
5.	3.	-6.	10.400	9.901	0.140	0.721
-8.	4.	-6.	5.320	5.296	0.040	0.874
6.	4.	-6.	9.200	8.910	0.080	0.759
-9.	5.	-6.	8.090	8.129	0.030	0.758
-7.	5.	-6.	6.720	7.367	0.050	0.830
5.	5.	-6.	9.360	8.901	0.050	0.754
-8.	6.	-6.	0.940	0.965	0.150	0.993
-7.	7.	-6.	3.850	4.266	0.140	0.913
-11.	0.	-5.	3.590	3.642	0.010	0.910
-9.	0.	-5.	3.650	3.668	0.010	0.933
1.	0.	-5.	3.770	3.632	0.170	0.912
3.	0.	-5.	8.060	7.638	0.220	0.756
5.	0.	-5.	2.180	2.043	0.160	0.973
7.	0.	-5.	6.080	5.875	0.180	0.854
-10.	1.	-5.	1.040	0.877	0.060	0.993
-8.	1.	-5.	5.770	5.888	0.060	0.865
2.	1.	-5.	4.910	4.413	0.160	0.871
4.	1.	-5.	5.340	5.082	0.080	0.866
6.	1.	-5.	5.830	5.286	0.100	0.859
-9.	2.	-5.	7.100	7.374	0.060	0.818
3.	2.	-5.	12.190	11.995	0.140	0.641
5.	2.	-5.	3.710	3.558	0.070	0.929
7.	2.	-5.	6.630	6.560	0.080	0.836
-10.	3.	-5.	3.920	4.099	0.040	0.912
-8.	3.	-5.	7.980	8.347	0.060	0.794
4.	3.	-5.	8.250	7.793	0.040	0.769
6.	3.	-5.	8.530	8.033	0.120	0.773
-9.	4.	-5.	4.850	5.010	0.030	0.887
5.	4.	-5.	2.620	2.247	0.150	0.963
7.	4.	-5.	6.990	7.178	0.140	0.825
6.	5.	-5.	3.550	3.750	0.060	0.938
8.	5.	-5.	2.400	2.317	0.060	0.967
7.	6.	-5.	6.840	7.251	0.110	0.827
9.	6.	-5.	4.730	5.269	0.060	0.873
8.	7.	-5.	4.120	4.297	0.090	0.901
-10.	0.	-4.	7.420	7.436	0.110	0.807
-8.	0.	-4.	8.530	9.032	0.070	0.776
0.	0.	-4.	7.020	6.308	0.040	0.750
2.	0.	-4.	2.630	2.590	0.110	0.948
4.	0.	-4.	14.650	15.577	0.500	0.573
6.	0.	-4.	9.240	9.209	0.170	0.739
-11.	1.	-4.	1.680	1.831	0.070	0.980
-9.	1.	-4.	7.570	7.857	0.070	0.807
3.	1.	-4.	9.420	8.993	0.110	0.692
5.	1.	-4.	5.420	5.102	0.070	0.862
7.	1.	-4.	3.850	3.985	0.070	0.927
-10.	2.	-4.	9.810	10.174	0.090	0.739
-8.	2.	-4.	2.920	3.097	0.030	0.956
2.	2.	-4.	11.010	10.737	0.040	0.639
4.	2.	-4.	10.860	10.545	0.100	0.670
6.	2.	-4.	1.170	0.582	0.250	0.992
-11.	3.	-4.	4.120	4.223	0.140	0.892
-9.	3.	-4.	9.210	9.259	0.070	0.759
5.	3.	-4.	11.240	11.032	0.030	0.680
7.	3.	-4.	3.960	3.855	0.070	0.925
-10.	4.	-4.	3.350	3.732	0.120	0.934
-8.	4.	-4.	4.300	4.360	0.030	0.914
4.	4.	-4.	4.590	4.180	0.090	0.896
6.	4.	-4.	6.160	6.030	0.070	0.849
-9.	5.	-4.	5.090	5.227	0.120	0.880

-7.	5.	-4.	2.780	2.909	0.020	0.960
-8.	6.	-4.	9.520	9.703	0.080	0.748
-6.	6.	-4.	12.870	14.077	0.240	0.672
9.	7.	-4.	0.720	0.104	0.270	0.996
-8.	8.	-4.	7.810	7.714	0.080	0.763
-11.	0.	-3.	5.140	5.069	0.250	0.874
-9.	0.	-3.	5.510	5.431	0.130	0.874
1.	0.	-3.	4.480	4.107	0.220	0.839
3.	0.	-3.	7.730	7.533	0.210	0.725
5.	0.	-3.	1.900	1.052	0.190	0.976
7.	0.	-3.	5.460	5.177	0.050	0.869
-10.	1.	-3.	1.130	0.872	0.030	0.992
2.	1.	-3.	5.670	5.227	0.140	0.798
4.	1.	-3.	6.690	6.256	0.110	0.789
6.	1.	-3.	7.040	6.664	0.150	0.804
8.	1.	-3.	4.720	4.424	0.070	0.900
-11.	2.	-3.	5.930	5.973	0.250	0.843
-9.	2.	-3.	8.630	8.596	0.090	0.775
3.	2.	-3.	12.070	12.195	0.060	0.601
5.	2.	-3.	4.580	4.134	0.150	0.889
7.	2.	-3.	6.550	6.228	0.160	0.833
-10.	3.	-3.	4.700	4.936	0.020	0.896
-8.	3.	-3.	9.400	9.396	0.100	0.751
4.	3.	-3.	9.050	8.729	0.030	0.719
6.	3.	-3.	9.430	9.240	0.120	0.734
-11.	4.	-3.	2.190	2.221	0.100	0.963
-9.	4.	-3.	4.760	4.767	0.070	0.897
5.	4.	-3.	2.240	2.261	0.100	0.971
7.	4.	-3.	7.130	6.903	0.120	0.818
-10.	5.	-3.	1.490	1.351	0.120	0.985
-8.	5.	-3.	3.320	3.263	0.070	0.944
6.	5.	-3.	2.220	1.727	0.110	0.973
-9.	6.	-3.	4.800	4.603	0.030	0.888
-7.	6.	-3.	7.890	7.546	0.050	0.797
-8.	7.	-3.	6.800	6.693	0.010	0.823
-12.	0.	-2.	4.930	5.590	0.270	0.860
-10.	0.	-2.	8.610	8.598	0.090	0.776
2.	0.	-2.	9.380	9.275	0.070	0.602
4.	0.	-2.	2.430	2.231	0.090	0.953
6.	0.	-2.	11.570	11.799	0.130	0.655
8.	0.	-2.	7.920	7.493	0.070	0.790
-11.	1.	-2.	6.640	7.535	0.500	0.827
-9.	1.	-2.	7.700	8.006	0.160	0.802
1.	1.	-2.	8.320	7.616	0.030	0.619
3.	1.	-2.	11.330	11.303	0.020	0.584
5.	1.	-2.	8.360	7.939	0.090	0.733
7.	1.	-2.	7.790	7.524	0.090	0.785
-12.	2.	-2.	2.520	2.874	0.080	0.947
-10.	2.	-2.	4.780	4.523	0.080	0.896
4.	2.	-2.	9.080	8.574	0.030	0.693
6.	2.	-2.	4.340	3.902	0.060	0.902
8.	2.	-2.	1.850	1.654	0.140	0.981
-11.	3.	-2.	7.880	8.166	0.490	0.782
-9.	3.	-2.	7.720	7.799	0.180	0.802
3.	3.	-2.	10.710	10.437	0.040	0.636
5.	3.	-2.	11.620	11.695	0.030	0.650
7.	3.	-2.	7.270	7.056	0.140	0.808
-10.	4.	-2.	6.980	7.003	0.210	0.819
-8.	4.	-2.	6.530	6.418	0.020	0.840
6.	4.	-2.	10.510	10.429	0.060	0.704

-11.	5.	-2.	4.850	5.201	0.150	0.859
-9.	5.	-2.	9.840	10.537	0.060	0.742
5.	5.	-2.	8.680	8.598	0.060	0.756
7.	5.	-2.	7.430	7.149	0.050	0.809
-10.	6.	-2.	3.370	3.243	0.090	0.929
-8.	6.	-2.	0.790	1.143	0.130	0.996
-9.	7.	-2.	6.720	6.566	0.010	0.817
-7.	7.	-2.	7.090	7.054	0.030	0.821
-11.	0.	-1.	2.320	2.229	0.060	0.968
-9.	0.	-1.	2.330	2.377	0.060	0.971
1.	0.	-1.	5.500	5.060	0.020	0.664
3.	0.	-1.	6.510	6.239	0.070	0.731
5.	0.	-1.	1.340	1.099	0.140	0.986
7.	0.	-1.	8.150	7.775	0.060	0.769
-12.	1.	-1.	5.840	5.740	0.030	0.832
-10.	1.	-1.	3.900	3.676	0.090	0.926
2.	1.	-1.	6.710	6.255	0.080	0.683
4.	1.	-1.	4.640	4.265	0.040	0.855
6.	1.	-1.	4.690	4.413	0.060	0.884
8.	1.	-1.	3.680	3.722	0.090	0.932
-11.	2.	-1.	4.810	4.646	0.180	0.889
-9.	2.	-1.	7.870	8.065	0.050	0.797
3.	2.	-1.	11.440	11.934	0.020	0.578
5.	2.	-1.	4.170	3.781	0.070	0.897
7.	2.	-1.	8.700	8.565	0.040	0.755
-10.	3.	-1.	2.530	2.512	0.040	0.965
4.	3.	-1.	9.650	9.949	0.030	0.679
6.	3.	-1.	10.410	10.417	0.030	0.695
8.	3.	-1.	10.240	10.326	0.100	0.725
-11.	4.	-1.	4.500	4.447	0.050	0.890
-9.	4.	-1.	6.330	6.440	0.090	0.847
5.	4.	-1.	2.720	2.592	0.110	0.956
7.	4.	-1.	6.130	5.657	0.130	0.849
-10.	5.	-1.	1.910	2.065	0.100	0.977
-8.	5.	-1.	3.810	3.621	0.030	0.930
6.	5.	-1.	3.360	3.083	0.110	0.942
-9.	6.	-1.	7.000	6.569	0.040	0.820
-7.	6.	-1.	6.200	6.025	0.020	0.851
-10.	7.	-1.	4.230	3.935	0.030	0.885
-8.	7.	-1.	4.330	4.171	0.040	0.910
-9.	8.	-1.	6.680	6.309	0.080	0.803
0.	-10.	0.	4.270	4.241	0.010	0.915
2.	-10.	0.	1.440	0.943	0.040	0.988
-5.	-9.	0.	5.670	5.674	0.040	0.867
-3.	-9.	0.	9.790	10.134	0.070	0.743
-1.	-9.	0.	8.270	8.328	0.040	0.784
-4.	-8.	0.	8.300	8.761	0.040	0.782
-2.	-8.	0.	9.730	10.149	0.060	0.735
0.	-8.	0.	4.390	4.161	0.050	0.908
-5.	-7.	0.	3.150	3.180	0.010	0.949
-3.	-7.	0.	4.170	4.200	0.040	0.914
-1.	-7.	0.	4.220	4.190	0.010	0.909
-8.	-6.	0.	1.020	0.405	0.070	0.994
-6.	-6.	0.	5.320	5.498	0.040	0.879
-4.	-6.	0.	7.950	8.456	0.030	0.777
-2.	-6.	0.	12.240	13.186	0.040	0.637
0.	-6.	0.	5.540	5.437	0.060	0.849

-3.	-5.	0.	11.050	12.016	0.050	0.656
-1.	-5.	0.	5.340	5.266	0.050	0.842
-4.	-4.	0.	13.430	15.500	0.060	0.593
-2.	-4.	0.	4.020	3.986	0.020	0.888
0.	-4.	0.	6.290	6.084	0.030	0.772
-1.	-3.	0.	8.750	9.430	0.040	0.636
-2.	-2.	0.	3.950	3.976	0.030	0.849
0.	-2.	0.	10.220	10.961	0.070	0.514
-12.	0.	0.	9.800	11.116	0.410	0.721
-11.	1.	0.	1.840	1.975	0.060	0.980
-12.	2.	0.	3.670	3.758	0.140	0.910
-11.	3.	0.	4.790	4.543	0.210	0.887
-10.	4.	0.	7.410	7.604	0.140	0.808
-11.	5.	0.	5.140	5.218	0.060	0.857
-10.	6.	0.	11.360	11.176	0.110	0.697
-9.	7.	0.	0.880	0.017	0.120	0.995
-8.	8.	0.	1.290	1.466	0.170	0.989

APPENDIX VI

The experiment on KDP at $T_c + 5^\circ\text{K}$ (127°K).

h , k , ℓ , f , \hat{f} , $\hat{\sigma}(f)$ and e.c., the extinction correction factor that has been included in \hat{f} , are listed in the following 3 pages; in that order; one set per line.

$\lambda = 0.871 \overset{\circ}{\text{A}}$. The final extinction parameter and scale factor were 0.00985 and 2.434 respectively.

H	K	L	f	f^2	$\sigma(f)$	e.c.
2.	0.	0.	8.037	8.667	0.092	0.570
4.	0.	0.	5.108	4.848	0.034	0.813
6.	0.	0.	4.841	4.605	0.058	0.868
8.	0.	0.	3.644	3.477	0.166	0.932
10.	0.	0.	3.920	3.678	0.062	0.932
12.	0.	0.	11.484	11.273	0.163	0.718
14.	0.	0.	10.092	10.080	0.048	0.753
3.	1.	0.	7.143	7.318	0.042	0.682
5.	1.	0.	4.140	4.240	0.063	0.884
7.	1.	0.	3.355	3.327	0.169	0.936
9.	1.	0.	7.857	7.791	0.072	0.795
11.	1.	0.	1.803	1.453	0.131	0.984
13.	1.	0.	3.657	3.607	0.065	0.942
15.	1.	0.	2.162	2.224	0.124	0.974
2.	2.	0.	2.751	2.819	0.054	0.906
4.	2.	0.	3.230	3.261	0.057	0.915
6.	2.	0.	10.419	10.977	0.122	0.669
8.	2.	0.	8.636	8.630	0.036	0.760
12.	2.	0.	4.334	4.316	0.067	0.923
14.	2.	0.	6.914	6.696	0.053	0.839
5.	3.	0.	9.145	9.800	0.079	0.697
7.	3.	0.	3.966	3.945	0.113	0.919
11.	3.	0.	5.339	5.207	0.091	0.891
13.	3.	0.	3.637	3.700	0.066	0.942
15.	3.	0.	4.637	4.558	0.061	0.899
4.	4.	0.	11.106	12.686	0.039	0.632
6.	4.	0.	6.623	7.041	0.037	0.816
8.	4.	0.	7.534	7.808	0.040	0.805
10.	4.	0.	7.120	7.149	0.072	0.832
12.	4.	0.	2.108	1.981	0.095	0.979
14.	4.	0.	0.898	0.888	0.269	0.996
7.	5.	0.	2.135	2.528	0.114	0.976
9.	5.	0.	5.599	5.542	0.050	0.879
11.	5.	0.	5.647	5.662	0.044	0.883
13.	5.	0.	2.334	2.157	0.099	0.973
6.	6.	0.	4.899	5.020	0.074	0.892
8.	6.	0.	0.841	0.045	0.318	0.996
10.	6.	0.	11.304	11.801	0.187	0.720
12.	6.	0.	7.966	7.669	0.085	0.811
14.	6.	0.	2.166	2.051	0.118	0.973
9.	7.	0.	0.810	0.019	0.386	0.997
11.	7.	0.	3.183	3.164	0.093	0.955
8.	8.	0.	2.448	2.188	0.133	0.972
10.	8.	0.	8.930	8.492	0.034	0.785
12.	8.	0.	5.987	5.785	0.038	0.865
3.	9.	0.	9.268	9.036	0.049	0.756
11.	9.	0.	7.451	7.159	0.035	0.822
10.	10.	0.	1.722	1.418	0.161	0.985
7.	13.	0.	0.999	0.677	0.245	0.994
1.	0.	1.	3.538	4.100	0.179	0.780
3.	0.	1.	5.163	4.850	0.051	0.781
5.	0.	1.	1.325	1.094	0.039	0.985
7.	0.	1.	6.701	6.632	0.009	0.811
9.	0.	1.	2.599	2.713	0.016	0.966
11.	0.	1.	2.960	2.979	0.020	0.960
13.	0.	1.	5.623	5.985	0.067	0.883
15.	0.	1.	1.024	1.304	0.035	0.994

2.	1.	1.	5.156	4.940	0.017	0.746
4.	1.	1.	3.521	3.280	0.014	0.898
6.	1.	1.	3.796	3.826	0.074	0.913
8.	1.	1.	3.175	3.237	0.033	0.947
10.	1.	1.	3.508	3.484	0.083	0.944
12.	1.	1.	5.598	5.631	0.042	0.884
14.	1.	1.	2.939	3.117	0.062	0.959
3.	2.	1.	8.961	9.581	0.050	0.637
5.	2.	1.	2.864	2.790	0.050	0.941
7.	2.	1.	7.085	6.995	0.041	0.801
9.	2.	1.	7.580	7.408	0.034	0.807
11.	2.	1.	4.454	4.489	0.070	0.919
13.	2.	1.	5.606	5.645	0.069	0.883
15.	2.	1.	4.983	5.103	0.038	0.889
4.	3.	1.	7.792	8.139	0.082	0.727
6.	3.	1.	8.412	8.640	0.047	0.744
8.	3.	1.	9.161	9.229	0.086	0.748
10.	3.	1.	2.889	2.736	0.072	0.961
12.	3.	1.	8.294	8.409	0.059	0.802
14.	3.	1.	4.050	4.129	0.046	0.926
5.	4.	1.	2.002	2.088	0.088	0.973
7.	4.	1.	4.904	5.055	0.052	0.889
9.	4.	1.	5.886	6.091	0.122	0.868
11.	4.	1.	4.408	4.385	0.049	0.921
13.	4.	1.	3.422	3.469	0.122	0.947
6.	5.	1.	2.138	2.347	0.106	0.974
8.	5.	1.	3.142	3.202	0.061	0.953
10.	5.	1.	1.236	1.265	0.168	0.993
12.	5.	1.	2.567	2.890	0.078	0.969
14.	5.	1.	1.564	1.513	0.102	0.986
7.	6.	1.	5.447	5.692	0.040	0.879
9.	6.	1.	6.228	6.418	0.041	0.861
11.	6.	1.	5.144	5.266	0.080	0.898
13.	6.	1.	4.550	4.528	0.041	0.911
8.	7.	1.	4.342	4.385	0.061	0.921
10.	7.	1.	4.218	4.150	0.050	0.926
12.	7.	1.	6.972	6.835	0.035	0.838
9.	8.	1.	6.996	7.065	0.052	0.840
11.	8.	1.	4.622	4.688	0.066	0.912
13.	8.	1.	3.669	3.527	0.043	0.930
10.	9.	1.	1.286	1.244	0.149	0.992
12.	9.	1.	6.000	5.753	0.035	0.858
11.	10.	1.	0.940	0.615	0.177	0.995
2.	0.	2.	7.441	7.186	0.198	0.657
4.	0.	2.	1.636	1.752	0.062	0.976
6.	0.	2.	9.693	9.581	0.010	0.692
8.	0.	2.	6.718	6.584	0.039	0.826
10.	0.	2.	8.460	8.466	0.031	0.787
12.	0.	2.	5.364	5.334	0.050	0.892
14.	0.	2.	1.490	1.626	0.110	0.988
1.	1.	2.	5.820	5.914	0.017	0.714
3.	1.	2.	8.998	8.999	0.069	0.638
5.	1.	2.	6.516	6.307	0.014	0.789
7.	1.	2.	6.235	6.049	0.040	0.833
9.	1.	2.	7.234	7.111	0.034	0.818
11.	1.	2.	6.943	6.869	0.039	0.840
13.	1.	2.	4.953	4.908	0.066	0.903
15.	1.	2.	6.566	6.732	0.097	0.838
4.	2.	2.	6.943	6.856	0.010	0.757

6.	2.	2.	3.383	3.236	0.054	0.932
8.	2.	2.	0.922	0.867	0.227	0.995
10.	2.	2.	4.156	4.226	0.119	0.926
12.	2.	2.	3.243	3.323	0.125	0.953
14.	2.	2.	3.958	4.091	0.046	0.929
3.	3.	2.	7.982	8.240	0.030	0.709
5.	3.	2.	9.250	9.479	0.029	0.703
7.	3.	2.	5.999	6.012	0.067	0.848
9.	3.	2.	7.011	7.058	0.058	0.829
11.	3.	2.	8.190	8.456	0.038	0.803
13.	3.	2.	5.147	5.083	0.018	0.897
6.	4.	2.	8.418	8.955	0.065	0.756
8.	4.	2.	5.633	5.604	0.039	0.872
10.	4.	2.	6.973	7.006	0.039	0.838
12.	4.	2.	4.291	4.313	0.048	0.924
14.	4.	2.	0.728	0.476	0.216	0.997
5.	5.	2.	6.719	7.516	1.155	0.814
7.	5.	2.	6.384	6.725	0.035	0.843
9.	5.	2.	9.262	9.833	0.031	0.765
11.	5.	2.	5.079	5.132	0.043	0.900
13.	5.	2.	5.842	6.000	0.037	0.872
8.	6.	2.	1.655	1.458	0.100	0.986
10.	6.	2.	3.346	3.480	0.058	0.951
12.	6.	2.	6.236	6.270	0.049	0.862
14.	6.	2.	5.766	5.833	0.030	0.860
7.	7.	2.	5.892	6.328	0.053	0.869
9.	7.	2.	6.352	6.497	0.036	0.860
11.	7.	2.	4.659	4.596	0.064	0.912
13.	7.	2.	4.396	4.453	0.040	0.911
10.	8.	2.	3.037	3.199	0.140	0.958
12.	8.	2.	2.864	2.682	0.052	0.959
9.	9.	2.	10.212	10.081	0.043	0.751
11.	9.	2.	4.785	4.746	0.034	0.904
1.	0.	3.	1.309	3.466	0.121	0.979
3.	0.	3.	6.110	5.765	0.122	0.777
5.	0.	3.	0.186	1.626	1.287	1.000
7.	0.	3.	4.636	4.415	0.049	0.895
9.	0.	3.	4.566	4.581	0.010	0.910
11.	0.	3.	4.327	4.158	0.063	0.923
13.	0.	3.	4.195	4.238	0.059	0.926
2.	1.	3.	3.525	3.627	0.045	0.891
4.	1.	3.	4.980	5.120	0.037	0.849
6.	1.	3.	4.924	4.818	0.046	0.876
8.	1.	3.	4.001	4.182	0.063	0.924
10.	1.	3.	1.344	0.886	0.177	0.991
12.	1.	3.	3.136	3.489	0.078	0.956
14.	1.	3.	1.539	1.620	0.147	0.987
3.	2.	3.	9.108	9.872	0.102	0.671
5.	2.	3.	3.218	3.134	0.081	0.935
7.	2.	3.	5.433	5.389	0.047	0.869
9.	2.	3.	7.584	7.904	0.049	0.811
11.	2.	3.	4.940	5.310	0.057	0.904
13.	2.	3.	4.147	4.248	0.061	0.927
4.	3.	3.	6.966	7.180	0.043	0.780
6.	3.	3.	7.337	7.398	0.039	0.793

APPENDIX VII

The experiment on DTGS at 80°C.

Sets of h , k , ℓ , f , \tilde{f} and $\check{O}(f)$ are listed on the following 15 pages. Each page has two columns of lines; each line consisting of one set.

h , k , ℓ are listed as integers and the f , \tilde{f} and $\check{O}(f)$ which follow are listed as real numbers.

H	K	L	f	\tilde{f}	$\sigma(f)$	3	5	0	9.06	8.13	0.10
						4	5	0	8.48	7.95	0.11
1	0	0	1.18	1.77	0.11	5	5	0	8.25	9.11	0.12
2	0	0	4.87	0.28	0.11	6	5	0	14.62	14.09	0.11
4	0	0	11.54	13.75	0.08	7	5	0	11.15	8.04	0.12
6	0	0	12.10	11.95	0.13	8	5	0	4.24	2.98	0.13
7	0	0	8.50	8.25	0.14	9	5	0	10.30	8.63	0.13
8	0	0	5.90	5.87	0.11	10	5	0	4.79	1.09	0.13
9	0	0	3.23	1.10	0.18	11	5	0	5.30	4.44	0.12
10	0	0	4.32	4.76	0.21	12	5	0	9.61	2.21	0.13
11	0	0	1.09	1.67	0.92	13	5	0	2.32	2.33	0.32
12	0	0	3.57	3.02	0.17	14	5	0	5.90	6.54	0.15
13	0	0	2.57	1.39	0.18	0	6	0	5.59	5.12	0.13
14	0	0	4.71	2.80	0.11	1	6	0	5.86	5.76	0.12
1	1	0	2.16	2.00	0.08	2	6	0	12.55	13.92	0.09
3	1	0	3.50	3.75	0.13	3	6	0	3.02	1.18	0.23
4	1	0	8.32	12.70	0.10	4	6	0	7.90	8.71	0.12
5	1	0	5.44	6.18	0.15	5	6	0	2.09	0.39	0.37
6	1	0	8.63	3.40	0.13	6	6	0	7.41	4.22	0.14
7	1	0	7.37	5.78	0.14	7	6	0	6.19	4.57	0.10
9	1	0	5.51	5.61	0.12	9	6	0	8.76	6.63	0.09
10	1	0	6.39	4.49	0.10	10	6	0	8.56	5.13	0.09
11	1	0	9.72	7.71	0.13	12	6	0	6.87	5.97	0.18
12	1	0	9.01	8.60	0.13	13	6	0	4.98	7.00	0.20
13	1	0	5.93	3.43	0.11	1	7	0	1.14	2.28	0.55
14	1	0	5.86	3.30	0.15	3	7	0	9.68	11.00	0.12
0	2	0	3.90	5.17	0.05	4	7	0	6.25	7.52	0.15
1	2	0	8.39	13.94	0.14	5	7	0	7.95	9.20	0.15
2	2	0	7.48	3.05	0.10	6	7	0	10.36	10.82	0.14
3	2	0	3.76	5.43	0.13	7	7	0	9.87	11.11	0.13
4	2	0	9.45	9.23	0.10	8	7	0	9.07	9.91	0.15
5	2	0	8.25	7.95	0.10	9	7	0	1.36	0.86	0.71
6	2	0	12.92	11.29	0.12	10	7	0	3.17	3.15	0.33
7	2	0	2.43	0.60	0.35	11	7	0	1.99	2.43	0.36
9	2	0	14.62	13.20	0.11	12	7	0	0.99	0.00	0.65
10	2	0	3.58	3.12	0.18	13	7	0	2.72	2.03	0.29
11	2	0	3.04	0.27	0.22	1	8	0	4.28	3.49	0.18
12	2	0	9.21	7.35	0.13	3	8	0	4.44	5.26	0.18
13	2	0	8.99	7.18	0.13	4	8	0	6.05	5.81	0.14
14	2	0	5.53	5.88	0.17	7	8	0	6.12	6.60	0.15
2	3	0	5.24	3.32	0.09	8	8	0	6.62	5.99	0.16
3	3	0	3.73	6.67	0.15	9	8	0	3.58	3.47	0.22
5	3	0	10.41	12.18	0.11	10	8	0	1.88	1.92	0.38
6	3	0	8.63	4.77	0.13	11	8	0	12.23	12.47	0.12
7	3	0	5.33	3.06	0.11	12	8	0	2.62	2.13	0.28
9	3	0	7.88	4.21	0.11	13	8	0	3.05	3.45	0.21
10	3	0	6.08	4.57	0.12	1	9	0	7.57	7.55	0.13
11	3	0	8.49	6.66	0.09	3	9	0	10.14	11.10	0.12
12	3	0	7.73	7.69	0.09	4	9	0	2.04	1.02	0.35
13	3	0	5.27	4.62	0.18	5	9	0	4.90	4.52	0.16
14	3	0	4.52	4.00	0.11	7	9	0	11.76	14.07	0.11
2	4	0	2.52	3.30	0.18	8	9	0	10.58	10.71	0.13
3	4	0	2.63	2.35	0.23	9	9	0	1.60	0.87	0.47
4	4	0	10.48	12.25	0.11	10	9	0	5.03	6.30	0.19
5	4	0	4.03	2.38	0.18	11	9	0	5.86	5.14	0.15
7	4	0	5.03	1.80	0.10	12	9	0	4.52	5.96	0.17
8	4	0	11.77	9.09	0.12	13	9	0	4.96	4.00	0.13
9	4	0	4.80	5.01	0.12	0	10	0	13.30	13.50	0.10
10	4	0	9.57	2.93	0.13	1	10	0	4.98	4.60	0.17
11	4	0	9.18	7.50	0.13	2	10	0	3.56	2.78	0.22
12	4	0	5.58	3.79	0.12	3	10	0	3.43	3.21	0.23
13	4	0	1.98	0.74	0.42	4	10	0	6.02	5.90	0.16
14	4	0	2.34	3.22	0.26	5	10	0	11.40	12.47	0.11
2	5	0	8.56	8.07	0.09	6	10	0	5.82	6.29	0.14

7	10	0	4.87	3.19	0.19	5	16	0	3.83	3.36	0.22
8	10	0	1.11	1.94	0.70	7	16	0	1.80	1.46	0.37
9	10	0	1.48	0.68	0.48	8	16	0	6.84	7.98	0.13
10	10	0	7.72	6.29	0.16	9	16	0	1.81	1.05	0.27
11	10	0	1.84	0.99	0.33	1	17	0	5.31	6.71	0.18
12	10	0	4.56	5.34	0.15	2	17	0	6.15	6.18	0.15
1	11	0	4.29	3.79	0.20	3	17	0	4.33	3.90	0.19
2	11	0	7.94	8.16	0.13	4	17	0	3.92	4.17	0.19
3	11	0	4.76	3.65	0.18	5	17	0	1.60	2.16	0.41
4	11	0	2.08	2.81	0.35	6	17	0	2.87	3.06	0.25
5	11	0	2.25	1.63	0.30	7	17	0	4.13	5.16	0.17
6	11	0	1.30	0.02	0.56	8	17	0	1.47	1.50	0.37
7	11	0	14.08	15.03	0.12	0	18	0	6.08	5.67	0.16
8	11	0	5.22	6.25	0.17	1	18	0	2.46	1.86	0.35
9	11	0	4.98	6.90	0.18	2	18	0	1.45	0.62	0.54
10	11	0	3.77	1.30	0.21	3	18	0	3.71	4.01	0.21
11	11	0	1.46	0.80	0.41	4	18	0	0.84	1.23	0.78
12	11	0	4.23	3.65	0.15	5	18	0	2.13	3.12	0.30
1	12	0	8.89	9.15	0.13	6	18	0	3.85	5.06	0.19
2	12	0	3.62	4.34	0.23	7	18	0	1.03	1.12	0.50
3	12	0	2.70	3.41	0.28	1	19	0	2.44	3.05	0.32
4	12	0	4.77	3.93	0.18	2	19	0	2.24	3.17	0.33
5	12	0	6.10	5.07	0.15	3	19	0	1.24	2.30	0.55
6	12	0	5.00	5.16	0.19	4	19	0	1.63	1.85	0.37
7	12	0	2.45	2.49	0.32	5	19	0	1.60	1.64	0.33
8	12	0	4.47	4.97	0.19	0	20	0	1.96	0.35	0.35
9	12	0	2.28	1.65	0.28	2	20	0	3.91	3.86	0.19
10	12	0	5.48	5.63	0.15	4	20	0	1.29	1.04	0.39
11	12	0	1.02	0.13	0.62	-15	0	1	3.80	5.66	0.15
1	13	0	1.25	0.05	0.58	-14	0	1	5.64	6.34	0.14
2	13	0	4.46	3.21	0.18	-13	0	1	5.10	3.63	0.13
3	13	0	1.71	0.65	0.41	-12	0	1	10.36	10.19	0.11
4	13	0	1.51	0.47	0.43	-11	0	1	9.12	9.43	0.12
5	13	0	1.10	1.32	0.68	-10	0	1	8.85	9.27	0.11
6	13	0	2.24	2.25	0.34	-9	0	1	5.90	5.87	0.14
7	13	0	6.08	5.76	0.15	-8	0	1	8.63	8.16	0.11
8	13	0	6.67	7.34	0.15	-6	0	1	12.99	14.23	0.09
9	13	0	1.19	0.15	0.56	-5	0	1	10.65	10.77	0.09
10	13	0	1.17	0.33	0.53	-1	0	1	1.74	2.71	0.15
11	13	0	1.23	1.52	0.41	0	0	1	1.66	1.25	0.11
0	14	0	2.21	3.37	0.43	5	0	1	3.15	1.89	0.12
1	14	0	8.18	8.37	0.13	6	0	1	1.22	1.21	0.32
2	14	0	3.08	3.85	0.25	7	0	1	10.20	10.36	0.11
3	14	0	5.05	4.31	0.18	8	0	1	6.33	6.57	0.14
4	14	0	3.25	2.82	0.24	9	0	1	7.37	7.15	0.13
5	14	0	1.99	1.80	0.40	10	0	1	5.13	4.82	0.14
6	14	0	12.74	13.69	0.12	11	0	1	6.87	6.68	0.15
7	14	0	5.79	4.95	0.16	12	0	1	7.55	7.67	0.14
8	14	0	1.03	1.33	0.65	13	0	1	2.30	1.61	0.27
9	14	0	1.93	2.31	0.31	-14	1	1	3.12	3.67	0.21
10	14	0	1.33	0.40	0.41	-13	1	1	2.00	2.67	0.31
1	15	0	3.10	2.66	0.27	-12	1	1	7.85	8.92	0.15
2	15	0	6.54	5.56	0.15	-11	1	1	8.76	10.25	0.11
3	15	0	6.60	6.29	0.15	-10	1	1	1.05	0.70	0.63
4	15	0	1.70	0.69	0.44	-9	1	1	3.12	2.16	0.23
6	15	0	4.92	5.20	0.19	-8	1	1	5.61	6.90	0.15
7	15	0	1.91	2.74	0.39	-7	1	1	3.74	2.79	0.10
8	15	0	1.35	0.24	0.47	-6	1	1	6.07	8.00	0.12
10	15	0	0.81	2.06	0.58	-5	1	1	11.13	12.05	0.10
0	16	0	6.34	5.18	0.16	-3	1	1	10.28	8.29	0.08
1	16	0	3.23	2.80	0.27	-2	1	1	11.24	8.73	0.08
2	16	0	2.64	1.39	0.30	0	1	1	5.60	3.99	0.09
3	16	0	3.12	3.70	0.27	1	1	1	12.74	8.76	0.10
4	16	0	3.82	2.98	0.21	2	1	1	2.72	3.73	0.14

3	1	1	1.16	0.85	0.19	5	4	1	9.20	9.51	0.10
4	1	1	4.89	2.80	0.13	6	4	1	1.37	3.10	0.25
6	1	1	2.80	1.08	0.13	7	4	1	3.73	3.85	0.15
7	1	1	9.18	9.27	0.10	8	4	1	4.98	3.68	0.12
8	1	1	6.96	7.84	0.12	9	4	1	5.98	5.98	0.12
9	1	1	7.26	7.80	0.11	10	4	1	1.37	1.49	0.47
10	1	1	1.97	0.16	0.29	13	4	1	1.64	0.32	0.35
11	1	1	1.21	0.41	0.54	-14	5	1	1.96	1.98	0.30
13	1	1	5.68	6.94	0.14	-11	5	1	2.26	2.37	0.31
-15	2	1	0.93	3.62	0.51	-10	5	1	3.95	4.06	0.17
-14	2	1	5.82	7.69	0.13	-9	5	1	8.62	8.74	0.12
-12	2	1	1.93	2.00	0.39	-8	5	1	1.44	0.44	0.52
-11	2	1	1.11	0.51	0.66	-7	5	1	12.32	11.98	0.10
-10	2	1	5.00	5.65	0.12	-6	5	1	5.60	5.13	0.12
-9	2	1	3.08	2.75	0.23	-5	5	1	10.22	9.51	0.10
-8	2	1	4.37	4.52	0.18	-4	5	1	1.74	2.18	0.31
-7	2	1	9.30	9.18	0.10	-2	5	1	5.73	5.05	0.11
-6	2	1	2.98	3.94	0.12	-1	5	1	8.06	5.73	0.09
-5	2	1	11.63	11.69	0.10	0	5	1	6.76	4.96	0.11
-3	2	1	8.77	9.79	0.09	1	5	1	11.49	11.71	0.10
-1	2	1	4.82	3.65	0.10	2	5	1	5.78	5.11	0.12
1	2	1	5.87	5.22	0.13	3	5	1	9.55	8.93	0.11
2	2	1	4.51	2.83	0.13	4	5	1	8.81	7.38	0.11
4	2	1	11.09	11.54	0.11	5	5	1	12.64	11.04	0.09
5	2	1	6.54	7.12	0.11	6	5	1	13.93	13.46	0.09
6	2	1	0.68	0.39	0.46	7	5	1	12.91	13.56	0.10
7	2	1	4.16	2.90	0.14	9	5	1	3.85	4.14	0.14
8	2	1	10.61	10.64	0.10	10	5	1	1.62	2.02	0.35
9	2	1	1.72	2.64	0.33	13	5	1	7.87	8.78	0.12
10	2	1	5.80	5.75	0.15	-14	6	1	4.92	4.85	0.13
11	2	1	2.28	2.15	0.24	-11	6	1	3.10	3.19	0.21
-14	3	1	0.85	1.29	0.73	-10	6	1	4.11	5.53	0.17
-12	3	1	4.25	6.62	0.18	-9	6	1	2.89	2.01	0.27
-11	3	1	8.34	8.62	0.12	-8	6	1	7.85	7.87	0.12
-9	3	1	4.08	4.28	0.18	-7	6	1	2.52	0.59	0.29
-8	3	1	11.57	11.39	0.10	-6	6	1	8.54	9.37	0.11
-7	3	1	9.22	9.60	0.10	-5	6	1	2.79	1.71	0.14
-5	3	1	4.37	3.65	0.10	-4	6	1	14.12	14.82	0.08
-4	3	1	9.33	8.60	0.09	-3	6	1	1.08	2.83	0.23
-3	3	1	10.57	11.44	0.09	-2	6	1	1.26	0.52	0.22
-2	3	1	1.07	0.23	0.23	-1	6	1	2.85	3.76	0.09
1	3	1	8.04	7.58	0.12	0	6	1	3.52	3.48	0.13
2	3	1	2.10	0.47	0.09	1	6	1	13.90	13.25	0.10
4	3	1	13.28	13.21	0.10	2	6	1	7.54	6.59	0.12
6	3	1	3.85	2.44	0.14	3	6	1	10.42	10.31	0.10
7	3	1	8.55	7.82	0.10	4	6	1	4.68	3.84	0.09
8	3	1	5.78	7.11	0.12	5	6	1	5.65	5.95	0.11
9	3	1	5.52	5.56	0.12	6	6	1	11.73	11.02	0.08
10	3	1	2.55	1.46	0.27	7	6	1	6.97	6.87	0.12
11	3	1	3.90	2.13	0.18	8	6	1	2.09	1.28	0.31
-12	4	1	5.34	6.87	0.16	13	6	1	3.70	6.44	0.17
-11	4	1	3.34	2.47	0.19	-14	7	1	3.94	3.56	0.16
-10	4	1	4.23	4.45	0.17	-13	7	1	2.88	1.74	0.23
-9	4	1	3.26	3.89	0.21	-11	7	1	6.20	5.61	0.14
-7	4	1	6.14	5.68	0.11	-10	7	1	1.62	1.58	0.36
-6	4	1	8.18	7.07	0.11	-9	7	1	8.87	9.24	0.12
-4	4	1	4.85	3.49	0.13	-8	7	1	13.91	14.70	0.10
-3	4	1	9.26	8.86	0.09	-7	7	1	6.01	6.70	0.15
-2	4	1	9.50	9.29	0.09	-6	7	1	11.31	11.03	0.10
0	4	1	12.87	14.17	0.08	-5	7	1	10.57	11.25	0.10
1	4	1	9.18	8.38	0.11	-4	7	1	3.50	3.26	0.20
2	4	1	1.73	2.31	0.13	-3	7	1	1.69	1.20	0.35
3	4	1	4.00	6.02	0.13	-2	7	1	12.04	12.41	0.08
4	4	1	2.93	2.54	0.11	-1	7	1	13.81	13.66	0.08

1	7	1	7.22	7.72	0.09	4	10	1	1.68	1.31	0.27
2	7	1	8.08	8.56	0.09	5	10	1	2.62	3.26	0.19
3	7	1	10.23	9.57	0.09	6	10	1	5.74	4.71	0.13
4	7	1	4.10	4.00	0.12	7	10	1	9.30	8.54	0.11
5	7	1	14.16	13.99	0.09	8	10	1	5.23	5.53	0.15
6	7	1	6.25	7.09	0.11	9	10	1	5.80	5.12	0.15
7	7	1	13.42	13.92	0.10	-12	11	1	2.66	2.38	0.24
8	7	1	1.15	0.06	0.49	-10	11	1	1.25	0.78	0.51
9	7	1	1.84	2.95	0.32	-9	11	1	3.61	3.96	0.21
10	7	1	3.79	2.71	0.19	-8	11	1	4.41	3.54	0.18
-13	8	1	3.61	3.03	0.19	-7	11	1	3.46	2.29	0.19
-10	8	1	1.73	3.28	0.37	-5	11	1	4.45	4.17	0.12
-9	8	1	1.88	1.79	0.34	-4	11	1	5.28	4.65	0.16
-7	8	1	7.80	7.15	0.12	-3	11	1	3.50	2.88	0.22
-6	8	1	1.41	0.19	0.32	-2	11	1	3.23	1.96	0.23
-5	8	1	3.13	3.19	0.16	-1	11	1	4.29	4.02	0.19
-4	8	1	3.74	4.42	0.19	0	11	1	12.09	12.23	0.11
-3	8	1	5.94	5.59	0.13	1	11	1	14.51	14.12	0.09
-2	8	1	8.65	7.20	0.10	2	11	1	8.41	8.60	0.10
0	8	1	11.17	10.49	0.10	3	11	1	1.77	2.01	0.27
1	8	1	4.83	4.27	0.11	4	11	1	5.78	5.45	0.11
2	8	1	1.81	2.01	0.21	6	11	1	3.51	3.79	0.19
3	8	1	6.80	6.45	0.10	7	11	1	0.95	0.78	0.51
4	8	1	8.01	8.46	0.10	8	11	1	2.06	3.47	0.33
5	8	1	5.43	4.61	0.12	-12	12	1	2.17	2.81	0.26
6	8	1	4.56	4.70	0.13	-11	12	1	4.03	3.66	0.18
7	8	1	6.80	5.90	0.11	-9	12	1	3.43	2.80	0.20
8	8	1	4.71	3.76	0.16	-8	12	1	1.79	0.97	0.38
9	8	1	1.63	0.82	0.34	-7	12	1	5.15	5.54	0.16
10	8	1	2.94	3.63	0.24	-6	12	1	0.98	0.04	0.61
-13	9	1	4.04	4.25	0.18	-5	12	1	2.29	2.24	0.21
-11	9	1	5.53	5.51	0.16	-4	12	1	4.18	3.69	0.19
-10	9	1	1.50	0.36	0.45	-3	12	1	6.28	6.61	0.14
-9	9	1	6.49	5.52	0.14	-2	12	1	8.36	7.88	0.12
-8	9	1	2.24	0.32	0.33	-1	12	1	2.31	3.18	0.31
-7	9	1	8.97	9.54	0.11	0	12	1	4.10	3.83	0.20
-5	9	1	4.47	4.29	0.12	1	12	1	6.38	6.04	0.11
-4	9	1	12.30	12.09	0.10	2	12	1	7.79	8.15	0.10
-3	9	1	0.99	1.88	0.69	3	12	1	7.29	6.69	0.10
-2	9	1	8.72	7.83	0.10	4	12	1	9.93	9.76	0.10
-1	9	1	11.10	11.24	0.09	5	12	1	7.57	6.78	0.12
1	9	1	9.11	8.80	0.09	6	12	1	11.18	12.16	0.11
3	9	1	4.52	3.97	0.12	7	12	1	2.81	2.00	0.25
4	9	1	6.88	6.15	0.11	10	12	1	3.67	3.22	0.19
5	9	1	7.59	7.16	0.11	11	12	1	2.39	3.52	0.25
6	9	1	10.12	10.12	0.10	-9	13	1	4.57	5.92	0.17
8	9	1	7.29	7.44	0.12	-8	13	1	1.19	0.57	0.54
9	9	1	2.12	1.78	0.32	-7	13	1	1.62	0.11	0.39
10	9	1	6.73	7.03	0.14	-6	13	1	3.53	3.36	0.21
-13	10	1	1.36	1.13	0.38	-5	13	1	3.31	3.66	0.19
-12	10	1	2.29	1.98	0.30	-4	13	1	3.52	3.05	0.23
-9	10	1	6.67	6.90	0.14	-3	13	1	3.57	1.92	0.21
-8	10	1	3.37	2.08	0.19	-2	13	1	2.24	0.98	0.33
-7	10	1	9.11	9.08	0.12	-1	13	1	5.89	5.48	0.15
-6	10	1	1.13	0.66	0.62	0	13	1	7.00	6.79	0.14
-5	10	1	3.53	3.83	0.16	1	13	1	2.79	1.79	0.18
-4	10	1	10.48	10.34	0.10	2	13	1	4.47	5.03	0.13
-3	10	1	6.09	6.68	0.15	3	13	1	1.91	0.96	0.25
-2	10	1	8.39	7.30	0.12	4	13	1	1.35	0.65	0.43
-1	10	1	1.76	1.78	0.42	5	13	1	3.41	2.95	0.18
1	10	1	7.19	7.14	0.10	6	13	1	4.66	4.67	0.17
2	10	1	5.30	4.95	0.11	7	13	1	7.59	8.70	0.13
3	10	1	1.19	1.02	0.39	9	13	1	3.82	3.29	0.18
						10	13	1	3.39	4.20	0.19

-10	14	1	3.32	1.68	0.19	-15	0	2	2.64	4.89	0.23
-8	14	1	4.80	6.21	0.16	-14	0	2	4.78	3.52	0.18
-7	14	1	1.58	1.21	0.37	-13	0	2	8.89	8.80	0.12
-6	14	1	4.71	4.41	0.18	-12	0	2	2.04	2.22	0.33
-5	14	1	6.78	5.46	0.12	-11	0	2	12.09	12.16	0.11
-4	14	1	11.63	11.22	0.10	-10	0	2	4.55	6.05	0.18
-3	14	1	7.39	8.11	0.13	-8	0	2	5.32	4.79	0.16
-2	14	1	3.63	3.84	0.19	-7	0	2	12.28	11.26	0.09
-1	14	1	10.08	10.66	0.12	-5	0	2	1.69	1.56	0.16
0	14	1	8.41	8.12	0.13	-4	0	2	7.45	7.62	0.10
1	14	1	10.29	9.88	0.10	-3	0	2	9.23	8.38	0.09
2	14	1	2.69	1.92	0.25	-2	0	2	1.38	2.63	0.14
3	14	1	6.75	5.66	0.12	2	0	2	8.55	8.56	0.10
4	14	1	10.94	11.02	0.10	3	0	2	2.53	1.83	0.13
5	14	1	2.11	3.56	0.33	4	0	2	2.80	4.55	0.22
6	14	1	8.12	7.36	0.12	6	0	2	4.52	4.55	0.13
9	14	1	3.81	2.10	0.17	7	0	2	6.06	7.00	0.14
10	14	1	2.64	2.35	0.21	8	0	2	6.79	6.70	0.13
-9	15	1	1.42	1.70	0.45	9	0	2	10.05	10.32	0.11
-7	15	1	2.09	2.06	0.31	10	0	2	8.37	9.56	0.11
-6	15	1	2.73	3.25	0.26	11	0	2	5.24	5.50	0.16
-5	15	1	4.67	4.21	0.15	13	0	2	0.96	0.22	0.52
-4	15	1	3.43	3.37	0.20	-14	1	2	1.15	0.33	0.49
-3	15	1	0.83	0.17	0.56	-12	1	2	1.21	1.52	0.55
-2	15	1	1.10	0.29	0.59	-11	1	2	5.42	5.16	0.16
-1	15	1	5.73	6.01	0.14	-10	1	2	2.57	2.50	0.30
0	15	1	4.95	4.75	0.17	-9	1	2	2.78	1.34	0.28
1	15	1	1.61	0.75	0.28	-7	1	2	8.27	8.07	0.12
2	15	1	1.81	1.45	0.35	-6	1	2	8.82	9.17	0.10
3	15	1	2.06	0.73	0.26	-5	1	2	8.11	7.48	0.11
4	15	1	1.49	0.28	0.30	-4	1	2	2.26	0.01	0.17
5	15	1	5.74	5.11	0.13	-3	1	2	7.74	7.71	0.12
9	15	1	2.40	2.78	0.25	-2	1	2	5.35	7.34	0.13
-8	16	1	1.41	0.83	0.47	2	1	2	2.90	1.49	0.10
-6	16	1	1.78	0.31	0.36	3	1	2	1.91	2.52	0.15
-5	16	1	1.79	2.09	0.37	4	1	2	6.50	6.68	0.09
-4	16	1	1.97	1.94	0.34	5	1	2	8.43	7.61	0.09
-3	16	1	1.32	1.05	0.56	6	1	2	6.60	6.18	0.12
-2	16	1	4.75	3.07	0.17	7	1	2	4.84	4.55	0.13
-1	16	1	4.26	3.11	0.18	8	1	2	5.89	6.77	0.12
0	16	1	1.29	0.32	0.48	9	1	2	4.89	4.69	0.16
1	16	1	7.25	6.62	0.13	10	1	2	3.69	4.23	0.19
2	16	1	1.67	0.87	0.28	-14	2	2	1.29	0.41	0.45
3	16	1	1.49	0.57	0.28	-13	2	2	5.08	4.21	0.18
4	16	1	2.84	2.24	0.17	-12	2	2	1.95	1.62	0.32
5	16	1	2.97	0.75	0.16	-11	2	2	11.54	13.18	0.11
-7	17	1	3.39	3.98	0.20	-7	2	2	4.61	2.75	0.15
-3	17	1	2.35	1.85	0.30	-6	2	2	7.65	7.66	0.10
-2	17	1	1.84	0.65	0.33	-5	2	2	3.12	1.31	0.18
-1	17	1	4.11	5.36	0.17	-4	2	2	4.62	4.50	0.12
0	17	1	5.68	7.09	0.15	-3	2	2	8.76	9.06	0.12
6	17	1	4.36	3.61	0.16	-2	2	2	5.42	6.43	0.10
7	17	1	3.46	4.06	0.18	-1	2	2	9.40	11.12	0.11
-7	18	1	2.16	2.09	0.26	1	2	2	3.88	4.37	0.12
-6	18	1	2.90	3.62	0.23	2	2	2	13.94	13.74	0.09
6	18	1	1.48	1.45	0.38	3	2	2	0.80	0.11	0.42
-6	19	1	3.50	4.62	0.17	4	2	2	4.15	3.70	0.11
-3	19	1	0.95	0.13	0.66	5	2	2	14.45	14.29	0.09
-2	19	1	2.49	2.39	0.27	6	2	2	3.62	2.52	0.16
-1	19	1	5.24	5.74	0.15	7	2	2	6.36	6.54	0.12
0	19	1	4.57	5.37	0.18	8	2	2	5.87	5.45	0.11
-2	20	1	1.68	2.62	0.38	10	2	2	3.84	4.31	0.17
0	20	1	4.51	4.63	0.16	-14	3	2	1.25	5.04	0.44
						-13	3	2	5.55	5.30	0.16

-12	3	2	7.52	7.59	0.12	10	5	2	0.880	0.01	0.70
-11	3	2	5.22	5.20	0.15	-13	6	2	1.530	5.69	0.37
-10	3	2	4.33	4.60	0.19	-12	6	2	6.250	4.13	0.13
-9	3	2	3.57	3.57	0.23	-11	6	2	1.540	0.78	0.41
-7	3	2	1.06	1.11	0.54	-10	6	2	5.730	3.31	0.14
-6	3	2	2.16	2.60	0.25	-8	6	2	2.020	1.01	0.37
-5	3	2	8.93	7.80	0.10	-7	6	2	12.030	12.71	0.12
-4	3	2	3.08	1.53	0.13	-6	6	2	2.300	2.84	0.29
-3	3	2	13.07	12.77	0.12	-5	6	2	5.800	5.64	0.13
-2	3	2	3.10	1.47	0.10	-4	6	2	4.620	5.62	0.15
-1	3	2	10.01	12.65	0.11	-3	6	2	0.910	1.19	0.58
2	3	2	1.73	0.85	0.16	-2	6	2	8.170	6.53	0.10
3	3	2	10.34	9.95	0.07	-1	6	2	5.010	5.33	0.12
4	3	2	8.97	8.86	0.09	1	6	2	9.590	9.46	0.09
5	3	2	8.62	7.49	0.10	2	6	2	9.390	9.31	0.09
6	3	2	11.94	12.48	0.09	3	6	2	7.400	7.06	0.09
7	3	2	3.31	3.20	0.15	4	6	2	5.320	5.03	0.11
8	3	2	1.34	1.05	0.32	5	6	2	1.070	1.13	0.48
9	3	2	1.97	2.35	0.31	6	6	2	7.430	6.93	0.11
10	3	2	2.54	2.65	0.26	7	6	2	5.390	5.65	0.11
-14	4	2	1.27	2.37	0.41	8	6	2	9.740	9.48	0.12
-13	4	2	5.60	5.25	0.15	9	6	2	1.600	0.39	0.41
-12	4	2	5.44	6.50	0.15	-13	7	2	1.380	2.87	0.43
-11	4	2	1.51	0.47	0.39	-12	7	2	8.980	9.58	0.13
-10	4	2	2.94	0.89	0.23	-11	7	2	3.350	3.51	0.21
-9	4	2	7.41	6.39	0.13	-10	7	2	10.150	9.79	0.12
-8	4	2	9.96	9.16	0.12	-9	7	2	2.470	1.73	0.28
-7	4	2	4.63	5.01	0.16	-8	7	2	3.100	2.95	0.24
-6	4	2	5.49	4.71	0.13	-6	7	2	4.500	4.40	0.18
-5	4	2	6.31	6.64	0.12	-4	7	2	3.480	3.10	0.19
-4	4	2	7.60	6.37	0.10	-3	7	2	8.640	7.83	0.10
-3	4	2	13.63	14.29	0.11	-2	7	2	12.200	12.80	0.10
-2	4	2	8.17	5.94	0.10	-1	7	2	4.900	4.28	0.15
-1	4	2	9.20	6.77	0.11	0	7	2	4.830	4.36	0.16
1	4	2	7.07	6.01	0.11	1	7	2	7.720	8.37	0.09
2	4	2	9.18	7.09	0.10	2	7	2	1.440	0.88	0.26
3	4	2	4.59	4.86	0.11	3	7	2	1.690	2.06	0.24
5	4	2	0.74	0.25	0.59	4	7	2	1.370	1.20	0.35
6	4	2	2.46	1.05	0.21	6	7	2	4.100	4.20	0.14
7	4	2	1.47	2.63	0.31	7	7	2	1.530	1.03	0.37
9	4	2	3.19	4.61	0.20	8	7	2	5.720	4.94	0.14
10	4	2	1.08	2.94	0.56	9	7	2	5.280	5.42	0.15
-13	5	2	2.16	3.06	0.34	-12	8	2	5.840	5.57	0.16
-12	5	2	5.41	5.30	0.16	-11	8	2	0.940	0.34	0.71
-11	5	2	8.52	7.88	0.12	-10	8	2	2.79	4.21	0.26
-10	5	2	1.34	0.43	0.48	-9	8	2	2.40	1.03	0.26
-9	5	2	11.06	11.39	0.12	-8	8	2	6.14	6.05	0.15
-7	5	2	1.31	0.47	0.48	-7	8	2	9.27	8.93	0.12
-5	5	2	2.37	1.40	0.23	-6	8	2	4.70	3.77	0.16
-4	5	2	10.08	8.74	0.10	-5	8	2	3.14	2.93	0.22
-2	5	2	5.24	5.25	0.12	-4	8	2	12.08	12.05	0.10
-1	5	2	7.08	6.18	0.10	-3	8	2	2.65	2.36	0.25
0	5	2	1.88	1.81	0.29	-2	8	2	12.57	12.28	0.10
1	5	2	7.67	6.39	0.11	-1	8	2	4.75	3.78	0.16
2	5	2	0.60	1.01	0.59	0	8	2	3.17	2.94	0.24
3	5	2	3.22	3.48	0.13	1	8	2	2.75	2.61	0.15
4	5	2	10.28	9.40	0.09	2	8	2	4.67	5.32	0.12
5	5	2	6.76	5.86	0.12	3	8	2	2.26	2.57	0.21
6	5	2	14.53	14.54	0.09	4	8	2	13.71	14.45	0.09
7	5	2	5.71	5.65	0.11	5	8	2	13.59	14.66	0.10
8	5	2	3.66	4.75	0.18	6	8	2	5.70	5.27	0.11
9	5	2	9.96	10.49	0.12	7	8	2	8.69	8.66	0.12

-13	9	2	0.89	4.79	0.56	0	12	2	1.38	0.66	0.55
-12	9	2	1.01	5.82	0.53	1	12	2	0.93	0.93	0.46
-11	9	2	0.87	1.09	0.73	2	12	2	11.03	9.80	0.10
-9	9	2	8.45	7.07	0.12	3	12	2	1.10	2.87	0.45
-8	9	2	3.72	2.88	0.20	4	12	2	5.28	5.13	0.15
-7	9	2	4.23	4.08	0.19	5	12	2	2.68	2.74	0.24
-6	9	2	2.54	2.77	0.27	6	12	2	3.60	3.01	0.19
-5	9	2	6.81	5.65	0.13	7	12	2	4.77	5.03	0.16
-4	9	2	3.68	4.35	0.19	-12	13	2	0.84	0.85	0.47
-3	9	2	12.70	13.22	0.10	-9	13	2	1.69	0.27	0.38
-1	9	2	0.81	0.05	0.52	-8	13	2	4.26	3.22	0.17
0	9	2	6.72	5.49	0.13	-7	13	2	3.45	2.59	0.21
1	9	2	2.86	2.50	0.15	-6	13	2	2.27	2.47	0.28
2	9	2	10.25	10.47	0.10	-5	13	2	8.72	8.38	0.12
3	9	2	14.72	14.89	0.09	-4	13	2	1.35	0.02	0.51
4	9	2	3.19	2.50	0.18	-3	13	2	2.19	1.34	0.32
5	9	2	7.64	7.98	0.10	-2	13	2	10.01	10.89	0.13
6	9	2	6.69	6.50	0.13	-1	13	2	1.89	1.14	0.36
7	9	2	9.28	9.08	0.12	0	13	2	12.95	13.21	0.11
8	9	2	2.89	2.16	0.21	2	13	2	6.13	5.35	0.13
-11	10	2	4.73	5.45	0.16	3	13	2	9.56	10.00	0.11
-10	10	2	4.69	4.40	0.15	4	13	2	1.70	0.54	0.37
-9	10	2	5.32	4.16	0.15	5	13	2	8.06	8.22	0.12
-8	10	2	1.40	1.22	0.46	6	13	2	1.06	2.35	0.62
-7	10	2	1.87	1.37	0.37	-8	14	2	1.71	1.52	0.33
-6	10	2	4.81	4.83	0.16	-7	14	2	6.45	7.91	0.14
-5	10	2	8.86	9.17	0.12	-6	14	2	9.88	9.24	0.12
-4	10	2	1.18	1.27	0.53	-5	14	2	4.71	3.33	0.18
-3	10	2	5.54	5.33	0.14	-4	14	2	1.97	0.16	0.35
-2	10	2	3.40	1.85	0.22	-3	14	2	4.38	4.45	0.18
-1	10	2	8.58	7.98	0.12	-2	14	2	8.20	8.20	0.11
0	10	2	7.78	7.68	0.13	0	14	2	7.53	7.42	0.14
1	10	2	7.48	6.85	0.10	1	14	2	3.73	3.20	0.18
3	10	2	2.66	2.16	0.21	2	14	2	2.62	2.36	0.24
4	10	2	6.59	6.61	0.11	3	14	2	1.28	1.26	0.50
6	10	2	2.03	1.45	0.31	4	14	2	12.03	10.66	0.11
7	10	2	2.82	3.39	0.23	5	14	2	4.68	4.55	0.17
8	10	2	2.10	2.25	0.31	-10	15	2	1.26	1.89	0.34
-11	11	2	0.78	4.72	0.70	-8	15	2	1.03	2.64	0.55
-10	11	2	6.27	6.22	0.13	-7	15	2	6.32	6.83	0.13
-9	11	2	2.65	3.21	0.25	-5	15	2	3.78	3.74	0.23
-8	11	2	5.44	4.96	0.14	-4	15	2	3.58	1.72	0.21
-7	11	2	11.09	11.37	0.11	-3	15	2	2.35	0.57	0.31
-5	11	2	5.71	4.39	0.14	-2	15	2	2.88	2.15	0.29
-4	11	2	1.13	0.12	0.41	-1	15	2	2.94	1.43	0.25
-3	11	2	1.21	0.48	0.53	0	15	2	7.35	7.40	0.15
-2	11	2	10.89	10.73	0.12	1	15	2	1.86	0.74	0.40
-1	11	2	13.17	13.50	0.12	2	15	2	1.81	1.90	0.33
0	11	2	9.62	9.35	0.12	3	15	2	2.14	0.51	0.37
1	11	2	1.30	2.51	0.38	4	15	2	1.55	1.27	0.42
2	11	2	1.60	1.13	0.27	-9	16	2	1.32	1.45	0.35
3	11	2	4.23	3.41	0.14	-8	16	2	1.07	1.70	0.48
4	11	2	1.51	1.43	0.30	-6	16	2	3.61	2.53	0.18
5	11	2	10.27	10.94	0.10	-5	16	2	4.38	3.32	0.17
6	11	2	5.88	6.91	0.13	-4	16	2	7.76	6.85	0.12
7	11	2	1.62	0.61	0.40	-3	16	2	3.54	0.18	0.20
-12	12	2	1.05	1.52	0.44	-2	16	2	2.53	0.13	0.28
-10	12	2	2.82	4.28	0.25	-1	16	2	10.39	10.26	0.13
-9	12	2	4.18	4.61	0.18	0	16	2	1.78	1.78	0.42
-8	12	2	2.65	2.39	0.24	1	16	2	5.12	5.98	0.16
-7	12	2	7.97	7.31	0.12	2	16	2	0.94	0.13	0.67
-6	12	2	10.47	9.80	0.10	0	17	2	3.06	2.42	0.22
-4	12	2	3.01	2.47	0.23	-15	0	3	5.80	4.56	0.15
-3	12	2	6.55	6.02	0.14	-14	0	3	4.82	5.28	0.18

-13	0	3	1.68	2.71	0.43	-9	3	3	1.83	1.25	0.39
-12	0	3	1.80	1.29	0.38	-8	3	3	1.16	0.05	0.37
-10	0	3	13.46	13.83	0.10	-7	3	3	5.25	5.10	0.15
-9	0	3	9.72	9.99	0.11	-6	3	3	9.14	9.39	0.12
-8	0	3	7.35	7.19	0.12	-5	3	3	0.98	0.40	0.59
-7	0	3	13.56	14.60	0.09	-4	3	3	0.64	1.09	0.46
-6	0	3	9.42	10.51	0.10	-3	3	3	2.15	2.52	0.26
-5	0	3	4.35	3.50	0.15	-2	3	3	9.53	8.23	0.11
-2	0	3	8.83	7.93	0.09	-1	3	3	1.93	2.13	0.26
-1	0	3	9.22	9.75	0.09	0	3	3	12.96	12.92	0.09
0	0	3	9.37	8.24	0.09	1	3	3	4.13	4.05	0.10
1	0	3	3.10	2.17	0.22	3	3	3	10.78	11.02	0.09
2	0	3	3.07	3.62	0.22	5	3	3	5.20	5.10	0.13
6	0	3	3.57	3.52	0.22	6	3	3	8.41	8.53	0.10
7	0	3	2.91	3.27	0.26	7	3	3	2.21	3.18	0.26
8	0	3	6.10	6.27	0.14	8	3	3	4.78	4.20	0.16
9	0	3	6.23	5.21	0.14	-14	4	3	1.73	5.54	0.27
11	0	3	4.23	5.12	0.19	-13	4	3	1.75	1.88	0.38
12	0	3	1.33	0.07	0.41	-12	4	3	5.02	3.53	0.18
-14	1	3	2.19	3.95	0.18	-11	4	3	8.45	8.76	0.13
-13	1	3	1.29	1.10	0.51	-10	4	3	7.86	8.83	0.15
-12	1	3	4.70	5.16	0.17	-9	4	3	9.14	8.76	0.14
-11	1	3	3.36	4.38	0.19	-7	4	3	1.49	0.94	0.44
-10	1	3	3.16	2.20	0.25	-6	4	3	4.66	4.53	0.17
-9	1	3	0.91	0.74	0.79	-5	4	3	11.85	12.32	0.11
-8	1	3	1.06	0.73	0.64	-3	4	3	1.63	1.99	0.36
-7	1	3	4.54	3.32	0.16	-2	4	3	2.95	1.56	0.20
-6	1	3	8.65	8.48	0.12	-1	4	3	5.95	6.54	0.12
-5	1	3	4.33	4.25	0.15	0	4	3	12.53	12.75	0.09
-4	1	3	2.94	3.66	0.14	1	4	3	7.77	8.65	0.09
-3	1	3	1.57	3.19	0.24	2	4	3	8.42	8.18	0.09
-2	1	3	3.19	5.73	0.16	3	4	3	10.07	10.77	0.09
2	1	3	1.76	0.91	0.20	4	4	3	12.35	12.41	0.09
3	1	3	6.78	7.25	0.10	5	4	3	9.44	9.99	0.10
4	1	3	10.92	11.17	0.09	6	4	3	3.20	2.42	0.16
5	1	3	10.84	11.63	0.10	7	4	3	10.47	10.77	0.10
6	1	3	1.96	1.36	0.22	8	4	3	3.45	2.97	0.23
7	1	3	5.60	6.56	0.11	9	4	3	2.13	0.55	0.32
8	1	3	6.08	5.86	0.13	-15	5	3	1.22	3.99	0.35
9	1	3	3.26	3.48	0.27	-14	5	3	1.29	1.41	0.39
-14	2	3	1.73	3.33	0.24	-13	5	3	0.96	4.89	0.32
-13	2	3	1.70	1.04	0.39	-12	5	3	7.10	6.70	0.15
-12	2	3	3.19	1.52	0.23	-10	5	3	12.13	12.65	0.10
-11	2	3	4.68	5.24	0.18	-9	5	3	3.87	4.15	0.20
-10	2	3	7.18	7.50	0.15	-8	5	3	10.39	10.49	0.12
-9	2	3	6.29	6.17	0.15	-4	5	3	2.02	1.51	0.32
-8	2	3	5.38	5.06	0.17	-3	5	3	4.19	4.33	0.15
-7	2	3	3.12	1.79	0.23	0	5	3	9.26	8.97	0.10
-6	2	3	7.64	7.56	0.12	1	5	3	1.79	2.12	0.21
-5	2	3	7.14	6.18	0.12	2	5	3	2.57	3.41	0.16
-4	2	3	9.41	9.45	0.11	3	5	3	6.66	6.85	0.10
-2	2	3	13.40	14.32	0.12	5	5	3	4.82	4.66	0.12
1	2	3	7.40	7.14	0.09	6	5	3	1.32	0.60	0.34
2	2	3	4.79	6.32	0.10	8	5	3	3.30	3.58	0.22
4	2	3	9.41	9.04	0.10	9	5	3	1.56	2.27	0.40
6	2	3	1.34	2.36	0.35	-12	6	3	4.85	5.67	0.17
7	2	3	7.82	7.12	0.11	-11	6	3	1.55	3.00	0.41
8	2	3	1.31	0.32	0.42	-10	6	3	3.34	4.78	0.21
9	2	3	2.40	0.64	0.31	-9	6	3	6.91	5.62	0.15
-14	3	3	2.09	7.94	0.20	-8	6	3	9.68	8.94	0.12
-13	3	3	4.92	4.45	0.17	-7	6	3	4.81	5.59	0.18
-12	3	3	7.25	5.54	0.15	-6	6	3	14.02	14.58	0.11
-11	3	3	4.22	4.01	0.15	-5	6	3	2.12	1.53	0.32
-10	3	3	12.51	12.49	0.12	-4	6	3	4.20	3.33	0.17

-3	6	3	13.24	12.98	0.11	1	9	3	3.69	3.39	0.17
-2	6	3	3.35	2.83	0.20	2	9	3	0.85	0.78	0.58
-1	6	3	1.85	2.20	0.33	3	9	3	4.87	4.62	0.12
0	6	3	7.91	6.80	0.12	4	9	3	1.18	0.41	0.38
1	6	3	10.04	9.47	0.09	5	9	3	12.12	12.19	0.10
2	6	3	7.87	7.39	0.10	6	9	3	0.94	0.66	0.62
3	6	3	8.43	8.01	0.10	7	9	3	2.37	0.92	0.27
4	6	3	12.87	13.13	0.10	-12	10	3	1.73	1.41	0.27
5	6	3	8.67	8.27	0.10	-10	10	3	5.23	5.03	0.15
7	6	3	2.53	1.83	0.24	-9	10	3	2.84	2.61	0.25
8	6	3	3.80	2.77	0.18	-8	10	3	9.14	8.39	0.11
-14	7	3	0.90	5.47	0.59	-7	10	3	3.46	3.68	0.24
-13	7	3	1.90	1.21	0.21	-6	10	3	6.69	6.14	0.15
-12	7	3	6.75	6.10	0.15	-5	10	3	0.99	1.28	0.70
-11	7	3	4.30	3.05	0.18	-4	10	3	5.30	4.56	0.16
-10	7	3	1.98	0.63	0.28	-3	10	3	7.83	7.65	0.13
-9	7	3	5.07	5.07	0.18	-2	10	3	13.07	13.63	0.12
-8	7	3	4.01	3.95	0.21	-1	10	3	8.07	8.77	0.13
-7	7	3	3.62	4.24	0.23	0	10	3	1.75	1.79	0.47
-6	7	3	8.66	8.18	0.14	1	10	3	5.56	4.77	0.13
-5	7	3	2.34	2.06	0.29	2	10	3	6.06	6.09	0.11
-3	7	3	1.16	0.50	0.32	3	10	3	6.70	6.21	0.11
-1	7	3	9.85	10.74	0.12	4	10	3	2.32	2.02	0.25
0	7	3	1.07	0.68	0.69	6	10	3	4.38	5.32	0.17
1	7	3	2.60	2.54	0.17	-11	11	3	1.44	1.86	0.24
2	7	3	4.49	4.61	0.13	-10	11	3	5.70	4.99	0.15
3	7	3	6.18	5.54	0.12	-9	11	3	1.85	0.24	0.34
4	7	3	10.26	10.12	0.10	-8	11	3	12.90	11.72	0.10
6	7	3	4.96	5.68	0.14	-7	11	3	11.08	10.43	0.11
7	7	3	6.07	7.08	0.15	-6	11	3	5.89	5.05	0.14
8	7	3	1.64	1.77	0.48	-5	11	3	9.06	8.19	0.13
-13	8	3	1.48	2.98	0.35	-4	11	3	9.77	10.41	0.12
-12	8	3	3.63	3.31	0.23	-3	11	3	7.89	7.51	0.13
-11	8	3	1.48	0.45	0.38	-1	11	3	6.94	6.57	0.15
-10	8	3	2.45	2.11	0.29	0	11	3	4.05	3.46	0.22
-9	8	3	14.21	13.91	0.10	1	11	3	3.78	3.04	0.15
-8	8	3	10.26	10.65	0.14	2	11	3	3.34	4.42	0.17
-7	8	3	8.10	8.50	0.14	3	11	3	13.13	13.86	0.10
-6	8	3	6.30	5.93	0.15	4	11	3	4.51	4.23	0.15
-5	8	3	4.02	3.62	0.21	5	11	3	2.25	1.20	0.27
-4	8	3	2.11	1.44	0.33	-12	12	3	1.56	1.52	0.28
-3	8	3	10.65	9.95	0.09	-11	12	3	1.39	2.99	0.36
-2	8	3	1.46	1.16	0.49	-10	12	3	2.08	2.01	0.30
-1	8	3	10.66	9.54	0.12	-8	12	3	5.07	5.43	0.14
0	8	3	0.62	0.46	0.60	-7	12	3	4.17	3.93	0.19
1	8	3	3.92	3.48	0.16	-6	12	3	3.42	2.87	0.21
3	8	3	2.58	1.80	0.21	-5	12	3	1.69	1.77	0.43
4	8	3	5.62	5.09	0.11	-4	12	3	13.31	14.38	0.12
6	8	3	3.66	3.32	0.18	-3	12	3	14.31	14.86	0.12
7	8	3	6.76	7.15	0.14	-2	12	3	2.38	2.56	0.34
8	8	3	5.49	5.30	0.15	-1	12	3	1.45	0.43	0.48
-13	9	3	0.84	1.60	0.60	1	12	3	5.55	5.51	0.14
-11	9	3	1.77	1.20	0.38	2	12	3	3.26	2.00	0.19
-10	9	3	1.82	0.31	0.36	3	12	3	6.39	5.99	0.13
-9	9	3	12.26	12.18	0.10	4	12	3	2.54	1.81	0.25
-8	9	3	11.34	10.64	0.12	5	12	3	1.73	1.98	0.32
-7	9	3	13.08	13.03	0.12	-10	13	3	1.66	1.19	0.24
-6	9	3	9.69	10.07	0.12	-9	13	3	5.10	5.88	0.16
-5	9	3	3.90	4.16	0.21	-8	13	3	1.66	1.51	0.40
-4	9	3	9.76	9.90	0.12	-7	13	3	5.95	5.24	0.13
-3	9	3	3.63	4.55	0.23	-6	13	3	7.49	6.90	0.13
-2	9	3	12.56	12.46	0.12	-5	13	3	0.78	0.09	0.77
-1	9	3	5.04	4.96	0.17	-4	13	3	2.98	2.45	0.21
0	9	3	10.25	9.13	0.12	-3	13	3	2.55	1.56	0.24

-2	13	3	7.90	7.39	0.12	6	0	4	7.23	7.88	0.12
0	13	3	4.88	3.91	0.16	7	0	4	6.74	6.81	0.13
1	13	3	1.16	0.14	0.52	8	0	4	5.27	5.11	0.15
2	13	3	1.03	0.51	0.57	-12	1	4	5.50	5.57	0.15
3	13	3	5.58	4.68	0.14	-11	1	4	4.40	3.84	0.16
4	13	3	0.95	1.58	0.65	-10	1	4	3.32	4.37	0.14
-9	14	3	1.65	3.68	0.21	-9	1	4	1.15	1.07	0.33
-8	14	3	4.59	5.00	0.18	-8	1	4	5.67	5.76	0.15
-7	14	3	2.14	0.54	0.31	-6	1	4	7.05	6.90	0.13
-6	14	3	3.18	2.55	0.22	-5	1	4	7.35	9.01	0.12
-5	14	3	3.97	2.58	0.18	-3	1	4	1.30	0.75	0.40
-4	14	3	1.61	0.22	0.43	-2	1	4	13.43	14.57	0.10
-3	14	3	11.79	12.36	0.11	-1	1	4	6.34	5.91	0.12
-2	14	3	1.03	0.64	0.71	0	1	4	7.19	6.80	0.14
-1	14	3	9.06	9.80	0.12	1	1	4	6.96	6.48	0.10
0	14	3	4.44	4.37	0.18	2	1	4	7.45	6.47	0.10
1	14	3	1.25	0.16	0.49	3	1	4	0.84	0.52	0.66
2	14	3	13.04	12.61	0.10	4	1	4	7.05	7.70	0.12
3	14	3	6.74	5.77	0.13	5	1	4	8.73	10.30	0.10
-10	15	3	0.88	1.60	0.52	7	1	4	5.16	4.54	0.15
-9	15	3	1.32	2.87	0.36	8	1	4	1.96	2.45	0.32
-8	15	3	1.72	1.47	0.19	-13	2	4	3.74	4.16	0.19
-7	15	3	1.72	2.40	0.37	-12	2	4	1.28	0.27	0.44
-6	15	3	5.40	5.15	0.16	-11	2	4	0.84	0.97	0.68
-5	15	3	3.45	2.86	0.21	-10	2	4	1.64	0.91	0.37
-4	15	3	6.85	6.89	0.14	-9	2	4	1.97	1.22	0.26
-3	15	3	4.90	4.71	0.14	-6	2	4	4.07	3.81	0.19
-2	15	3	3.69	3.41	0.18	-5	2	4	4.74	3.81	0.16
0	15	3	2.52	1.50	0.24	-4	2	4	6.51	5.72	0.13
1	15	3	1.81	3.15	0.32	-3	2	4	5.11	4.85	0.15
2	15	3	1.06	0.73	0.58	-2	2	4	5.36	5.46	0.13
-8	16	3	1.75	0.81	0.27	-1	2	4	1.06	0.53	0.55
-7	16	3	1.57	5.35	0.30	0	2	4	8.94	8.18	0.11
-6	16	3	1.32	4.51	0.24	2	2	4	2.52	3.10	0.20
-5	16	3	1.14	0.02	0.59	4	2	4	1.55	0.55	0.28
-4	16	3	6.58	7.11	0.15	5	2	4	0.76	1.48	0.58
-3	16	3	6.41	7.32	0.14	6	2	4	0.87	0.23	0.64
-2	16	3	4.59	3.40	0.17	7	2	4	8.67	8.62	0.12
-1	16	3	4.44	5.05	0.17	8	2	4	6.37	6.95	0.15
-8	17	3	0.82	2.90	0.58	-13	3	4	4.91	4.67	0.16
-6	17	3	1.31	6.90	0.40	-12	3	4	3.53	3.69	0.20
-5	17	3	2.78	2.73	0.19	-11	3	4	1.83	1.71	0.31
-4	17	3	1.10	2.10	0.46	-10	3	4	11.43	10.35	0.10
-1	17	3	1.48	6.63	0.43	-9	3	4	10.06	10.33	0.10
-4	18	3	0.79	2.54	0.70	-8	3	4	2.07	2.22	0.34
-2	18	3	1.63	3.59	0.31	-7	3	4	6.88	6.72	0.15
-1	18	3	1.48	0.05	0.39	-6	3	4	9.26	9.13	0.12
-1	19	3	1.16	1.73	0.43	-5	3	4	1.41	1.47	0.46
-15	0	4	1.08	0.79	0.64	-4	3	4	3.93	2.59	0.18
-13	0	4	6.35	5.67	0.13	-3	3	4	9.50	9.11	0.10
-12	0	4	1.79	1.30	0.33	-2	3	4	7.49	7.46	0.12
-11	0	4	9.19	9.28	0.11	-1	3	4	12.89	13.50	0.10
-10	0	4	8.57	8.48	0.12	0	3	4	2.06	0.16	0.36
-9	0	4	10.12	10.90	0.11	1	3	4	7.35	7.17	0.10
-8	0	4	7.46	8.00	0.13	2	3	4	5.65	4.99	0.13
-7	0	4	11.02	11.09	0.11	3	3	4	10.18	9.85	0.10
-6	0	4	8.08	8.16	0.12	5	3	4	2.44	1.40	0.20
-5	0	4	14.18	13.69	0.09	6	3	4	10.58	10.44	0.10
-4	0	4	10.40	10.02	0.10	7	3	4	4.89	4.89	0.14
-3	0	4	2.48	2.99	0.25	8	3	4	3.18	1.75	0.20
-1	0	4	2.21	2.45	0.27	-12	4	4	6.33	6.83	0.15
0	0	4	1.60	0.19	0.40	-11	4	4	4.45	3.88	0.17
4	0	4	4.56	4.22	0.18						
5	0	4	1.94	1.05	0.31						

-10	4	4	3.18	3.03	0.21	-1	7	4	1.56	1.48	0.41
-9	4	4	1.31	1.76	0.33	1	7	4	4.54	4.12	0.13
-8	4	4	3.86	3.92	0.19	2	7	4	4.18	3.63	0.12
-7	4	4	10.67	10.81	0.12	3	7	4	4.51	4.30	0.13
-6	4	4	3.28	3.82	0.24	4	7	4	2.00	2.65	0.31
-4	4	4	8.42	8.73	0.12	5	7	4	8.28	7.92	0.12
-3	4	4	6.16	6.94	0.13	6	7	4	2.83	3.17	0.20
-2	4	4	6.61	7.11	0.13	-14	8	4	0.98	1.92	0.44
1	4	4	9.84	10.33	0.10	-13	8	4	0.99	0.43	0.27
2	4	4	9.52	9.40	0.10	-11	8	4	0.81	0.08	0.74
3	4	4	2.10	1.06	0.25	-10	8	4	3.27	3.41	0.20
4	4	4	4.81	4.24	0.12	-9	8	4	10.84	9.99	0.10
5	4	4	8.17	6.44	0.12	-8	8	4	9.45	8.66	0.12
6	4	4	7.52	6.83	0.12	-7	8	4	8.23	8.62	0.10
7	4	4	2.44	3.16	0.24	-6	8	4	1.44	0.44	0.46
-12	5	4	1.17	1.86	0.54	-4	8	4	2.13	1.58	0.32
-11	5	4	1.17	1.62	0.56	-3	8	4	12.12	12.26	0.12
-10	5	4	2.57	1.63	0.25	-2	8	4	10.21	10.05	0.12
-9	5	4	6.36	6.84	0.11	-1	8	4	2.73	2.63	0.26
-8	5	4	5.96	5.76	0.15	0	8	4	1.53	1.47	0.56
-7	5	4	12.22	12.48	0.12	1	8	4	5.33	5.55	0.11
-6	5	4	12.55	12.14	0.12	2	8	4	5.36	5.48	0.12
-5	5	4	1.70	0.69	0.38	3	8	4	8.34	8.74	0.10
-4	5	4	4.27	4.62	0.18	4	8	4	7.89	8.24	0.13
-3	5	4	12.01	12.61	0.10	5	8	4	2.01	1.49	0.26
-2	5	4	4.85	4.87	0.15	6	8	4	4.81	4.05	0.13
-1	5	4	1.53	2.16	0.38	-13	9	4	1.83	2.69	0.19
0	5	4	5.93	5.00	0.13	-11	9	4	2.58	3.01	0.27
1	5	4	11.66	11.20	0.09	-10	9	4	7.27	7.63	0.13
2	5	4	12.57	12.78	0.09	-9	9	4	7.01	8.43	0.13
3	5	4	10.26	10.74	0.10	-8	9	4	1.61	1.68	0.45
4	5	4	2.30	2.88	0.21	-7	9	4	1.94	1.68	0.31
5	5	4	3.47	3.19	0.21	-6	9	4	4.16	2.71	0.13
6	5	4	1.23	1.15	0.44	-5	9	4	5.92	5.98	0.16
7	5	4	1.01	0.92	0.51	-3	9	4	1.78	1.37	0.39
-14	6	4	1.39	4.09	0.23	-2	9	4	3.30	2.46	0.22
-13	6	4	0.80	6.99	0.39	-1	9	4	1.91	0.39	0.34
-11	6	4	2.31	1.84	0.26	0	9	4	2.00	1.83	0.40
-10	6	4	3.03	1.65	0.22	1	9	4	0.91	0.77	0.50
-9	6	4	9.29	8.64	0.12	2	9	4	0.72	1.36	0.62
-8	6	4	7.18	6.64	0.11	3	9	4	2.11	1.34	0.29
-7	6	4	11.74	12.70	0.12	4	9	4	3.52	3.53	0.18
-5	6	4	1.56	0.07	0.40	5	9	4	7.83	7.38	0.12
-4	6	4	1.37	1.81	0.28	-9	10	4	8.05	7.90	0.13
-2	6	4	7.60	6.60	0.13	-8	10	4	1.82	0.82	0.35
-1	6	4	4.57	4.28	0.16	-7	10	4	4.54	3.89	0.16
0	6	4	12.61	10.94	0.11	-5	10	4	1.27	0.77	0.33
1	6	4	6.77	5.76	0.12	-4	10	4	12.97	13.47	0.10
2	6	4	12.94	12.32	0.09	-3	10	4	4.90	4.23	0.12
3	6	4	7.02	6.69	0.10	-2	10	4	8.21	8.51	0.10
4	6	4	11.83	12.99	0.10	-1	10	4	1.40	1.90	0.32
5	6	4	1.50	1.73	0.39	0	10	4	0.90	2.20	0.88
6	6	4	7.19	7.06	0.11	2	10	4	4.01	4.12	0.16
7	6	4	9.52	8.95	0.12	4	10	4	1.77	1.88	0.29
-12	7	4	3.06	1.99	0.22	5	10	4	1.14	0.53	0.45
-11	7	4	2.49	2.12	0.28	-12	11	4	1.70	7.38	0.21
-9	7	4	2.03	2.43	0.31	-11	11	4	1.11	0.42	0.33
-8	7	4	1.46	0.89	0.29	-10	11	4	2.59	2.86	0.25
-7	7	4	3.32	3.31	0.22	-9	11	4	4.76	4.86	0.17
-6	7	4	11.03	11.29	0.12	-8	11	4	5.79	4.62	0.14
-5	7	4	1.28	1.08	0.52	-7	11	4	9.77	9.51	0.11
-4	7	4	4.91	4.96	0.17	-6	11	4	2.43	1.57	0.28
-3	7	4	9.68	10.21	0.12	-5	11	4	7.59	7.24	0.13
-2	7	4	3.09	2.29	0.23	-4	11	4	12.66	12.36	0.10
						-3	11	4	0.86	0.55	0.78

-2	11	4	4.47	4.09	0.18	-9	1	5	1.88	1.67	0.26
-1	11	4	8.87	8.66	0.12	-8	1	5	4.19	4.08	0.13
0	11	4	7.94	8.59	0.12	-7	1	5	9.74	8.82	0.11
1	11	4	12.85	12.38	0.10	-5	1	5	5.47	4.90	0.13
2	11	4	9.73	9.76	0.11	-4	1	5	2.82	2.64	0.20
3	11	4	5.43	5.42	0.13	-3	1	5	12.02	11.34	0.09
4	11	4	1.67	2.64	0.30	-2	1	5	9.40	9.46	0.11
-10	12	4	1.02	2.57	0.67	-1	1	5	3.49	4.24	0.17
-9	12	4	2.08	2.46	0.33	0	1	5	7.86	6.41	0.14
-8	12	4	3.09	4.14	0.24	3	1	5	1.20	1.38	0.36
-7	12	4	3.33	2.86	0.22	4	1	5	5.76	5.16	0.13
-6	12	4	2.38	2.22	0.33	5	1	5	2.23	2.99	0.31
-5	12	4	4.24	3.33	0.17	6	1	5	3.45	2.91	0.17
-4	12	4	2.46	2.16	0.24	-12	2	5	2.54	2.41	0.25
-3	12	4	7.40	7.20	0.13	-11	2	5	2.62	2.65	0.27
-2	12	4	5.09	4.63	0.16	-10	2	5	6.05	6.43	0.14
-1	12	4	8.47	8.09	0.12	-9	2	5	0.93	0.59	0.63
0	12	4	5.73	5.00	0.15	-8	2	5	13.64	14.48	0.10
1	12	4	5.92	6.29	0.14	-7	2	5	6.89	7.21	0.11
2	12	4	4.89	4.82	0.14	-6	2	5	2.78	2.17	0.20
3	12	4	3.33	2.78	0.17	-5	2	5	8.64	8.26	0.11
4	12	4	5.88	4.87	0.13	-3	2	5	9.26	8.32	0.11
-7	13	4	2.68	3.15	0.26	-2	2	5	4.82	4.64	0.13
-6	13	4	4.93	4.36	0.15	-1	2	5	8.08	7.43	0.11
-5	13	4	3.09	2.84	0.21	0	2	5	8.99	10.04	0.12
-4	13	4	5.58	5.45	0.15	2	2	5	4.28	4.85	0.15
-3	13	4	3.79	3.99	0.18	3	2	5	5.26	6.20	0.12
-2	13	4	4.64	3.98	0.16	4	2	5	2.59	3.97	0.23
-1	13	4	1.12	1.14	0.44	5	2	5	11.33	13.07	0.11
0	13	4	1.39	0.96	0.37	-12	3	5	1.96	1.38	0.32
1	13	4	4.16	3.36	0.15	-11	3	5	4.49	5.27	0.14
2	13	4	1.03	0.29	0.48	-10	3	5	12.06	12.09	0.10
3	13	4	3.84	2.09	0.17	-9	3	5	14.61	14.70	0.10
-6	14	4	2.76	3.25	0.24	-8	3	5	5.10	5.90	0.12
-5	14	4	4.97	6.27	0.16	-7	3	5	7.50	7.37	0.10
-4	14	4	3.29	2.80	0.18	-6	3	5	4.20	2.91	0.14
-2	14	4	4.95	5.12	0.13	-5	3	5	12.50	11.17	0.09
-1	14	4	3.84	3.26	0.15	-3	3	5	13.64	13.03	0.09
0	14	4	3.91	3.46	0.19	-2	3	5	12.02	11.63	0.10
1	14	4	2.64	3.37	0.25	-1	3	5	1.40	1.57	0.37
-3	15	4	3.05	3.75	0.21	0	3	5	8.04	7.62	0.14
-2	15	4	4.23	4.41	0.17	1	3	5	6.20	5.97	0.11
0	15	4	0.96	1.14	0.79	2	3	5	5.04	5.39	0.12
-15	0	5	2.24	2.82	0.31	5	3	5	4.74	5.65	0.15
-12	0	5	4.16	3.71	0.17	6	3	5	6.00	4.61	0.13
-11	0	5	6.87	7.43	0.13	-11	4	5	4.70	4.40	0.16
-9	0	5	8.46	9.44	0.11	-10	4	5	6.08	7.09	0.14
-8	0	5	9.41	10.33	0.10	-9	4	5	1.17	1.41	0.37
-7	0	5	5.94	6.12	0.12	-8	4	5	8.71	8.49	0.10
-5	0	5	9.92	9.59	0.11	-7	4	5	4.95	4.31	0.11
-3	0	5	12.60	12.51	0.09	-6	4	5	8.70	8.80	0.10
-2	0	5	6.20	5.61	0.14	-5	4	5	7.02	6.62	0.10
-1	0	5	6.08	6.13	0.14	-4	4	5	4.88	4.82	0.13
0	0	5	3.77	1.87	0.19	-3	4	5	12.31	11.70	0.09
1	0	5	4.45	4.41	0.21	-2	4	5	2.14	1.60	0.22
2	0	5	7.19	6.76	0.14	-1	4	5	1.96	1.08	0.26
3	0	5	2.42	1.54	0.32	0	4	5	9.23	9.31	0.11
4	0	5	6.07	4.98	0.14	1	4	5	9.00	9.51	0.10
5	0	5	8.63	7.62	0.12	2	4	5	2.47	1.64	0.19
6	0	5	5.45	5.89	0.14	3	4	5	9.83	10.39	0.11
7	0	5	0.84	5.35	0.58	4	4	5	4.01	3.25	0.17
-12	1	5	4.20	2.67	0.16	5	4	5	5.32	6.40	0.14
-11	1	5	6.67	6.71	0.13	6	4	5	2.06	2.65	0.30
-10	1	5	12.04	12.28	0.10	-11	5	5	10.41	10.99	0.12
						-9	5	5	4.99	5.21	0.15

-8	5	5	3.29	3.50	0.15	1	9	5	3.31	2.53	0.19
-7	5	5	3.42	2.67	0.15	2	9	5	1.64	0.55	0.31
-6	5	5	4.28	4.46	0.13	3	9	5	8.29	8.36	0.11
-5	5	5	7.62	7.00	0.10	4	9	5	3.70	4.68	0.19
-4	5	5	5.23	4.86	0.13	-9	10	5	4.05	4.60	0.17
-3	5	5	5.75	5.64	0.12	-8	10	5	8.89	8.75	0.11
-2	5	5	10.61	9.87	0.10	-7	10	5	3.03	4.10	0.21
-1	5	5	1.43	2.67	0.33	-6	10	5	5.02	5.11	0.14
0	5	5	4.80	4.18	0.11	-5	10	5	2.45	2.79	0.24
1	5	5	2.01	1.27	0.23	-3	10	5	0.84	0.15	0.49
2	5	5	8.42	8.54	0.10	-2	10	5	4.88	3.49	0.15
3	5	5	1.41	0.90	0.38	-1	10	5	9.94	8.80	0.11
4	5	5	10.65	11.64	0.12	0	10	5	3.81	2.76	0.18
5	5	5	2.07	0.12	0.31	1	10	5	4.01	3.08	0.14
-11	6	5	4.74	4.76	0.16	2	10	5	1.98	1.08	0.34
-10	6	5	7.29	6.70	0.12	3	10	5	1.18	1.16	0.56
-9	6	5	2.00	1.41	0.32	-8	11	5	9.91	10.18	0.12
-8	6	5	3.98	4.00	0.15	-7	11	5	4.67	4.59	0.15
-7	6	5	10.90	11.92	0.10	-6	11	5	1.47	0.68	0.33
-6	6	5	7.09	7.13	0.10	-5	11	5	4.39	3.59	0.15
-5	6	5	7.99	8.28	0.10	-4	11	5	2.99	2.38	0.18
-4	6	5	2.72	1.96	0.17	-3	11	5	10.90	11.89	0.10
-3	6	5	1.82	2.05	0.27	-2	11	5	9.14	9.22	0.11
-2	6	5	8.25	7.84	0.10	-1	11	5	2.62	3.20	0.26
-1	6	5	4.23	3.82	0.13	0	11	5	5.79	5.14	0.17
0	6	5	9.99	8.27	0.12	1	11	5	4.45	3.22	0.14
1	6	5	0.90	0.01	0.52	2	11	5	8.75	9.91	0.12
2	6	5	7.70	7.98	0.12	-7	12	5	2.90	2.17	0.23
3	6	5	8.19	8.40	0.12	-6	12	5	0.97	1.76	0.50
4	6	5	12.76	14.35	0.10	-5	12	5	2.12	3.30	0.32
5	6	5	2.29	0.11	0.23	-4	12	5	3.26	3.56	0.20
-10	7	5	9.71	9.51	0.11	-3	12	5	2.38	1.87	0.27
-9	7	5	6.19	5.78	0.12	-2	12	5	6.69	6.92	0.13
-7	7	5	5.00	4.41	0.14	-1	12	5	0.96	0.22	0.53
-5	7	5	11.24	11.49	0.10	0	12	5	3.16	3.20	0.26
-4	7	5	13.08	12.90	0.10	-5	13	5	1.78	1.03	0.33
-3	7	5	4.82	4.87	0.12	-4	13	5	2.24	2.27	0.31
-1	7	5	7.64	7.33	0.10	-3	13	5	2.75	2.67	0.24
0	7	5	11.31	11.32	0.10	-2	13	5	8.92	10.12	0.12
2	7	5	2.43	2.57	0.24	-1	13	5	1.14	1.02	0.56
3	7	5	4.23	3.59	0.17	0	13	5	4.38	3.24	0.19
4	7	5	1.70	2.46	0.32	-11	0	6	5.80	5.27	0.15
5	7	5	1.92	3.35	0.32	-10	0	6	5.47	4.54	0.16
-10	8	5	1.82	1.16	0.37	-9	0	6	4.78	4.96	0.16
-9	8	5	7.73	7.96	0.12	-8	0	6	4.29	5.07	0.17
-8	8	5	7.29	5.94	0.11	-7	0	6	3.46	4.43	0.23
-7	8	5	2.23	1.69	0.27	-6	0	6	13.31	14.25	0.11
-6	8	5	4.49	4.47	0.15	-5	0	6	10.40	10.74	0.11
-4	8	5	8.33	8.37	0.10	-4	0	6	9.93	10.75	0.12
-3	8	5	5.50	5.43	0.11	-3	0	6	5.94	6.36	0.14
-2	8	5	3.87	3.54	0.15	-1	0	6	10.85	10.68	0.11
-1	8	5	3.88	4.08	0.15	0	0	6	4.90	2.93	0.18
0	8	5	2.47	1.64	0.27	1	0	6	5.85	6.54	0.13
2	8	5	3.85	4.28	0.19	2	0	6	6.78	6.38	0.15
3	8	5	3.85	3.24	0.17	3	0	6	3.65	2.79	0.15
4	8	5	6.54	6.97	0.13	4	0	6	5.66	6.22	0.15
-9	9	5	2.13	1.86	0.31	5	0	6	3.21	4.45	0.23
-7	9	5	3.60	2.03	0.18	-11	1	6	2.32	1.87	0.29
-6	9	5	1.42	2.02	0.42	-10	1	6	12.31	13.04	0.10
-5	9	5	1.36	0.66	0.31	-9	1	6	2.64	2.01	0.23
-4	9	5	5.68	5.52	0.12	-8	1	6	1.19	1.25	0.39
-3	9	5	5.75	5.74	0.13	-7	1	6	1.55	0.22	0.25
-2	9	5	12.61	12.83	0.10	-6	1	6	8.44	8.48	0.10
-1	9	5	3.21	2.97	0.18	-5	1	6	11.93	12.41	0.10
0	9	5	6.39	6.09	0.13	-4	1	6	3.32	3.33	0.14

-3	1	6	3.80	3.43	0.13	3	5	6	4.61	4.57	0.16
-2	1	6	7.10	8.69	0.10	-10	6	6	6.01	6.76	0.15
0	1	6	8.19	7.15	0.14	-9	6	6	11.46	10.88	0.11
1	1	6	2.71	2.60	0.22	-8	6	6	5.36	4.41	0.15
2	1	6	0.95	0.42	0.57	-7	6	6	5.86	6.03	0.13
3	1	6	2.77	3.24	0.22	-6	6	6	4.76	4.72	0.14
4	1	6	1.67	1.67	0.36	-5	6	6	1.36	1.09	0.39
-11	2	6	5.58	5.82	0.15	-4	6	6	7.57	7.76	0.11
-10	2	6	9.44	7.57	0.11	-2	6	6	2.27	2.07	0.25
-9	2	6	3.68	3.88	0.18	0	6	6	0.97	0.74	0.53
-8	2	6	3.28	2.84	0.18	1	6	6	4.24	3.64	0.16
-7	2	6	0.88	0.75	0.57	2	6	6	8.22	8.11	0.12
-6	2	6	3.43	3.68	0.14	3	6	6	1.67	1.78	0.35
-5	2	6	10.64	11.88	0.10	-9	7	6	0.93	2.38	0.65
-4	2	6	9.77	10.60	0.10	-8	7	6	6.10	2.85	0.13
-3	2	6	4.20	4.11	0.13	-7	7	6	3.09	2.46	0.23
-2	2	6	7.38	8.34	0.10	-6	7	6	1.58	0.29	0.37
-1	2	6	3.78	4.37	0.13	-5	7	6	4.17	3.44	0.16
0	2	6	2.79	1.80	0.25	-4	7	6	2.63	1.85	0.23
1	2	6	4.13	4.35	0.15	-2	7	6	2.96	2.12	0.19
2	2	6	6.50	7.21	0.13	-1	7	6	1.69	2.28	0.33
4	2	6	1.77	2.01	0.33	0	7	6	2.05	0.12	0.28
-11	3	6	8.72	9.75	0.12	1	7	6	1.83	0.72	0.35
-10	3	6	2.23	1.50	0.25	2	7	6	5.78	4.54	0.15
-9	3	6	3.72	1.94	0.16	-9	8	6	5.76	6.41	0.13
-8	3	6	8.88	9.15	0.11	-8	8	6	2.69	0.09	0.24
-7	3	6	4.46	4.36	0.15	-7	8	6	8.16	6.36	0.12
-6	3	6	5.53	6.00	0.11	-6	8	6	4.84	2.11	0.16
-5	3	6	7.16	8.52	0.11	-5	8	6	5.46	4.18	0.14
-4	3	6	4.61	4.94	0.12	-4	8	6	7.86	9.16	0.12
-3	3	6	5.39	5.23	0.11	-3	8	6	3.62	4.91	0.18
-2	3	6	2.93	2.82	0.16	-2	8	6	2.09	1.87	0.28
-1	3	6	6.59	7.19	0.11	-1	8	6	2.27	0.60	0.29
0	3	6	7.84	7.77	0.15	0	8	6	2.67	1.88	0.24
1	3	6	8.97	10.50	0.11	1	8	6	3.00	1.65	0.23
2	3	6	6.33	6.17	0.13	2	8	6	4.83	5.98	0.16
3	3	6	6.93	4.81	0.13	-7	9	6	4.89	3.09	0.16
4	3	6	4.73	3.74	0.16	-6	9	6	3.82	2.80	0.17
-10	4	6	2.51	0.26	0.26	-5	9	6	4.61	1.36	0.17
-9	4	6	1.13	0.50	0.54	-4	9	6	8.66	7.79	0.12
-8	4	6	0.95	0.28	0.57	-3	9	6	8.43	9.71	0.12
-7	4	6	3.89	4.42	0.15	-2	9	6	2.71	2.42	0.25
-6	4	6	8.83	8.64	0.11	-1	9	6	0.96	0.67	0.70
-5	4	6	10.01	10.70	0.10	0	9	6	2.72	1.39	0.24
-2	4	6	1.93	0.54	0.21	-5	10	6	9.14	7.46	0.12
-1	4	6	6.35	5.65	0.12	-4	10	6	7.17	6.21	0.13
0	4	6	3.27	2.35	0.25	-3	10	6	4.52	5.65	0.17
1	4	6	2.97	3.52	0.20	-2	10	6	4.59	3.24	0.16
2	4	6	4.70	2.94	0.16	-1	10	6	5.56	5.40	0.15
3	4	6	3.37	1.13	0.21	0	11	6	5.87	6.51	0.17
4	4	6	2.46	2.51	0.25	-10	0	7	4.39	4.86	0.20
-10	5	6	10.65	11.48	0.11	-9	0	7	5.77	6.42	0.15
-9	5	6	3.84	1.57	0.19	-8	0	7	10.13	9.10	0.11
-7	5	6	6.76	6.26	0.13	-7	0	7	7.64	6.52	0.12
-6	5	6	1.29	1.55	0.30	-6	0	7	2.13	2.11	0.30
-5	5	6	10.61	10.89	0.09	-5	0	7	13.53	14.18	0.11
-4	5	6	5.90	5.30	0.11	-4	0	7	9.62	9.23	0.13
-3	5	6	2.06	3.04	0.23	-3	0	7	4.95	4.87	0.17
-2	5	6	3.13	3.24	0.17	-2	0	7	1.42	1.84	0.47
-1	5	6	2.68	3.24	0.15	-1	0	7	6.90	6.39	0.14
0	5	6	5.12	5.98	0.14	0	0	7	7.50	7.89	0.13
1	5	6	4.21	4.81	0.15	1	0	7	7.49	7.95	0.15
2	5	6	3.76	1.84	0.19	-8	1	7	2.83	0.66	0.23

-7	1	7	3.80	1.23	0.19
-6	1	7	5.84	2.69	0.15
-5	1	7	4.28	3.60	0.20
-4	1	7	10.70	8.94	0.15
-3	1	7	10.93	7.72	0.15
-2	1	7	7.29	6.69	0.12
-1	1	7	6.16	5.60	0.13
0	1	7	8.64	6.16	0.12
-8	2	7	2.90	0.18	0.24
-7	2	7	4.72	2.29	0.16
-6	2	7	4.90	3.31	0.15
-5	2	7	2.03	1.16	0.41
-4	2	7	4.34	4.54	0.22
-3	2	7	11.55	10.57	0.13
-2	2	7	8.58	6.82	0.12
-1	2	7	3.48	3.10	0.19
0	2	7	2.37	3.42	0.28
-8	3	7	4.53	5.02	0.16
-7	3	7	5.55	4.84	0.15
-6	3	7	1.64	0.33	0.36
-5	3	7	5.19	4.46	0.16
-4	3	7	12.00	11.60	0.11
-3	3	7	5.54	5.67	0.15
-1	3	7	3.74	2.21	0.20
0	3	7	1.89	0.92	0.34
-8	4	7	4.14	4.67	0.19
-7	4	7	2.22	0.66	0.29
-6	4	7	7.10	5.87	0.12
-5	4	7	2.41	2.90	0.29
-4	4	7	5.74	6.29	0.15
-3	4	7	2.04	2.13	0.32
-2	4	7	0.84	0.48	0.76
-1	4	7	2.92	1.82	0.23
0	4	7	2.86	3.15	0.25
-7	5	7	1.88	0.25	0.33
-5	5	7	2.08	0.45	0.31
-4	5	7	7.62	8.26	0.12
-3	5	7	2.10	2.59	0.31
-2	5	7	1.11	0.57	0.57
-1	5	7	1.03	0.22	0.60
-6	6	7	11.52	12.21	0.11
-5	6	7	12.40	12.72	0.11
-4	6	7	1.22	1.35	0.50
-3	6	7	2.98	3.60	0.24
-2	6	7	0.90	0.30	0.69
0	6	7	8.53	9.29	0.15

APPENDIX VIII

Published work.

The following 3 papers make use of the data collection and analysis described in this thesis.

The first two listed papers were given at the Third International Meeting on Ferroelectricity 1973.

The last listed paper made use of preliminary analysis of preliminary data off DKDP.

The Crystal Structure of the Paraelectric Phase
of $K(D_{0.88}H_{0.12})_2PO_4$

V.R. Eiriksson, K.D. Rouse* and R.J. Nelmes

Department of Physics, University of Edinburgh,
Edinburgh EH9 3JZ, Scotland

*A.E.R.E., Harwell, Didcot,
Berkshire, England

Full three-dimensional neutron data have been collected from a single crystal of $K(D_{0.88}H_{0.12})_2PO_4$ (DKDP) at $294^{\circ}K$ and also just above the ferroelectric transition ($T_c = 209^{\circ}K$) at $T_c + 5^{\circ}K$ and $T_c + 10^{\circ}K$. The low-temperature data sets were extended to greater resolution along the a and b axes than along c (the tetrad). The techniques of constrained least-squares refinement and statistical testing have been applied to determine the significance of important features of the structure. Particular attention has been paid to the position and distribution of the deuterium in the short O-D-O bonds. The tests applied and the results of the analysis will be discussed. The structures at $294^{\circ}K$ and just above T_c will be compared.

Preliminary results from the data collected at $294^{\circ}K$ have been published (Solid State Commun. (1972) 11, 1261).

Structural Studies of the System KH_2PO_4 - KD_2PO_4

R.J. Nelmes and K.D. Rouse*

Department of Physics, University of Edinburgh,
Edinburgh EH9 3JZ, Scotland

*A.E.R.E., Harwell, Didcot,
Berkshire, England

Full three-dimensional neutron data have been collected from a single crystal of KH_2PO_4 (KDP) at 294°K and also just above the ferroelectric transition ($T_c = 123^\circ\text{K}$) at $T_c + 4^\circ\text{K}$. The techniques of constrained least-squares refinement and significance testing have been applied as in the analysis of the structure of DKDP discussed in an earlier paper. Particular attention has been given to the position and distribution of the hydrogen in the short O-H-O bonds. The structures at 294°K and just above T_c will be compared. A comparison will also be made with the structural results for DKDP presented in the earlier paper; the effect of deuteration on the tetragonal phase of the KH_2PO_4 - KD_2PO_4 system will be discussed.

A preliminary comparison of the KDP and DKDP structures at room-temperature has been published (Solid State Commun. (1972) 11, 1261), which shows some significant structural changes with deuteration in the tetragonal phase. Further, it is known that at very high levels of deuteration a monoclinic form crystallises at room-temperature and that DKDP also undergoes a transition from the tetragonal phase to a monoclinic phase on heating. It is thus necessary to view the system KH_2PO_4 - KD_2PO_4 as a whole, and the currently available information on the phases in the system will be summarised. The results of a structural study of the room-temperature monoclinic phase will be given.

Reprinted from
SOLID STATE COMMUNICATIONS

STRUCTURAL STUDIES OF THE SYSTEM KH_2PO_4 – KD_2PO_4

R.J. Nelmes and V.R. Eiriksson

Department of Physics, University of Edinburgh,
The King's Buildings, Mayfield Road, Edinburgh EH9 3JZ

and

K.D. Rouse

Atomic Energy Research Establishment, Harwell, Didcot, Berkshire

(Received 2 August 1972 by R.A. Cowley)

Current least-squares refinement techniques have been applied to the KDP structural data collected by Bacon and Pease and to recent room-temperature data from DKDP. The results in the paraelectric phase of both salts (i) show that in the short oxygen–oxygen bonds the protons (deuterons) are disordered, and (ii) suggest a significant isotope effect on the orientation of their distribution relative to the oxygen–oxygen line.

COMPARED with the wealth of dynamical experiments and theoretical work on KH_2PO_4 (KDP) and $\text{K}(\text{D}_{x-1}\text{H}_{1-x})_2\text{PO}_4$ (DKDP) there is a paucity of detailed structural knowledge, and there is growing evidence that some commonly held assumptions about their structures are incorrect. The structure of DKDP has not hitherto been investigated. The most recent structural work on KDP is that of Bacon and Pease in 1955.¹ In the tetragonal paraelectric phase [space group $\bar{1}42d$, $a = b = 7.453$, $c = 6.959$ Å (room-temperature);² $a = b = 7.426$, $c = 6.919$ Å (at 132°K, see 1 and 2)] they collected ($hk0$) and ($h0l$) data at room-temperature³ and ($h0l$) data at 132°K¹ (their work on the ferroelectric phase¹ is not considered here). This provided accurate parameters for the K, P and O atoms, but some details of the proton distribution in the short oxygen–oxygen hydrogen bonds remained uncertain.¹ For example, the important distinction between the protons being 'ordered' in a single minimum or 'disordered' in a double minimum potential well is held to have been left unresolved.^{1,4,9} The analyses of experiments performed on DKDP

have had to use the structural parameters of KDP: this approximation is now inadequate.⁹

Recently, incoherent elastic and coherent inelastic neutron scattering techniques have been used to study the proton motion and distribution in KDP^{5–8} and the deuteron motion in DKDP.^{9,10} Plessner and Stiller⁵ found the proton distribution in KDP at room-temperature to be concentrated at sites 0.40 ± 0.03 Å apart (Δ in Fig. 1), with the line joining the sites (AB in Fig. 1) inclined at $6 \pm 3^\circ$ to the ab plane (θ in Fig. 1). In DKDP Wallace *et al.*¹⁰ found θ to be 22° using the dynamical data of Skalyo *et al.*⁹ collected at 225°K. These investigations showed that the proton (deuteron) sites for a double minimum well, or the direction of high thermal motion in a single minimum well, do *not* lie along the oxygen–oxygen (O–O) line, and suggested an isotope effect of surprising magnitude. This and the uncertainties mentioned before indicated the need for an accurate structural study of both DKDP and KDP.

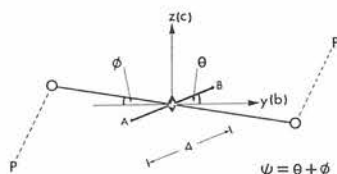


FIG. 1. The hydrogen bond in KDP or the deuterium bond in DKDP. The bond is viewed down the x -axis and has a two-fold symmetry axis (diad) at its centre as shown. The open circles denote the oxygen atoms. A and B are the sites of the two 'half' H(D) atoms in the double minimum model; the line AB is the direction of the principal thermal motion for the single minimum model, in which the H(D) atoms lie on the diad. Δ is the distance A to B . The approximate location of the phosphorus to which each oxygen is attached is indicated: the x -coordinate of the phosphorus is less than that of the oxygen.

While starting the data collection from DKDP current techniques of constrained least-squares refinement and significance testing¹¹ were applied to the KDP data of Bacon and Pease^{1,3} to see if more information could be obtained than previously given. These techniques permit a statistical significance level to be attached to structural features. For example, to answer the question 'Does the x -coordinate of the hydrogen, x_H , differ from that of the oxygen, x_O ?' the structure is refined with $x_H = x_O$ and then with this constraint removed. From the known probability distribution for the ratio of the 'goodness of fit' indices of the two refinements, the statistical significance of the difference between x_H and x_O is obtained. This procedure is of considerably greater rigour than any depending on a single unconstrained refinement and the least squares 'errors' derived therefrom.¹¹ Details of the refinements and tests applied in this study — out of place here — will be presented in a subsequent paper.

In discussing the results, the model in which the proton occupies a single minimum well will be referred to as 'ordered', and that in which it occupies a double minimum well as 'disordered'. The direction of highest thermal motion of the proton in the ordered model will be designated the 'principal axis'.

Using the data collected at 132°K it was found

- (i) that it is only 90% probable that the x -coordinate of H, x_H , differs from that of O, x_O (see Fig. 1),
- (ii) that tilting of the principal axis of proton motion off the O—O line in the ordered model is also significant at the 90% level, and
- (iii) that the disordered model gives a very significantly better fit to the data than does the ordered model: it is 99.9% probable that the disordered model is correct.

For the ordered model the refinement gives $\psi = 6 \pm 4^\circ$ [see (ii) above], and $\phi = 0.5 \pm 0.1^\circ$ (Fig. 1). This is to be compared with the result of Plessner and Stiller⁵ that $\theta = 6 \pm 3^\circ$ at room-temperature. In the disordered model the refinement gives a site separation, Δ , of $0.34 \pm 0.02 \text{ \AA}$ [see (iii) above]. x_H is probably less than x_O [see (i) above].

The same procedure was followed through with the room-temperature ($h0l$) data.³ Generally lower levels of significance were obtained, as expected, but the improvement of the disordered model over the ordered model was still significant at the 99% level, with $\Delta = 0.34 \pm 0.02 \text{ \AA}$.

It is interesting to note that Bacon and Pease¹ performed their final least-squares refinement with a two minima model and the parameters and errors obtained give $\Delta = 0.34 \pm 0.04 \text{ \AA}$. This would seem significantly different from zero! It was perhaps a sign of the times that this was not regarded as conclusive in the light of the evidence from the Fourier map.

Neutron data collection at room-temperature (294°K) on a single crystal of DKDP has been completed very recently. The specimen has a $D/D + H$ ratio of 0.88 ± 0.01 , and cell dimensions $a = b = 7.468 \pm 0.001$, $c = 6.979 \pm 0.001 \text{ \AA}$.¹² The data were collected with a wavelength of 1.15 \AA using a Ferranti Mk. II 4-circle diffractometer on the PLUTO reactor at A.E.R.E., Harwell. To obtain preliminary results for comparison with the KDP refinements part of the 'crude' data set was selected (corrections for absorption, extinction

and small drifts in the 'standard' intensity have yet to be completed). Observed (hkl) reflections in the range $40^\circ < \theta_{\text{Bragg}} < 70^\circ$ and a few ($h0l$) reflections with $\theta_{\text{Bragg}} < 40^\circ$ were used – excluding the strongest reflections, for which high extinction was expected.

The procedure of the KDP refinements was followed. It was found

- (i) that it is 99% probable that the x -coordinate of D, x_D , differs from that of O, x_O (see Fig. 1),
- (ii) that the inclination of the principal axis of deuteron motion to the O–O line in the ordered model is significant at the 99% level,
- (iii) that the separation of the deuterium onto two sites (disordered model) is significant at somewhat above the 99.9% level, and
- (iv) that it is 99.5% probable that these sites lie off the O–O line.

The disordered model refinement gives a deuteron site separation, Δ , of $0.44 \pm 0.01 \text{ \AA}$ [see (iii) above] – a larger separation than in KDP, as expected; x_D is probably less than x_O [see (i) above]; the O–O distance is $2.516 \pm 0.004 \text{ \AA}$ (compare 2.484 \AA in KDP); θ is $8.0 \pm 2.5^\circ$ [see (iv) above], and ϕ is $0.25 \pm 0.15^\circ$. This low value of ϕ is important in relation to the work of Skalyo *et al.*⁹ Assuming KDP structural parameters (which give $\phi = 0.5 \pm 0.1^\circ$) they found a large distortional movement of the oxygen tetrahedra in the ferroelectric mode. But for $\phi = 0$ this motion cannot be determined from their results. The need to analyse experiments on DKDP using structural parameters for DKDP is underlined.

The ordered model refinement gives $\psi = 11 \pm 3^\circ$ and $\phi = 0.4 \pm 0.2^\circ$. The data used by Wallace *et al.*¹⁰ to obtain a value of 22° for θ was measured at 225°K ,⁹ on a specimen with $D/D + H \sim 0.92$ as estimated¹² from the given⁹ transition temperature. Here a determination of the 'static' deuteron distribution from diffraction data is being compared with the result of a dynamical experiment. Nevertheless, the difference in θ values is not expected to be so large. There

is also the temperature difference which might account for the discrepancy; but again it would be an effect of surprising magnitude – and quite different from KDP (see above).

These results show that in the tetragonal phase of both KDP and DKDP the separation of the protons (deuterons) onto two sites in the short hydrogen (deuterium) bonds is highly significant. There is also a marked isotope effect on the angle, ψ , that the line joining these sites makes with the O–O direction.

The increase in ψ and the O–O separation for DKDP [$\text{K}(\text{D}_{0.88}\text{H}_{0.12})_2\text{PO}_4$ here] compared with KDP – hence weakening of the bond – suggests an explanation for the transition from a tetragonal to a monoclinic phase at high deuteration levels.¹³ A monoclinic phase is also obtained on heating tetragonal DKDP;¹⁴ there is evidence that these two monoclinic phases have very similar structures.^{15,16}

There are thus reasons for carrying out a full structural study of the system $\text{KH}_2\text{PO}_4\text{--KD}_2\text{PO}_4$. Nemes has recently determined the structure of the high deuteration monoclinic phase from X-ray data.¹⁷ Full neutron data have been collected for the room-temperature phase of DKDP, and work on the ferroelectric phase is now in progress. Neutron experiments are planned for the near future on the paraelectric and ferroelectric phases of KDP, on the high deuteration monoclinic phase (to locate the deuteriums more precisely) and on the high temperature monoclinic phase.

Acknowledgements – The authors would like to thank Professor W. Cochran for his generous encouragement and advice and Dr. B.J. Isherwood for his kind assistance. The support of a Science Research Council Fellowship for R.J.N. and of the Icelandic Science Foundation for V.R.E. are gratefully acknowledged.

REFERENCES

1. BACON G.E. and PEASE R.S., *Proc. R. Soc.* **A230**, 359 (1955).
2. MEGAW H.D., *Ferroelectricity in Crystals*. Methuen, London (1957).
3. BACON G.E. and PEASE R.S., *Proc. R. Soc.* **A220**, 397 (1953).
4. JONA F. and SHIRANE G., *Ferroelectric Crystals*. Pergamon, London (1962).
5. PLESSER TH. and STILLER H., *Solid State Commun.* **7**, 323 (1969).
6. FELCHER G. and PELAH I., *J. Chem. Phys.* **52**, 905 (1970).
7. GRIMM H., STILLER H. and PLESSER TH., *Phys. Status Solidi* **42**, 207 (1970).
8. ARSIC-ESKINJA M., GRIMM H. and STILLER H., *Symposium on Neutron Inelastic Scattering*. IAEA/SM-155/G2 (1972).
9. SKALYO J., FRAZER B.C. and SHIRANE G., *Phys. Rev.* **B1**, 278 (1970).
10. WALLACE E.A., COCHRAN W. and STRINGFELLOW M., *Suppl. J. de Physique*, **33**, C2-59 (1972).
11. PAWLEY G.S., *Advances in Structure Research by Diffraction Methods*. Vol. 4. (edited by HOPPE W. and MASON R.) Pergamon, Oxford (1972).
12. ISHERWOOD B.J., Private communication.
13. UBBELOHDE A.R. and WOODWARD I., *Nature, Lond.* **144**, 632 (1939).
14. GRUNBERG J., LEVIN S., PELAH I. and WIENER E., *Solid State Commun.* **5**, 863 (1967).
15. BLINC R., O'REILLY D.E., PETERSON E.M. and WILLIAMS J.M., *J. Chem. Phys.* **50**, 5408 (1969).
16. GRUNBERG J., LEVIN S., PELAH I. and GERLICH D., *Phys. Status Solidi (b)* **49**, 857 (1972).
17. NELMES R.J., *Phys. Status Solidi (b)* **52**, K89 (1972).

Des techniques récentes d'affinement aux moindres carrés ont été appliquées aux données obtenues par Bacon et Pease sur la structure du KDP, aussi bien qu'à des données recueillies récemment sur le DKDP à la température ambiante. Les résultats dans la phase paraélectrique des deux matériaux: (i) démontrent que les protons (deutrons) sont désordonnés dans les liens courts oxygène-oxygène; (ii) suggèrent que l'orientation de leur distribution relativement à la ligne oxygène-oxygène dépend de l'isotope.

REFERENCES

- Arndt, U.W. and Willis, B.T.M., 1966, Single Crystal Diffractometry. Cambridge University Press.
- Bacon, G.E. and Pease, R.S., 1953, Proc. R. Soc. A220, 397.
- Bacon, G.E. and Pease, R.S., 1955, Proc. R. Soc. A230, 359.
- Bacon, G.E., 1972, Acta Cryst. A28, 357.
- Blinic, R., 1960, J. Phys. Chem. Solids 13, 204.
- Blinic, R., Dimic, V., Kolar, V., Lahajnar, G., Stepisnik, I., Zumer, S. and Vene, N., 1968, J. Chem. Phys. 49, No. 11, 4996.
- Blinic, R., O'Reilly, D.E., Peterson, E.M. and Williams, Jack M., 1969A, J. Chem. Phys. 50, No. 12, 5408.
- Blinic, R., Ferraro, J.R. and Postmus, C., 1969B, J. Chem. Phys. 51, No. 2, 732.
- Brockhouse, B.N., 1966, Phonons in perfect lattices and in lattices with point imperfections. Ed. Stevenson, R.W.H. Edinburgh: Oliver and Boyd.
- Bunn, C.W. and Emmett, H., 1949, Discussions Faraday Soc. III, 119.
- Busch, G. and Scherrer, P., 1935, Naturwissenschaften 23, 737.
- Chynoweth, A.G., 1959, Phys. Rev. 113, 159.
- Cochran, W., 1951, Acta Cryst. 4, 408.
- Cochran, W., 1960, Advances in Physics 9, 387.
- Cochran, W., 1961, Advances in Physics 10, 401.
- Cochran, W. and Cowley, R.A., 1962, J. Phys. Chem. Solids 23, 447.
- Cochran, W., 1969, Advances in Physics 18, No. 72, 157.
- Cochran, W., 1972, Private Communications.
- Cochran, W., 1973, The Dynamics of Atoms in Crystals. London: Edward Arnold.
- Cooper, M.J. and Rouse, K.D., 1970, Acta Cryst. A26(2), 214.
- Cowley, R.A., 1962, Phys. Rev. Lett. 9, 159.
- de Quervain, M., 1944, Helv. Phys. Acta 17, 509.
- Devonshire, A.F., 1954, Advances in Physics 3, No. 10, 85.
- Eiriksson, V.R. and Placido, F., 1971, unpublished work.

REFERENCES (Contd.)

- Eiriksson, V.R., Nelmes, R.J. and Rouse, K.D., 1973, Proceedings of the Third International Meeting on Ferroelectricity (in press)
- Fatuzzo, E. and Mertz, W.J., 1967, Ferroelectricity. Amsterdam: North Holland Publishing Co.
- Fletcher, S.R., Skapaski, A.C. and Keve, E.T., 1971, J. Phys. C. 4, L 255.
- Frazer, B.C., 1971, Structural Phase Transitions and Soft Modes. Ed. Samuelsen, E.J. Oslo: Universitetsforlaget.
- Frazer, B.C. and Pepinsky, R., 1953, Acta Cryst. 6, 273.
- Fujii, Y. and Yamada, Y., 1971, J. Phys. Soc. Japan 30, No 6, 1676.
- Gilman, J.J., 1966, (Editor) The Art and Science of Growing Crystals. New York: Wiley.
- Grunberg, J., Levin, S., Pelah, I. and Wiener, E., 1967, Solid State Commun. 5, 863.
- Grunberg, J., Levin, S., Pelah, I. and Gerlich, D., 1972, Phys. Stat. Sol. (b) 49, 857.
- Hamilton, W.C., 1964, Statistics in Physical Science. New York: The Ronald Press Co.
- Hamilton, W.C., 1965, Acta Cryst. 18, 502.
- Hewat, A., 1973, Proceedings of the Third Internationale Meeting on Ferroelectricity (in press).
- Hosino, S., Okaya, Y. and Pepinsky, R., 1959, Phys. Rev. 115, 323.
- International Tables for X-ray Crystallography, 1962, Birmingham: Kynoch Press.
- Isherwood, B.J., 1972, Divisional Report No. 13016/C, The General Electric Company, Wembley, Middlesex.
- Itoh, K. and Mitsui, T., 1973, Ferroelectrics 5, 235.
- Jona, F. and Shirane, G., 1962, Ferroelectric Crystals. London: Pergamon Press.
- Kaminow, I.P. and Damen, T.C., 1968, Phys. Rev. Lett. 20, 1105.
- Keve, E.T. et al., 1973, Proceedings of the Third International Meeting on Ferroelectricity (in press).
- Kiehl, S.J. and Wallace, G.H., 1927, J. Am. Chem. Soc. 49, 375.
- Levy, H.A., Peterson, S.W. and Simonsen, S.H., 1954, Phys. Rev. 93, 1120.
- Lipson, H. and Cochran, W., 1966, The Determination of Crystal Structures. London: Bell.

REFERENCES (Contd.)

- Lyddane, R.H., Sachs, R.G. and Teller, E., 1941, Phys. Rev. 59, 673.
- Megaw, H.D., 1957, Ferroelectricity in Crystals. London: Methuen.
- Matthias, B.T., Miller, C.E. and Remeika, J.P., 1956, Phys. Rev. 104, 849.
- Moore, M.A. and Williams, H.C.W.L., 1972, J. Phys. C. 5, 3168.
- Nakano, J., Shiozaki, Y. and Nakamura, E., 1973A, Proceedings of the Third International Meeting on Ferroelectricity (in press).
- Nakano, J., Shiozaki, Y. and Nakamura, E., 1973B, J. Phys. Soc. Japan 34, 1423.
- Nelmes, R.J., 1971, Acta Cryst. B27, 272.
- Nelmes, R.J., 1972, Phys. Stat. Sol. (b) 52, K89.
- Nelmes, R.J., Eiriksson, V.R. and Rouse, K.D., 1972, Solid State Commun. 11, 1261.
- Nelmes, R.J. and Rouse, K.D., 1973, Proceedings of the Third International Meeting on Ferroelectricity (in press)
- Nitsche, R., 1958, Helv. Phys. Acta 31, 306.
- O'Keefe, M. and Perrino, C.T., 1967, J. Phys. Chem. Solids 28, 211.
- Paul, G.L., Cochran, W., Buyers, W.J.L. and Cowley, R.A., 1970, Phys. Rev. B11, No. 2, 4603.
- Pawley, G.S., 1969, Acta Cryst. A25, 531.
- Pawley, G.S., 1970, Acta Cryst. A26, 691.
- Pawley, G.S., 1972, in: Advances in Structure Research by Diffraction Methods. Oxford: Pergamon Press.
- Peckham, G.E., Saunderson, D.H. and Sharp, R.I., 1967, Brit. J. Appl. Phys. 18, 473.
- Pepinsky, R., Okaya, Y. and Jona, F., 1957, Bull. Am. Phys. Soc. Ser. II 2, 220.
- Pereverzeva, L.P., Pogoskaya, N.Z., Poplavko, Yn.M., Pakhomov, V.I., Rez, I.S. and Sil'nitskaya, G.B., 1972, Sov. Phys. Solid State 13, No. 11, 2690.
- Peterson, S.W., Levy, H.A. and Simonsen, S.H., 1953, J. Chem. Phys. 21, 2084.
- Pippard, A.B., 1964, The Elements of Classical Thermodynamics Cambridge: University Press.

REFERENCES (Contd.)

- Pirrene, J., 1949, Physica 12, 1019.
- Pirrene, J., 1955, Physica 21, 219.
- Plessner, T.H. and Stiller, H., 1969, Solid State Commun. 7, 323.
- Rapoport, E., 1970, J. Chem. Phys. 53, No. 1, 311.
- Riste, T., Samuelsen, E.J. and Otnes, K., 1971, Structural Phase Transitions and Soft Modes. Ed. Samuelsen E.J.
Oslo: Universitetsforlaget.
- Shibuya, I. and Mitsui, T., 1961, J. Phys. Soc. Japan 16, 479.
- Skalyo, J., Frazer, B.C. and Shirane, G., 1970, Phys. Rev. B1, 278.
- Slater, J.C., 1941, J. Chem. Phys. 9, 16.
- Togunaga, M., 1966, Progress in Theoretical Physics 36, No. 5, 857.
- Togunaga, M. and Matsubara, T., 1966, Progress in Theoretical Physics 35, No. 4, 581.
- Ubbelohde, A.R. and Woodward, I., 1939, Nature, Lond, 144, 632.
- Ubbelohde, A.R. and Woodward, I., 1947, Proc. Roy. Soc. A188, 358.
- Wallace, E.A., Cochran, W. and Stringfellow, M., 1972, Suppl. J. de Physique 33, C2-59.
- West, J., 1930, Z. Krystallogr. 74, 306.
- Wood, E.A. and Holden, A.N., 1957, Acta Cryst. 10, 145.
- Zheludev, I.S., 1971, The Physics of Crystalline Dielectrics, Vol. 1, Crystallography and Spontaneous Polarization.